APPLICATION OF CELLULOSE NANOWHISKER AND LIGNIN IN PREPARATION OF RIGID POLYURETHANE NANOCOMPOSITE FOAMS

A Dissertation
Presented to
The Academic Faculty

by

Yang Li

In Partial Fulfillment
of the Requirements for the Degree
Doctor of Philosophy in the
School of Chemistry and Biochemistry

Georgia Institute of Technology
August, 2012

APPLICATION OF CELLULOSE NANOWHISKER AND LIGNIN IN PREPARATION OF RIGID POLYURETHANE NANOCOMPOSITE FOAMS

Approved by:

Dr. Arthur J. Ragauskas, Advisor
School of Chemistry and Biochemistry
Georgia Institute of Technology

Dr. Stefan France
School of Chemistry and Biochemistry
Georgia Institute of Technology

Dr. Charles L. Liotta
School of Chemistry and Biochemistry
Georgia Institute of Technology

Dr. Yunlin Deng
Chemical and Biomolecular Engineering
Georgia Institute of Technology

Dr. Preet Singh
School of Materials Science and Engineering
Georgia Institute of Technology

Date Approved: [May 15, 2012]

ACKNOWLEDGEMENTS

It has been a long way full of happiness to go from the starting of graduate study at Georgia Institute of Technology in August 2007 to the accomplishment of the Ph. D. dissertation. This would not be possible without the love, care, support, and advice from many individuals. I would like to sincerely say 'thank you' to all of them.

First and foremost, I would like to acknowledge my advisor, Dr. Arthur J. Ragauskas, for his guidance, encouragement, advice, and mentorship throughout my doctoral research. I would also like to thank my committee members, Dr. Charles L. Liotta, Dr. Stefan France, Dr. Yulin Deng, and Dr. Preet Singh, for their insightful comments and support from the initial to the final level of this project.

I am grateful to my co-workers at Georgia Tech, especially Dr. Shaobo Pan, Dr. Nan Jiang, Dr. Yunqiao Pu, and Dr. Dong Ho Kim, for their support in many aspects during the completion of this project.

I owe my deepest gratitude to my husband, Hongfeng Ren. Without his guidance and encouragement, I would not have the first step out towards my goal; without his continuous support and constructive suggestions, I would not have today's accomplishments.

I also would like to thank my parents and sister their strong support and complete understanding all the way, and all my good friends in the United States for the wonderful times and lasting memories we shared together.

Finally, I would like to acknowledge the financial support from the Paper Science and Engineering Fellowship program at the Institute of Paper Science and Technology.

TABLE OF CONTENTS

LIST OF TABLES

LIST OF FIGURES

LIST OF SYMBOLS AND ABBREVATIONS

AC	Aggregated cellulose nanowhiskers
AFM	Atomic force microscopy
BDO	1,4-butane diol
CC	Coated cellulose nanowhiskers
CCD	Charge coupled device
$CDCl_3$	Deuterated chloroform
CNW	Cellulose nanowhiskers
conc.	Concentration
CP/MAS	Cross polarization/magnetic angle spinning
CTC	Cellulose tricarbanilate
D	Polydispersity index
DABCO	1,4-diazabicyclofoctane
DEG	Diethylene glycol
DI	Deionized
DMA	Dynamic mechanical analysis
DMAc	Dimethylacetamide
DMF	Dimethyl formamide
DMPA	Dimethylol propionic acid
DMSO	Dimethyl sulfoxide
DMSO-d6	Deuterated dimethyl sulfoxide
DPG	Dipropylene glycol
DP_N	Number-average degree of polymerization
DP_V	Viscosity-average degree of polymerization

DP_W	Weight-average degree of polymerization
DSC	Differential scanning calorimetry
ECF	Elemental chlorine free
EG	Ethylene glycol
EO	Ethylene oxide
EOL	Ethanol organosolv lignin
FAO	Food agricultural organization
FE-SEM	Field emission-scanning electron microscopy
FT-IR	Fourier transform infrared
G	Guaiacyl
GC	Grafted cellulose nanowhiskers
gg	gauche-gauche
GPC	Gel permeation chromatography
gt	gauche-trans
H	*p*-hydroxyl phenyl
HCl	Hydrochloric acid
HDI	Hexamethylene diisocyanate
HFC-245fa	1,1,1,3,3-pentafluoropropane
HFC-134a	1,1,1,2-tetrafluoroethane
H_2SO_4	Sulfuric acid
HW	Hardwood
I_{OH}	Hydroxyl index
IP	Intellectual property
IPDI	Isophorone diisocyanate
KBr	Potassium bromide

KOH	Potassium hydroxide
LiCl	Lithium chloride
LiTFSI	Trifluoromethanesulfonylimide
MCC	Microcrystalline cellulose
MDI	Diphenylmethane diisocyanate
$MgSO_4$	Magnesium sulfate
ML	Middle lamella
MMD	Molar Mass distribution
M_n	Number-average molecular weight
M_v	Viscosity-average molecular weight
M_w	Weight-average molecular weight
MWCO	Molecular weight cut off
MW_{glu}	Molecular weight of anhydroglucose
NaCl	Sodium chloride
NHND	N-hydroxy-5-norborene-1,3-dicarboximide
NMR	Nuclear magnetic resonance
P	Primary cell wall
PCL	Polycaprolactone
PEG	Poly(ethylene glycol)
PLA	Poly(lactic acid)
PLLA	Poly(L-lactide)
PMMA	Polymethylmethacrylate
PO	Propylene oxide
PPG	Polypropylene glycol
ppm	Parts per million

PPO	Poly(propylene oxide)
PU	Polyurethane
PVA	Polyvinyl alcohol
PVAc	Polyvinyl acetate
S	Syringyl
SAXS	Small angle X-ray scattering
SEM	Scanning electron microscopy
S.D.	Standard deviation
SW	Softwood
S1	The outer layer of the secondary cell wall
S2	The middle layer of the secondary cell wall
S3	The inner layer of the secondary cell wall
T	Temperature
T_d	Decomposition temperature
TDI	Toluene diisocyanate
TEA	Triethylamine
TEDA	Triethylenediamine
TEM	Transmission electron microscopy
TFE	Thermally-assisted field emission
T_g	Glass transition temperature
tg	trans-gauche
TGA	Thermogravimetric analysis
THF	Tetrahydrofuran
T_m	Melting temperature
TMDP	2-Chloro-4,4,5,5-tetramethyl -1,3,2-dioxaphospholane

TMP	Trimethylolpropane
UV	Ultraviolet
WPU	Waterborne polyurethane
WAXS	Wide angle X-ray scattering
XRD	X-ray diffraction
3D	3 dimensional
η	Viscosity

SUMMARY

Though the rapid development of human society, concerns on the fossil fuel shortage, pollution, and end-of-life disposal issues are attracting the most attention nowadays. Therefore, more efforts from governments, industries, and research institutes have been paid to the sustainable development than it has ever been done before. Cellulose, lignin and hemicellulose are the major components of biomass and also the most abundant biopolymers in nature. They are widely available, renewable, biodegradable, non-edible, and have low stable market prices which are competitive with petroleum-derived polymers. Moreover, their unique structures have huge potentials to be explored. Not only being used as a raw material in pulp and paper mills, cellulose has been found to have a lot of superior properties when hydrolyzed into cellulose nanowhiskers (CNWs), which can be applied to structural materials and nanocomposites synthesis. As a major waste from the paper-making process, lignin has lead to the prosperity of the biobased chemicals and macromolecules instead of being burned directly as a low value fuel, attributing to its unique phenolic structures.

The first study in the thesis investigates the reinforcing effect of CNWs in preparation of rigid polyurethane (PU) foam, one of the most diverse and widely used plastic materials with an ever-growing global market. The control foam was prepared by first mixing polyols, catalysts, and surfactant, and then adding blowing agent and diisocyanate under strong stirring. Freeze dried CNWs of up to 1 wt% were added by dispersing in dimethyl formamide (DMF) and then mixing with polyols followed by DMF removal under high vacuum. The resulting control foam and nanocomposite

foams exhibited different density and closed cell size. Therefore, the mechanical properties of the prepared foams were compared based on the unit mass data. Tensile property, especially compressive property was enhanced with increasing CNWs addition as compared to the control. FT-IR spectra indicated CNWs acted as a crosslinking reagent in the PU synthesis, which is one of the reasons for the improvement of mechanical and dynamic mechanical properties of the nanocomposites.

The second study presents the application of Kraft lignin in preparation of rigid PU foams. A commercial softwood Kraft pine lignin was derived from its solid form into a liquid polyol through a chain extension reaction with propylene oxide under the catalysis of potassium oxide. The structure, composition, and properties of the lignin polyol were studied by different techniques including FT-IR, GPC, and NMR. It has proven that the Kraft lignin polyol has characteristics suitable for rigid PU foam preparation. Later, a series of formulation optimization experiments was set up by gradually replacing commercial polyols, which were used in the control foam preparation, with lignin polyol, in order to prepare a rigid PU foam with superior mechanical strength. The compressive study showed that the foam prepared with only one type of polyol, lignin polyol, possessed the optimal properties.

Based on the results of the previous formulation optimization study, the preparation of an ethanol organosolv lignin (EOL)-based rigid PU foam reinforced with higher content of CNWs (up to 5 wt%) was reported in the third study. EOL, which is largely produced by the biorefineries today, was used instead of Kraft lignin due to its higher purity, lower molecular weight, and less condensed structure compared to Kraft lignin, and its sulfur free characteristic. In order to improve the content of CNWs to a

level above 1 wt%, its aqueous suspension was directly mixed with the EOL polyol followed by water removal under high vacuum. Instead of using freeze dried CNWs, which is difficult to be well dispersed in organic solvents, e.g., DMF, this method can easily improved the CNWs content in PU formulation with a homogeneous dispersion of CNWs. With increasing CNWs contents, the closed cell size of rigid PU foams was decreased resulted in a slight increase of the density. However, the density was still in the value range of the commercial low density rigid PU foams. The prepared nanocomposites possessed significant improvements of both mechanical properties and thermal stability which were shown by the compressive testing, differential scanning calorimetry (DSC) analysis, and thermogravimetric analysis (TGA).

CHAPTER 1

INTRODUCTION

Biobased polymers and biomaterials are a relatively new and growing market in light of recent societal concerns including dwindling petroleum reserves, environmental and end-of-life disposal issues. Polymers derived from plants, especially those from non-food resources, are attracting the attention of governments, industries, and research institutes, primarily attributed to their environmental compatibility, unique physical properties, and low stable market prices which are competitive with petroleum-derived polymers.

Cellulose, as the most abundant biopolymer on earth with a total annual biomass production of about 1.5×10^{12} tons [1], has led to a large body of research due to its renewable nature, wide availability, non-food agricultural based economy, low density, high specific strength and modulus, high aspect ratio, and reactive surface [2]. Cellulose nanowhiskers, the acid hydrolysis product of cellulose fibers, exhibit not only a high elastic modulus of 143 GPa [3-4], but also significant changes in electrical, optical, and magnetic properties in comparison to native cellulosic fibers [2]. There has been a growing interest in CNW-based novel materials and CNWs reinforced nanocomposites in the last decade, and improvements in mechanical and thermal properties are readily achieved [4-9].

Lignin, the most abundant phenolic biopolymer, plays an important role in the biomaterials industry nowadays. As of 2010, the pulp and paper industry generated ~55 million tons of lignin each year, most of which is burned in a recovery furnace facilitating the recovery of pulping chemicals and energy [10]. To date, the existing market for

lignin products remains limited (~2%) and focused primarily on low value products such as agents for dispersing, binding, and emulsion stabilization in the form of water soluble lignosulphonates [11-12]. Since lignin contains a large number of aliphatic and phenolic hydroxyl groups, researchers have applied lignin in the fields of phenolic resin, epoxy polymer, acrylics, and polyurethanes in the form of both original lignin and chemically modified lignin [13-15].

The purpose of this dissertation deals with the application of CNWs and lignin in novel biomaterials preparation. The incorporation of CNWs into rigid PU foam would have positive effect on the mechanical and thermal properties of the product as a result of the unique characteristics of CNWs and the chemical interactions between CNWs and the polymer matrix. Lignin is a promising polyol precurser for the preparation of rigid PU foam thanks to its large amount of hydroxyl groups as reactive sites as well as the wide availability, renewability, and biodegradability. Chapter 2 introduces the structure, properties and applications of cellulose, lignin and polyurethane with an emphasis on the application of cellulose nanowhisker and lignin in preparation of polyurethanes. Chapter 3 summarizes the materials, experimental procedures and analysis procedures used in the present thesis study. Chapter 4 reports a preliminary study of the reinforcing effect of CNWs up to 1.00 wt% on the mechanical and thermal properties of rigid polyurethane foams prepared from commercial chemicals and polymers. The reason that PU has been selected as the polymer matrix is that it has rapidly grown to be one of the most diverse and widely used materials with a continuously increasing global market. Moreover, there is a new trend of PU industry towards the biobased PU with better environmental compatibility and nanocomposite PU with enhanced properties.

Following this trend, Chapter 5 describes the application of softwood Kraft pine lignin in the synthesis of polyurethane. An oxypropylation reaction of Kraft pine lignin was performed to render the solid lignin into a liquid polyol. Then, a formulation optimization study was designed to determine the best formulation by using three types of polyols, namely lignin polyol, sucrose polyol, and glycerol polyol. The last two are the most common polyols currently used in the rigid PU industry. Based on this study, the preparation of ethanol organosolv lignin-based rigid polyurethane foam was described in Chapter 6. CNW was employed as the reinforcing filler in this study. The CNWs content has been increased to 5 wt% by directly mixing its aqueous suspension with polyols instead of using the DMF suspension of freeze dried CNWs dispersed in Chapter one.

The major objectives set in this dissertation are summarized as follows:

- Study the reinforcing effect of CNWs in preparation of rigid PU foam
- Investigate the application of Kraft lignin in preparation of rigid PU foam through oxypropylation
- Determine the optimal formulation for the best mechanical performance of the rigid PU foam by using three different polyols: lignin polyol, sucrose polyol, and glycerol polyol
- Explore the synergetic function of EOL and CNWs in view of the preparation of a biobased rigid PU foam.

CHAPTER 2

LITERATURE REVIEW[1]

2.1 Problem Statement

In recent times there has been a drive to utilize non-oil-based polymers due to a predicted diminishing supply of this feedstock for polymeric materials. Cellulose, being the most abundant polymer in nature, is a prime candidate for replacing several oil-based feedstocks.

Nanotechnology, defined as the manipulation of materials measuring 100 nm or less in at least one dimension, where the physical, chemical, or biological properties are fundamentally different from those of the bulk material, represents a major opportunity for wood and wood-based materials to improve their performance and functionality, develop new generations of products, and open new market segments in the coming decades [16]. The use of cellulose nanowhiskers derived from annually renewable resources as a reinforcing filler in polymeric matrix provides positive environmental benefits with respect to ultimate disposability, raw material use as well as strong mechanical properties. By comparing with inorganic fillers, the main advantages of cellulose nanowhiskers are [2]:

- Renewable nature

[1] The sections that regard to cellulose nanowhiskers and its applications in polyurethane were accepted for publication as a book chapter in Advances in Diverse Industrial Applications of Nanocomposites, 2011. It is entitled as "Cellulose Nano Whiskers as a Reinforcing Filler in Polyurethanes". The other author is Arthur J. Ragauskas from the Institute of Paper Science and Technology and School of Chemistry and Biochemistry at Georgia Institute of Technology.

- Wide availability
- Non-food agricultural based economy
- Low energy consumption
- Low cost
- Low density
- High specific strength and modulus
- High sound attenuation of lignocellulosic based composites
- Relatively reactive surface, which can be used for grafting specific groups
- Easier recycling by combustion of cellulose nanowhiskers filled composites

Polyurethanes, similar to other plastics, are widely used across a number of industries such as construction, electronics, and packaging, in the form of insulation, footwear, coatings, sealants, elastomers, and adhesives [17-18]. It has an ever-growing global market as shown in Figure 1. Recently, Global Industry Analysts, Inc. announces the release of a comprehensive global report on polyurethane foam market [19]. The global market for polyurethane foam is projected to reach 9.6 million tons by the year 2015, driven by resurgent demand from construction, furniture and bedding, and automotive markets. The need for low-cost and long-lasting materials and rising significance of energy efficiency in appliances and buildings is expected to foster growth in the foamed plastics market.

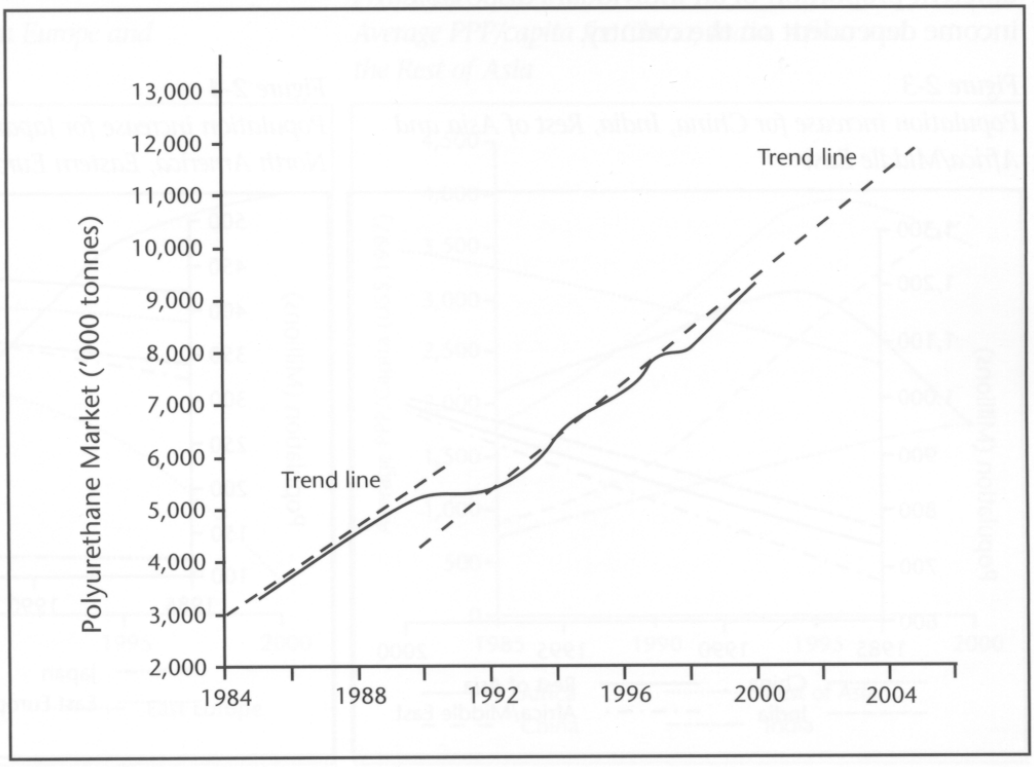

Figure 1. Volume growth of the global polyurethane market [20].

Polyols used for rigid polyurethane applications usually prepared from high functionality initiators such as sucrose and sorbitol. Those initiators have food value and require productive agricultural lands. Because of thesir high viscosity, carbohydrate initiated polyol is often added, e.g, glycerin or diethylene glycol which is derived from fossil fuels, as a co-initiator in order to lower the viscosity for easy handling and processing [21]. From the view of sustainable development, research focus has shifted toward polyol produced from lignocellulosic biomass. Lignin, as a by product of the paper making industry and modern biorefinery which is mainly burned as a low value fuel, is a promising candidate due to:

- Non-food agricultural based economy

- Large quantity
- Biodegradability
- High functionality of hydroxyl groups suitable for the preparation of rigid application polyol

In conclusions, the environmental issues, the diminishing fossil fuel reserves, the competition between food and industry, and the prosperous polyurethane foam market spurred the utilization of biobased polymers, namely cellulose, lignin and hemicelluloses. The application of cellulose nanowhiskers and lignin in preparation of rigid polyurethane nanocomposites foam is a response to the above mentioned demands and is fully studied in the present research.

2.2 Lignocellulose

Lignocellulosic biomass is composed of three major constituents: cellulose, hemicelluloses and lignin (Figure 2), as well as smaller amounts of pectin, protein, extractives and ash, which together form a complex and rigid structure [22-23]. Table 1 summarizes the distribution of the three major biopolymers in several hardwoods, softwoods and agricultural residue species [24].

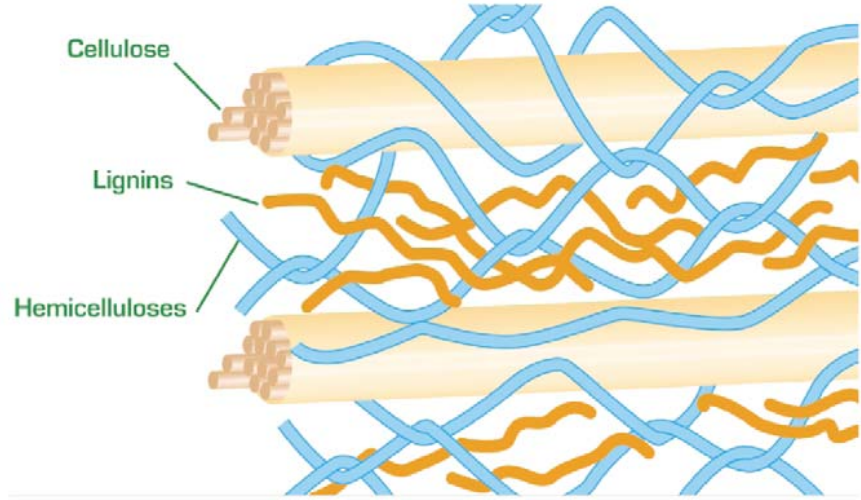

Figure 2. Schematic representation of the secondary cell wall containing cellulose, hemicelluloses and lignin [25].

Table 1. Cell wall macromolecule composition of different softwoods, hardwoods and agricultural residue species [24, 26].

	Wood Macromolecules[a]		
Wood Species	**Cellulose (%)**	**Lignin (%)**	**Hemicelluloses (%)**
Softwoods			
Picea glauca	41	27	31
Abies balsamea	42	29	27
Pinus strobes	41	29	27
Tsuga canadensis	41	33	23
Norway spruce	46	28	25
Loblolly pine	39	31	25
Thuja occidentalis	41	31	26
Hardwoods			
Eucalyptus globulus	45	19	35
Acer rubrum	45	24	29
Ulmus americana	51	24	23
Populus tremuloides	48	21	27
Betula papyrifera	42	19	38
Fagus grandifolia	45	22	29
Agricultural residues			
Corn stover	40	25	17
Wheat straw	30	50	20
Switchgrass	45	30	12

[a]All samples were analyzed extractives free.

Cell wall in biomass is composed mainly of middle lamella (ML) [27], primary

cell wall (P), and secondary cell wall (S) (Figure 3) [28]. ML is an amorphous intercellular region, containing mostly lignin that glues the fibers together. The primary cell wall is a thin layer (0.1–1 μm) contains a loose, random network of cellulose microfibrils embedded in a matrix that consists of amorphous pectins and hemicelluloses lacking structural orientation [29]. The secondary cell wall is thicker than the primary wall (10–20 μm) and is divided into three sublayers due to differences in the microfibrillar orientation. These layers are: the outer layer of the secondary wall (S1), the middle layer of the secondary wall (S2), and the inner layer of the secondary wall (S3). The S1 layer contains fibrils that are arranged in a cross-hatch pattern; the S2 layer accounts for a major part of the cell wall volume and is composed of parallel fibrillar units oriented at a slight angle to the cell axis; the S3 contains parallel fibrillar units forming a flat helix in the transverse direction [29].

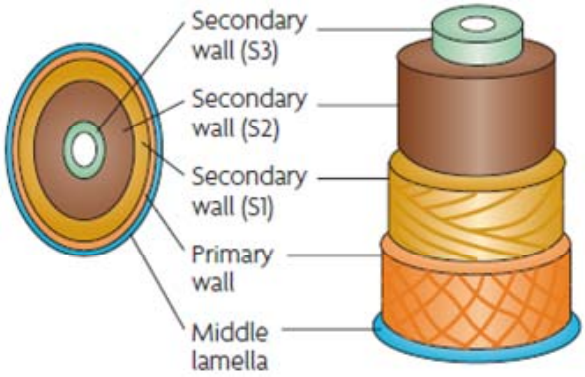

Figure 3. Schematic representation of plant cell [28].

2.3 Cellulose

2.3.1 Cellulose Structure and Properties

Cellulose was first discovered by the French scientist Anselme Payen in 1838, when he noticed a resistant fibrous solid that remained behind after treating plant tissue with acids and ammonia. Cellulose is a polydispersed linear polymer of *β*-(1,4)-D-glucose [1]. A cellulose fiber is composed of bundles of microfibrils where the cellulose chains are stabilized laterally by inter- and intra-molecular hydrogen bonding (Figure 4) [30]. Microfibrils are comprised of elementary fibrils where monocrystalline domains are linked by amorphous domains. Generally, monocrystalline cellulose has been reported with length ranges from 100 to 300 nm and diameter between 5 and 20 nm. In other words, cellulose monocrystalline has a high aspect ratio of 20-60 [5, 31-34]. Table 2 summarizes the degree of crystallinity and the lateral dimension of elementary fibrils from several cellulose samples measured by X-ray diffraction (XRD). The tensile strength and modulus of the perfect native cellulose crystallites are approximately 10 GPa and 150 GPa, respectively [16]. It could compete in equal or better conditions with other engineering materials (Table 3), and it is possible to consider that this can be used in high-end technological applications.

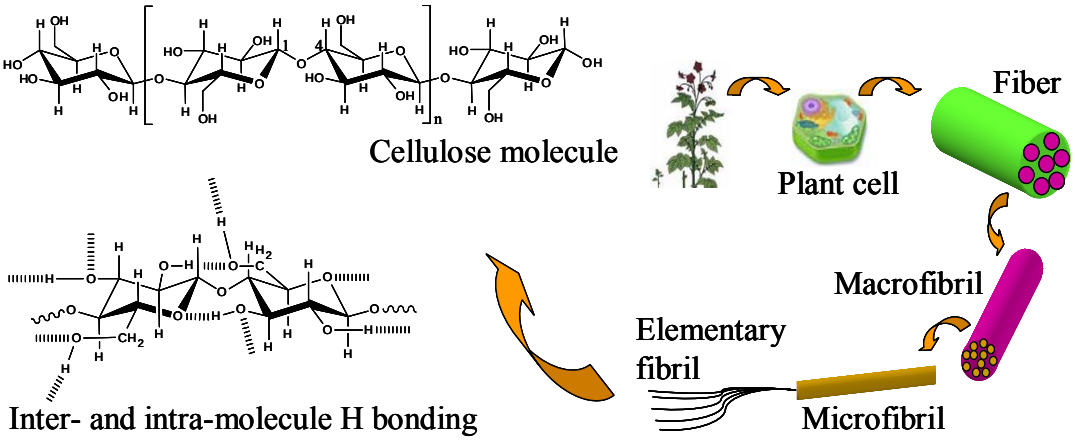

Figure 4. Schematic representation of cellulose fiber.

Table 2. Degree of crystallinity and lateral dimension of elementary fibrils from several cellulose samples [35-39].

Sample	Crystallinity, %	Lateral dimension, nm
Natural softwood/hardwood cellulose	60-62	3-4
Isolated sulfite spruce cellulose	62-63	5-6
Isolated Kraft spruce cellulose	64-65	6-7
Natural cotton cellulose	68-69	5-6
Isolated cotton cellulose	70-72	7-8
Natural flax or ramie cellulose	65-66	4-5
Isolated flax or ramie cellulose	67-68	6-7
Bacterial cellulose	75-80	7-8
Algae cellulose	75-80	10-15

Table 3. Strength and stiffness of several reinforcing materials [40].

Material	Tensile strength (GPa)	Tensile modulus (GPa)
Cellulose nanocrystals	7.5	150
Glass fiber	4.8	86
Steel wire	4.1	207
Kevlar	3.8	130
Graphite whiskers	21	410
Carbon nanotubes	11-73	270-970

2.3.1.2 Polymorphs of Cellulose

Cellulose displays six different polymorphs, namely I, II, III_I, III_{II}, IV_I, and IV_{II} with the possibility of conversion from one form to another (Figure 5). Native cellulose in plants is a composite of three crystalline allomorphs: cellulose Iα, cellulose Iβ, and paracrystalline cellulose; and the noncrystalline form amorphous cellulose at accessible and inaccessible fibril surface [41-44]. Accessible fibril surfaces are those in contact with water, while the inaccessible fibril surfaces are fibril-fibril contact surfaces and surfaces resulting from distortions in the fibril interior [45] (Figure 6).

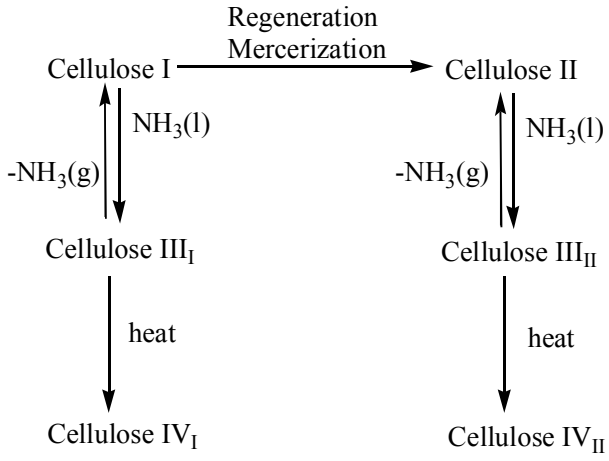

Figure 5. Interconversion of the polymorphs of cellulose.

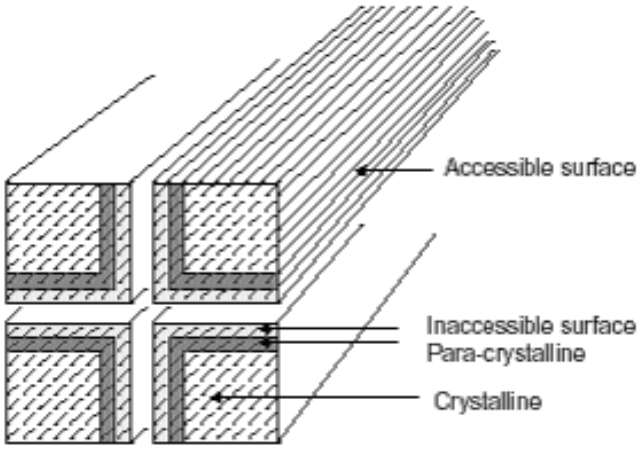

Figure 6. A proposed representation of the fibril structure [46].

Cellulose Iα, a one chain triclinic unit cell, is the dominant form in bacterial and algal cellulose, whereas cellulose Iβ, a monoclinic two-chain unit cell, is dominant in higher plants, such as wood [44]. Cellulose Iα is meta-stable in nature and can be converted to the thermodynamically more stable allomorph (cellulose Iβ) by annealing [44, 47]. Nishiyama *et al*. proposed that slippage of the glucan chains is the most likely mechanism for conversion of cellulose Iα to cellulose Iβ [47]. Both chains in cellulose

Iα and Iβ are organized in sheets packed in a parallel-up fashion, with the hydroxymethyl groups in the *tg* conformation. Paracrystalline cellulose is the form that is less ordered than cellulose Iα and cellulose Iβ but more ordered than the amorphous cellulose. The presence of disordered phases was supported by experimental results from solid-state cross polarization/magic angle spinning (CP/MAS) ^{13}C NMR, tensile tests of cellulose fibers, and wide-angle (WAXS) and small-angle X-ray scattering (SAXS). The estimation of the phases composition of native cellulose is possible using different techniques such as FT-IR, ^{13}C NMR, and synchrotronradiated X-ray diffraction. CP/MAS ^{13}C NMR spectroscopy is a technique that has been used to determine the relative intensities of these various cellulose structures as well as cellulose crystallinity. Table 4 summarizes the cellulose crystallinity and ultrastructure from several biomass determined by CP/MAS ^{13}C NMR spectroscopy [48].

Table 4. Cellulose crystallinity and ultrastructure from several biomass determined by CP/MAS ^{13}C NMR spectroscopy [48].

Origin	Crystallinity (%)	Iα	Iα+β	*para*-Crystalline	Iβ	Accessible fibril surfaces	Inaccessible fibril surfaces
Hybrid poplar[a]	63	5.0	14.2	31.1	19.8	10.2	18.3
Loblolly pine[b]	63	0.1	30.7	24.8	6.9	33.1	15.6
Alamo switchgrass[b]	44	2.3	8.8	27.3	4.5	5.7	51.3

[a]Cellulose was isolated from holocellulose by HCl hydrolysis which was isolated from the extracted samples by exposure to $NaClO_2$ and acetic acid. [b]Cellulose was isolated by two-step dilute acid pretreatment.

2.3.1.3 Hydrogen Bonding of Cellulose Molecules

Cellulose are composed of 1,4-linked β-D-glucose chains in $^4C_1$ chair

conformation. The ultrastructure of cellulose is largely due to the presence of covalent bonds, hydrogen bonds and van der Waals forces. Interchain hydrogen bonds are existing in addition to hydrogen bonding within the cellulose chains and might introduce order or disorder into the system, depending on its regularity [49].

When considering hydrogen bonding, it is essential to note the conformation of the C(6) hydroxymethyl group. There are three possible minimum energy orientations for this substituent to the pyranose ring; *trans-gauche* (*tg*), *gauche-trans* (*gt*) and *gauche-gauche* (*gg*), as illustrated in Figure 7 [50]. The reason for the difference in stability between these three staggered conformers is the relative proximity of the oxygen and carbon substituents. X-ray diffraction study of oriented cellulose fibrous samples prepared by aligning cellulose microcrystals from tunicin and freshwater alga showed a *tg* orientation in cellulose I [47, 51]. For cellulose II, both regenerated [52] and mercerized [53] forms were reported to have a *gt* conformation throughout the cellulose chain at the corner of the unit cell, but a *tg* arrangement for the centre chain. However, some rotation about the suggested minimum orientations (*tg*, *gt* and *gg*) was accepted as being possible [49]. The majority view, expressed in the literature, is that cellulose I has a *tg* conformation and cellulose II has a *gt* conformation throughout the chains [54-55].

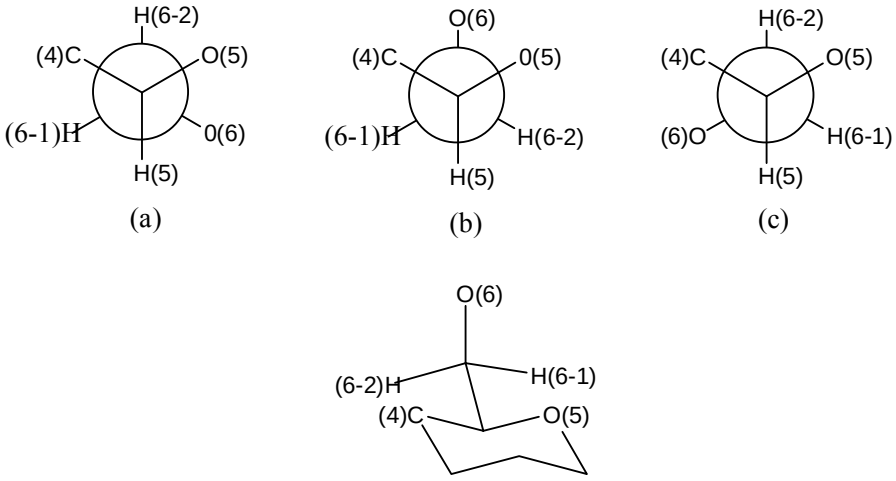

Figure 7. Three most probable rotational positions of the hydroxymethyl group: (a)*gt*, (b)*gg*, (c)*tg*.

Derived from the study of hydroxymethyl orientations, intra- and inter-molecular hydrogen bond patterns were suggested for cellulose I and II. The former has two intramolecular hydrogen bonds at (O)5-(OH)3 and (OH)2-(O)6 and an interchain hydrogen bond between (O)6-(O)3 as shown in Figure 8 [56-59]. Cellulose II is reported as having intrachain hydrogen bonding at (OH)3-(O)5 and an intermolecular hydrogen bond at (OH)6-(O)2 for corner chains and (OH)6-(O)3 for centre chains. An extra dimension was also added to the hydrogen bonding in cellulose II over cellulose I, in the form of an inter-sheet interaction between (OH)2 (corner chain) - (O)2 (centre chain), absent in native cellulose.

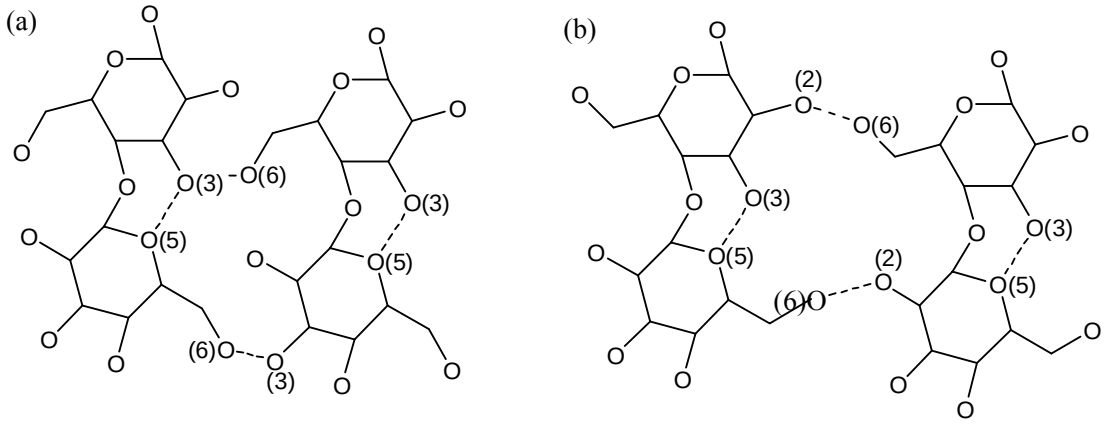

Figure 8. Hydrogen bonding pattern for (a) cellulose I and (b) cellulose II.

Differences in the hydrogen bonding patterns reported for models of cellulose I and II are not solely derived from deviations in hydroxymethyl conformation but also from the fact that the polarity of the chains are thought to differ; a parallel arrangement [60] is attributed to cellulose I and an antiparallel arrangement is attributed to cellulose II.

A further consideration, in view of recent evidence, is the conformation which exists in each of the native cellulose polymorphs Iα and Iβ. Molecular dynamics simulations carried out by Heiner et al. [61] indicate that the Iα has a *tg* hydroxy-methyl conformation in more than 90% of cases. For the Iβ polymorph, 81.0% of hydroxymethyl groups were found to be *tg*. In each situation the remainder of the percentage is represented by a mixture of the *gg* and *gt* conformations. This agrees with carbon NMR studies carried out by Yamamoto and Horii [62].

Cellulose III_I has intramolecular hydrogen bonds between (OH)3-(O)5 and (O)2-(OH)6 and intermolecular associations between (O)3-(O)6 as in cellulose I [49]. For celluloses IV_I and IV_{II}, in addition to the usual two intramolecular hydrogen bonds present in most of other crystalline celluloses, both polymorphs seem to be well established by the intermolecular hydrogen bonding along the plane that is parallel to all

the cellulose chains [49].

2.3.1.4 Cellulose Degree of Polymerization

2.3.1.4.1 Definition of Degree of Polymerization and Common Measurement Techniques

Degree of polymerization (DP) can be defined in terms of the number-average DP (DP_N), weight-average DP (DP_W), or viscosity-average DP (DP_V), according to the following equations [63]:

$$DP_N = \frac{M_n}{MW_{glu}} = \frac{\sum N_i M_i}{\sum N_i} / MW_{glu}$$

$$DP_W = \frac{Mw}{MW_{glu}} = \frac{\sum N_i M_i^2}{\sum N_i} / MW_{glu}$$

$$DP_V = \frac{M_V}{MW_{glu}} = \frac{\sum N_i \eta}{\sum N_i} / MW_{glu} \text{ , where } \eta = K_m M_i^{\alpha+1}$$

where N_i is the number of moles of a given fraction i having molar mass M_i, M_N is the number-average molecular weight, M_W is the weight average molecular weight, M_V is the viscosity-average molecular weight, MW_{glu} is the molecular weight of anhydroglucose (162 g/mol), η is viscosity, K_m is a constant, and the value of α for cellulose and cellulose derivatives in most cases ranges from 0.75 – 1 [63].

The two most commonly used techniques to measure the DP of cellulose are the viscometry and the gel-permeation chromatography (GPC) methods. Viscometry measurements are relatively quick and convenient and are used to measure the DP_V of cellulose [64]. However, it has three limitations: 1) it provides only M_V, which is not an absolute average since it depends of the solvent/temperature conditions, 2) it provides no

information concerning the molar mass distribution (MMD), and 3) the complex metal solutions used along with the method can degrade cellulose [64]. On the other hand, GPC provides DP_n, DP_w, all three molecular weights (M_N, M_W, and M_V), as well as the MMD. Similar to viscometry, GPC does not give the absolute molar mass because it is calculated based on the molecular weight of a set of standards which is frequently a set of well defined polystyrene standards with varying molecular weights.

2.3.1.4.2 Determination of Cellulose Degree of Polymerization

The determination of the DP of cellulose begins with its dissolution. The two most practiced techniques are: 1) dissolving cellulose in metal complex solutions, and 2) forming cellulose derivatives by nitration or tricarbanilation. These solutions have been used for measuring the DP of cellulose either viscosimetrically or by using GPC [65-66]; however, the metal complex solutions have been frequently used with the viscosimetric technique [67-74].

Measuring the DP of cellulose viscometrically after nitration was a technique developed in the 1940s, in which extractive-free wood meal is treated in a mixture of nitric acid, phosphoric acid, and phosphorous pentoxide, resulting in the isolation of cellulose nitrates, which is then solubilized in either acetone or ethyl acetate [75-77]. In the 1950s, Timell extensively investigated this technique and determined the DP of several native wood celluloses [76-78]. A list of the DP of cellulose determined by nitration followed by measurement of viscosity is provided in [75-79]. An advantage of this method is that it does not require pre-isolation of cellulose through the holocellulose pulping and the base-catalyzed hydrolysis of the hemicellulose. The DP values ranged from ~925 – 5500. Table 5 shows that agricultural residues, such as bagasse and wheat straw, have lower

cellulose DP (~1000) than hardwoods and softwoods, which possess higher DP cellulose in the range of 4000 – 5500. Today the nitration methodology is rarely used due, in part, to the uncertainty arising from possible acid hydrolysis of the cellulose chain during derivatization as well as the instability of the derivative [65].

Table 5. DP of native wood and non-woody celluloses after nitration using the viscometric method [75-79].

Species	DP
Trembling aspen	5000
Beech	4050
Red maple	4450
Eastern white cedar	4250
Eastern hemlock	3900
Jack pine	5000
Tamarack	4350
White spruce	4000
Balsam fir	4400
White birch	5500
Eucalyptus regnans	1510
Pinus radiata	3063
Bagasse	925
Wheat straw	1045

Cellulose tricarbanilate (CTC) is another cellulose derivative for DP measurement, which is usually done by GPC [65, 73, 80]. CTC is the most utilized derivative for GPC studies due to following advantages: 1) complete substitution, 2) no depolymerization occurs during derivatization, 3) stability of the derivative, and 4) solubility and stability in THF [65]. Cellulose tricarbanilation is commonly performed by reaction of cellulose with phenyl isocyanate in either dimethylsulfoxide (DMSO) or pyridine as the solvents. However, it has been shown that cellulose oxidation and degradation occur during derivatization of cellulose in the presence of DMSO but not in pyridine [80]. Therefore, pyridine is most commonly used solvent for the derivatization, since it is important not to

detrimentally affect its chain length during the isolation and preparation of samples.

DP values of several native woody and non-woody cellulose samples are listed in Table 6 [67, 70-71, 74, 81]. It appears from the data in Table 6 that viscometry is more popular in determining DP of cellulose in lignocellulosic biomass. In fact, Kumar *et al*., stated that the viscometry technique is more adequate to analyze cellulose DP, given the complexity of lignocellulosic biomass [67]. The cellulose DP range is ~1500 – 4500. Hardwoods, such as poplar and aspen, have a cellulose DP of 3500 and 4500, respectively. Sweet *et al.* reported a DP of 1450 for southern pine, which is significantly less than the DP values reported for hardwoods [81]. Agricultural residues varied over a range of 1800 – 4000. Cellulose in jute fiber has a large DP value when compared to corn kernels, cotton stalks, wheat straw, and rice straw. DP of Nalita cellulose increased from ~3200 to 3600 as the tree became older (12 months to 30 months), suggesting that cellulose DP increases as the tree develops [71]. Nalita is a common name to *Trema orientalis*, a fast-growing shade tree with soft foliage, found in warm and wet regions of southern Africa and Asia [82].

Table 6. DP of native wood and non-woody celluloses [67, 70-71, 74, 81]

Species	Measurement Technique	DP
Southern Pine	GPC	1450
DDGS	Viscometry	2243
Corn kernels	Viscometry	1693
Dhaincha	Viscometry	2520
Cotton stalks	Viscometry	1820
Jute fiber	Viscometry	3875
Wheat straw	Viscometry	2660
Rice straw	Viscometry	1820
Corn stover	Viscometry	2520
Poplar	Viscometry	3500
Aspen	Viscometry	4581
Nalita (12 months)	Viscometry	3181
Nalita (18 months)	Viscometry	3383
Nalita (24 months)	Viscometry	3518
Nalita (30 months)	Viscometry	3611

[a]Cellulose tricarbanilate, [b]Viscometry technique gives DP_v

2.3.2 Cellulose Nanowhiskers

2.3.2.1 Preparation

Cellulose nanowhisker, is defined by Eichhorn as a fibrous form of cellulose produced by the acid hydrolysis of plant (or animal or bacterial) based cellulose, with lateral dimensions ranging from 3–30 nm [83]. There are many other names used to describe cellulose nanowhiskers, such as cellulose nanocrystals, cellulose nanofibres and cellulose whiskers, which are not going to be used here. During the past twenty years, research on CNWs has been extensively developed. Softwood (SW) Kraft pulp [9, 84-86], SW sulfite pulp [87], hardwood (HW) elemental chlorine free (ECF) pulp [87], recycle pulp [88], cotton fiber [84, 89-96], sisal fiber [95, 97], flax fiber [4], ramie fiber [98-100], wheat straw [31], bamboo residue [101], bacterial microfibrils [39], grass fiber [102], tunicate cellulose [3, 95, 98, 103-106], and microcrystalline cellulose (MCC) [5, 107-111] have all been utilized as sources for CNWs preparation. CNWs dimension

depends on both the origin of cellulose and reaction conditions employed. In general, wood and cotton CNWs have a smaller length and cross section compared to those derived from tunicate, bacterial and algae [39, 87, 112-113], which is in agreement the lateral dimension of their corresponding elementary fibrils. CNWs exhibit not only a high elastic modulus of 143 GPa [3], but also show significant changes in electrical, optical, and magnetic properties in comparison to native cellulosic fibers [2]. Therefore, there is a growing research interest in CNWs reinforced composites, and improvements in mechanical and thermal properties of the resulting materials are readily achieved [4-9, 33, 107, 114-115].

Under certain acid hydrolysis conditions, transverse cleavage of the cellulose fibers happens primarily in the amorphous zone and releases needle-like cellulose nanowhiskers. The most common CNWs preparation method is acid hydrolysis, including sulfuric acid and hydrochloric acid. Other methods, such as enzymatic hydrolysis and mechanical disintegration have also been used [88, 116].

2.3.2.1.1 Sulfuric Acid Hydrolysis

Cellulose fibers are usually disintegrated by a Wiley mill into a small size before hydrolysis. Sulfuric acid concentrations of 60-70% (w/w), more often 64% [84], are preferred. Acid treatment can range from 10 min at 70˚C to 3 h at 45˚C at selected acid to cellulose ratios which depends on the type of cellulose fibers. The reaction is typically quenched by diluting with a 10 fold addition of deionized (DI) water. The sediment, CNWs, is collected and neutralized by repeated centrifugation and prolonged dialysis against DI water until the pH of the CNWs suspension does not change. For specific investigation and/or application purposes, all ions except H^+ associated with

sulfate groups on the surface of H_2SO_4 generated CNWs need to be removed. This can be achieved by treating the CNWs suspension with a mixed bed ion exchange resin and filtering through a 0.45 μm membrane [89]. Finally, ultrasonic treatment is necessary to well separate CNWs, where a plastic reaction flask is preferred to avoid the release of ions from the glass container and the solution needs to be chilled to avoid overheating which could cause desulfation [90]. A comprehensive compilation of preparation conditions employing sulfuric acid and the average dimensions of CNWs derived from different sources is summarized in Table 7.

Table 7. Dimensions of CNWs prepared under different sulfuric acid hydrolysis conditions [4, 31, 84-87, 89-90, 92-93, 97, 103, 108-111].

Cellulose sources	H_2SO_4 conc., (%, w/w)	Time, min	Temperature, ˚C	Acid/cellulose, mL/g	Dimension, nm
SW pulp	64	10	70	8.75	~ 200 × 5
	60	50	< 70	8.75	~ 200 × 5
	65	10	70	10	185 ± 75 × ~ 3.5
	65	60	45	8.75	185 ± 75 × ~ 3.5
	64	45	45	17.5	100-250 × 5-15
HW pulp	64	25	45	8.75	147 ± 7 × 3-5
	64	25	45	8.75	141 ± 6 × 5.0 ± 0.3
	64	45	45	8.75	120 ± 5 × 4.9 ± 0.3
	64	45	45	17.5	105 ± 4 × 4.5 ± 0.3
Cotton	64	120	45	8.75	~ 200 × 5
	64	60	45	8.75	115 ± 10 × ~ 7
	64	45	45	17.5	176 ± 21 × 13 ± 3
	64	120	60	8.33	70-150 × 10-20
	65	60	45	8.75	100-150 × 5-10
Sisal	65	15	60	16.2	~ 250 × 4
Flax	64	240	45	8.33	327 ± 108 × 21 ± 7
Wheat straw	65	60	25	34.3	150-300 × ~ 5
MCC	63.5	130.3	44	10	200-400 × <10
	64	300	45	8.75	41-320 × < 100
	64	180	45	17.5	60-120 × 8-10
	64	-	45	8.75	100-225 × 10-15

The effects of sulfuric acid hydrolysis temperature, time, and ultrasonic treatment duration on the properties of CNWs were investigated thoroughly by other researchers [90]. The experimental setup is summarized in Table 8. It was shown that with 64% (w/w) sulfuric acid, and at an acid to microcrystalline cellulose ratio of 8.75 mL/g and 25˚C, 18 h was required to generate CNWs. At 65˚C, hydrolysis of cellulose was so fast that a yellow color appeared at the first 10 min, and the sample became black after 1 hour. Side reactions, e.g., dehydration, were presumed to occur under this condition. A temperature of 45˚C was proposed to be optimal and could lead to an efficient hydrolysis yielding an ivory-white colored suspension with a reported yield of 44% after 1 hour. The sulfur content and surface charge of CNWs gradually increased when increasing the hydrolysis reaction time from 10 to 240 min at 45˚C. The CNWs size decreased in the early stage of the hydrolysis and a relatively stable dimension was achieved after 1 hour as summarized in Table 9. The appearance of the CNWs suspension could be white with some starting pulp particles (low yield), ivory white viscous suspension (optimal), yellowish or even black viscous suspension (over hydrolyzed) [90]. The particle size decreased within the first 5 min of ultrasonic treatment but no further change was observed upon extended treatment, while the surface charge of CNWs remained constant [90]. Table 10 shows the effect of ultrasonic treatment on the CNWs dimensions. Similar results were obtained with MCC prepared from Norway spruce sulfite pulp [108]. Briefly, the optimal condition was determined to be sulfuric acid concentration of 63.5% (w/w), acid to cellulose ratio of 10 mL g^{-1}, and 130 min hydrolysis at 44˚C followed by approximately 30 min ultrasonic treatment, which produced CNWs of 200 to 400 nm in length and less than 10 nm in width and a yield of 30% of the initial weight.

Table 8. Effect of sulfuric acid hydrolysis condition on the appearance of CNWs suspension and the yield of CNWs [90].

Sample	T, ˚C.	Time, h	Appearance of the suspension	Yield, % (w/v)
1	25	1	White, with pulp particles	89.8
2	25	18	Ivory white, viscous	34.4
3	45	1	Ivory white, viscous	43.5
4	65	0.25	Yellow, very viscous	48.1
5	65	1	Black	N/A

Table 9. Effect of sulfuric acid hydrolysis time at 45˚C on the sulfur content and length of CNWs [90].

Sample	Hydrolysis time, min	Sulfur content, %	CNWs length, nm
1	10	0.53	390
2	20	0.50	332
3	30	0.58	276
4	45	0.62	226
5	60	0.69	197
6	120	0.74	179
7	240	0.75	177

Table 10. Effect of ultrasonic treatment on the length and surface charge of CNWs [90].

Treatment time, min	CNWs length, nm	Surface charge as S %
1	214	0.484
2	205	0.487
5	182	0.482
10	183	0.489
20	176	0.507
40	182	0.503

The same study was performed on black spruce sulfite pulp and bleached eucalyptus Kraft pulp treated with 64% (w/w) sulfuric acid at 45˚C [87]. Longer hydrolysis time and higher acid to cellulose ratio produced shorter, less polydispersed CNWs. Compared to MCC, cellulose fiber requires less time to produce CNWs of similar size. The same type of cellulose fibers used in various literature researches are usually of enormous size difference yet the same size cellulose nanowhiskers are

achieved [4, 31, 84-87, 89-90, 92-93, 97, 103, 108-111]. It implies that the original dimension of cellulose fibers will only affect the treatment conditions to obtained cellulose nanowhiskers while the size of cellulose nanowhiskers is only determined by the origin of cellulose fibers, more specifically, the structure of cellulose fibers.

2.3.2.1.2 Hydrochloric Acid Hydrolysis

With regards to the hydrochloric acid hydrolysis, cellulose fibers are usually treated with 4 N HCl at 80˚C for approximately 4 h at an acid to cellulose ratio of 30-35 mL/g. Centrifugation, dialysis against DI water, and ultrasonic treatment are followed at the same conditions as used for CNWs preparation with sulfuric acid. The overall mass yield of HCl-CNWs is 10-20% and the pH value of its suspension is ~6, while the yield of H_2SO_4-CNWs is 70-75% and the pH of H_2SO_4-CNWs levels off at 2-3 due to the sulfate groups [86, 91]. HCl-CNWs of SW Kraft pulp were reported to be approximately 180 nm in length and 3.5 nm in width, while the cotton yielded HCl-CNWs were around 100 nm in length and 5-10 nm in width [85-86, 91].

2.3.2.1.3 Comparison between Sulfuric Acid and Hydrochloric Acid Hydrolyzed CNWs

Compared to the hydrochloric acid procedure, sulfuric acid hydrolysis employs lower temperature, lower acid to cellulose ratio, and less time to produce CNWs of similar dimensions as shown in Table 11. Moreover, H_2SO_4-CNWs suspension is more stable due to the static repulsion between negatively charged sulfates compared to the easily aggregated HCl-CNWs and it was the same reason given for the time independence of viscosity of the H_2SO_4-CNWs suspension [16]. In order to investigate the influence of sulfate groups on the viscosity properties of the CNWs suspension, Araki

et al. [85, 91] introduced sulfate groups to HCl-CNWs by postsulfonation. Briefly, HCl-CNWs precipitated after centrifugation were mixed with 65% (w/w) sulfuric acid to yield a final acid concentration of 55% (w/w) and reacted in a water bath at 40˚C or 60˚C for 2 h, which was then quenched by adding large amounts of cold water. The number of sulfate groups was controlled by changing experimental factors, such as time and temperature. For example, treatment of an HCl-CNWs suspension with equal weight amount of concentrated sulfuric acid at 60˚C overnight resulted in a sulfate content of 38 mmol kg^{-1}, which was much lower than that of H_2SO_4-CNWs (140 mmol kg^{-1}) [91]. An increase of sulfate groups was observed when the postsulfonation reaction was conducted at 40˚C for 2 h [85]. A high concentration aqueous suspension of CNWs with a low content of sulfate groups showed a slight viscosity increase with time, though it was not as significant as HCl-CNWs. However, the suspension of HCl-CNWs treated with sulfuric acid at 40˚C had nearly the same level of viscosity properties as a H_2SO_4-CNWs suspension. The viscosity was also found to be strongly affected with a surface charge content that ranges between 50 mmol kg^{-1} and 60 mmol kg^{-1}. In summary, although the microscopic size and shape of CNWs could be the same irrespective of preparation method, the introduction of the surface charge drastically reduced the viscosity of its suspension and removed its time dependency.

Table 11. Comparion of acid (sulfuric acid and hydrochloric acid) hydrolysis conditions to prepared CNWs of similar dimensions [85].

Acid	Acid/cellulose, ml/g	Time, min	T, ºC	CNWs dimension, nm
H_2SO_4, 65%(w/w)	8.75	60	45	185 ± 75 × ~3.5
HCl, 4 N	30	225	80	180 ± 80 × 3.5 ± 0.5

2.3.2.1.4 Enzymatic Hydrolysis

Cellulases are composites of endoglucanases, exoglucanases and cellobiohydrolases. These enzymes act synergistically in the hydrolysis of cellulose. Endoglucanase randomly attacks and hydrolyzes the amorphous region whilst exoglucanase attacks the cellulose polymer chain from either the reducing or non-reducing ends [117]. Cellobiohydrolases hydrolyze cellulose from either the C1 or the C4 ends using a protein in each case, into cellobiose units [117]. Since CNWs are produced from the crystalline region of the cellulose fiber, the selectivity of enduglucanase enzyme to hydrolyze the amorphous regions leaving the crystalline CNWs was studied by Filson et al.[88]. The highest yield of CNWs was obtained by treatment with 84 EGU of endoglucannase per 200 mg recycled pulp at 50˚C for 60 min assisted by microwave or conventional heating. Microwave treatment of the recycled pulp was reported to give a higher yield than conventional heating. Endoglucanase hydrolyzed CNWs were found to have a relatively larger size than acid hydrolyzed CNWs, typically 30 to 80 nm in width and 100 nm to 1.8 μm in length.

2.3.2.1.5 Mechanical Disintegration

In addition, a chemical swelling/ultrasonic separation method was also used to prepare wood-based CNWs [116]. MCC (10 wt%) was dissolved in a swelling solution of dimethylacetamide (DMAc) with 0.5 wt% of LiCl and treated at 70˚C for 12 h with stirring. The slightly swollen particles were further separated in an ultrasonic bath for 3 h over a period of 5 days with long intervals. The CNWs were estimated to be less than 10 nm in width and 200 to 400 nm in length.

2.3.2.2 Chemistry Involved in Acid Hydrolysis of Cellulose

2.3.2.2.1 Chemistry of Acid Hydrolysis of Cellulose

The hydrolysis of cellulose begins with the reaction of acidic proton and oxygen that bonds two glucose units, forming corresponding conjugated acid. Then, a cleavage of the C-O bond occurs, and a cyclic carbocation is formed [118]. In the next step, after a rapid addition of water, a hydrolyzed cellulose molecule is formed, and a proton is released. In the first step, protonation has two pathways, the dominant one is at O1 and the other one is at O5. An illustration of the acid hydrolysis mechanism is shown in Figure 9.

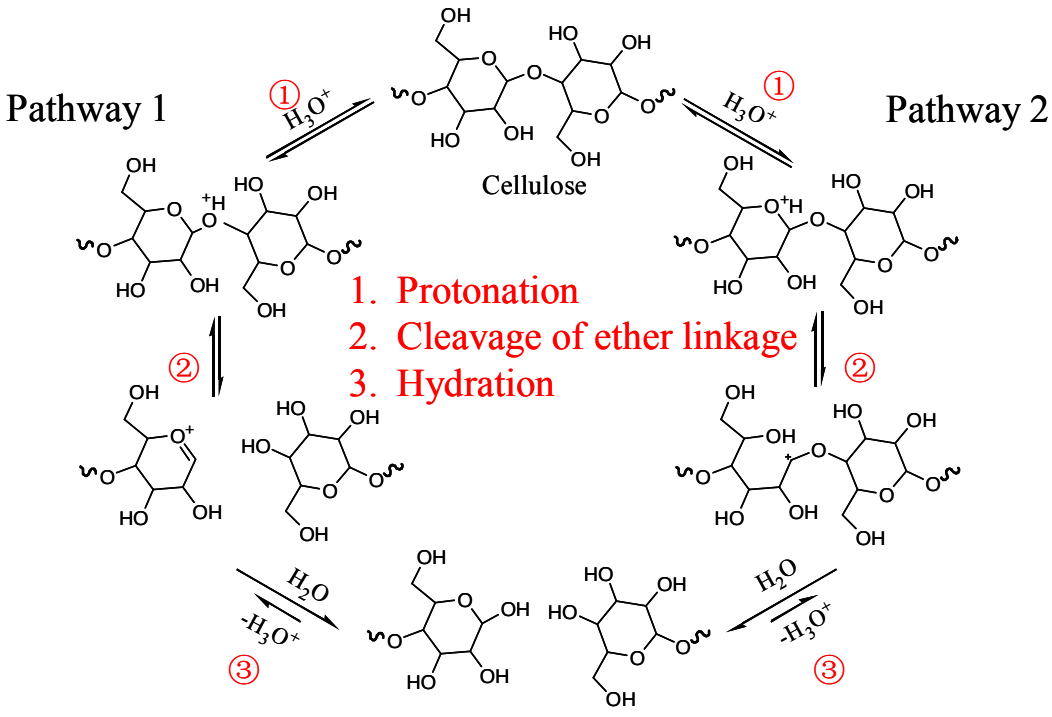

Figure 9. Illustration of the acid hydrolysis mechanism [118].

2.3.2.2.2 Sulfation of Cellulose during Sulfuric Acid Hydrolysis

During sulfuric acid hydrolysis, the sulfation of cellulose to form cellulose sulfate is an example of a typical sulfation reaction (Figure 10). It introduces negative charges to the CNWs and the static repulsion improves the stability of CNWs suspension. The sulfation reaction of the primary and secondary hydroxyl groups of cellulose doesn't basically differ from that of other alcohols. The peculiarities lie in the macromolecular structure of the cellulose molecule. The splitting of the molecule chain competes with the catalyzed esterification, but can be fairly controlled under appropriate conditions [119]. The mechanism of the sulfation reaction of cellulose molecule is shown in Figure 11, where the hydrogen sulfate ion, HSO_3^- is the sulfating species [120]. First of all, one proton of the sulfuric acid molecule transfers to the hydroxyl oxygen of another sulfuric acid molecule, leaving a sulfate ion. Then, the oxygen of the primary and/or secondary hydroxyl groups of cellulose molecules is protonated. In the last step, the sulfate ion attacks the carbon connected to the protonated hydroxyl oxygen and a water molecule is lost forming a cellulose ester.

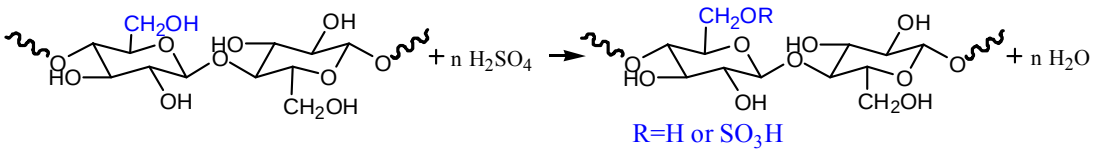

Figure 10. Illustration of the sulfation of cellulose hydroxyl groups during sulfuric acid hydrolysis.

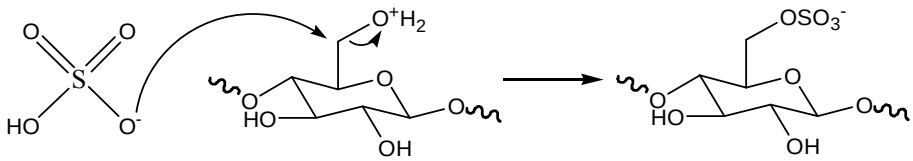

Figure 11. Mechanism of the sulfation of cellulose hydroxyl groups during sulfuric acid hydrolysis [120].

2.3.2.2.3 Determination of the Sulfur Content of Sulfuric Acid Generated CNWs

The sulfate content of CNWs can be determined by a conductimetric method described elsewhere [86]. Briefly, a CNWs suspension (~0.01 g mL^{-1}, 45 mL) is mixed with a NaCl solution (0.01 M, 5 mL) before measurement. For samples with poor or no sulfonation, 3 mL of water is replaced by 0.01 M HCl in order to obtain a preferred value. An alkaline solution (0.1 N NaOH) is then added to the suspension at a rate of 0.5 mL per 5 min with continuous stirring. The change in conductivity is recorded by an electric conductometer. Theoretically, the two branches of the titration curve should intercept the volume axis at the same value which is the equivalence-point volume as shown in Figure 12(a). However, in some cases, the abscissa intercepts due to the dissociation of cellulosic carboxylic acid groups after the stronger sulfate groups have been neutralized [121]. The actual equivalence-point volume is then determined as the average of the two volumes as shown in Figure 12(b). The degree of sulfonation relies highly on the acid to cellulose ratio and the reaction time as shown in Table 12.

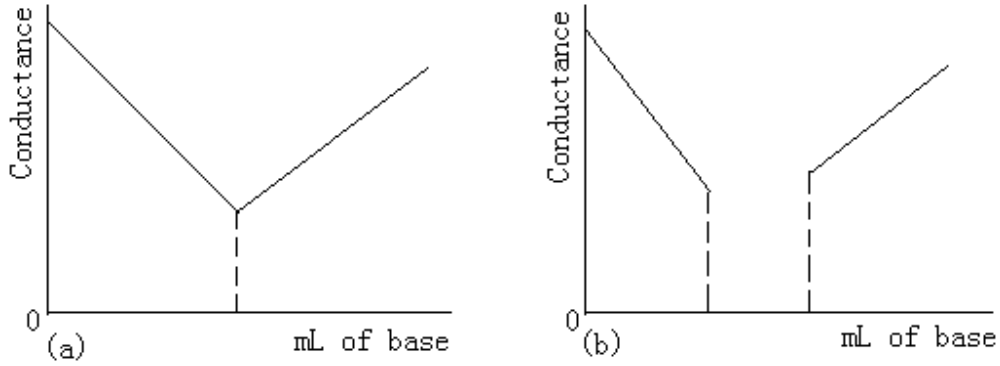

Figure 12. Typical conductimetric titration curves: (a) strong acid with a strong base, (b) weak acid with a strong base [122].

Table 12. Effect of sulfuric acid (72 %, w/w) hydrolysis condition on the degree of sulfonation of liner pulp [123].

Pulp:acid	Reaction time, min	Sulfur group[a], %	DS[b]
1:4	16	49.540	1.670
	17	59.290	2.000
	45	56.670	1.910
1:6	15	59.110	1.995
	19	59.840	2.020
	18	46.260	1.560
1:8	15	62.260	2.102
	20	59.440	2.013
	45	53.290	1.793
1:10	15	60.700	2.049
	23	63.100	2.129
	22	61.500	2.076

[a]Sulfur content is the percentage of the sulfur groups based on the total number of the hydroxyl groups and sulfur groups. [b]Degree of substitution (DS) was calculated as the average number of hydroxyl groups in the anhydroglucose that are substituted in the particular product.

2.3.2.3 Characterization and Properties of Cellulose Nanowshikers

2.3.2.3.1 Dimension Measurement of Cellulose Nanowhiskers

Transmission electron microscopy (TEM) is a microscopy technique whereby a beam of electrons is transmitted through an ultra thin specimen, interacting with the specimen as it passes through. An image is formed from the interaction of the electrons transmitted through the specimen; the image is magnified and focused onto an imaging device, such as a fluorescent screen, on a layer of photographic film, or to be detected by a sensor such as a CCD camera [124]. TEM is capable of measuring the size of cellulose nanowhiskers. A sample is usually prepared by drying a drop of dilute CNWs suspension (~0.1%, w/v) on a carbon coated microscope grid [90]. The particle dimension can be determined by manual counting from TEM micrographs at a high magnification, and the distributions of particle length and diameter are calculated by counting several individual particles in each sample. Details in the light microscope

samples can be enhanced by stains that absorb light; similarly TEM samples can also utilize high atomic number stains to enhance contrast. The stain absorbs electrons or scatters part of the electron beam which otherwise is projected onto the imaging system. On some occasions, the CNWs TEM sample was stained with a uranyl acetate solution to enhance the resolution [97, 106, 109]. This method is capable of providing information about structural details often finer than those visible in thin sections, replicas, or shadowed specimens.

Atomic force microscopy (AFM) is another useful technique to characterize CNWs. AFM provides a 3D profile of the surface on a nanoscale, by measuring forces between a sharp probe (<10 nm) and surface at very short distance (0.2-10 nm probe-sample separation) [125]. Probes are typically made from Si_3N_4 or Si and have different dimensions according to the specific tip shape. A detailed description of the tip dimension can be found elsewhere [126]. The probe is supported on a flexible cantilever. The AFM tip "gently" touches the surface and records the small force between the probe and the surface. The AFM can be used to study a wide variety of samples (i.e. plastic, metals, glasses, semiconductors, and biological samples such as the walls of cells and bacteria). Unlike scanning electron microscopy (SEM) it does not require a conductive sample. However there are limitations in achieving atomic resolution. The physical probe used in AFM imaging is not ideally sharp. As a consequence, an AFM image does not reflect the true sample topography, but rather represents the interaction of the probe with the sample surface. This is called tip convolution [125]. In Beck-Candanedo et al.'s study [87], CNWs suspension was diluted, filtered, dropped on the mica which was already stained with poly-L-lysine

solution, washed off with water and dried. The mica was then attached to an AFM specimen disk and analyzed. In addition, particle size distribution, average molecular weight and zeta potential of CNWs can also be determined by dynamic light scattering [88].

2.3.2.3.2 Thermal Property of Cellulose Nanowhiskers

The structure changes from cellulose fiber to cellulose nanowhiskers, e.g., aspect ratio, surface charge and crystallinity, lead to different thermal performance. Untreated cellulose fibers exhibited many steps of degradation according to the thermogravimetric analysis (TGA) results. It included an initial moisture loss at 110˚C, and intermediate loss at 280˚C and 352˚C. As to H_2SO_4-CNWs, two well separated degradation processes, one from 220˚C to 280˚C and the other between 330˚C to 500˚C, with initial moisture loss at 120˚C were observed [127]. The increase of the moisture loss temperature was attributed to the strong adhesion of water molecules to the large surface of CNWs. The main degradation between 220˚C and 280˚C was due to the depolymerization, dehydration, and decomposition of glycosyl units followed by the formation of a char. The degradation above 325˚C could be ascribed to the oxidation and breakdown of the char to lower molecular weight gaseous products [93]. The low degradation temperature of CNWs bearing sulfate groups was due to the increasing numbers of free end chains and sulfate groups at the surface, which were liable to early decomposition [128].

2.3.2.3.3 Optical and Orientation Properties

At very low concentrations, cellulose nanowhiskers randomly suspended in water

and form an isotropic phase [129]. As the CNWs are rigid rod-like particles, they have a strong tendency to align along a vector director. This rod alignment creates a macroscopic birefringence that can be directly observed through crossed polarizers (Figure 13). This birefringent character of the CNWs suspension was first observed in 1959 by Marchessault et al. [130]. In the isotropic phase, CNWs appear as spherical or oval droplets as investigation by polarized optical microscopy [84]. The initial ordered domains are similar to the "tactoids" described for other systems [131-133]. As the concentration increases, for instance by water evaporation, the tactoids coalesce to give an anisotropic phase. This phase is characterized by the self-orientation of cellulose nanowhiskers in the same direction along a vector director resulting in a nematic liquid crystalline alignment [129]. When the suspension reaches a critical concentration the CNWs can form a chiral nematic ordered phase displaying optical characteristics of a typical cholesteric liquid crystal [84, 89, 130]. This is because of the self-alignment of the particles along a vector director in a packed nematic plane such that the angle of the vector director in each subsequent plane is in a spiral stairway packing of CNWs rods about a cholesteric axis [129]. The critical concentration for anisotropic phase formation can be measured by observing the amounts of isotropic and anisotropic phases in a series of samples with different concentrations [89-90]. The anisotropic phase separates at relatively low concentration, e.g., 4 wt% for a salt-free CNWs suspension. The critical concentration was slightly increased and the biphasic range became narrower with longer hydrolysis time and/or higher acid to cellulose ratio [87]. It is not possible to observe any chiral nematic phase of CNWs hydrolyzed by acids other than sulfuric aicd. Postsulfonated CNWs suspension showed a birefringent glassy phase different

from the chiral nematic phase as shown in Figure 14 [91].

Figure 13. Birefringent character of isotropic cellulose nanowhiskers suspension.

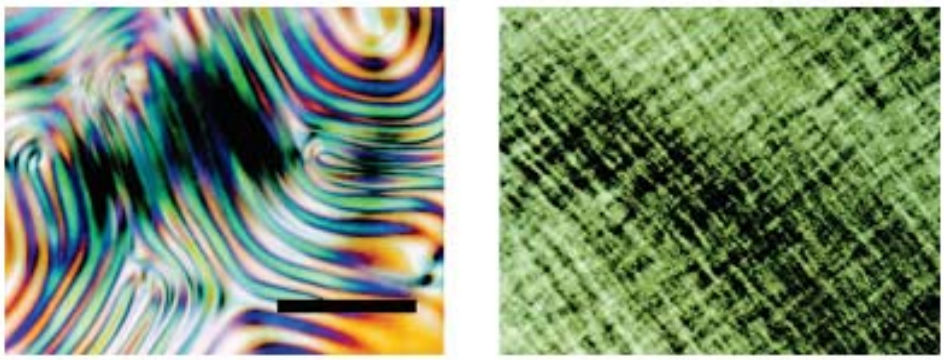

Figure 14. Polarized-light micrographs of cellulose nanowhiskers suspensions: (left) fingerprint pattern in the chiral nematic phase of the directly H_2SO_4-hydrolyzed suspension (initial solid content, 5.4%); (right) cross-hatch pattern of postsulfated suspension (solid content, 7.1%) [134].

2.3.2.4 Applications of CNWs in Nanocomposites Preparation

2.3.2.4.1 Application with Hydrophilic Polymers

Tunicate CNWs with a length of 100 nm to several μm and a width of 10-20 nm were incorporated into poly(styrene-co-butyl acrylate) latex at a content of 6% (w/w)

[103]. The TEM image revealed that the CNWs were distributed throughout the structure, without segregation or association. The mechanical properties of the polymer film were improved and particularly striking when it was heated above the glass transition temperature. The shear modulus G of the pure matrix remained constant at around 1 GPa below T_g, and dropped rapidly to 1 MPa during the crossing of the glass-rubber transition temperature. Above this temperature, it behaved as a viscous liquid, with G decreasing rapidly with increasing temperature. The films that contained cellulose whiskers had a slight increase in their G value below T_g, but the drop in G value above T_g was dramatically reduced: only from 1 to 0.1 GPa for a film reinforced by 6% (w/w) whiskers. Above T_g, the reinforced films behaved as rubbers as their G value stayed constant all the way to 500 K, a temperature at which cellulose starts to decompose. With the same polymer matrix, Helbert et al. [31] studied the reinforcing effect of wheat straw CNWs (150-300 nm × ~5 nm) in a range from 0 to 30 wt%. The relaxed modulus of the nanocomposite films were improved especially above the glass transition temperature compare to the pure film, e.g. a thousand times higher with a CNWs content of 30 wt%. The improvements were attributed to not only the geometry and stiffness of the CNWs but also to the interactions of the CNWs which probably formed CNWs clusters through hydrogen bonds. Pu et al. [9] prepared three closely related acrylic latex films employing acacia pulp fibers (0.62 mm × ~0.02 mm), CNWs (100-250 nm × 5-15 nm), and nanocellulose balls (~80 nm). Surface roughness measurement by AFM provided a value of 1.86 for 5% CNWs reinforced films in comparison to 8.86 and 2.78 for the control film and 5% nanocellulose balls reinforced film indicating decreased surface roughness. The composites reinforced with cellulose

nanowhiskers exhibited a threefold increase in TEA whereas the addition of acacia fibers had a negative effect and the nanocellulose balls had no effect on TEA values. Tensile strength of the 5% CNWs reinforced films was more than double of the strength of control film and films reinforced with 5% nanocellulose balls or 5% acacia fibers. The improvements of mechanical properties can be attributed to the formation of hydrogen-bonded network of cellulose nanowhiskers in the composite that is governed by a percolation mechanism as well as the high aspect ratio of cellulose nanowhiskers.

Oksman et al. [116] incorporated DMAc/LiCl swelled and separated CNWs into maleic anhydride modified poly(lactic acid) (PLA) to prepare a novel nanocomposite. The structure of the composites was made up of partly separated CNWs when poly(ethylene glycol) (PEG) used as processing aid to lower the viscosity. The mechanical properties of the nanocomposite were improved, e.g., the elongation at break was increased about 800%, though DMAc/LiCl seemed to cause degradation of the composites at high processing temperature. The dispersion optimization of CNWs and the degradation prevention need to be resolved in the future.

Water uptake was found to increase with increasing Sisal CNWs (~250 nm × ~4 nm) content in the polyvinyl acetate (PVAc) matrix with a plateau value established once CNWs percolation occurs [97]. Above the threshold, water uptake was not found to plasticize the composite significantly. Below this, the composite was plasticized significantly at high water uptake, whereas at low values plasticization was not found to occur, presumably due to strong CNW-PVAc interactions. Therefore, there is a potential of CNWs to stabilize polar matrices at low content under humid conditions.

2.3.2.4.2 Application with Hydrophobic Polymers

Due to the strong hydrogen bonding interactions between the hydroxyl groups of CNWs, it is difficult to obtain well separated CNWs in organic solvents especially non-polar solvents, and that restricts its application in hydrophobic polymer matrix. To resolve this difficulty, dispersion of CNWs in polar solvent, addition of surfactant such as phosphoric ester to CNWs aqueous suspension, and surface modification of CNWs were studied [5, 94-95, 105, 111].

In polar organic solvent such as dimethylformamide (DMF) and dimethylsulfoxide (DMSO), dilute well dispersed CNWs suspensions were obtained by vigorous mixing and intensive ultrasonic treatment of dry CNWs, owing to the high value of the dielectric constant of polar solvent and the medium wettability of CNWs. Samir et al. [5] prepared a polyether nanocomposite reinforced with tunicate CNWs (500 nm-1-2μm × 15 nm) by using a CNWs DMF suspension. The addition of CNWs reduced the crosslinking density but had no effect on the thermal stability of the polyether nanocomposite. CNWs DMF suspension was also used to prepare polymethylmethacrylate (PMMA) film by the solution casting method [111]. The nanocomposite film retained good transparency and thermal stability but a significantly enhanced storage modulus compared to the pure film. In another study, cotton CNWs (aspect ratio of ~10) and tunicate CNWs (aspect ratio of ~80) were dispersed in DMF first, and then mixed with an oligomeric difunctional diglycidyl ether of bisphenol A (an epoxide equivalent weight of 185-192) and a diethyl toluene diamine-based curing agent to prepare the epoxy nanocomposite films [95]. The CNWs content systematically varied between 4 and 24% v/v. The storage modulus of the nanocomposites was increased modestly below T_g and significantly above T_g. The mechanical properties of

the novel nanocmposite were well described by the percolation model as the result of the formation of a percolating CNWs network in which stress transfer was facilitated by strong interactions between CNWs. Solvent exchange from water to acetone and then to DMF through several successive centrifugation steps, is another way to disperse CNWs in DMF.

In non-polar solvent, e.g., toluene, CNWs can be well dispersed with the assistance of a surfactant, e.g., phosphoric ester. Ljungberg et al. [105] used three different types of CNWs (one to several micrometers in length, 10-20 nm in diameter) to prepare isotactic polypropylene nanocomposite films. The first type was aggregated CNWs (AC) in toluene which were obtained by redispersion of freeze dried CNWs. The second type was CNWs grafted with maleated polypropylene (PPgMA) (GC) and then redispersed in toluene by mechanical mixing. The final type is surface coated CNWs (CC) with phosphoric ester of polyoxyethylene-9-nonylphenyl ether, freeze dried and then resispersed in toluene. The linear mechanical properties above T_g were found to be drastically enhanced for all three nanocomposites as compared to the neat polypropylene. It was attributed to a mechanical coupling between the polypropylene crystallites and filler/filler interactions. However, at large deformations, the dispersion quality of the CNWs played a major role resulting in enhanced ultimate mechanical properties. As a result, the surface coated CNWs showed the best reinforcing effect.

Surface modification of CNWs is an alternative method to suspend CNWs in non-polar organic solvents. Cotton CNWs, functionalized by partial silylation through reaction with n-dodecyldimethylchlorosilane in toluene, can easily form stable suspensions in tetrahydrofuran (THF) and chloroform [94]. It has been used as biobased

nucleation reagent to increase the crystallization rate of poly(L-lactide)(PLLA). The tensile modulus and strength of the PLLA /modified CNWs (1 wt%) nanocomposite film were more than 20% higher compared to the pure PLLA.

2.4 Lignin

The term lignin is derived from the Latin word "lignum," for wood [135-136]. In plant cell walls, lignin fills the spaces between cellulose and hemicellulose, and it acts like a resin that holds the lignocellulose matrix together [137]. Lignin is considered to be the most recalcitrant biopolymer in the plant cell wall and provide three main functions [136]. First, lignin decreases the permeability of water across the cell walls, which is an important role for the transport of water and nutrients. Second, it provides rigidity and structural support to the cell wall to resist compression and bending. Third, lignin can protect the cell wall from microorganisms by providing resistance against the penetration of destructive enzymes into the cell wall. The composition, molecular weight, and amount of lignin differ from plant to plant, with lignin abundance generally decreasing in the order of softwoods (25-30%), hardwoods (19-23%), and grasses. Its amount is determined not only by the vegetation, but also by a number of other factors: climatic zone, soil, tree age, and content in various parts of a plant [138-140].

2.4.1 Lignin Structure and Biosythesis

Lignin is an amorphous, cross-linked, and three dimensional phenolic polymer consisting of methoxylated phenylpropane structures. Although the exact structure of native lignin found in plants is still unknown, its biosynthesis is thought to involve the

polymerization of three primary monomers: *p*-coumaryl alcohol (*p*-hydroxyphenyl), coniferyl alcohol (guaiacyl), and sinapyl alcohol (syringyl), depicted in Figure 15 [138-139, 141-144]. Coniferyl alcohols constitute approximately 90% of SW lignin, whereas roughly equal proportions of coniferyl alcohol and sinapyl alcohol appear in HW lignin, although many exceptions are known. Table 13 gives out the molar percentages of guaiacyl, syringyl, and *p*-hydroxyphenyl units in several biomass lignins. The polymerization process is initiated by the oxidation of the monolignol phenolic hydroxyl groups. The oxidation itself has been shown to be catalyzed via an enzymatic route [145-146]. It is believed that both peroxidases and laccases are involved in lignin synthesis, where laccase is primarily responsible for the initial polymerization of monolignols to oligolignols, while peroxidases, on the other hand, catalyze the reactions of oligolignols leading to the extended lignin macropolymer [146].

The enzymatic dehydrogenation is initiated by an electron transfer that yields reactive monolignol species with free radicals as shown in Figure 16. A monolignol with a free radical can then couple with another monolignol with a free radical to generate a dilignol. For example, the formation of β-O-4 interlinkage via radical coupling is shown in Figure 17 [135]. Subsequent nucleophilic attack by water, alcohols, or phenolic hydroxyl groups on the benzyl carbon of the quinone methide intermediate will restore the aromaticity of the benzene ring [30, 147]. The generated dilignols will then undergo further polymerization. The common linkages in lignin structure are shown in Figures 18. Table 14 [148] lists the relative abundance of the various linkages in softwoods, including spruce, and hardwoods, such as birch and eucalyptus. A schematic representation of a proposed softwood and hardwood lignin

structures are depicted in Figure 19 and Figure 20, respectively [149-150]. The additional methoxy groups on the aromatic rings in HW lignin prevent formation of 5-5 or dibenzodioxocin linkages, resulting in more linear structures relative to SW lignin.

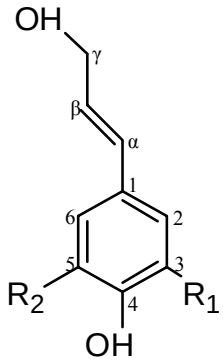

Sinapyl alcohol/Syringyl: R_1=R_2=OMe
Coniferyl alcohol/guaiacyl: R_1=OMe, R_2=H
***p*-Coumaryl** alcohol/*p*-hydroxyphenyl: R_1=R_2=H

Figure 15. Methoxylated phenylpropane structures in lignin.

Table 13. Molar percentage of guaiacyl (G), syringyl (S), and *p*-hydroxyphenyl (H) units in several biomass lignin.

Origin	G	S	H
Wheat straw [151]	45	46	9
Loblolly pine [152]	87	0	13
Spruce [153]	98	2	0
Beech [154]	56	40	4
Eucalyptus globulus [155]	14	84	2
Alamo Switchgrass [156]	51	41	8

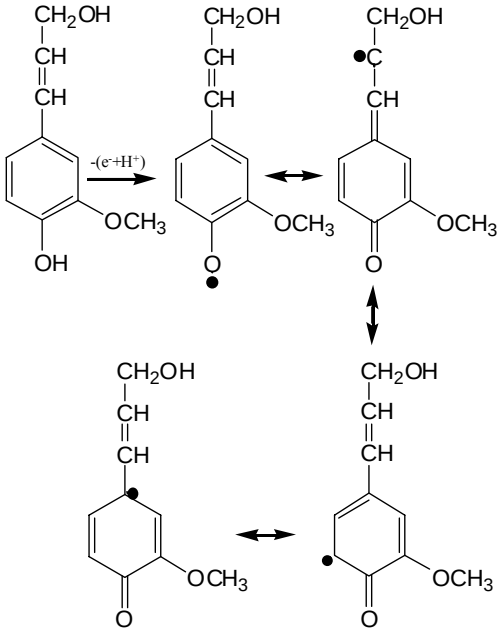

Figure 16. Phenylpropane radicals to form various linkages in lignin structure [143].

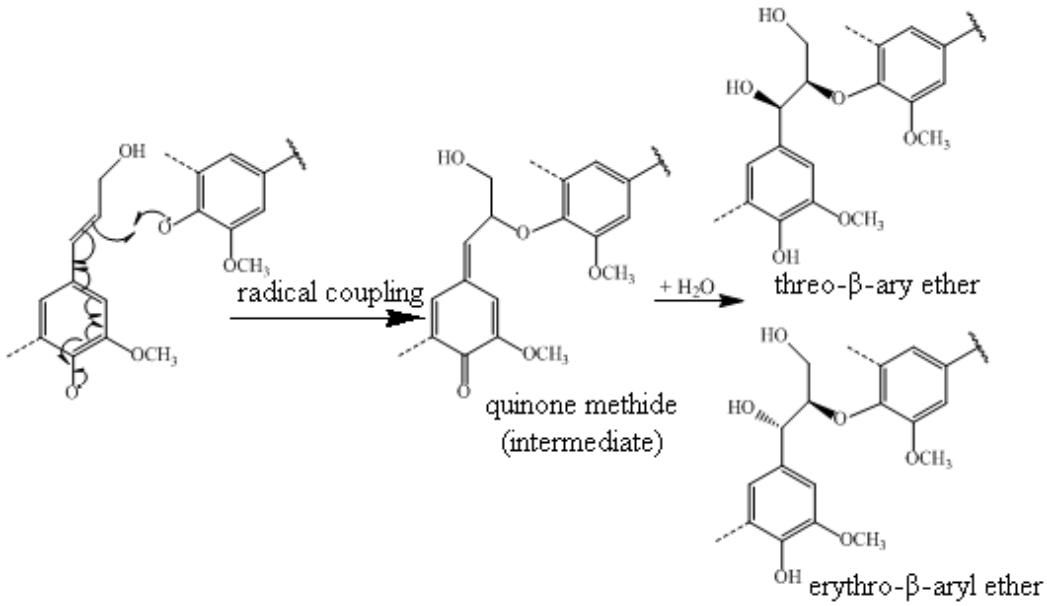

Figure 17. Formation of *β*-O-4 interlinkage via radical coupling [135].

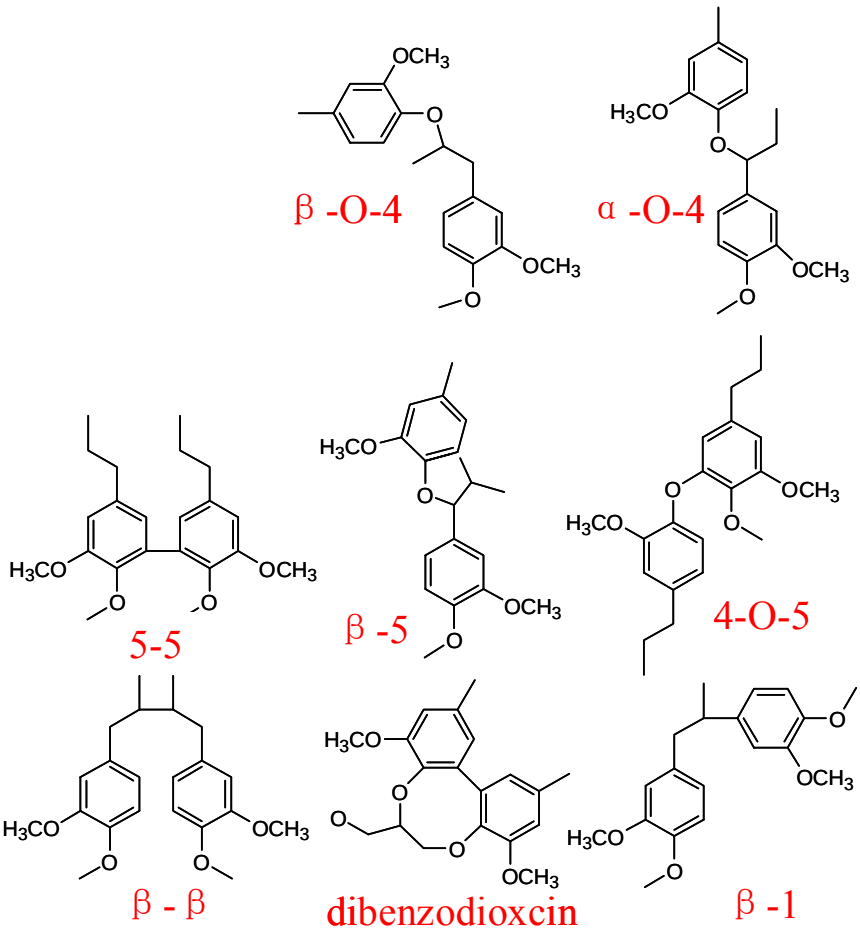

Figure 18. Common linkages in lignin structure.

Table 14. Inter monolignolic linkages as percent of the total linkages [148].

Name	Type of linkage	Softwood (%)	Hardwood (%)
β-aryl ether	*β*-O-4’	35-60	50-70
Diaryl ether	4-O-5’	<4	7
Phenyl coumarane	*β*-5’	11-12	4-9
Dihydroxy biphenol	5-5’	10	~5
Diaryl propane 1,3-diol	*β*-1’	1-2	1
Pinoresinol	*β*-*β*’	2-3	3-4
Dibenzodioxocin	5-5’-O-4	4-5	Trace
Spiro-dienone	*β*-1’ α-O-*α*’	1-3	2-3

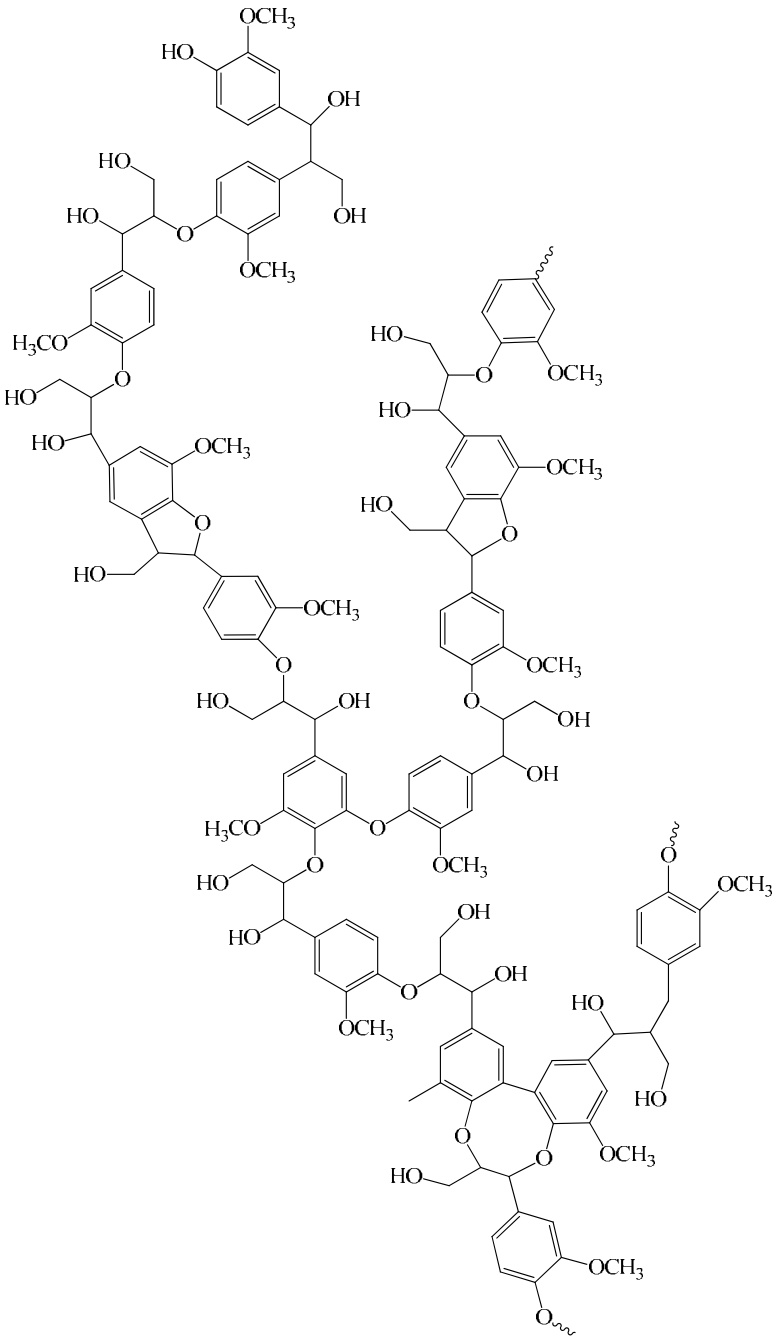

Figure 19. Example for structure of native softwood lignin [149].

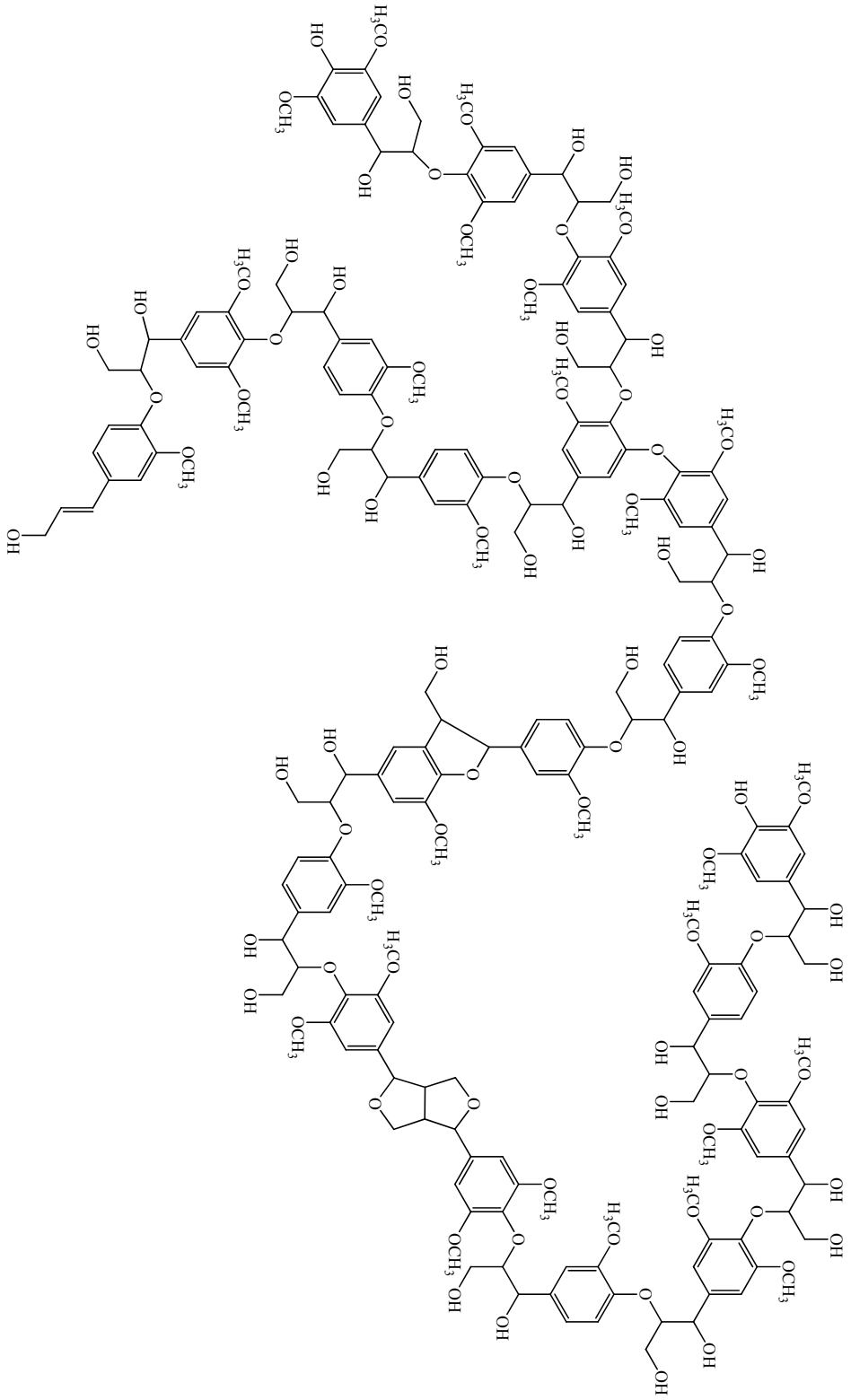

Figure 20. Model for poplar milled wood lignin [150].

2.4.2 Lignin Extraction

Lignins from trees, plants, and agricultural crops with different chemical composition and properties can be obtained by using several extraction methods. Commercial chemical pulping processes (sulfite and Kraft processes) produce lignosulfonate and Kraft lignin in the cooking liquor as residue. Lignin can also be prepared from organosolv pretreatment following organic-solvent-based procedures. The effects of pretreatment on lignocellulosic materials are illustrated in Figure 21. Ideally, an effective pretreatment method has to [157]:

- Result in high recovery of all carbohydrates
- Result in high removal of hemicelluloses and lignin
- Produce no or very limited amounts of sugar and lignin degradation products
- Have a low energy demand
- Have a low operational/capital cost

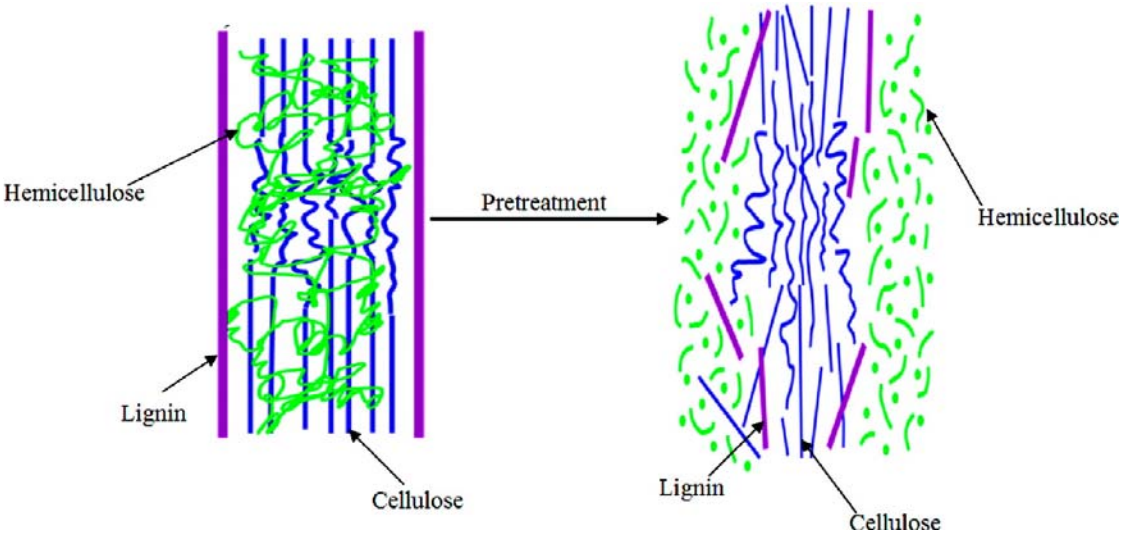

Figure 21. The effect of pretreatment on lignocellulosic materials [158].

It is practically impossible to isolate pure lignin quantitatively from cell walls in an intact state. The lignin isolated by known methods (physical, chemical or enzymatic treatments) is a mixture of degraded or solubilized lignin from various morphological regions.

2.4.2.1 Kraft Pulping

Kraft pulping is the most dominant chemical pulping technique [138]. It employs high pH and considerable amounts of aqueous sodium hydroxide and sodium sulfide. Lignin is degraded at temperatures between 150˚C and 180˚C for about 2 h in a stepwise process [159]. Kraft lignin can be precipitated and extracted from the black liquor in a two-step acidification process. First, carbon dioxide is used to reduce the pH of the liquor till 9–10, and about 75% of the lignin is precipitated as a sodium salt [160]. For further purification, this lignin is suspended in water and acidified with H_2SO_4 to a pH lower than 3 [138].

In the Kraft pulping process lignin is primarily degraded through cleavage of β-O-4 structures [161]. The extensive cleavage of β-O-4 structures yields a large number of phenolic end-groups in the dissolved lignin with the concomitant formation of partially degraded and partially modified side chains with far fewer oxygenated carbons than are found in native wood lignin [162]. It is important to note that 5-5 linkages are highly refractory because they typically survive and are even formed during the Kraft pulping process.

2.4.2.2 Kraft Lignin

Kraft lignin is a dark-colored and water- and solvent-insoluble product but can dissolve in alkali owing to its high concentration of phenolic hydroxyl groups [163].

Kraft lignin contains a small number of aliphatic thiol groups that give the isolated product a characteristic odor, especially during heat treatment [163]. Kraft lignin does not undergo a distinctive glass-to-rubber transition when heated, despite the fact that lignin in wood has a T_g of under 100˚C [164]. Initial degradation of Kraft pine lignin occurs between ~120˚C and ~300˚C from bond fragmentation in the phenyl propane side chains evidenced by the formation of formic acid, formaldehyde, carbon dioxide, water, and sulfur dioxide [165]. Major decomposition initiates at ~300˚C and extends to 480˚C at which point 50% of the initial weight has been lost. Methanol, 2-methoxyphenol (gauiacol), and a 2-methoxy-4-alkyl-substituted phenol are the most apparent species evolving in this region which indicates the fragmentation of the major chain linkages between the monomeric phenol units in the lignin structure [165].

Data from the Food and Agricultural Organization of the United Nations (FAO) revealed that, in 2006, 9.8×10^7 tons of Kraft pulp were produced in worldwide developed countries from a total chemical pulp production of 1.03×10^8 tons [166]. A very small amount of Kraft lignin is isolated from pulping liquors in the United States and Europe [167]; the vast majority is used as in-house fuel required for the recovery of chemicals [163]. The commercial Kraft lignin is generally sold in the sulphonated form or as lignin amines [138].

2.4.2.2 Organosolv Pretreatment

In an organosolv pretreatment, hemicelluloses and lignin are hydrolyzed by treating the biomass in an organic or aqueous-organic solvent mixture with the addition of an inorganic acid catalyst, e.g., H_2SO_4 or HCl [157]. Typically, solvents such as methanol, ethanol, acetone, ethylene glycol, triethylene glycol, and phenol are used in the

organosolv process [157]. During pretreatment, the hydrolyzed lignin is extracted into the organophilic phase and is recovered as the filtrate, the cellulose is recovered as the solid residue, and the hemicellulose is recovered in the water-soluble fraction as monomeric and oligomeric sugars [48, 168]. Pan et al. did a process optimization of ethanol organosolv pretreatment of hybrid poplar [169] and lodgepole pine [170] using response surface methodology. The typical conditions for the highest yield of EOL were summarized in Table 15.

Table 15. Typical ethanol organosolv pretreatment conditions for a high yield of ethanol organosolv lignin [169-170]

Wood species	Temperature (˚C)	Time (min)	H_2SO_4 (% of wood)	Ethanol concentration (% (v/v))	EOL yield (% of wood)
Poplar	195	80	1.50	65	20.90
Pine	170	80	1.20	70	22.00

The attractive features of solvent pulping have been demonstrated with the construction and operation of a demonstration scale facility in Mirimichi, New Brunswick, Canada from 1989-1996 using the Alcell process. Repap owned the IP to the process when taken over by hedge funds in 1997. The process uses aqueous ethanol solutions (40-60% v/v) to delignify wood at temperatures from 180-210°C and 2-3.5 MPa. Solvent is recovered with flash evaporation, vapour condensation and vacuum stripping [171]. The pilot plant boasted superior environmental performance, excellent bleached pulp, an economically attractive scale of 300 tons/day, and commercially attractive by-products. It is said that the technology can be used to produce fully bleachable pulps from hardwood with physical and optical properties similar to those of Kraft pulp [172].

Moreover, it is able to exploit small regions of hardwood resource that could not support a modern sized Kraft mill [173]. When compared to the conventional Kraft pulping process, the Alcell process offers a number of advantages, namely economical pulping on a smaller scale, easy recovery and recycle of organic solvents, separate streams of cellulose, hemicelluloses, and lignin, allowing valorization of all components of lignocellulosic biomass, and a sulphur-free therefore an environmentally benign process [174-175]. The major byproduct of the process is the lignin fraction, known as Alcell lignin or ethanol organosolv lignin (EOL), and can be used for several coproducts [172].

Pan and co-workers have extensively studied the ethanol organosolv pretreatment of poplar and pine by examining the effects of various process parameters on the yield and distribution of cellulose, hemicellulose, and lignin in three fractions (solid fraction, ethanol organosolv lignin fraction, and water-soluble fraction) [168, 170]. The process parameters were cooking temperature (T), time at the cooking temperature (t), sulfuric acid concentration (S), and ethanol concentration (E). Typical conditions are within the following ranges: T = 150–200°C; t = 30–90 min; S = 0.5–1.5%, w/w; E = 25–80%, v/v [168, 170, 176]. Finding the optimum condition was based on recovering solids with high glucose content and low lignin content, and high recovery of the hemicelluloses in the water fraction. Table 16 summarizes the composition of the three fractions after ethanol organosolv pretreatment of poplar and pine at the optimum condition, and compared these values to the untreated raw materials [168, 170]. In both cases, the resulting solid substrates of poplar and pine mainly contain glucose with minimal amounts of lignin and other sugars such as xylose and mannose. Most of the hemicelluloses were recovered in the water soluble fraction, which also contains

considerable amounts of soluble lignin due to lignin hydrolysis. However, the majority of the lignin is recovered in the EOL fraction.

Table 16. Compositional analysis of the raw materials and the three fractions after ethanol organosolv pretreatment of poplar and pine at the optimum condition [168, 170].

Content[a]	Untreated poplar	Pretreated poplar[b]	Untreated pine	Pretreated pine[c]
EOL		15.53		19.57
Solid		54.19		43.05
Klason lignin	20.95	5.88	24.79	4.17
Acid-soluble lignin	2.30	0.30	0.29	0.1
Glucose	48.95	43.16	50.46	37.63
Xylose	17.85	3.36	7.21	0.56
Mannose	3.388	1.49	13.09	0.59
Galactose	0.38	-	2.22	-
Arabinose	0.26	-	1.42	-
Water-soluble		16.98		20.06
Acid-soluble lignin		5.22		4.76
Glucose		0.55		4.19
Xylose		9.37		3.23
Mannose		1.29		5.37
Galactose		0.33		1.73
Arabinose		0.22		0.78

[a]% (w/w) in oven-dried wood. [b]Pretreatment conditions: 1.25 % w/w H_2SO_4, 50 % v/v ethanol, 180°C, and 60 min. [c]Pretreatment conditions: 1.10 % w/w H_2SO_4, 65 % v/v ethanol, 170°C, and 60 min.

2.4.2.3 Ethanol Organosolv Lignin (EOL)

β-O-4 linkages are the predominant substructures present in lignin from the starting material, as well as after the pretreatment [177]. During ethanol organosolv treatment, acid-catalyzed cleavage of *β*-O-4 linkages and ester bonds were the major mechanisms of lignin cleavage [178]. Comparing to other pulping methods, such as Kraft pulping, steam explosion, dilute-acid pretreatment, and hot-water treatment, where the only proposed use for the lignin is as a boiler fuel, EOL is usually high-purity, low molecular weight, narrow polydispersity, less condensed, sulfur free, and low ash content

product with relatively narrow molecular weight distributions [139, 177-178]. Table 17 summarizes the characteristics of pine and poplar EOL [169, 179].

Table 17. Weight-average molecular weight (M_w), number-average molecular weight (M_n), polydispersity index (D = M_n/M_w), and functional groups of pine and poplar EOL [169, 179].

	Molecular weight and polydispersity index			Functional group[b], mmol g^{-1} lignin	
EOL[a]	M_w	M_n	D	ArOH	AlkOH
Pine	1280	3010	2.35	3.41	4.43
Poplar	1093	2105	1.93	3.48	3.85

[a]Ethanol organosolv lignin produced under 1.10 % w/w H_2SO_4, 65 % v/v ethanol, 170°C, and 60 min for pine, and 1.25 % w/w H_2SO_4, 50 % v/v ethanol, 180°C, and 60 min for poplar. [b]ArOH = phenolic hydroxyl group; AlkOH = aliphatic hydroxyl group.

EOL shows a low glass transition temperature and exhibits flow when heated [163]. It is highly soluble in organic solvents, very hydrophobic and practically insoluble in water [163]. It has more abundant phenols and carboxylic acids and less aliphatic carbons which is suitable as antioxidants, soil conditioner, precursor for green diesel via hydrogenation, a precursor for chemicals such as vanilla, and a host of phenol derivatives [177].

2.4.3 Lignin Applications in Polymer and Materials Industries

As of 2004, the pulp and paper industry alone produced 50 million tons of extracted lignin, but only approximately 2% is commercially used which the remainder burned as a low value fuel [10-12]. The commercially available lignin comprise two categories [138]: (1) the sulphur-free lignin, mainly obtained from biomass conversion technologies focused on biofuel production, organosolv pulping processes [160, 180], and soda pulping based on alternative resources like agricultural residues and non-wood fibers [163]; and (2) the sulphur containing lignin, which resulted essentially from Kraft

and sulphite pulping processes [138]. This last category comprises almost the whole market of commercially available lignin. The total annual capacity of technical lignin production is around 785,000 tons [138].

Besides the traditional use as energy source and in leather tanning, lignin is now applied for stabilization of food and feed, due to its antioxidant and antifungal properties [142]. Also, anti-carcinogenic and antibiotic activities of lignin have been reported [181]. With regard to polyolefin polymer UV stabilization, the lignins (NovaFiber and Kraft) utilized by Gosselink et al. [182] were comparable to a common, but relatively expensive, commercially applied stabilizer (Hindered Amine Light Stabilizer, HALS). In this case, the price benefit should drive the commercial uptake of lignin provided the brown coloration it imparts to these blends does not affect their applications. An increasingly important factor surrounding plastics in general but specifically polyolefin-based products is that of their recalcitrance to biodegradation. However, this is one area where there are significant benefits to be had by the incorporation of lignin [13]. Variation of the degree of lignin incorporation is reported to be accompanied by increases in the degree and rate of biodegradation [183-186].

Following the biomass pretreatment, lignin is susceptible to a wide range of chemical transformations to form valuable chemicals. For instance, through catalytic reduction reactions, which involve the removal of the extensive functionality of the lignin subunits, simple monomeric compounds such as phenols, benzene, toluene, and xylene can be formed [139]. These simple aromatic compounds can then be hydrogenated to alkanes or used to synthesis other fine chemicals using the technology already developed in the petroleum industry [139]. Vanillin and dimethyl sulphoxide are the only two low

molecular chemicals produced in large quantities from technical lignin, particularly from lignosulphonates [138].

The promoting factors for utilizing lignin as raw material for polymeric synthesis can be summarized as follows [187]: (1) renewable and abundant raw material that constitutes about 15–30% of the wood and 12–20% of other annual plants; (2) material with intrinsic biodegradability which is expected to be transmitted to polymers where lignin is incorporated; (3) presence of various reactive points that can be used in a wide range of chemical reactions; (4) byproduct of the pulp industry that available in large quantities. As a result, lignin should be an obvious candidate for application as a phenol substitute in phenol formaldehyde resins but its chemical heterogeneity is the limiting factor and, at an additive level of 5–10% of the resin weight, has led to the production of resins with increased M_w [188]. This can be countered however via several avenues. Biochemical modification of the lignin, i.e., reaction with enzyme systems to oxidatively crosslink the lignin [189] or pre-reaction of the lignin with methylolated phenols increased its reactivity [190]. Employing lignin from novel processes, e.g., acetosolv [191], acid hydrolysis [192], and organosolv [192-194] were shown to be effective phenol diluents in phenol-based resin. For example, the use of acetosolv lignin in phenol–formaldehyde resin and subsequent plywood board formation produced board knife-test results better than those obtained with a commercial phenol–formaldehyde resin [191]. Similarly, Cetin and Ozman [194] showed that the direct replacement of organosolv lignin for phenol in phenol–formaldehyde resins exhibited satisfactory resin properties and had good curing properties compared to the lignin free resin.

The epoxy resin market is economically vibrant and with specific reference to

phenol–epoxy resin, in which lignin could flourish as a crosslinking agent [13]. Moreover, because of the high contents of aromatic moieties, lignin has been exploited to prepare carbonaceous materials with interesting results in various forms of activated carbons as well as in the preparation of carbon fibers from blends with poly(ethylene oxide) [27, 195].

2.5 Polyurethane

Polyurethane is any polymer consisting of a chain of organic units joined by urethane linkages (-NHCOO-). PU has rapidly grown to be one of the most diverse and widely used plastics with a continuously increasing global market since its first lab synthesis in 1937 by Otto Bayer and co-workers [196]. Nowadays, PU is primarily used for construction, packaging, insulation, bedding, upholstery, footwear, and vehicle parts, in the form of rigid, semi-rigid, and flexible foams of a wide range of densities, as well as elastomers [17-18]. Compared to conventional materials, e.g., wood and metals, polyurethane has its own unique merits, such as low density, low thermal conductivity and moisture permeability, a high strength to weight ratio, and high dimensional stability [197]. Moreover, the formulation and reaction conditions of polyurethane synthesis can be readily adjusted and additives can be used to produce PU with desired properties for specific applications [20, 187]. Despite the significant benefits of PU, it still exhibits some drawbacks including poor degradability and toxicity due to the use of isocyanates which have evoked researchers to find more environmental friendly starting materials. Besides, the mechanical and thermal properties of PU are not optimal in comparison to some other synthetic polymers like polystyrene [198]. These drawbacks have continued

to spur research into PU composites, especially nanocomposites, considering the superior properties that can be acquired by the introduction of nanoparticles into a PU product.

2.5.1 Polyurethane Synthesis

2.5.1.1 Chemicals

For the manufacture of PU, two groups of at least bifunctional substances are needed as reactants; compounds with isocyanate groups, and compounds with active hydrogen atoms. The physical and chemical character, structure, and molecular size of these compounds influence the polymerization reaction, as well as the ease of processing and final physical properties of the resulting PU. In addition, additives such as catalysts, surfactants, blowing agents, crosslinkers, flame retardants, light stabilizers, and fillers are used to control and modify the reaction process and performance characteristics of the polymer.

2.5.1.1.1 Isocyanate

The first essential component of a PU polymer is the isocyanate. Molecules that contain two isocyanate groups are called diisocyanates. These molecules are also referred to as monomers or monomer units, since they themselves are used to produce polymeric isocyanates that contain three or more isocyanate functional groups. An example of a polymeric isocyanate is polymeric diphenylmethane diisocyanate, which is a blend of molecules with two, three, and four or more isocyanate groups, with an average functionality of 2.7. Isocyanates can be classed as aromatic, such as diphenylmethane diisocyanate (MDI) or toluene diisocyanate (TDI); or aliphatic, such as

hexamethylene diisocyanate (HDI) or isophorone diisocyanate (IPDI). The structures of those diisocyanates are drawn in Figure 22.

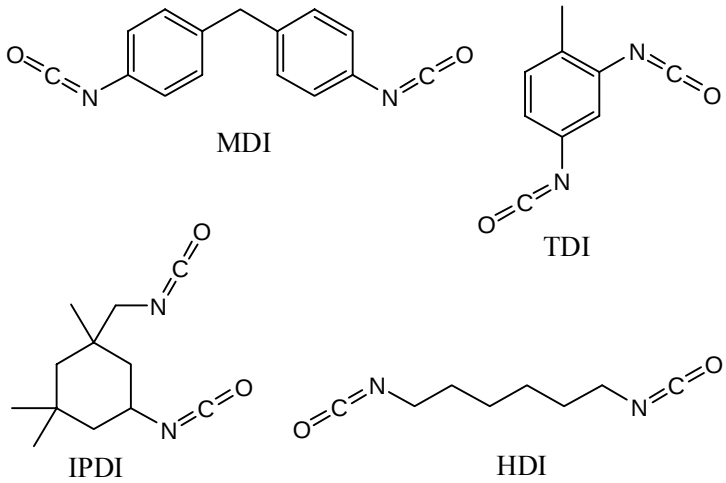

Figure 22. Structures of common diisocyanates

2.5.1.1.2 Polyol

The second essential component of a PU polymer is the polyol. Molecules that contain two hydroxyl groups are called diols, those with three hydroxyl groups are called triols, etc. In practice, polyols are distinguished from short chain or low-molecular weight glycol as chain extenders and crosslinkers such as ethylene glycol (EG), 1,4-butane diol (BDO), diethylene glycol (DEG), glycerine, and trimethylolpropane (TMP) [199]. Polyols are formed by base-catalyzed addition of propylene oxide (PO) or ethylene oxide (EO) onto a hydroxyl or amine containing initiator, or by polyesterification of a di-acid, such as adipic acid, with glycols, such as ethylene glycol or dipropylene glycol (DPG). Polyols extended with PO or EO are polyether polyols. Polyols formed by polyesterification are polyester polyols.

2.5.1.1.3 Catalysts

The PU polymerization reaction is catalyzed by tertiary amines, such as dimethylcyclohexylamine, and organometallic compounds, such as dibutyltin dilaurate or bismuth octanoate [200]. Furthermore, catalysts can be chosen based on whether they favor the urethane (gel) reaction, such as 1,4-diazabicyclo[2.2.2]octane (also called DABCO or TEDA), or the urea (blow) reaction, such as bis-(2-dimethylaminoethyl)ether, or specifically drive the isocyanate trimerization reaction, such as potassium octoate [199].

2.5.1.1.4 Blowing Agent

One of the most desirable attributes of PU is their ability to be turned into foams. Blowing agents such as water, certain halocarbons such as HFC-245fa (1,1,1,3,3-pentafluoropropane) and HFC-134a (1,1,1,2-tetrafluoroethane), and hydrocarbons such as n-pentane, can be incorporated into the poly side or added as an auxiliary stream [200-202]. Halocarbons and hydrocarbons are chosen such that they have boiling points at or near the room temperature. Since the polymerization reaction is exothermic, these blowing agents volatilize into a gas during the reaction process. They fill and expand the cellular polymer matrix, creating a foam.

2.5.1.1.5 Surfactant

Surfactants are used to modify the characteristics of the polymer during the foaming process. They are used to emulsify the liquid components, regulate cell size, and stabilize the cell structure to prevent collapse and surface defects [199-200]. Rigid foam surfactants are designed to produce very fine cells and very high closed cell content.

Flexible foam surfactants are designed to stabilize the reaction mass while at the same time maximizing open cell content to prevent the foam from shrinking. The need for surfactant can be affected by the choice of isocyanate, polyol, component compatibility, system reactivity, process conditions and equipment, tooling, part shape, and shot weight.

2.5.1.2 Synthesis

Softer, elastic, and more flexible polyurethanes result when linear difunctional polyether polyols are used to create the urethane links. The chemical reaction to synthesis a linear or low crosslinked PU is shown in Figure 23. The reaction mechanism involved in PU synthesis is illustrated in Figure 24, taking tertiary amine catalysis as an example. This strategy is used to make spandex elastomeric fibers and soft rubber parts, as well as foam rubber. For example, a diol such as polycaprolactone (PCL) and polypropylene glycol (PPG), an isocyanate such as isophorone diisocyanate and 2,4-toluene diisocyanate, an organic acid, typically dimethylol propionic acid (DMPA), and a catalyst, e.g., triethylamine (TEA) were used in preparation of waterborne PU films [4, 93, 203]. More rigid products result if polyfunctional polyols are used, as these create a three-dimensional crosslinked structure which, again, can be in the form of low-density foams. Even more rigid foams can be made with the use of specialty trimerization catalysts which create cyclic structures within the foam matrix, giving a harder, more thermally stable structure, designated as polyisocyanurate foams. Such properties are desired in rigid foam products used in the construction sector. For instance, sucrose-based and glycerol-based polyols, polymeric MDI, dimethylcyclohexylamine, 1-methyl-4-(2-dimethylaminoethyl) piperazine, silicone surfactant, and pentane were used by Li et al. [204] in the synthesis of rigid PU foams.

Polyurethane synthesis is essentially a formation of urethane linkages between polyols and isocyanates. However, linkages other than urethane bonds may also formed, such as allophanate bonds which can arise from the reaction of excess diisocyanates with urethane groups [205]. Moreover, isocyanate dimerization and trimerization reactions can also occur. Figure 25 shows all possible reactions.

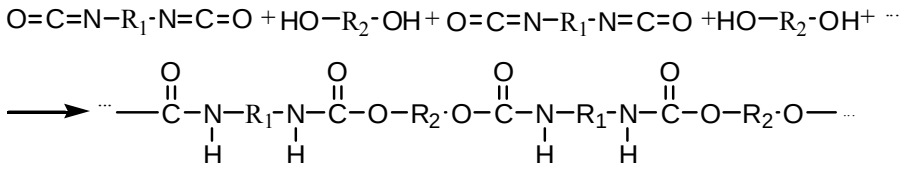

Figure 23. Chemical reaction to synthesize linear polyurethanes.

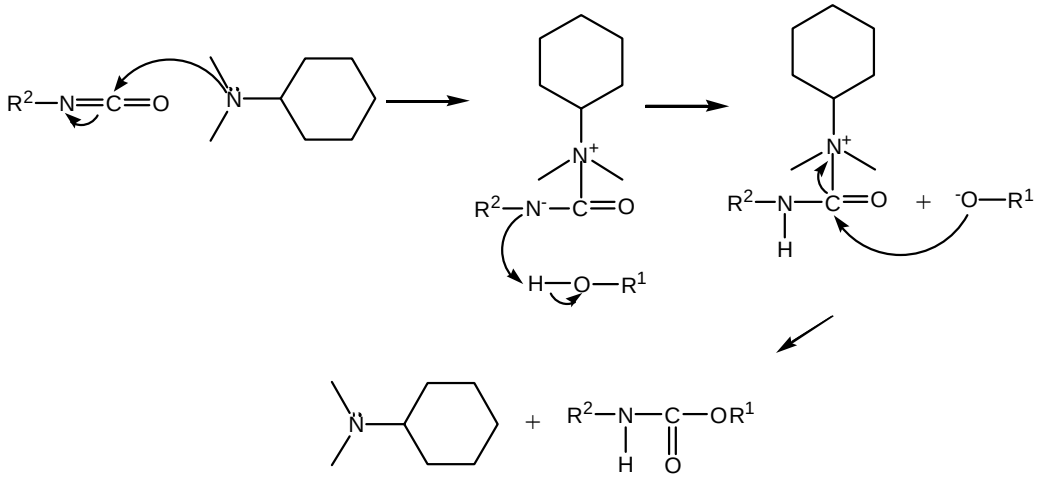

Figure 24. Reaction mechanism involved in polyurethane synthesis.

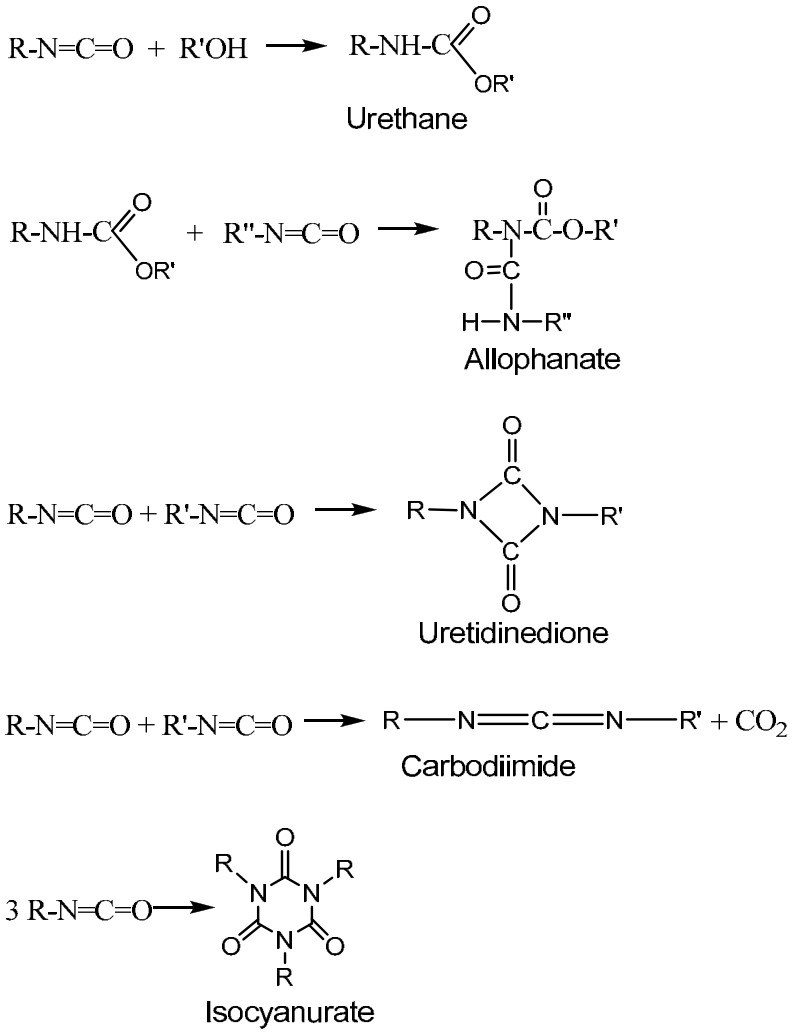

Figure 25. Possible reactions involved in the preparation of PU.

2.5.2 Rigid Polyurethane Foam

2.5.2.1 Global Market and Typical Properties

Over three quarters of the global consumption of PU products is in the form of foams, with flexible and rigid types being roughly equal in market size. In both cases, the foam is usually behind other materials: flexible foams are behind upholstery fabrics in commercial and domestic furniture; rigid foams are inside the metal and plastic walls of most refrigerators and freezers, or behind paper, metals and other surface materials in the

case of thermal insulation panels in the construction sector [206].

Rigid polyurethane foam is a highly cross-linked polymer with an essentially closed-cell structure. Its low density, low moisture permeability, high strength to weight ratio, and especially low thermal conductivity have made rigid PU foam a dominant synthetic material on a global basis [17, 20]. The thermal insulating property of rigid PU foam is known to be superior to those of other insulating materials such as expanded polystyrene, mineral wool, cork, softwood, fireboard, concrete blocks, and brick which are less expensive but require a larger quantity of material to attain the same insulating performance as that of rigid PU foams [199-200]. Table 18 summarizes some typical properties of rigid polyurethane foams [199].

Table 18. Typical properties of rigid polyurethane foams [199].

Density (kg m^{-3})	24-32
Tensile strength (MPa)	0.2-0.28
Compression strength at yield (MPa)	
Parallel to foam rise	0.14-0.31
Perpendicular to foam rise	0.07-0.17
Compression at yield (%)	5-10
Closed cells (%)	92-98
Dimensional stability (% volume change)	
70˚C, 100% relative humidity, 2 weeks	7-15
100˚C, 2 weeks	5-10
-40˚C, 2 weeks	0-2

2.5.2.2 Synthesis of Rigid PU Foams

The popularity and recognized performance of rigid PU foams are greatly dictated by the contribution of the components included in its formulations. Nowadays, a wide range of products are commercially available offering the possibility to establish almost

unlimited formulation regarding the required end properties of rigid PU foams. A typical rigid PU formulation normally includes an isocyanate, a polyol, a co-crosslinking agent, physical and/or chemical blowing agents, a catalyst, and a surfactant, having each one a specific role in the chemical reactions involved in the formation of rigid PU foams. The reactions involved in this process include urethane formation, crosslinking reactions, and foaming reactions if chemical blowing agent is used. The formation of a urethane linkage has already been shown in Figure 23. The formed urethane group has thereafter the possibility to further react with an isocyanate group to form allophanate as shown in Figure 26. This reaction contributes to introduce chemical crosslinking into the polymer.

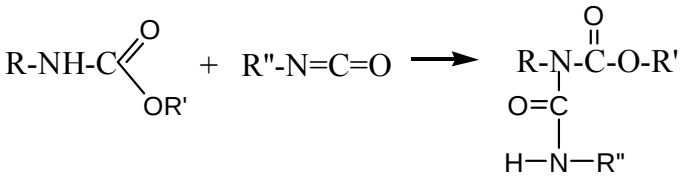

Figure 26. Formation of allophanate.

2.5.2.2.1 Isocyanate

The more commonly used isocyanates in rigid PU foam formulations are TDI and polymeric MDI, although the latter have gained increasing popularity in recent years. The used NCO index (100×(Actual amount of NCO used) / (Theoretical amount of NCO required)) is usually between 1.05 and 1.20, corresponding to a NCO excess of 5-20%. An exception is however observed in the production of polyisocyanaurate foams; where a high NCO index is used (normally between 2 and 5) in order to favor the trimerization reaction between NCO groups (Figure 27) [200].

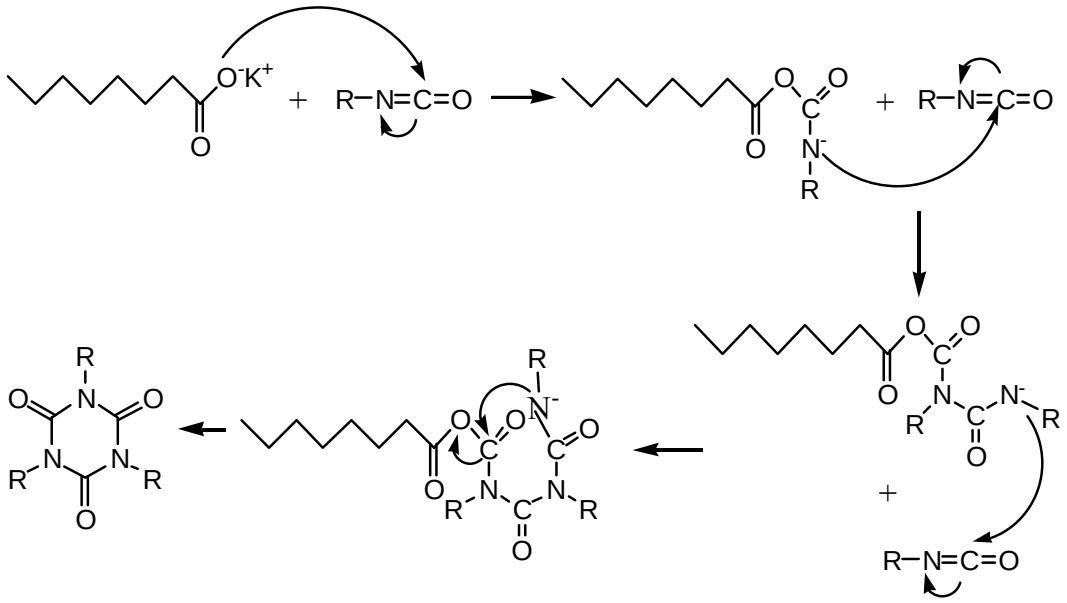

Figure 27. Trimerization reaction of isocyanates.

2.5.2.2.2 Polyol

The most important polyols used in rigid PU foam formulations are primary and secondary hydroxyl terminated polyether polyols followed by polyester polyols, normally of aromatic nature. This tendency results from the enormous variety of molecular structures regarding hydroxyl functionality and molecular weight of polyether polyols. More recently, some aromatic polyester polyols have gained an increased attention from rigid PU foam producers, partly motivated by its low cost and also due to its aromatic nature which ensures more internal cohesion of the materials [200]. The polyols used in rigid PU foam formulations have normally a high hydroxyl number (the weight of KOH in milligrams that will neutralize the acid from 1 gram of polyol) between 300 and 800 mg KOH/g [207].

2.5.2.2.3 Catalyst, Blowing Agent and Surfactant

As previously discussed, a variety of catalysts, blowing agent and surfactant can be selected for desired properties of rigid PU foams. Surfactants present several functions along the process of foam formation, namely: (1) reduction of surface tension, (2) emulsification of reactive mixture components, (3) promotion of bubble nucleation during mixing, and (4) stabilisation of cell walls during foam expansion. Currently, the most commonly used surfactants in rigid PU foam synthesis are polydimethyl siloxane-polyether copolymers [199-200].

2.5.2.2.4 Additives

Additives can be added to improve foam properties. For such purpose, a wide range of compounds could be used, including air, inert gases, dyes and pigments, plasticizers, flame retardants, synthetic fibers, and organic and inert fillers [199]. Lignin has also been used for such purpose, more concretely as filler or, from a more realistic point of view, as reactive filler. Lignin participation in the polymerization reaction has been detected through the reaction of some surface hydroxyl groups [208-209].

2.6 Cellulose Applications in Polyurethanes

2.6.1 Cellulose Fibers and Microfibrils Reinforced Polyurethanes

The mechanical properties of PU elastomers reinforced by bacterial cellulose microfibers of different aspect ratios were investigated by Bicerano and Brewbaker [210]. Microfibers of high aspect ratio nearly doubled the Young's modulus and tripled the strength of the pure elastomer, which far surpassed those observed for microfibers of modest aspect ratios. Green algae cellulose fibers of 500 to 600 μm in length and 20 to

200 μm in width were used to prepare PU composite foams [211]. The peak mechanical properties of the composite were obtained at a dry fiber content of 5-10 wt% based on the total weight of isocyanate and polyol. Vegetal cellulose fibers reinforced polyurethanes were also studied [212]. Hydrogen bonding interactions between cellulose fibers and polyurethane matrix were detected by FT-IR as (1) N-H absorption band with bonded hydrogen shifted from 3290 cm^{-1} in the control PU to 3309 cm^{-1} and 3307 cm^{-1} in the PU reinforced with 3% and 5% cellulose fibers; (2) an intensification of the band in the form of a shoulder characterized in the control PU at 1708 cm^{-1} is observed in both composite spectra, and this is attributed to the stretching of C=O with hydrogen bond interactions; (3) the band at 1667 cm^{-1} associated with the stretching of C=O and the deformation of N-H with hydrogen bond interactions disappears; (4) there is a reduction in the composite spectral relative intensity of N—H symmetrical deformation absorption at 798 cm^{-1} of PU. Later on, Wu et al. [213] compared the reinforcing effect of cellulose fiber (1-2 mm in length) versus nanofibril (20 to 40 nm in diameter and 450-900 nm in length) in PU elastomers. Table 19 indicated that the addition of cellulose nanofibrils significantly improved the tensile properties of resulting PU, while cellulose fibers only resulted in a mild increase of tensile modulus but a decrease of tensile strength and the strain-to-failure. It was likely that the less successful reinforcement was due to micron rather than nanoscale dispersion of the fillers [213]. In Mosievicki et al.'s study [214], MCC was found to be poorly dispersed in the PU matrix due to the agglomeration of crystalline particles which resulted in lower mechanical and dynamic mechanical properties; however, the thermal stability was enhanced at high temperatures.

Table 19. Reinforcing comparison between cellulose fibers and nanofibrils in terms of tensile properties [213].

Fillers	Tensile modulus change,%	Tensile strength change, %	Strain-to-failure change, %
Cellulose fiber, 5 wt%	+28.6	-20.5	-62.7
Cellulose nanofibril, 5 wt%	+163.3	+110.3	+169.8

2.6.2 Cellulose Nanowhiskers Reinforced Polyurethanes

Cellulose nanowhiskers up to 5 wt% [8] and up to 1 wt% [110, 215] were used as nanofillers to prepare thermoplastic polyurethanes. Briefly, a CNWs DMF suspension was first added to the polyol under stirring and followed by ultrasonic treatment and solvent evaporation at 70˚C. Afterward, certain amount of isocyanate was added and mixed thoroughly. As isocyanate is a very reactive chemical that can easily react with a trace of water present in the system and/or react with it self to form trimers, a molar ratio of isocyanate groups to hydroxyl groups higher than 1.0 is necessary for a complete reaction of polyol [196, 216-217]. The mixture was then cast into an open mold and cured. SEM images of the resulting nanocomposites indicated a well dispersion of CNWs in the polymer matrix [8, 215]. Tensile modulus of the products was significantly improved at small loadings of CNWs, i.e., 0.5–5 wt%, and this was more apparent at higher loadings such as 2.5 and 5.0 wt% [8]. The creep deformation decreased with increasing CNWs content. For instance, incorporation of 1 wt% CNWs resulted in a tensile modulus improvement of ~53% and creep reduction of ~36% (Table 20) [215]. A phase separation of soft and hard domains was favored by CNWs addition which led to an upward shift in melting temperature (T_m) of the crystalline phase, an increase in Young's modulus, and a decrease in deformation at break [110, 215].

The application of cellulose nanowhiskers can also be found in the synthesis of

waterborne polyurethanes (WPU) [4, 93]. Polycaprolactone and dimethylol propionic acid (DMPA) were introduced into a reaction flask equipped with a mechanical stirrer and a dropping funnel and heated to 80-85˚C until the PCL melted; isophorone diisocyanate was then added dropwise under a dry nitrogen atmosphere for several h until the isocyanate content reached a desired value. Subsequently, a CNWs DMF suspension was added, and the reaction lasted for several hours. Afterward, DMF was removed under reduced pressure at 60-80˚C, and acetone was added to reduce the viscosity of the pre-polymer. Carboxylic groups of DMPA were neutralized with triethylamine for 30 min, and the product was dispersed in DI water with vigorous stirring at room temperature overnight. The solid content could be further increased to above 25 wt% by rotary vacuum evaporation at 30˚C. The suspension was finally casted in Teflon petri dishes and dried in an oven at 40-50˚C for 10 h to 20 h depending on the water content. CNWs were well dispersed in the polymer matrix as shown by SEM images of the nanocomposites [4]. FT-IR spectra revealed a good adhesion in the interfacial area attributed to strong hydrogen bonding [4]. The detailed changes of the mechanical properties of the polyurethane nanocomposites can be found in Table 20. The polyurethane chains were found to form crystalline domains on the surface of CNWs which expedited the crystallization of PCL in the nanocomposites [93]. This co-crystallization phenomenon was believed to induce the formation of a co-continuous phase between the filler and the matrix which significantly enhanced the interfacial adhesion and consequently contributed to the improvements in thermal stability and mechanical strength of the resulting nanocomposites. The formation of a three dimensional network of CNWs through intermolecular hydrogen bonding is another

reason for the improvements [4].

Table 20. Improvements of the mechanical and thermal properties of cellulose nanowhiskers reinforced polyurethane nanocomposite films [4, 8, 93, 110, 203, 215].

Thermoplastic PUs	CNWs dimesion, nm × nm	CNWs content, wt%	Young's modulus change,%	Tensile strength change,%	Elongation at break change, %	T_g change, %	T_d change, %	T_m change, %	
								S[c]	H[d]
Polyol mixture and polymeric MDI	100-225 × 10-15	0.5	+55.1	-18.48[a]	-43.6	-	-	-	-
		1.0	+50.6	-48.5[a]	-54.5	-	-	-	-
		2.5	+102.8	-29.0[a]	-50.9	+53.5[b]	-	-	-
		5.0	+143.6	-37.8[a]	-52.7	-	-	-	-
Commercial polyester PU	Hundreds × 10-20	0.1	-	-	-	+0.55	-	+0.73	+2.27
		0.5	-	-	-	+1.37	-	+2.93	+4.25
		1.0	-	-	-	+2.19	-	+5.12	+2.05
PEG 650 and MDI (48 wt %)	2500-5000 × 50-100	0.1	-	-	-	-	-	-	-
		0.5	-2.29	-	+11.3	-	-	-	-
		1.0	-1.16	-	-14.2	-	-	-	-
PEG 2000 and MDI (45 wt%)		0.1	-	-	-	-	-	+18.3	0
		0.5	-29.4	-	-92.1	-	-	+60.0	
		1.0	-21.6	-	-81.8	-	-	+35.0	
PEG 2000 and MDI (40 wt%)		0.1	-	-	-	-	-	+9.6	0
		0.5	+37.9	-	-83.3		-	+57.7	
		1.0	+34.0	-	-75.9	-	-	+55.8	
PEG 2000 and MDI (32 wt%)		0.1	-	-	-	-	-	+38.2	0
		0.5	+49.1	-	-82.9	-	-	+70.6	
		1.0	+53.6	-	-89.9	-	-	+32.4	
PEG 2000 and MDI (23 wt%)		0.1	-	-	-	-	-	+73.3	-
		0.5	+42.5	-	-87.9	-	-	+50.7	
		1.0	+44.5	-	-93.4	-	-	+56.0	
Waterborne PU	70-150 × 10-20	2	+218	+43.2	+21.3	+6.65	~15.8	42.51˚C	
		4	+1224	+70.5	+29.1	+5.67		41.76˚C	
		6	+2335	+102	-2.1	+7.07		42.56˚C	
		8	+3171	+114	-21.2	+5.63		41.66˚C	
		10	+6218	+120	-40.3	+9.38		42.63˚C	
	327 ± 108 × 21 ± 7	5	+40.0	+116	-9.19	-1.75	-	-	-
		10	+1460	+137	-32.3	-2.92	-	-	-
		15	+940	+181	-43.4	-3.31	-	-	-
		20	+23220	+186	-61.3	-4.67	-	-	-
		25	+47280	+230	-68.6	-4.47	-	-	-
		30	+66780	+247	-82.9	-5.25	-	-	-
	700-800 × 80-100	0.4	+140	+66.7	-4.11	-7.00[b]	+11.1[e]	-	-

[a]Yield strength change,%. [b]Based on T_α (glass-rubber relaxation temperature). [c]Softsegments. [d]Hardsegments. [e]Based on 30% weight loss temperature .

Rigid PU nanocomposite foams reinforced with cellulose nanowhiskers were studied by Li et al. [204, 218]. The CNWs DMF suspension was mixed with the polyol under vigorous stirring and then the solvent was removed under reduced pressure. Catalysts and blowing agent were added and mixed when the mixture cooled down to room temperature. Certain amount of polymeric MDI was then added and vigorously stirred for ~20s until foaming. The products were left at room temperature for at least 48 h before any physical testing. The nanocomposite foams had closed cells homogeneously dispersed in the polymer matrix. The cell size was around 350 μm and decreased slightly with increasing CNWs content. This was presumably because CNWs served as nucleation sites to facilitate the bubble nucleation process, and the increased number of nucleation sites led to a finer cell structure. The detailed changes of the mechanical and thermal properties of the resulting nanocomposites were summarized in Table 21. Chemical interactions between CNWs hydroxyl groups and isocyanate groups served as one reason for the increase of the glass transition temperature and also had a positive effect on the tensile properties of the nanocomposites.

Table 21. Improvements of the mechanical and thermal properties of cellulose nanowhiskers reinforced rigid polyurethane nanocomposite foams [218].

CNWs content, wt%	Tensile modulus change,%	Yield strength change,%	Tensile strength change,%	Compressive strength change,%	Compressive modulus change,%	T_g change, ˚C	T_d change, ˚C
0.25	-16.7	-16.7	0	+166.7	+66.7	+6	-4
0.50	0	-16.7	-11.1	+166.7	+133.3	+12	-2
0.75	+37.5	+16.7	+11.1	+183.3	+133.3	+9	+3
1.00	+112.5	+33.3	+22.2	+100.0	+133.3	+9	+10

CNW is considered superior to other traditional nanofillers due to its wide availability, renewable and biodegradable features, simple hydrolysis process, high

intrinsic strength and modulus, and high aspect ratio and reactivity. The reinforcing effect of CNWs in PU is accomplished through both crosslinking and hydrogen bonding between CNWs and the polymer matrix. Improvements on the mechanical and thermal properties of the nanocomposites are remarkable compared to other inorganic fillers as well as cellulose fibers and microfibrils. The dispersion difficulty due to the hydrophilicity of CNWs can be overcome by either physical or chemical methods as discussed before. Techniques to produce less polydispersed CNWs are being developed, and it will facilitate the property control of CNWs and ensuing nanocomposites and thus broaden its applications in the future.

2.7 Lignin Applications in Polyurethanes

2.7.1 The Global Trend of Lignin Applications in Polyurethanes

It is worth to mention that the interest for developing lignin-based applications, including lignin-based polymers and materials, became more intense during the last few years. Two major factors are related to this situation, namely (1) the availability of new lignin sources such as sulphur-free lignins, and (2) the growing interest in biorefinery process where lignin valorization is important [138]. The interest to explore lignin as a raw material for polyurethane synthesis has lead, in the past few decades, to some research works due to (1) the random non-crystalline network structure of lignin which is related to mechanical properties and thermal stability [12]; (2) the natural properties of lignin which also contribute to an improvement of the moisture and flame resistance of polyurethanes [219]; (3) its aliphatic and phenolic hydroxyl functionalities provide good reacting sites towards isocyanates [12]. Various types of lignin-based polyurethane

materials including elastomers and foams have been produced using a wide range of chemical systems [138]. The exhibited properties were similar or in some cases even superior to those of the conventional polyurethanes[138]. The importance of these achievements leads to the appearance of some patented results [219-221].

2.7.2 Lignin Application in Preparation of Polyurethanes

Preparation of polyurethane from lignin is not an easy process because of the complex structure of lignin. The utilization of lignin in polyurethane synthesis follows two global approaches [138]: (1) the direct utilization of lignin without any preliminary chemical modification, alone or in combination with other polyols, and (2) by making hydroxyl functions more readily available by chemical modification, such as esterification and etherification reactions.

2.7.2.1 Direct Application

The first lignin which was incorporated as such into polyurethane formulations was a byproduct of Kraft pulping [222]. Kraft lignin contributed chemically to the formation of a three dimensional network. At low lignin contents, the resulting polyurethanes exhibited considerable toughness at specific values of [NCO]/[OH] ratios. However, at high lignin contents (>30 wt%), the corresponding polyurethanes were hard and brittle regardless of the [NCO]/[OH] ratio used. The effect of the molecular weight of the Kraft lignin on the properties of polyurethanes was studied by Yoshida et al. [223]. Polyurethanes prepared with low molecular weight lignin (M_w=620) were more flexible than those obtained with lignin of medium (M_w=1290) and high values (M_w=2890). When Kraft lignin content was higher than 30 wt%, rigid and glassy products were

obtained regardless of the molecular weight of the lignin used.

2.7.2.2 Oxypropylated Lignin Application

Preparation of low-cost polyols from abundant and renewable biomass resources has long been an important subject in the polyurethane industry. Simple sugars and some short chain molecules such as glycerol are commonly used for that purpose [224]. Nevertheless, scientific interest in exploring other biomass components has recently grown [224]. A very persistent attention was paid to the use of lignin as polyol precursor in the polyurethane synthesis. Lignin polyol is able to overcome the technical limitations and constraints imposed by the polymeric nature of lignin when directly used as a macromonomer for synthesis purposes. Among different liquefaction techniques, oxypropylation was regarded as the most promising one. Through oxypropylation, the hydroxyl groups, particularly the phenolic ones that are entrapped inside the molecule and difficult to access, are liberated from the steric and/or electronic constraints, and at the same time, the solid lignin becomes a liquid polyol, as a result of the introduction of multiple ether moieties [224].

Oxypropylation is actually a chain extension reaction of lignin macromolecules and it always accompanied by the homopolymerization of propylene oxide through transfer reactions during the anionic grafting mechanism (Figure 28) [224]. In fact, when H_2O is the initiating species, e.g. from aqueous KOH, propylene oxide (PO) can be activated directly, whereas when alkoxy anions are formed from the OH moieties on the substrate to be oxypropylated, chain growth starts at those sites, but monomer transfer can provoke the detachment of the anionic active species and give rise to PO homopolymerization [225]. A simple mechanism in Figure 29 shows that above 95% of

secondary hydroxyl groups formed due to steric hindrance that makes RO^- more likely to attack CH_2 instead of CH in propylene oxide. The produced polyol is, in fact, a mixture of oxypropylated lignin bearing as many hydroxyl functions as the original substrate and some low-molecular-weight products, poly(propylene oxide) (PPO) oligomers. These oligomers are normally left in the final mixture because they constitute a very useful bifunctional comonomer, decreasing viscosity and glass transition temperature of the polyol [224].

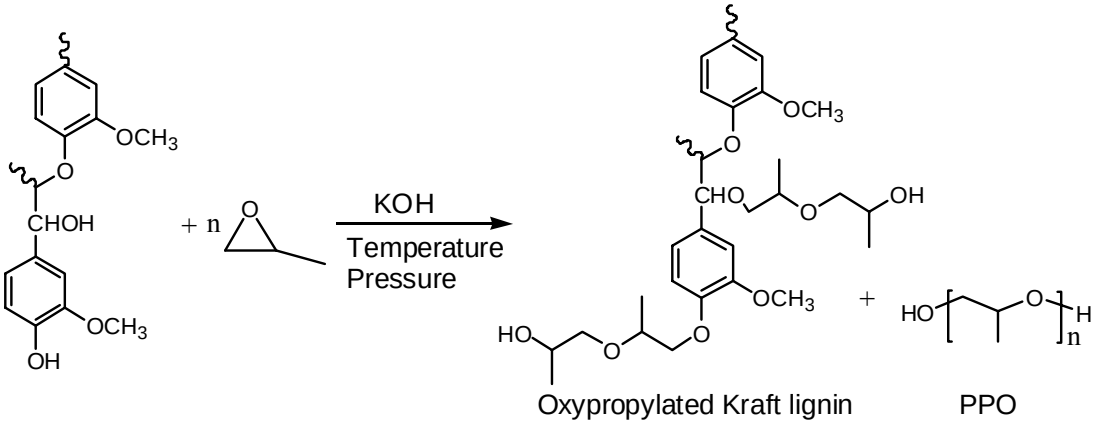

Figure 28. Reaction involved in the oxypropylation of lignin

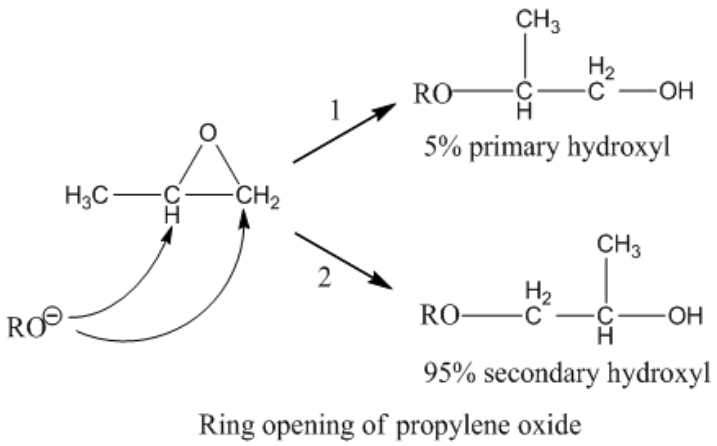

Figure 29. Oxypropylation reaction mechanism.

Lignin oxypropylation has been the subject of some prior work that accomplished with or without catalyst, and in the presence or absence of solvent, for several lignin/propylene oxide (L/PO) ratios [208, 226-228]. The documented experimental conditions required high temperatures and pressures [228], rendering the process, from the energetic point of view, less attractive. Furthermore, the presence of solid fractions was also detected if quite mild experimental conditions were applied, this could also be due to the complex nature of lignin itself [229-234]. Some researchers have carried out the oxypropylation of lignin by diluting them in organic solvents (acetone, toluene, and etc.) [235], which did not involve the total dissolution of lignin. This decreased the contribution of self-condensation reactions, but increased the reaction time and required the removal of the solvents [226].

The high functionality associated with lignin-based polyols makes them ideal for the synthesis of rigid polyurethane foams. Most of the work dedicated to the incorporation of oxypropylated lignins into rigid PU foams has been performed by Gandini's research group. The produced rigid PU foams were found to have insulating properties, dimensional stability and an accelerated aging behavior very similar to those prepared with commercial counterparts [208, 226]. For example, rigid PU foams obtained from lignin polyols together with 10 wt% of glycerol as a chain extender exhibited good thermal properties and dimensional stability, even after aging [236]. Glasser's research group has also conducted some studies devoted to the use of lignin-based polyols in the synthesis of rigid PU foams. Among others, their studies were mainly concerned with the study of flame resistance properties of the resulting cellular materials [237].

2.8 Composite Materials

A composite is a structural material that consists of two or more combined constituents that are combined at a macroscopic level and are not soluble in each other. One constituent is called the reinforcing phase and the one in which it is embedded is called the matrix. The reinforcing phase material may be in the form of fibers, particles, or flakes. The matrix phase materials are generally continuous. Examples of composite systems include concrete reinforced with steel and epoxy reinforced with graphite fibers, etc.

2.8.1 Types of Composite Materials

Composites are classified by the geometry of the reinforcement (particulate, flake, and fibers) (Figure 30) or by the type of matrix (polymer, metal, ceramic, and carbon) [238].

- Particulate composites consist of particles immersed in matrices such as alloys and ceramics. They are usually isotropic because the particles are added randomly. Particulate composites have advantages such as improved strength, increased operating temperature, oxidation resistance, etc. Typical examples include use of aluminum particles in rubber; silicon carbide particles in aluminum; and gravel, sand, and cement to make concrete.
- Flake composites consist of flat reinforcements of matrices. Typical flake materials are glass, mica, aluminum, and silver. Flake composites provide advantages such as high out-of-plane flexural modulus, higher strength, and low cost. However, flakes cannot be oriented easily and only a limited

number of materials are available for use.

- Fiber composites consist of matrices reinforced by short (discontinuous) or long (continuous) fibers. Fibers are generally anisotropic and examples include carbon and aramids. Examples of matrices are resins such as epoxy, metals such as aluminum, and ceramics such as calcium–alumino silicate. The fundamental units of continuous fiber matrix composite are unidirectional or woven fiber laminas. Laminas are stacked on top of each other at various angles to form a multidirectional laminate.
- Nanocomposites consist of materials that are of the scale of nanometers (10 nm). The accepted range to be classified as a nanocomposite is that one of the constituents is less than 100 nm. At this scale, the properties of materials are different from those of the bulk material. Generally, advanced composite materials have constituents on the microscale (10 μm). By having materials at the nanometer scale, most of the properties of the resulting composite material are better than the ones at the microscale. Not all properties of nanocomposites are better; in some cases, toughness and impact strength can decrease.

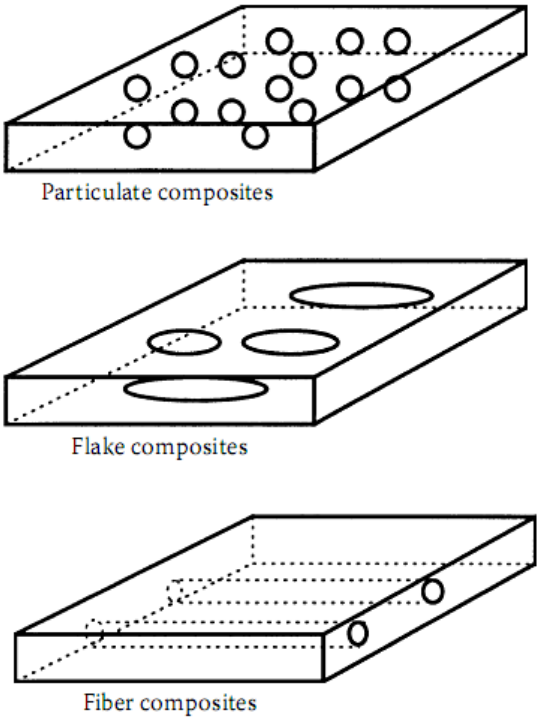

Figure 30. Types of composite based on reinforcement shape.

2.8.2 Reinforcing Factors of Fiber/Whisker-Polymer Composites

Synthetic composites are often reinforced with high-strength fibers or whiskers (short fibers). Such reinforcements are obtained via special processing schemes that generally result in low flaw/defect contents. Due to their low flaw/defect contents, the strength levels of whiskers and fibers are generally much greater than those of conventional bulk materials in which higher volume fractions of defects are present [239]. This is shown in Table 22 in which the strengths of monolithic and fiber/whisker materials are compared. The higher strengths of the whisker/fiber materials allow for the development of composite materials with intermediate strength levels, i.e., between those of the matrix and reinforcement materials. Similarly, intermediate values of modulus and other mechanical/physical properties can be achieved by the use of

composite materials.

Table 22. Summary of basic mechanical properties of selected composites constituents: fiber versus bulk properties [239].

Reinforcements	Young's modulus (GPa)	Strength[a] (MPa)
Alumina: fiber	300	2000
monolithic	382	332
Carbon: fiber	290	3100
monolithic	10	20
Glass: fiber	76	1700
monolithic	76	100
Polyethylene: fiber	172	2964
monolithic	0.4	26
Silicone carbide: fiber	406	3920
monolithic	410	500

[a]Tensile and flexural strengths for fiber and monolithic, respectively.

Fiber reinforcements of a thin diameter are of interest because [238]:

- Actual strength of materials is several magnitudes lower than the theoretical strength. This difference is due to the inherent flaws in the material. Removing these flaws can increase the strength of the material. As the fibers become smaller in diameter, the chances of an inherent flaw in the material are reduced. A steel plate may have strength of 689 MPa, while a wire made from this steel plate can have strength of 4100 MPa.
- For higher ductility and toughness, and better transfer of loads from the matrix to fiber, composites require larger surface area of the fiber–matrix interface. For the same volume fraction of fibers in a composite, the area of the fiber–matrix interface is inversely proportional to the diameter of the fiber. This implies that, for a fixed fiber volume in a given volume of composite, the area of the fiber–matrix interface is inversely proportional to the diameter

of the fiber.

- Fibers able to bend without breaking are required in manufacturing of composite materials, especially for woven fabric composites. Ability to bend increases with a decrease in the fiber diameter and is measured as flexibility. Flexibility is defined as the inverse of bending stiffness and is proportional to the inverse of the product of the elastic modulus of the fiber and the fourth power of its diameter.

The actual balance of properties of a given composite system depends on the combinations of materials that are actually used. Since it is generally restricted to mixtures of metals, polymers, or ceramics, most synthetic composites consist of mixtures of the different classes of materials that are shown in Figure 31(a). However, during composite processing, interfacial reactions can occur between the matrix and reinforcement materials. These result in the formation of interfacial phases and interfaces (boundaries), as shown schematically in Figure 31(b) [239]. Since light weight is often of importance in a large number of structural applications, especially in transportation vehicles such as cars, boats, airplanes, etc., specific mechanical properties are often considered in the selection of composite materials [239]. Specific properties are given by the ratio of a property (such as Young's modulus and strength) to the density. For example, the specific modulus is the ratio of Young's modulus to density, while specific strength is the ratio of absolute strength to density.

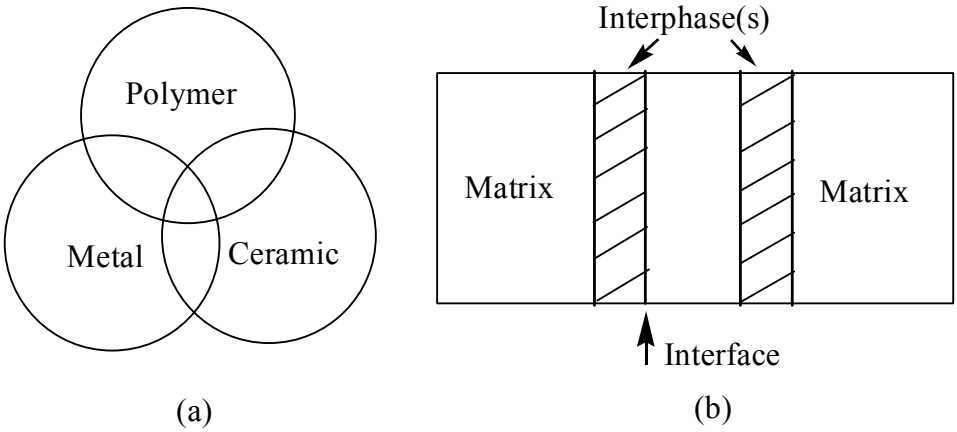

Figure 31. Schematic illustration of (a) the different types of composites and (b) interface and interphases formed between the matrix and reinforcement materials.

Four fiber/whisker factors contribute to the mechanical performance of a composite [238]:

- Length: The fibers can be long or short. Long, continuous fibers are easy to orient and process, but short fibers cannot be controlled fully for proper orientation. Long fibers provide many benefits over short fibers. These include impact resistance, low shrinkage, improved surface finish, and dimensional stability. On the other side, due to the existence of defects, the actual measured strengths of solids are generally a few orders of magnitude below the predicted theoretical strengths. Since the maximum possible crack size per unit volume increases with increasing fiber size, fiber strengths will decrease with increasing fiber length. This is because failure is more likely to initiate from larger flaws, which are more likely to exist in longer fibers. Short fibers have fewer flaws and therefore have higher strength. Short fibers also provide low cost, are easy to work with, and have fast cycle time fabrication procedures.
- Orientation: Composite architectures can be tailored to support loads in

different directions. Unidirectional fiber-reinforced architectures are, therefore, only suitable for structural applications in which the loading is applied primarily in one direction. The composite fiber may be oriented to support axial loads in such cases. Similarly, bidirectional composite systems (with two orientations of fibers) can be oriented to support loads in two directions. The fibers may also be discontinuous in nature, in which case they are known as whiskers. Whiskers generally have high strengths due to their low defect densities. Fibers oriented in one direction give rise to very high stiffness and strength in the direction of alignment. It also applies to other anisotropic properties, i.e., properties that vary significantly with changes in direction. If the fibers are oriented in more than one direction, such as in a mat, there will be high stiffness and strength in the directions of the fiber orientations. However, for the same volume of fibers per unit volume of the composite, it cannot match the stiffness and strength of unidirectional composites. Random orientations of fibers will tend to result in lower average strengths in any given direction, but have no effect on relatively isotropic properties, i.e., properties that do not vary as much in any given direction. .

- Shape: In general, the cross-sectional form of the reinforcing fibers/whiskers in composites is round-shape because handling and manufacturing them is easy. In structural mechanics, as the optimization of the stress distribution of materials some design engineers prove that noncircular or hollow-shape is better than round solid in mechanical properties and they have applied in

many structural materials, such as I-beam train road, construction support pipe/pile rod, etc. The non-round fiber cross-sections and the smaller diameter round fibers induce a larger resistance per unit volume than the larger diameter fibers. One reason for this is the larger surface interaction area between the fibers and the surrounding matrix, resulting in a higher bond and shear friction resistance. Although hexagon and squareshaped fibers are possible, their advantages of strength and high packing factors do not outweigh the difficulty in handling and processing.

- Material: Once the fibers are incorporated into the composite structure, matrix loads are transmitted to the fibers by shear. Since the fibers are stronger, they will support greater loads than the matrix can. This means that the load-carrying ability of most composites is provided by the fibers. This is always the case for polymer matrix composites in which the matrix strength and moduli are generally much less than those of the fibers. The resulting composite properties are, therefore, dependent on the fiber properties, and the polymer matrix serves mostly as a ‘‘glue’’ that keeps the structure bonded, and the fibers separated from each other. The bonding between the matrix and the fiber materials also enables stresses to be transmitted from the matrix to the fiber via shear. Since the material of the fiber directly influences the mechanical performance of a composite, fibers are generally expected to have high elastic moduli and strengths. This expectation and cost have been key factors in the graphite, aramids, and glass dominating the fiber market for composites.

Use of fibers by themselves is limited, with the exceptions of ropes and cables. Therefore, fibers are used as reinforcement to matrices. The matrix functions include binding the fibers together, protecting fibers from the environment, shielding from damage due to handling, and distributing the load to fibers. Although matrices by themselves generally have low mechanical properties compared to those of fibers, the matrix influences many mechanical properties of the composite. These properties include transverse modulus and strength, shear modulus and strength, compressive strength, interlaminar shear strength, thermal expansion coefficient, thermal resistance, and fatigue strength.

Other than the fiber and matrix other factors influence the mechanical performance of a composite include the fiber–matrix interface. Interfaces are among the most important yet least understood components of a composite material. In particular, there is a lack of understanding of processes occurring at the atomic level of interfaces, and how those processes influence the global material behavior. There is a close relationship between the processes that occur on the atomic, microscopic, and macroscopic levels. In fact, knowledge of the sequences of events occurring on these different levels is extremely important in understanding the nature of interfacial phenomena. Interfaces in composites, often considered as surfaces, are in fact zones of compositional, structural, and property gradients, typically varying in width from a single atom layer to micrometers. Among the many factors that govern the characteristics of composites involving a fibrous material, such as carbon, glass, or ceramic, and a macromolecular matrix, it is certain that the adhesion between fiber and matrix plays a predominant part. The stress transfer at the interface requires an efficient coupling

between fiber and matrix. It is important to optimize the interfacial bonding since a direct linkage between fiber and matrix gives rise to a rigid, low impact resistance material. For tough composites, the fiber-matrix interface must be sufficiently weak to allow debonding at the interface, yet strong enough for effective load transfer from the matrix to the fiber. Chemical, mechanical, and reaction bonding may form the interface [238]. In most cases, more than one type of bonding occurs. The interface bonding can be controlled either by selecting fiber and matrix materials which are thermodynamically stable at the processing and service temperatures or by applying coatings that act as diffusion barriers, thereby preventing a strong bond between the fiber and the matrix.

- Chemical bonding is formed between the fiber surface and the matrix. Some fibers bond naturally to the matrix and others do not. Coupling agents are often added to form a chemical bond. Coupling agents are compounds applied to fiber surfaces to improve the bond between the fiber and matrix. For example, silane finish is applied to glass fibers to increase adhesion with epoxy matrix.
- The natural roughness or etching of the fiber surface causing interlocking may form a mechanical bond between the fiber and matrix.
- If the thermal expansion coefficient of the matrix is higher than that of the fiber, and the manufacturing temperatures are higher than the operating temperatures, the matrix will radially shrink more than the fiber. This causes the matrix to compress around the fiber.
- Reaction bonding occurs when atoms or molecules of the fiber and the matrix

diffuse into each other at the interface. This interdiffusion often creates a distinct interfacial layer, called the interphase, with different properties from that of the fiber or the matrix. Although this thin interfacial layer helps to form a bond, it also forms microcracks in the fiber. These microcracks reduce the strength of the fiber and thus that of the composite. Weak or cracked interfaces can cause failure in composites and reduce the properties influenced by the matrix. They also allow environmental hazards such as hot gases and moisture to attack the fibers.

Weak or cracked interfaces can cause failure in composites and reduce the properties influenced by the matrix. They also allow environmental hazards such as hot gases and moisture to attack the fibers. Although a strong bond is a requirement in transferring loads from the matrix to the fiber, weak debonding of the fiber–matrix interface is used advantageously in ceramic matrix composites. Weak interfaces blunt matrix cracks and deflect them along the interface. This is the main source of improving toughness of such composites up to five times that of the monolithic ceramics.

In conclusion, the mechanical properties of a composite depend on the reinforcements, the matrix, and the interactions between those two. For a specific polymer matrix and chemical structure of the particle, the performances of the composite are affected by the particle size (length and diameter), particle aspect ratio, the native strength of the particle, and the possible chemical interactions between them. While the smaller diameter, the high aspect ratio, and high strength of the particle always play a positive role, the length of the particle and any possible chemical interactions have dual character as discussed above.

CHAPTER 3

EXPERIMENTAL MATERIALS AND PROCEDURES

3.1 Materials

3.1.1 Chemicals

Sucrose polyol, glycerol polyol, polymeric methylene diphenyl diisocyanate, dimethylcyclohexylamine and 1-methyl-4-(2-dimethylaminoethyl) piperazine were kindly provided by Huntsman Polyurethanes (The Woodlands, TX, USA). Silicone surfactant was obtained from Air Products (Allentown, PA, USA). All other chemicals were purchased either from Sigma-Aldrich (St. Louis, MO, USA) or VWR (West Chester, PA, USA), and used as received without further purification. Water in all experiments was deionized water.

3.1.2 Pulp for Preparation of Cellulose Nanowhiskers

A commercial fully bleached softwood Kraft pulp was obtained from a southeastern U.S.A manufacturing facility. It was grounded in a Wiley mill to pass through a 0.85 mm screen before sulfuric acid hydrolysis.

3.1.3 Wood for Ethanol Organosolv Pretreatment

Wood used for ethanol organosolv pretreatment originated from two loblolly pine (Pinus taeda) trees from a tree farm in North Georgia (Bowater Incorporated). They were approximately 25 years old, and were void of any visual diseases. Wood chips of 2-8 mm in thickness were first grounded into sawdust by using a Wiley mill to pass a 5 mm screen and then stored in a cold room at -5°C for future use.

3.2 Experimental procedure

3.2.1 Cellulose Nanowhiskers Preparation

Cellulose nanowhiskers were prepared following a published sulfuric acid hydrolysis procedure [87]. In brief, softwood Kraft pulp was grounded in a Wiley mill to pass through a 0.85 mm screen and then treated with sulfuric acid (64 wt%) in a ratio of 1.00 ml/g pulp at 45°C for 45 min with vigorous stirring. The reaction was halted by adding 10-fold of DI water. The sediment was centrifuged for 10 min at 12,000 rpm and the precipitate was collected, redispersed, and recentrifuged twice. The precipitate was dialyzed against water using the regenerated cellulose dialysis tubing with an approximate 12,000–14,000 molecular weight cut off until the pH did not change. To get a homogeneous nanowhiskers aqueous solution, sonication was performed for 20 min by a GEX 500 ultrasonic processor. The resulting colloidal suspension was centrifuged for 5 min at 5000 rpm and the cloudy supernatant nanowhiskers were collected and kept in the refrigerator until used.

3.2.2 Ethanol Organosolv Lignin Preparation

Pine wood chips (160 g) were first grounded into sawdust with a 5 mm screen Wiley mill and extracted with toluene and ethanol (2:1, v/v, 2L) for 48 h. Pretreatment was carried out in a Parr reactor filled with extracted sawdust, ethanol (65 %, 7:1, v/w), and concentrated sulfuric acid (1.1 wt%) at 170°C for 60 min [170]. The pretreated sawdust was washed with distilled water and separated from the liquid portion by filtration. Water was then added in the liquid to precipitate EOL which was then filtered, washed, and oven dried for future use.

3.2.3 Lignin Oxypropylation

3.2.3.1 Oxypropylation Kraft Lignin

Lignin oxypropylation reaction was carried out in a 160 mL Parr reactor equipped with a thermal mantle, mechanical stir, pressure gauge, and temperature controller. Lignin was dried at 50°C in a vacuum oven for 24 h before use. Lignin, PO, and KOH were mixed in a glass liner, sealed in the Parr reactor, and heated to 150°C [240]. The reaction completed when the pressure went back to 0. Table 23 summarizes the reactant formulations and conditions employed.

Table 23. Oxypropylation formulation and conditions of Kraft lignin.

Kraft lignin (g)	Propylene oxide (mL)	Potassium hydroxide (g)	T_{set}[a] (ºC)	T_{max} (ºC)	P_{max} (MPa)	Time[b] (min)
10	40	0.5	150	285	1.75	~9

[a] T_{set} is the reaction initiation temperature.
[b] Reaction time was recorded from the initiation temperature to the pressure reached zero.

3.2.3.2 Oxypropylation of Ethanol Organosolv Lignin

Oxypropylation of EOL was performed according to a published method [240]. EOL (20.00 mg) was mixed with PO (80.00 mL) and KOH (1.00 mg) in a 250 mL Parr reactor which was then closed and heated under stirring till 160°C. The return of the relative pressure to zero indicated the end of the reaction. The reactor was cooled and the ensuing polyol was recovered.

3.2.4 Rigid Polyurethane Foam Preparation

3.2.4.1 Preparation of Rigid PU Foam from Commercial Polyols

Rigid polyurethane foam was prepared by a literature based one-shot method [216]. This procedure involved mixing certain amount of polyols (Jeffol FX 31-240 and Jeffol SD–361), blowing agent (neopentane), catalysts (Jeff cat DMCHA and Jeff cat TR-52), and surfactant (DABCO DC 5604) at 600 rpm for 1 min. Polymeric MDI was then added under stirring at 1500 rpm for 20 s. After reacting for 3 min, sufficient polymerization and cross-linking had occurred to solidify the mixture. The foam was cured at room temperature for at least 48 h before use. Table 24 gives the formulation to prepare the control rigid polyurethane foam.

Table 24. Formulation of the control rigid polyurethane foam.

Chemicals	wt%
Sucrose based polyol	27.90
Glycerol based polyol	16.70
Polymeric MDI	40.60
Dimethycyclohexylamine	1.30
1-methyl-4-(2-dimethylaminoethyl) piperazine	0.90
neopentane	11.20
Silicone surfactant	1.40

3.2.4.2 Preparation of Rigid PU Foam from Kraft Lignin Polyol

Rigid PU foams were prepared by a one-shot method [216]. Briefly, it is formed by first mixing polyol(s) with catalysts and surfactant for ~1 min, followed by adding pentane and polymeric MDI under strong stirring until foaming was induced. All foams cured at room temperature for at least 48 h prior to characterizations, which allowed for the complete reaction of diisocyanates forming hard rigid polyurethane foams. Table 25 summarizes the amounts of each component used for individual foam preparation.

DMCHA (1.80 g) and Mannich base (0.90 g) as catalysts, pentane (10.00 g) as a blowing agent, and surfactant (1.50 g) were used at the same amounts for all formulations. The value of [NCO]/[OH] ratio was set at 1.2.

Table 25. Formulation optimization experiments set up.

Lignin polyol (wt%[a])	Sucrose polyol (g)	Glycerol polyol (g)	Polymeric MDI (g)
0	25.00	15.00	36.37
10	22.50	15.00	36.66
30	17.50	15.00	37.24
60	10.00	15.00	36.07
100	0.00	15.00	39.24
Only lignin polyol	0.00	0.00	42.20

[a]Weight percentage is based on 25.00 g of sucrose polyol used in the control foam.

3.2.4.3 Preparation of Rigid PU Foam from EOL Polyol

EOL polyol (40.00 g) was premixed with DMCHA (1.80 g), Mannich base catalyst (0.90 g), and surfactant (1.50 g) for 1 min., pentane (10.00 g) was then added together with polymeric MDI (41.59 g) under strong stirring for 25 s. Foams were cured at RT for at least 48 h.

3.2.5 Rigid Polyurethane Nanocomposite Foam Preparation

3.2.5.1 Preparation of Rigid PU Nanocomposite Foams from Commercial Polyols

Varying amounts of freeze dried cellulose nanowhiskers (based on the percentage of the total weight of polyols and polymeric MDI) were dispersed in DMF as described by Marcovish [8], and followed by the addition of sucrose-based and glycerol-based polyols under sonication. DMF was then removed under reduced pressure. The same

process steps were followed as the control foam preparation except a longer mixing time due to a higher viscosity. Foams were also cured at room temperature for at least 48 h before use.

3.2.5.2 Preparation of Rigid PU Nanocomposite Foams from EOL Polyol

Foam reinforced with 0, 1 and 5 wt% of CNWs were prepared by a one-shot method [241]. A water suspension of CNWs was directly mixed with EOL polyol followed by the removal of water under high vacuum. Compared to its dimethylformamide suspension, this method avoided freeze drying of CNWs which would cause the agglomeration of CNWs and a difficulty in redispersion as well as the large use of DMF.

3.3 Analysis procedure

3.3.1 FT-IR

3.3.1.1 FT-IR of Rigid PU Foams

Fourier transform infrared spectra of the control and nanocomposite foams were recorded between 600 and 4000 cm^{-1} with a resolution of 4.00 cm^{-1} and 64 scans on a Magna 550 Fourier transform infrared spectrometer. A fine powder of PU foam was prepared by manually grinding the foam and mixing with KBr to obtain pellets with a 1 mm thickness using an air-powered pellet press.

3.3.1.2 FT-IR of Lignin and Oxypropylated Lignin

FT-IR spectra of lignin before and after oxypropylation were recorded between 4,000 and 600 cm^{-1} with a resolution of 4.0 cm^{-1} and 64 scans on a Magna 550 FT-IR Spectrometer. KBr powders were used to obtain lignin (1%, w/w) pellets with a

thickness of 1 mm using an air-powered pellet press.

3.3.2 SEM

3.3.2.1 SEM of Commercial Polyol-based Rigid PU Foams

The cell structure of the control foam and nanocomposite foams were examined by a LEO 1530 field emission scanning electron microscope (FE-SEM). A small sample of the foam (5 mm×5mm×1 mm) was cut and placed on one side of a double-sided carbon tape. Samples were coated with gold palladium using Electron Microscopy Sciences 350 sputter coating to prevent charge build-up during SEM analysis. Images were obtained under a 5 kV accelerating voltage.

3.3.2.2 SEM of Kraft Lignin/EOL-based Rigid PU Foams

SEM images of the prepared rigid PU foams were taken by a Hitachi S-800 FE-SEM. Five samples (5 mm × 5 mm × 1 mm) were cut from different parts of each foam by using a sharp blade and placed on one side of a double-side carbon tape. Samples were coated with a gold palladium sputter coater to prevent charge build up during imaging. Images were taken under an accelerating voltage of 10 kV and magnification of 40. Five images from different parts of each foam were taken for an average cell size analysis.

3.3.3 AFM of Cellulose Nanowhiskers

The atomic force microscope was used to examine the dimensions of cellulose nanowhiskers using Digital Instruments Dimension 3100 Nanoscope equipped with a Digital Instruments IIIa controller (Veeco Instrument Inc, Santa Babara, CA, USA) in multimode. All the samples were imaged in tapping mode. Amplitude images at 5 μ and 2.5 μ scans were recorded. A drop of diluted suspension of cellulose nanowhiskers was deposited onto the freshly cleaved mica and left to dry at room temperature for 12 h.

3.3.4 NMR Spectroscope

All NMR experiments were performed with a Bruker Avance-400 spectrometer (Billerica, MA, USA). The data analysis was done using Mnova NMR Data Processing software (Mestrelab Research SL, Santiago de Compostela, Spain).

3.3.4.1 ^{1}H NMR Characterization of Kraft Lignin before and after Oxypropylation

^{1}H NMR spectra were acquired on dry samples (~20 mg) in DMSO-d_6 (450 μL) applying 90^{o} pulse angle and 15 s pulse delay. 120 scans were collected at room temperature. The spectrum was processed with 1.0 Hz line broadening and no zero filling.

3.3.4.2 ^{13}C NMR Characterization of Kraft Lignin before and after Oxypropylation

Quantitative ^{13}C NMR spectra were also collected on dry samples (80-120 mg) dissolved in DMSO-d_6 (450 μL). An inverse-gated decoupling pulse sequence was used. 10,000 scans were collected at 100.59 MHz operating frequency, 90^{o} pulse angle, and a 12 s pulse delay at room temperature. The spectrum was processed with 10.0 Hz line broadening and no zero filling.

3.3.4.3 ^{31}P NMR Characterization of Kraft/EOL Lignin before and after Oxypropylation

2-Chloro-4,4,5,5-tetramethyl -1,3,2-dioxaphospholane (TMDP) was used as a phosphitylation reagent for the ^{31}P NMR analysis [242]. Briefly, a relaxation reagent solution (chromium (III) acetylacetonated, 3.6 mg mL^{-1}) and an internal standard solution (N-hydroxy-5-norborene-1,3-dicarboximide (NHND), 4mg mL^{-1}) were prepared in a mixed solvent of pyridine and $CDCl_3$ (1.6:1, v/v). 20-25 mg of lignin/lignin polyol was dissolved in 0.5 mL solvent in a vial, followed by TMDP (0.1 mL) addition which was

stirred for 10 min prior to NMR analysis [243]. Quantitative ^{31}P NMR spectra were acquired using an inverse-gated decoupling pulse sequence with 90° pulse angle, 25 s pulse delay. 200 scans were collected at room temperature. The spectrum was processed with 4.0 Hz line broadening and no zero filling.

3.3.5 GPC Analysis of Lignin before and after Oxypropylation

Acetylation of the GPC samples was carried out according to a published method [243]. In brief, dry lignin/oxypropylated lignin (~20 mg) was added to a solution of acetic anhydride and pyridine mixture (1:1, v/v, 2 mL) and then stirred at room temperature for 72 h. The solvent mixture was removed under reduced pressure at 50°C. The acetylated product was dissolved in chloroform (50 mL) and washed with water (20 mL). The chloroform phase was dried over anhydrous $MgSO_4$ and then concentrated under reduced pressure. The dry acetylated lignin/oxypropylated lignin was then dissolved in THF (~1 mg mL^{-1}) for GPC analysis.

The molecular weight of lignin before and after oxypropylation was examined by GPC employing an Agilent Technologies 1200 series analysis system consisting of an autosampler, a UV detector, and four columns of Styragel HR 0.5, HR 2, HR4, and HR 6 (Waters, Inc., Milford, MA) linked in series using THF as the eluent (1.0 mL min^{-1}). The acetylated sample was dissolved in THF (1 mg mL^{-1}), filtered through a 0.45 μm filter, injected (20 μL) into the GPC system, and detected by a UV detector at 270 nm. A calibration curve was constructed based on eight narrow polystyrene standards ranging in molar weight from 1.5×10^3 to 3.6×10^6 g mol^{-1}. Data collection and processing were performed using Polymer Standards Service WinGPC Unity software (version 7.2.1, Polymer Standards Service USA, Inc., Warwick, RI).

3.3.6 Mechanical Testing

3.3.6.1 Tensile Testing of Commercial polyol-based Rigid PU Foams

Tensile testing was performed on the Instron Corporation tensile testing machine 5566 according to ASTM D 638-08 using type IV specimen with dimension: thickness = 4 mm, width = 6 mm, gage length = 25 mm [244]. The crosshead speed was 5 mm min^{-1}. Wedge type grips were employed to clamp specimen ends. Load displacement data were recorded during the experiment using a data acquisition system for further analysis.

3.3.6.2 Compression Testing of Commercial Polyol-based Rigid PU Foams

Compression testing was carried out with a 17-71 TMI Monitor Compression tester according to ASTM C 365M-05 on cylindrical specimens with dimension: diameter = 30 mm, height = 15 mm [244]. The crosshead speed was 6 mm min^{-1}. The tests were terminated when the applied load reached a densification level of 80%. Specimen displacement was recorded from the crosshead movement using a data acquisition system.

3.3.6.3 Compression Testing of Kraft/EOL-based Rigid PU Foams

Compression testing was carried out on a MTS Insight 2 universal test machine according to ASTM C365/C365M-05. Five specimens with a square section of 25 mm × 25 mm and a thickness of 15 mm were cut off from each foam. The crosshead speed was 4 mm min^{-1}. Tests were terminated when it reached a densification level of 80%. Specimen displacement was recorded from the crosshead movement by a data acquisition system.

3.3.7 Dynamic Mechanical Analysis (DMA) of Commercial Polyol-based Rigid PU

Foams

DMA was carried out with a Q800 TA Instrument in tension clamps. The specimen was rectangular strips with dimensions of 10 mm × 6 mm × 5 mm. Measurements were performed at 1 Hz frequency. A temperature scan mode was used from room temperature to 180ºC with a heating rate of 2 ºC min^{-1}.

3.3.8 Differential Scanning Calorimetry (DSC) Analysis of Rigid PU Foams

DSC Experiments were performed using a Q200 TA instrument. Sample of approximately 10 mg was heated up from −80°C to 150°C at a heating rate of 10 °C min^{-1} under a nitrogen gas atmosphere. The heat flow as a function of temperature was recorded during the experiment by a Universal Analysis 2000 data acquisition system.

3.3.9 Thermogravimetric Analysis (TGA) of Rigid PU Foams

TGA was performed by using a TGA Q5000 TA instrument. Experiments were carried out under nitrogen gas flux of 25 mL min^{-1}. Samples were cut into small rectangular pieces weighing 7–10 mg. The samples were placed in a platinum sample pan, sealed in the furnace, and heated to 700°C at a heating rate of 10 °C min^{-1}. The real time weight loss as a function of the temperature was recorded during the experiment by a Universal Analysis 2000 data acquisition system.

CHAPTER 4

RIGID POLYURETHANE FOAM REINFORCED WITH CELLULOSE NANOWHISKERS[2]

4.1 Introduction

Cellulose is the most abundant renewable polymer in nature, representing about 1.5×10^{12} tons of the total annual biomass production, and is considered a valuable bioresource to address the increasing demand of environmentally friendly and biocompatible products [1]. Cellulose is composed of assemblies of microfibrils where the polymeric chains of β-(1,4)-D-glucose molecules are stabilized by inter and intramolecular hydrogen bonding [116]. The microfibrils consist of crystalline domains separated by amorphous domains with length varies from 100 nm to several microns [1, 116]. Upon acid hydrolysis, transverse cleavage typically occurs at the amorphous regions, and under certain conditions cellulose nanowhiskers (CNWs) are released. The diameter of CNWs is typically on the order of 10-20 nm and the length ranges from 100-300 nm for wood-based CNWs to a few microns when derived from tunicate cellulose [1]. These highly ordered nanostructures exhibit high bending strength of 10

[2] The preliminary data of this research was accepted for publication in Nano-Micro Letters, 2010. It is entitled as "Rigid Polyurethane Foam Reinforced with Cellulose Whiskers: Synthesis and Characterization". The other authors are Arthur J. Ragauskas from the Institute of Paper Science and Technology and School of Chemistry and Biochemistry at Georgia Institute of Technology and Hongfeng Ren from School of Materials Science and Engineering at Georgia Institute of Technology. The full data of this research was accepted for publication in Journal of Nanoscience and Nanotechnology, 2011. It is entitled as "Rigid Polyurethane Foam/Cellulose Whisker Nanocomposites: Preparation, Characterization, and Properties". The other authors are Arthur J. Ragauskas from the Institute of Paper Science and Technology and School of Chemistry and Biochemistry at Georgia Institute of Technology and Hongfeng Ren from School of Materials Science and Engineering at Georgia Institute of Technology.

GPa, high elastic modulus of 143 GPa, and significant changes in electrical, optical, and magnetic properties compared to the typical micron sized cellulose fibers [2-4] . There has been a growing interest in nanocomposite preparation by adding CNWs into natural or synthetic polymers in the last decade [4-8, 245]. A good dispersion of cellulose nanowhiskers within the polymer matrix is critical since CNWs have a strong tendency to aggregate via hydrogen bonding [246-247]. The resulting nanocomposites exhibited improved mechanical and thermal properties which are primarily due to the extensive hydrogen bonding between cellulose nanowhiskers and the polymer matrix, and in some cases, chemical interactions as well [3, 6-8, 87, 245].

Polyurethane is an important commercial plastic possessing a wide range of physical and chemical properties based on various formulations [20]. It is used in a wide variety of applications to create all manner of consumer and industrial products. Rigid PU foam is a highly crosslinked polymer with a closed-cell structure. It is typically prepared from polymeric MDI and polyether polyols with hydroxyl index (I_{OH}) of 300-800 mg KOH/g and viscosity below 300 Pa·s [240, 248]. Rigid PU foam offers low density, low thermal conductivity, and low moisture permeability properties along with a high strength to weight ratio as a performance attribute [17, 20]. It is one of the most common polymeric foam used on a global basis, which is reflected in its multitude of applications including ship-building, automotive, furniture, footwear, packaging, etc [20]. One of the largest applications of rigid polyurethane foam comes about from its use as a core for sandwich panels, which are high performance materials exhibiting exceptional strength properties while having low density. There is a growing application of light weight sandwich panels in transportation systems as the high strength

to weight property reduces the amount of fuel used in transporting these materials [31, 249]. However, rigid PU foam is not as stiff as other traditional materials, such as wood and steel, and due to weak core properties failures can occur in the form of wrinkling of the skin, crushing of core, core–shear and core-skin debonding [250]. Therefore, a substantial effort has been directed towards developing high performance rigid PU foams. Cellulose fiber modified water-blown soy polyol-based PU foams were reported to have increased density and rigidity [17, 251]. Rigid PU foams reinforced with spherical TiO_2, platelet nanoclay, rod-shaped carbon nanofibers, and pristine and organically-modified layered silicates have also been investigated and shown to significantly enhance the thermal and mechanical properties of the nanocomposites [196, 244, 250].

The application of cellulose nanowhiskers in polyurethanes has been recently studied by several groups. Polyurethane elastic films were prepared in either organic medium [8, 110, 215], i.e., DMF, or water medium [4, 203-204, 218]. Hydrogen bonding interactions between cellulose nanowhiskers and the polymer matrix were found to favor CNWs dispersion in polyurethane and provide a good adhesion in the interfacial areas [4, 8, 215]. The addition of CNWs can significantly increase the tensile modulus of polyurethane elastomers at very low filler loading though a decrease of the creep deformation [4, 8, 93, 203, 215]. It is believed the three dimensional network linked by intermolecular hydrogen bonding of cellulose nanowhiskers and chemical bonding between nanowhiskers hydroxyl groups and isocyanate groups are part of the reason for the improvement [4, 8]. Cellulose nanowhiskers promoted the phase separation of soft and hard domains of polyurethane which resulted in an increased crystallinity of the soft domain and generated an upward shift of the glass transition temperature, an increase in

tensile modulus, and a decrease in deformation at break of the nanocomposite [110, 215].

In present study, we summarized the benefits of reinforcing rigid PU foams with varying amounts of cellulose nanowhiskers, particularly with respect to the improvements in mechanical properties of the resulting nanocomposites. Scanning electron microscope was used to characterize the cell structure of nanocomposite foams. FT-IR spectra were recorded to study the chemical structure of the nanocomposites. Tensile and compressive properties as well as thermal stability and thermal mechanical property were compared between the control foam and nanocomposite foams.

4.2 Experimental section

4.2.1 Chemicals and materials

A commercial fully bleached softwood Kraft pulp was used to prepare cellulose nanowhiskers. Sulfuric acid (98%, w/w), DMF and neopentane were purchased from VWR. Polymeric MDI with an average functionality of 2.7 and NCO content of 31.5% (Rubinate M), sucrose-based polyether polyol (Jeffol SD-361), glycerol-based polyether polyol (Jeffol FX 31-240), dimethylcyclohexylamine (Jeff cat DMCHA), and 1-methyl-4-(2-dimethylaminoethyl) piperazine (Jeff cat TR-52) were all kindly provided by Huntsman Polyurethanes. Silicone surfactant (DABCO DC 5604) was obtained from Air Products and Chemicals, Inc. All chemicals were used as received. The characteristic parameters of polyols and polymeric MDI were summarized in Table 26.

Table 26. Technical characteristics of polyols and polymeric MDI.

Chemical	M_n	Functionality	I_{OH}[a]	NCO(%)[b]
Sucrose-based polyol	690	4.4	360	-
Glycerol-based polyol	700	3.0	240	-
Polymeric MDI	340	2.7	-	31.1

[a]Hydroxyl index I_{OH} is defined as the weight of KOH in mg that will neutralize the acetic anhydride capable of reacting by acetylation with 1 g polyol. [b]Isocyanate content *NCO*(%) is the weight percentage of reactive isocyanate groups in an isocyanate.

4.2.2 Preparation of Cellulose Nanowhiskers

Cellulose nanowhiskers were prepared as described in Chapter 3 (3.2.1 Cellulose nanowhiskers preparation).

4.2.3 Preparation of Rigid Polyurethane Foam

Rigid polyurethane foam was prepared as described in Chapter 3 (3.2.4.1 Preparation of rigid PU foam from commercial polyols). As isocyanate is a very reactive chemical and can easily react with trace water present in the starting materials and/or react with itself forming trimers, a molar ratio of isocyanate (NCO) to hydroxyl (OH) higher than 1.0 is often used [196, 216-217]. A molar ratio of 1.1 was chose in present study to ensure a complete reaction of hydroxyl groups.

4.2.4 Preparation of Rigid Polyurethane Nanocomposite Foam

Rigid polyurethane nanocomposite foams were prepared as described in Chapter 3 (3.2.5.1 Preparation of rigid PU nanocomposite foams from commercial polyols). The same formulation as the control foam was used for all nanocomposites preparation except for the amounts of cellulose nanowhiskers added.

4.2.5 Materials Characterization

The dimension of sulfuric acid hydrolyzed cellulose nanowhiskers was measured by AFM as described in Chapter 3 (3.3.3 AFM of Cellulose Nanowhiskers).

The cell structure of the control and nanocomposite foams were examined by a LEO 1530 FE-SEM as described in Chapter 3 (3.3.2.1 SEM of commercial polyol-based rigid PU foams). FT-IR spectra of the control and nanocomposite foams were recorded as described in Chapter 3 (3.3.1.1 FT-IR of rigid PU foams).

4.2.6 Tensile Testing

Tensile properties of the prepared foams were studied as described in Chapter 3 (3.3.7.1 Tesile testing of the commercial polyol-based rigid PU foams). The tensile modulus was calculated from the slope of the initial linear part of the stress-strain curve, while the maximum stress of the initial linear part and the stress at failure were taken as the yield strength and tensile strength. For each data point, five samples were tested, and the average value was calculated along with the standard deviation.

4.2.7 Compression Testing

Compressive properties of the resulting foams were studied as described in Chapter 3 (3.3.7.2 Compression testing of the commercial polyol-based rigid PU foams) The initial slope of the stress-strain curve is used to calculate the compressive modulus and the intersection point between the initial slope and the plateau slope is used to calculate the strength [250]. For each data point, five samples were tested, and the average value was calculated along with the standard deviation.

4.2.8 DSC Analysis

The glass transition temperature of the control foam and nanocomposite foams was determined by DSC analysis as described in Chapter 3 (3.3.9 Differential scanning

calorimetry (DSC) analysis of rigid PU foams).

4.2.9 Thermogravimetric Analysis

The thermal stability of the control foam and nanocomposite foams was studied by TGA using a Q5000 TA Instrument as described in Chapter 3 (3.3.10 Thermogravimetric analysis (TGA) of rigid PU foams)

4.2.10 Thermal Mechanical Testing

The thermomechanical response of the resulting foams was studied by DMA as previously described in Chapter 3 (3.3.8 Dynamic mechanical analysis (DMA) of commercial polyol-based rigid PU foams) The main relaxation temperatures associated with T_g were determined from the temperature position of the maximum in tan δ.

4.3 Results and Discussion

Two sensitive and important factors to make rigid PU nanocomposite foams are the presence of water and the dispersion of cellulose nanowhiskers in the polymer matrix. As water can act as a chemical blowing agent due to the release of carbon dioxide when reacting with isocyanates, its content in cellulose nanowhiskers needs to be controlled. Hence, for this study freeze dried cellulose nanowhiskers were dispersed in DMF by sonication to assist the mix with polyurethane reagents. Pentane was used as a physical blowing agent due to its general availability and reported benefits to the physical properties of the PU foam [252], while water is usually used for flexible PU foam preparation.

Several experiments were set up with different formulations in order to prepare rigid polyurethane foam with adequate reaction time, easy process, and proper foam shape (no shrinkage), according to both literature and industrial data. The best formulation finally chosen to use in this study was listed in Table 24 in Chapter 3 (3.2.4.1 Preparation of Rigid PU Foam from Commercial Polyols). The control foam was synthesized with a density of 53.8 kg m^{-3} (a standard deviation of 0.5 kg m^{-3}). Repeating the same experiments in presence of varying amounts of cellulose nanowhiskers (Figure 32: 150-250 nm in length and 10-20 nm in width) generated PU nanocomposite foams. Nanocomposite foam reinforced with 0.75 wt% of CNWs were produced with a similar density (53.6 ± 0.3 kg m^{-3}) as the control foam, while other nanocomposite foams had either a lower or higher density than the control foam. This was primarily due to the high volatility of n-pentane (36.1ºC) which resulted in differing losses of the blowing agent during mixing. Table 27 reports the densities of foams prepared in this study.

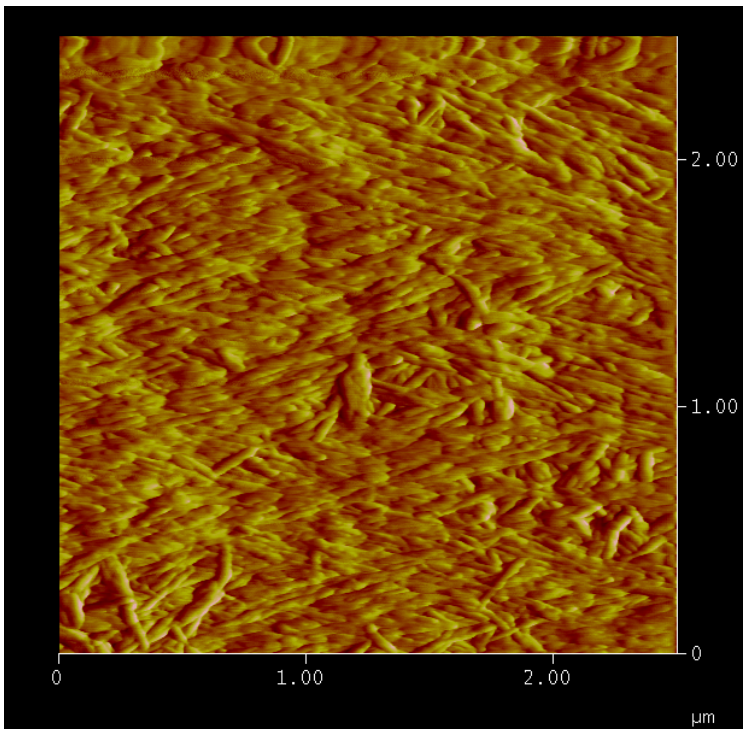

Figure 32. AFM image of sulfuric acid hydrolyzed cellulose nanowhiskers.

Table 27. Density of the control foam and nanocomposite foams.

CNWs (wt %)	Density (kg m^{-3})
0	53.8 ± 0.5
0.25	41.4 ± 0.5
0.50	46.2 ± 0.6
0.75	53.6 ± 0.3
1.00	82.0 ± 0.6

Scanning electron microscope images in Figure 33 show the cell structure of the control foam and nanocomposite foams reinforced with 0.25, 0.50, 0.75 and 1.00 wt% of cellulose nanowhiskers. The closed cells were homogeneously dispersed in the nanocomposites. The cell size was around 350 µm and decreased slightly with increasing CNWs content as summarized in Table 28. This is presumably because cellulose nanowhiskers served as nucleation sites to facilitate the bubble nucleation process and the increased number of nucleation sites led to a finer cell structure

[253-254].

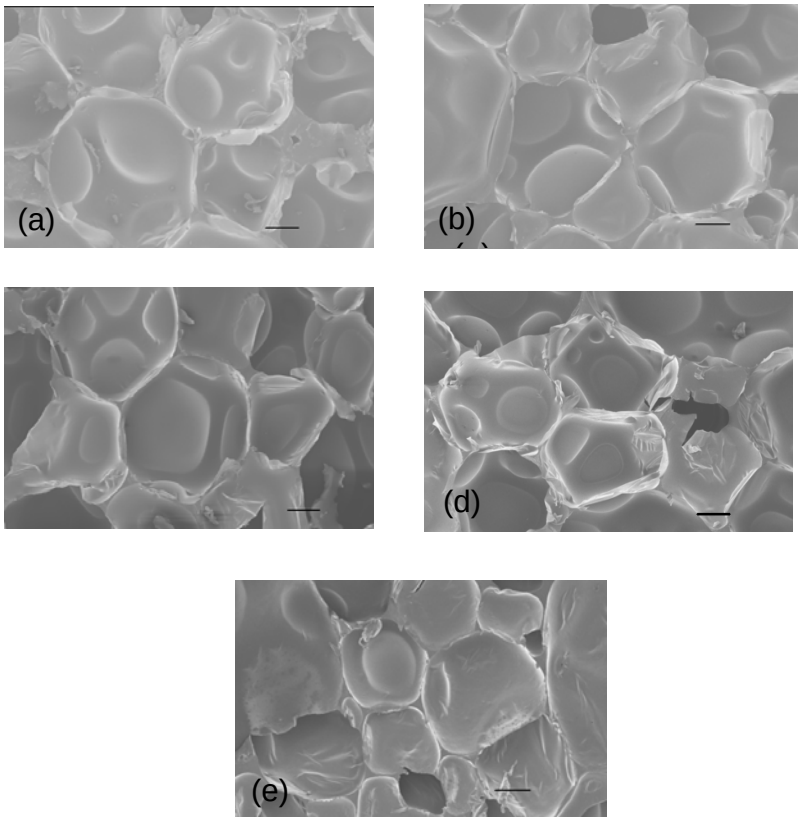

Figure 33. SEM images of (a) the control foam and foams reinforced with (b) 0.25, (c) 0.50, (d) 0.75, and (e) 1.00 wt% of cellulose nanowhiskers. Scale bar: 100 μm.

Table 28. Individual cell size of the control foam and nanocomposite foams.

CNWs (wt %)	Cell size (μm)
0	376 ± 41
0.25	358 ± 25
0.50	345 ± 54
0.75	339 ± 28
1.00	323 ± 23

FT-IR spectroscopy was utilized to study the chemical structures of rigid PU foams. The FT-IR spectra of the control foam and nanocomposite foams are shown in

Figure 34. The presence of urethane linkages could be readily observed due to the NH stretching and bending vibration absorptions at 3320 cm^{-1} and 1530 cm^{-1}, OC=O stretching vibration at 1730 cm^{-1}, and CO-NH vibration at 1600 cm^{-1}. Methyl group at 2930 cm^{-1}, O-CO at 1230 cm^{-1} and C-O at 1090 cm^{-1} were primarily from the polyether polyol [248], while a minor contribution was from cellulose nanowhiskers. Most of these functional groups were nearly identical for both the control foam and nanocomposite foams, which indicated the dominant chemical structure of the foam was not altered by the presence of cellulose nanowhiskers. Extensive hydrogen bonding was a characteristic of polyurethane matrix [255]. Functional groups acting as acceptors in the hydrogen bonding with NH are the urethane carbonyl (-C=O) in hard segment, ether (-C-O-C) in soft segment of polyurethane, and hydroxyl groups and ether oxygens of cellulose nanowhiskers [4]. Some researchers found other changes in FT-IR spectra when reinforcing PU with cellulose derivatives or cellulose nanocrystals, such as additional peaks at 1100 cm^{-1} (C-O-C) from cellulose anhydroglucose unit, and increased OH signal intensity at 3300 cm^{-1} [217]. The filler contents in those studies ranged from 5 wt% to 30 wt%, which were much higher than 1.00 wt% used in present study. It is most likely the reason that these features were not observed in Figure 34. However, we did observe that the peak of the carbonyl stretching vibration shifts from 1732 to 1736 cm^{-1} gradually, though this change was smaller compared to that of Cao et al.'s work with a 30% maximum incorporation of cellulose nanocrystals [4]. The shift suggested the incorporation of cellulose nanowhiskers in PU matrix disturbed the hydrogen bonding between NH and C=O and improved the microphase separation between hard and soft segments due to the strong interaction between cellulose nanowhiskers and PU [4, 110,

215].

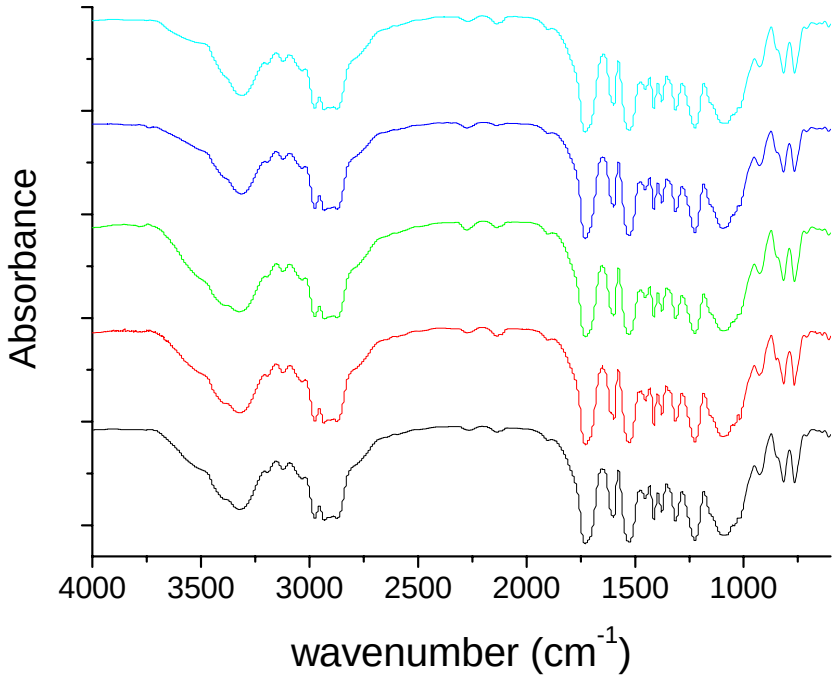

Figure 34. FT-IR spectra of the control foam, nanocomposite foams reinforced with 0.25, 0.50, 0.75 and 1.00 wt% cellulose whiskers (from bottom to top).

In order to investigate other interactions that may exist between cellulose nanowhiskers and the polyurethane matrix, a spectrum of the control foam and 1.00 wt% cellulose nanowhiskers mixed mechanically after PU polymerization was recorded in Figure 35. Compared to the mixture, the nanocomposite foam showed a reduction in the intensity of the signal center at 3500 cm^{-1} which was ascribed to the cellulose O-H stretching vibration and polyurethane N-H stretching vibration. The intensity decrease can be attributed to the crosslinking of cellulose hydroxyl groups with isocyanate units during polyurethane synthesis.

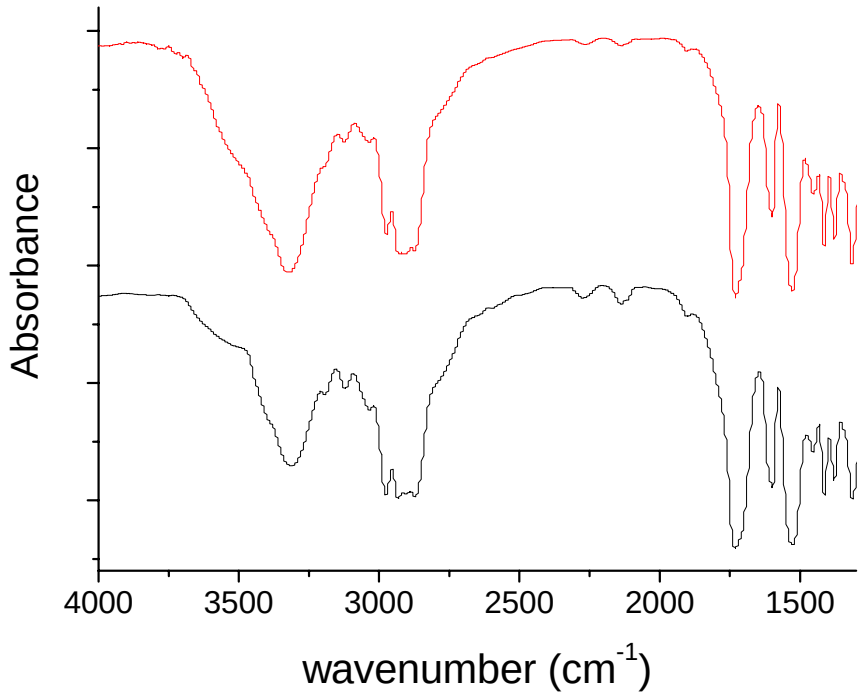

Figure 35. FT-IR spectra of the nanocomposite foam reinforced with 1.00 wt% nanowhiskers (bottom) and the mechanical mixture of the control foam and 1.00 wt% nanowhiskers (top).

Tensile stress-strain curves of the control foam and nanocomposite foams are shown in Figure 36. The tensile properties were reported in terms of tensile modulus, yield strength and tensile strength as summarized in Table 29. Since density plays an important role in the mechanical properties of rigid PU foam, data were present as the unit mass value for comparison between different samples. The incorporation of 0.25 and 0.50 wt% cellulose nanowhiskers slightly reduced tensile strength and modulus. However, rigid polyurethane foam reinforced with 0.75 wt% cellulose nanowhiskers exhibited higher tensile modulus, yield strength and tensile strength by 37.5%, 16.7% and 11.1%, respectively, compared to the control foam. An even significantly improvement was observed at 1.00 wt% cellulose nanowhiskers reinforced PU foam. The tensile modulus, yield strength and tensile strength were dramatically enhanced by 112.5%,

33.3% and 33.3%, respectively

.

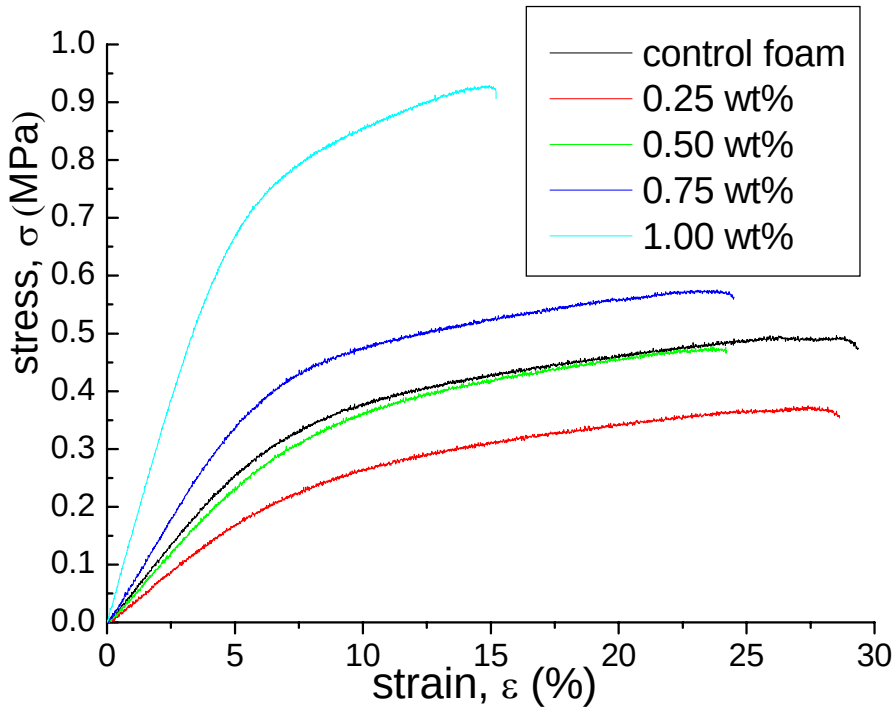

Figure 36. Tensile stress-strain curves of the control foam and nanocomposite foams.

Table 29. Tensile properties of the control foam and nanocomposite foams.

CNWs	Tensile modulus (MPa)		Yield strength (MPa)		Tensile strength (MPa)	
(wt%)	Average	per unit mass	Average	per unit mass	Average	per unit mass
0	4.37 ± 0.41	0.08	0.316 ± 0.031	0.006	0.485 ± 0.043	0.009
0.25	3.04 ± 0.05	0.07	0.208 ± 0.013	0.005	0.354 ± 0.018	0.009
0.50	3.47 ± 0.10	0.08	0.244 ± 0.012	0.005	0.381 ± 0.011	0.008
0.75	5.98 ± 0.37	0.11	0.364 ± 0.025	0.007	0.552 ± 0.015	0.010
1.00	14.30 ± 0.70	0.17	0.670 ± 0.035	0.008	0.966 ± 0.058	0.012

Compressive stress-strain curves of the control foam and nanocomposite foams are shown in Figure 37. The compressive properties were given in terms of compressive modulus and compressive strength as summarized in Table 30. Data were also present as unit mass value for comparison between different foams. All curves

showed three stages of deformation: initial linear behavior, linear plateau region, and densification. It was observed that the incorporation of cellulose nanowhiskers had a more remarkable impact on compressive modulus in comparison to compressive strength. Rigid PU foam reinforced with 0.25 wt% cellulose nanowhiskers showed a strength improvement of 66.7% and it leveled off at cellulose nanowhiskers content of 0.50 wt% and above. However, the compressive modulus of the nanocomposites was enhanced by 116.7%, 166.7% and 183.3%, respectively, with increasing cellulose nanowhiskers content from 0.25 wt%, 0.50 wt% to 0.75 wt%. Its effect was reduced at 1.00 wt% cellulose nanowhiskers content as the compressive modulus was only increased by 100% compared to the control foam. Overall, substantial improvement of the compressive properties of rigid polyurethane foam reinforced with cellulose nanowhiskers was observed at much lower filler content (≤ 1.00 wt%) in comparison to foams reinforced with other inorganic particles [196, 244, 250].

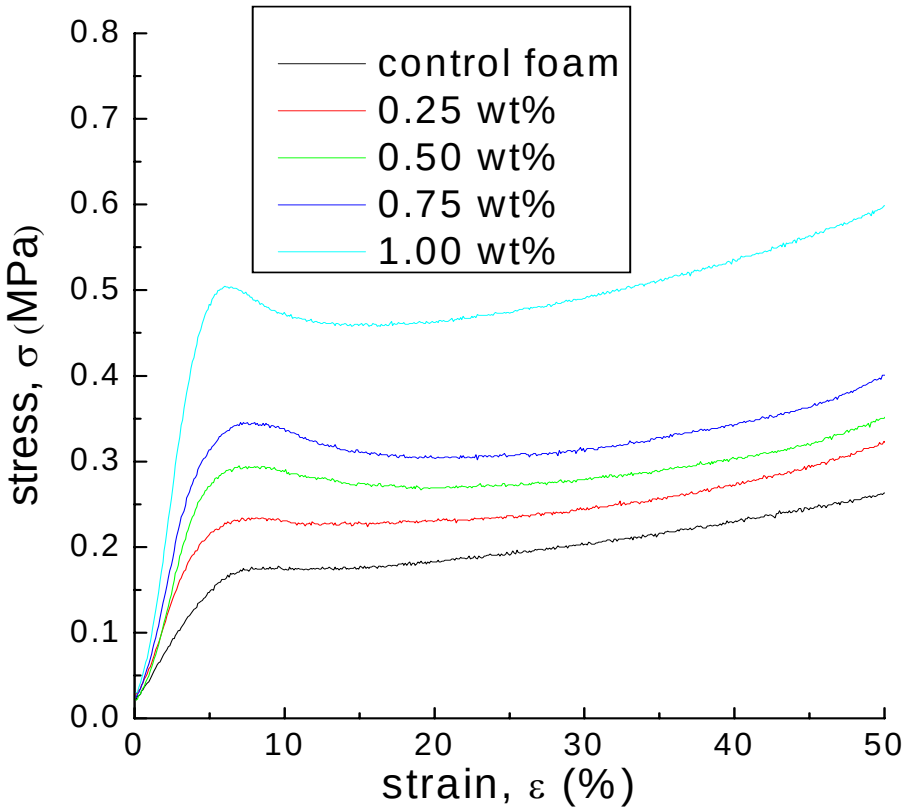

Figure 37. Compressive stress-strain curves of the control foam and nanocomposite foams.

Table 30. Compressive properties of the control foam and nanocomposite foams.

CNWs (wt%)	Compressive modulus (MPa)		Compressive strength(MPa)	
	Average	per unit mass	Average	per unit mass
0	3.29 ± 0.58	0.06	0.145 ± 0.045	0.003
0.25	5.48 ± 0.27	0.13	0.187 ± 0.016	0.005
0.50	7.19 ± 0.12	0.16	0.335 ± 0.000	0.007
0.75	9.21 ± 0.00	0.17	0.353 ± 0.007	0.007
1.00	10.20 ± 0.81	0.12	0.536 ± 0.000	0.007

In general, tensile property especially compressive property of rigid polyurethane foams were improved by the addition of cellulose nanowhiskers as reinforcing fillers at low contents (≤ 1.00 wt%). Several factors are associated with the observed improvements. First of all, cellulose nanowhiskers have an intrinsic high bending

strength of 10 GPa, high elastic modulus of 143 GPa, and high aspect ratio [3-4, 244], which undoubtedly contributed to the enhancement of mechanical properties of the nanocomposites. The high specific surface area of cellulose nanowhiskers also made a significant contribution as it introduced higher potential for chemical crosslinking and hydrogen bonding between CNWs and the polyurethane matrix. The well dispersed cellulose nanowhiskers may also serve as nucleating agents in the foaming process for a fine cell structure as stated in a previous study [116]. Finally, a common explanation for the improvement of mechanical properties of nanocomposites is the creation of multiple crack sites and/or multiple cracks branching due to the presence of nanoparticles into the polymer which delays the fracture processes in nanocomposites [250].

The thermograms of differential scanning calorimetry in Figure 38 indicate that T_g of the nanocomposite foams is higher than that of the control foam, and it shifts to a higher value with increasing cellulose nanowhiskers content as shown in Table 31. It is the same result as previous researches on cellulose nanowhiskers reinforced polyurethane elastic films [110, 215]. Cellulose nanowhiskers interrupted the interaction between soft and hard segments of polyurethane resulting in improved microphase separation. This promoted the crystallization of soft segment and resulted in an increase of T_g. Alternatively, the solid surface of cellulose nanowhiskers induced a restricted mobility of polyurethane chains by forming hydrogen bonds and chemical crosslinking within the polymeric matrix, which also resulted in the shift of T_g toward a higher value.

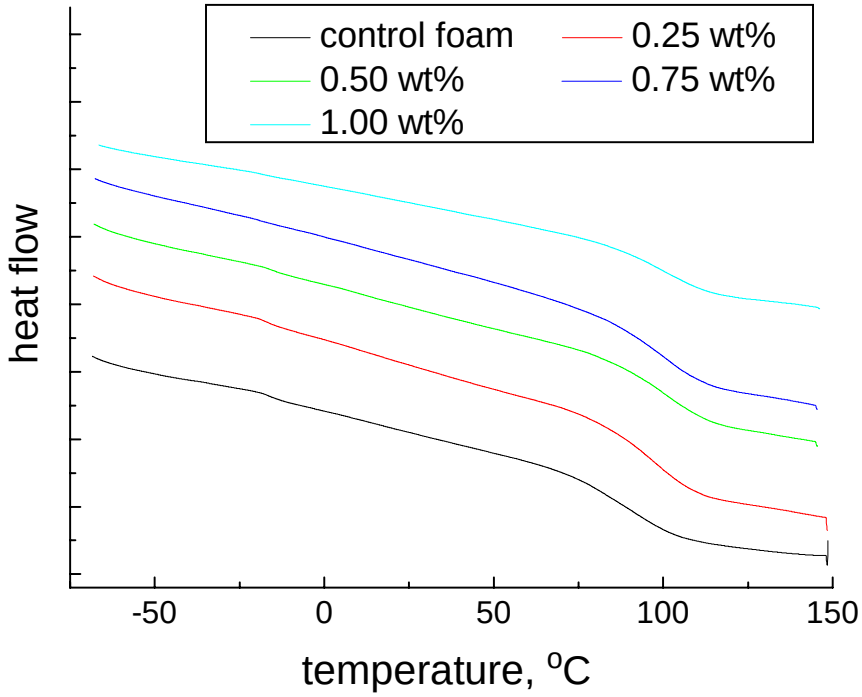

Figure 38. DSC curves of the control foam and nanocomposite foams. The DSC curves were shifted showing a relative value of heat flow for easy illustration.

The thermograms of thermogravimetric analysis of the control foam and nanocomposite foams are shown in Figure 39. Polyurethane decomposition starts at around 250ºC. The change of T_d is not obvious at low cellulose nanowhiskers contents. However, when the content reaches 1.00 wt%, T_d is increased by 10ºC as shown in Table 31 indicating a higher thermal stability of the nanocomposite foam.

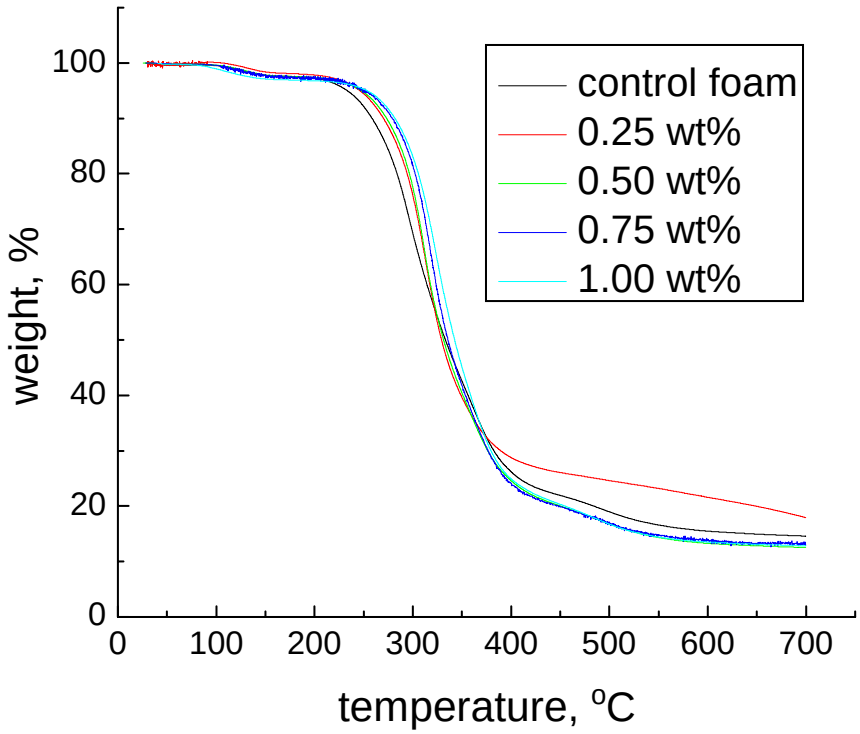

Figure 39. TGA curves of the control foam and nanocomposite foams.

Table 31. Glass transition temperature and decomposition temperature of the prepared rigid PU foams.

CNWs (wt%)	0	0.25	0.50	0.75	1.00
T_g (ºC)	88	94	100	97	97
T_d (ºC)	333	329	331	336	343

DMA is a thermal analysis technique that measures the properties of materials as they are deformed under periodic stress. Storage modulus, loss modulus and tan δ can be directly given by the test. A variety of other fundamental material parameters can be defined from them, e.g., glass transition temperature T_g. Figure 40 shows the typical DMA curves of storage modulus and tan δ within a temperature range from 25ºC to 180ºC. An abrupt diminution of the storage modulus which relates to the mechanical failure of the material can be observed. The appearance of a tan δ peak which is

so-called sample damping is associated with the material transition and is used historically in literature to define T_g. The modulus value of the nanocomposite foam is a lot higher than the control foam at temperature below T_g. It agrees with the statement that the high mechanical strength of cellulose nanowhiskers and the crosslinking and hydrogen bonding introduced by cellulose nanowhiskers contributes to the improved mechanical properties of rigid PU nanocomposite foams. It was also observed that T_g values of the nanocomposite foam is higher than that of the control foam, indicating higher thermal stability is achieved by the reinforcement of polyurethane with cellulose nanowhiskers.

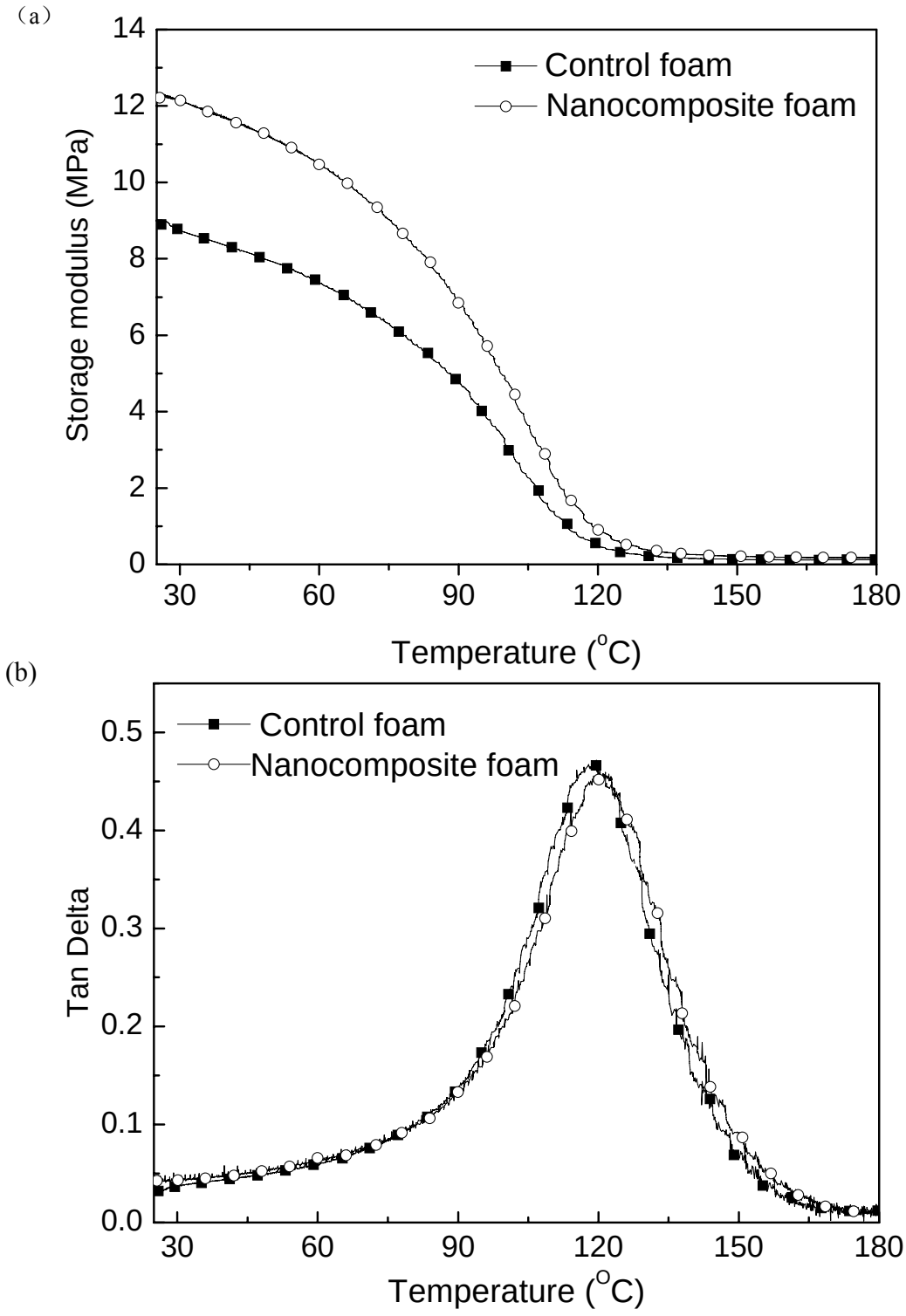

Figure 40. Curves of (a) storage modulus and (b) tan δ vs. temperature for the control foam and the nanocomposite foam.

4.4 Conclusion

Novel rigid polyurethane nanocomposite foams were prepared by the polymerization of a sucrose-based polyol, a glycerol-based polyol and polymeric diphenylmethane diisocyanate in presence of cellulose nanowhiskers. Varying amounts of cellulose nanowhiskers produced by sulfuric acid hydrolysis of commercial fully bleached softwood Kraft pulp (0.25, 0.50, 0.75 and 1.00 wt%) were incorporated into polyurethane matrix to investigate its effect on the mechanical and thermal properties of the resulting nanocomposites. Analysis of the prepared foams by FT-IR spectroscopy indicated that all samples exhibited signals attributed to polyurethanes including the NH stretching and bending vibrations at 3320 cm^{-1} and 1530 cm^{-1}, the OC=O vibration at 1730 cm^{-1} and the CO-NH vibration at 1600 cm^{-1}. FT-IR analysis also showed that cellulose nanowhiskers were crosslinked with polyurethane chains as the signal intensity of the OH stretching vibration centered at 3500 cm^{-1} was significantly reduced in comparison to the spectral data acquired for a control sample prepared from the pure polyurethane foam mixed with cellulose nanowhiskers. FT-IR spectra of the nanocomposite foams also suggested that the incorporation of cellulose nanowhiskers in PU matrix disturbed the hydrogen bonding between NH and C=O which improved the microphase separation between hard and soft segments in polyurethanes. A higher crystallinity of the soft segments led to a higher glass transition temperature of the nanocomposites. The closed cells of the control foam and nanocomposite foams were homogeneously dispersed and the cell sizes were approximately 350 μm in diameter as observed by scanning electron microscope. A substantial improvement of mechanical properties at low cellulose nanowhiskers content (≤1.00 wt%) was obtained. Cellulose

nanowhiskers showed more remarkable impact on compressive properties of rigid polyurethane foam as compared to the tensile properties, and on a relatively high CNWs content (≥ 0.75 wt%). The thermal stability of the nanocomposites was also enhanced as determined by differential scanning calorimetry and thermogravimetric analysis. Dynamic mechanical analysis results testified the improvements of mechanical properties and showed a better thermal stability of the nanocomposite foams.

In summary, rigid polyurethane nanocomposite foams reinforced with differing amounts of cellulose nanowhiskers were prepared through a one-shot method. These foams had homogeneous cell dispersion and uniform cell size. The intrinsic high strength and aspect ratio of cellulose nanowhiskers, cellulose nanowhisker-polyurethane hydrogen bonding and crosslinking, and the effect of cellulose nanowhiskers acting as nucleation sites to facilitate the bubble nucleation process resulted in improved mechanical and thermal properties of foams, particularly at relatively high filler contents (≥ 0.75 wt%).

CHAPTER 5

KRAFT LIGNIN-BASED RIGID POLYURETHANE FOAM[3]

5.1 Introduction

Lignin, the most abundant aromatic biopolymer in nature, is a three dimensional amorphous polymer which is derived from *p*-coumaryl alcohol, coniferyl alcohol, and/or sinapyl alcohol [138-139, 143]. In the secondary cell walls of vascular plants, lignin fills the spaces between cellulose and hemicellulose, providing mechanical strength to the lignocellulose matrix [137]. The structure and amount of lignin depends not only on the type of plant, but also a number of other factors: climate, soil, tree age, and portion of a tree [138-140]. The largest source of lignin is the Kraft pulping process [138]. A small amount of lignin in the form of water-soluble lignosulphonates is produced by the sulphite pulping process. Kraft pulping employs sodium hydroxide (~20% on oven dried wood) and sodium sulfide (~5% on oven dried wood) at temperatures between 150-180°C for about 2-3 h to degrade and extract lignin from wood [159]. As of 2010, the pulp and paper industry generated ~55 million tons of lignin each year, most of which is burned in a recovery furnace facilitating the recovery of pulping chemicals and energy [10]. To date, the existing markets for lignin products remains limited (~2%) and focused primarily on low-value products such as agents for dispersing, binding, and emulsion stabilization in the form of water soluble lignosulphonates from the sulphite pulping process [11-12]. Since lignin contains a large number of aliphatic and phenolic

[3] This manuscript was accepted for publication in Journal of Wood Chemistry and Technology, 2012. It is entitled as "Kraft Lignin-based Rigid Polyurethane Foam". The other author is Arthur J. Ragauskas from the Institute of Paper Science and Technology and School of Chemistry and Biochemistry at Georgia Institute of Technology.

hydroxyl groups, researchers have begun to examine the preparation of lignin modified phenolic resin, epoxy polymer, acrylics, and polyurethanes [13-15].

Polyurethane is among the most widely used synthetic polymers for assorted applications including coatings, adhesives, elastomers, foams, and fibers [18]. These numerous applications can be attributed to polyurethane's predominant and controlled mechanical and thermal performance depending on the synergistic effect of soft- and hard-segments of the polymer matrix as well as various optional species, such as chain extender, cross-linker, UV absorber, light stabilizer, antioxidant, and flame retardant [187]. Rigid PU foam is a highly crosslinked polymer with a closed-cell structure. Its low density, low thermal conductivity, low moisture permeability, high dimensional stability, and good adhesive property lead to the broad uses in construction, refrigeration appliances, and technical insulations [20].

Since lignin has a random non-crystalline network structure, it possesses unique properties that relate to mechanical properties and thermal stability. The natural properties of lignin also contribute to an improvement of moisture and flame resistance of PU foams [219]. Moreover, its aliphatic and phenolic hydroxyl functionalities provide good reacting sites towards isocyanates [12]. Kraft lignin was first incorporated into PU formulations together with a polyether triol and it has been shown to contribute chemically to the formation of a crosslinked network [222]. At low lignin contents, the resulting PUs exhibited considerable toughness at specific values of [NCO]/[OH] ratios. However, at high lignin contents (> 30 wt%), the corresponding PUs were hard and brittle regardless of the [NCO]/[OH] ratio used [222-223]. In a later study by Yoshida et al. [223], it was found that PUs prepared with low molecular weight lignin (M_w=620)

were more flexible than those obtained with lignin of medium (M_w=1290) and high values (M_w=2890). When Kraft lignin contents in PUs were higher than 30 wt%, rigid and glassy products were obtained, regardless of the molecular weight of the lignin used. A recent study on the acetic acid lignin-containing PU showed that hydrogen bonding was established between lignin and the polymer matrix and the thermal stability was improved with increasing lignin concentration up to 50%, however, a maximum lignin content of 43.3% can be reached for the continuous film formation [256].

In order to improve the content of lignin in PU formulation for a product with suitable performance, extensive attention has been directed towards its application as a polyol precursor through liquefaction instead of the direct use of underivatized lignin [205, 234, 257-261]. Recently, oxypropylation has been recognized as a viable and promising approach to overcome the technical limitations and constraints imposed by the polymeric nature of lignin when directly used as a macromolecule for synthetic purposes [240]. Direct oxypropylation of lignin under alkaline condition was found to be more efficient than acidic condition [236]. After oxypropylation, the starting solid lignin becomes a liquid polyol as a result of the introduction of multiple ether moieties [224]. A study of rigid PU foams obtained from lignin polyols together with 10 wt% of glycerol as a chain extender has shown that it resulted in a rigid PU foam yielding good thermal properties and dimensional stability, even after aging [226].

In the current rigid polyurethane foam industry, sucrose polyol and glycerol polyol are the most widely used polyols. Whether the use of lignin polyol can result in a product with comparable or even superior properties as compared to the conventional polyols will determine its future applications in this field. Herein, we compared lignin

polyol with commercial polyols in view of the mechanical property of the corresponding rigid PU foams. A series of rigid PU foams was synthesized from commercial polyols and lignin polyol with varying combinations, which started from a control foam made from only commercial polyols to a foam solely based on lignin polyol. The results demonstrated the first preparation of lignin-based rigid PU foam without the assistance of any other polyols which provides a significant improvement of the mechanical property of the resulting PU as compared to its commercial counterpart.

5.2 Experimental Section

5.2.1 Chemicals and Materials

A commercial USA softwood Kraft pine lignin (Indulin AT) was used. According to the product prescription, it is completely free of hemicellulosic materials and has an ash content of 3%. Sucrose polyol, glycerol polyol, polymeric MDI, DMCHA, and Mannich base catalyst were commercial products the same as those used in Chapter 4. Other chemicals used in this work were purchased from VWR or Sigma Chemical Co., and used as received.

5.2.2 Oxypropylation of Kraft Lignin

Oxypropylation of Kraft lignin was performed as described in Chapter 3 (3.2.3.1 Kraft lignin oxypropylation). Upon heating, the pressure gradually rose with increasing temperature, and once it reached 150°C the pressure increased to a maximum value of ~1.75 MPa in seconds and then quickly returned to 0 in less than 9 min, indicating the completion of the reactants. The formulation of oxypropylation reaction was determined according to literature which was able to produce a lignin polyol with an

acceptable hydroxyl index between 300 and 800 mg KOH/g and a low viscosity for the purpose of rigid PU foam synthesis [224].

5.2.3 Acetylation of Lignin/Oxypropylated Lignin

Kraft lignin and oxypropylated Kraft lignin samples were acetylated for GPC analysis as described in Chapter 3 (3.3.5 GPC analysis of Kraft lignin before and after oxypropylation).

5.2.4 Phosphitylation of Lignin/Oxypropylated Lignin

The Kraft lignin/oxypropylated Kraft lignin phosphitylation procedure for ^{31}P NMR analysis was accomplished as described in Chapter 3 (3.3.4.3 ^{31}P NMR characterization of Kraft/EOL lignin before and after oxypropylation).

5.2.5 Optimization Experiments

A control foam was prepared from sucrose polyol, glycerol polyol, and polymeric MDI. Sucrose polyol was then gradually replaced by lignin polyol in weight percentages of 10%, 30%, 60%, and 100% since they have a similar hydroxyl index. The last foam was made with only lignin polyol without the addition of sucrose polyol or glycerol polyol. The formulation is summarized in Chapter 3 (3.2.4.2 Preparation from Kraft Lignin Polyol)

5.2.6 Preparation of Kraft Lignin-based Rigid PU Foam

Rigid polyurethane foams in this study were prepared as described in Chapter 3 (3.2.4.2 Preparation from Kraft lignin polyol).

5.2.7 Characterizations

All prepared lignin polyols were extracted three times with hot hexane under

reflux to obtain pure oxypropylated lignin by removing poly(propylene oxide) oligomers according to the literature [228, 242, 262].

The molecular weight (M_w and M_n) of Kraft lignin before and after oxypropylation was determined by GPC as described in Chapter 3 (3.3.5 GPC analysis of Kraft lignin before and after oxypropylation). Molecular weights (M_n and M_w) were calculated by the software relative to the universal polystyrene calibration curve. Polydispersity index was determined by dividing M_w by M_n.

FT-IR spectra of Kraft lignin before and after oxypropylation were recorded as described in Chapter 3 (3.3.1.2 FT-IR of Kraft lignin and oxypropylated Kraft lignin).

All NMR experiments including ^{1}H, ^{13}C and ^{31}P NMR were performed with a Bruker Avance-400 spectrometer (Billerica, MA, USA) as described in Chapter 3 (3.3.4 NMR spectroscope).

SEM images of the prepared rigid PU foams were taken by a Hitachi S-800 FE-SEM as described in Chapter 3 (3.3.2.2 SEM of Kraft lignin/EOL-based rigid PU foams).

The density of each foam was calculated as the average value of mass divided by volume of five samples (25 mm × 25 mm × 15 mm).

5.2.8 Mechanical Testing

The compressive testing of Kraft lignin-based rigid polyurethane foams were conducted on a MTS Insight 2 universal test machine according to ASTM C365/C365M-05 as described in Chapter 3 (3.3.7.3 Compression testing of Kraft/EOL-based rigid PU foams). The intersection point between the initial slope and the plateau slope in the stress-strain curves was determined as the yield strength and the initial slope was termed as the compressive modulus. The average value of 5 data

points of each foam together with the standard deviation (S.D.) was recorded for comparison.

5.3 Results and Discussion

Oxypropylation, the chain extension reaction of Kraft lignin, is always accompanied by the homopolymerization of propylene oxide through transfer reactions following the anionic grafting mechanism [225, 240]. The resulting polyol is, in fact, a mixture of oxypropylated lignin and PPO oligomers. In other words, the PPO oligomers exist either as the grafts of lignin or a polymer by itself. The independent PPO oligomers are normally left in the final mixture because they constitute a very useful bifunctional co-polyol, decreasing the viscosity and glass transition temperature of the lignin polyol [240]. The oxypropylation with lignin is illustrated in Figure 28 in Chapter 2.

Lignin oxypropylation was accomplished following the conditions summarized in Table 23 in Chapter 3 (3.2.3.1 Kraft Lignin Oxypropylation). Most of the propylene oxide was reacted either to form the lignin grafts or the homopolymer of PPO which are two competitive reactions during oxypropylation. The traces of PO were removed by placing the lignin polyol in a vacuum oven at 40°C until a constant weight was achieved. The weight of the crude product equals the total weight of the starting Kraft lignin and propylene oxide. The potassium ion remained with the lignin polyol for PU preparation. Pure oxypropylated lignin was separated from the PPO oligmers by extracting the polyol mixture with hot hexane under reflux three times, according to the procedure described by Pavier and Gandini [225]. They were subsequently vacuum dried until a constant

weight was achieved and the PPO content was determined to be 46 ± 5 wt%. The original Kraft lignin has a broad molecular weight distribution and the large molecules were degraded to some extent during oxypropylation resulting in a smaller polydispersity index of the oxypropylated lignin. The detailed data were summarized in Table 32. The amount of PPO grafts per oxypropylated lignin macromolecule was determined to be ~38.9 wt% in average according to the M_n values of the original and oxypropylated Kraft lignin.

Table 32. Molecular weight change of Kraft lignin after oxypropylation (Samples were acetylated for GPC analysis).

	Kraft lignin	Oxypropylated lignin
M_w (g mol^{-1})	7.6×10^3	4.2×10^3
M_n (g mol^{-1})	1.1×10^3	1.8×10^3
D	7.0	2.4

FT-IR spectra of the original and the oxypropylated Kraft lignin are shown in Figure 41. The spectra are normalized to the intensity of the lignin aromatic ring vibrations at 1600 cm^{-1} [263]. In both spectra, the O-H stretching vibration is easily seen at ~3450 cm^{-1} and the intensity remains generally the same. However, the oxypropylated Kraft lignin exhibits increasing band intensity at 2868–2937 cm^{-1} which is assigned to the O-H stretching vibration in methylene groups [263]. Moreover the increasing band intensity at 1034–1096 cm^{-1} in the spectra of oxypropylated Kraft lignin, corresponding to the aliphatic C-H and C-O stretching vibrations, are also due to the PPO grafts. [264].

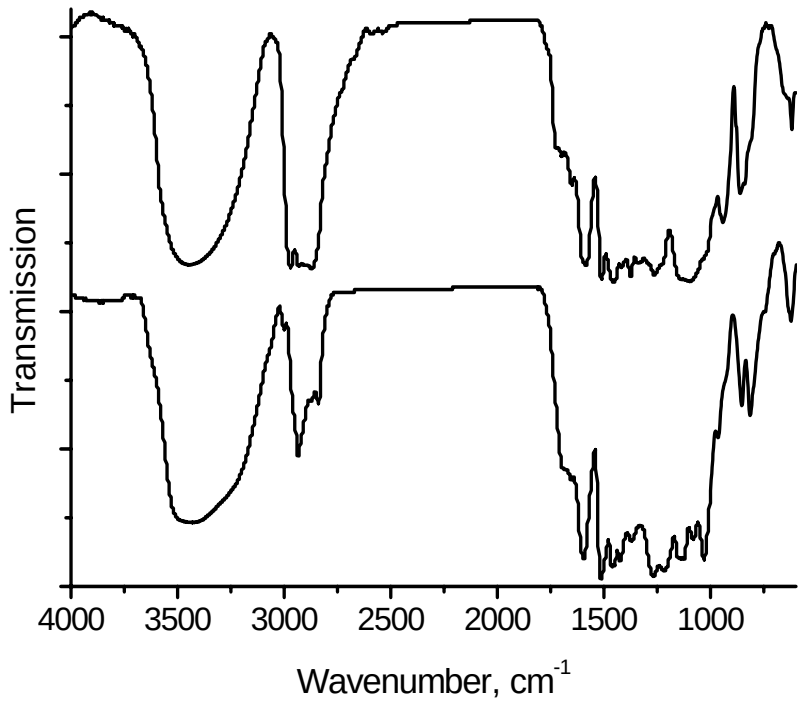

Figure 41. FT-IR spectra of Kraft lignin (bottom) and oxypropylated lignin (top).

Compared to the starting Kraft lignin, the oxypropylated lignin exhibited apparent differences in the ^{1}H NMR spectral data (Figure 42). Introducing large amounts of PPO grafts generated peaks of CH_3 groups at 1.0 ppm, CH_2 groups at 3.4 ppm, and CH groups at 3.7 ppm which were also seen by Nadji et al. [226]. Protons from aromatic rings (~6.3-7.7 ppm) were clearly identified although the relative signal intensity was diminished due to the dominance of PPO grafts.

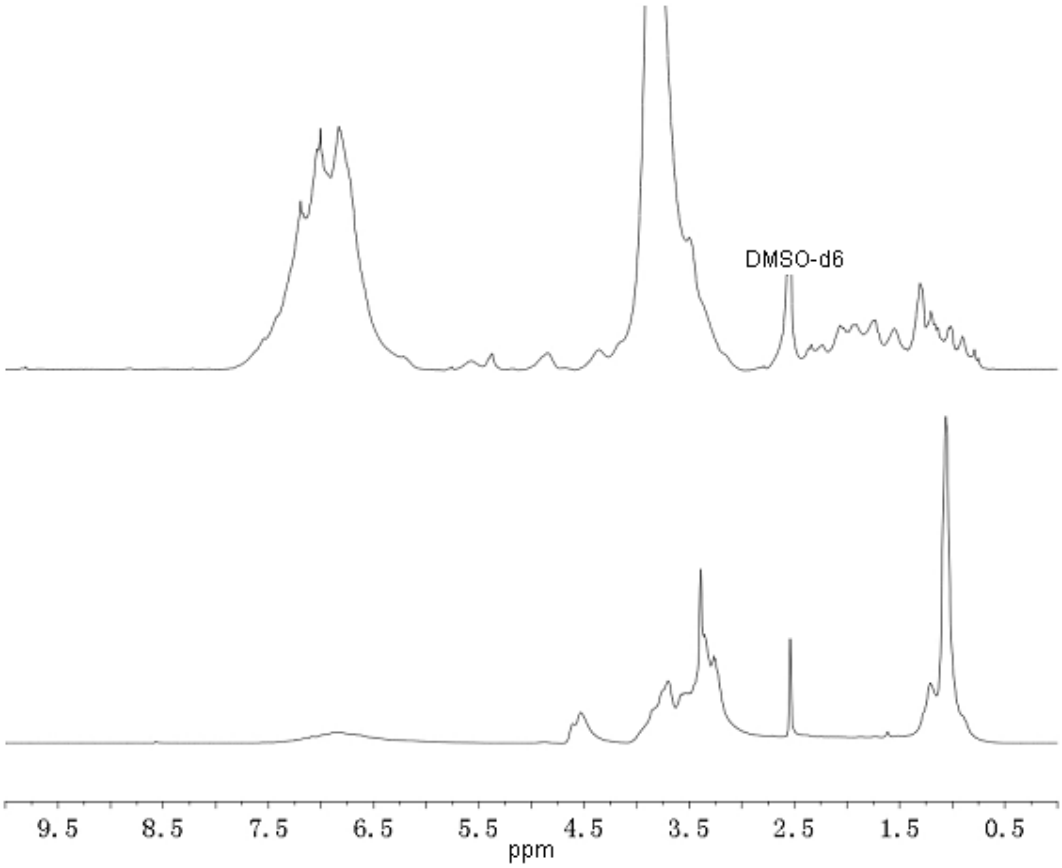

Figure 42. ^{1}H NMR spectra of Kraft lignin (top) and oxypropylated lignin (bottom).

The signals in the ^{13}C NMR spectra (Figure 43) can be divided into three main types: 1) those corresponding to carbonyl and carboxyl carbons (160-200 ppm); 2) those associated to aromatic carbons, which can be divided further into quaternary (125-160 ppm) and protonated carbons (100-125 ppm); 3) and those assigned to aliphatic carbon atoms which allow the observation of the main linkages between phenylpropane units (10-100 ppm). The strong signal at 56-57 ppm was readily assigned to the methoxyl group in guaiacyl units [265]. In the spectrum of oxypropylated lignin the grafted PPO oligomers chains generated intense aliphatic carbon peaks. CH_3 resonances were identified at 17 and 20 ppm, respectively for the pendant and terminal methyl groups.

CH_2 and CH resonances were identified between 71.4 and 77.4 ppm. The terminal CH-OH carbons were identified at 65 and 67 ppm [266].

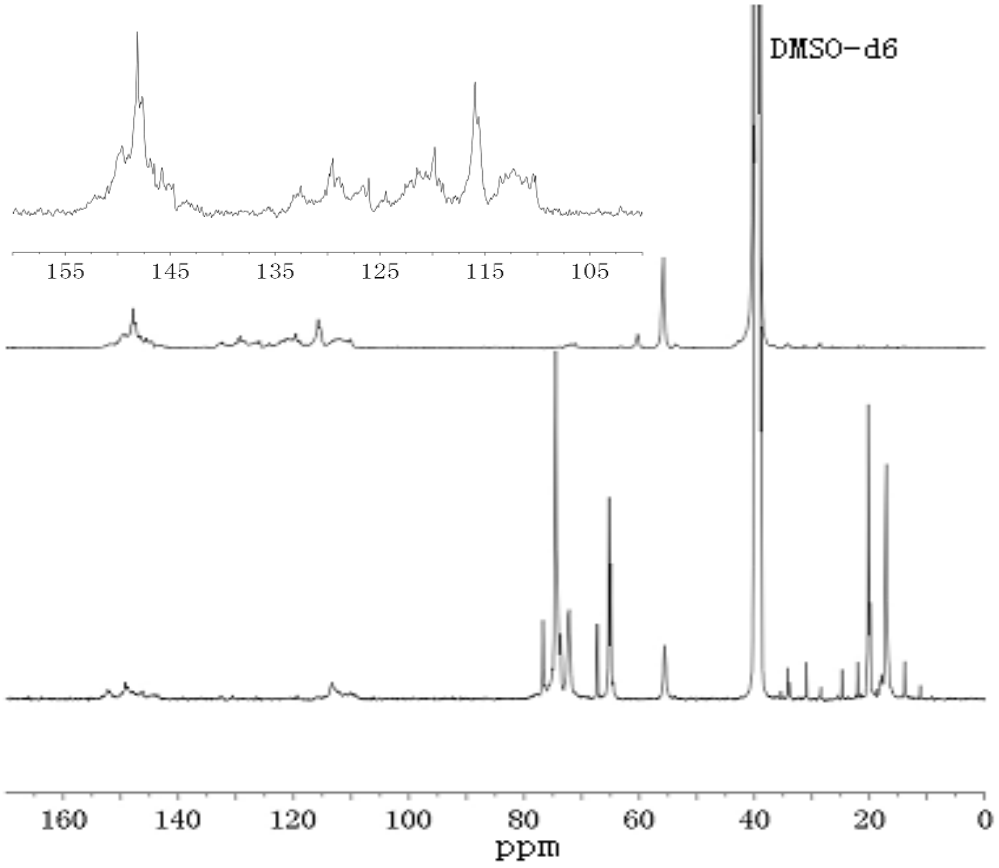

Figure 43. ^{13}C NMR spectra of Kraft lignin (top) and oxypropylated lignin (bottom).

Quantitative ^{31}P NMR was used not only to investigate the structure change of the Kraft lignin before and after oxypropylation but also as a direct and fast tool for hydroxyl index calculation. The spectrum of Kraft lignin shows aliphatic, condensed phenolic, guaiacyl, and a small amount of carboxylic hydroxyl groups, while in the spectrum of oxypropylated lignin exhibited only aliphatic and carboxylic hydroxyl groups as can be seen in Figure 44. This indicates a successful chain extension reaction after which all

phenolic hydroxyl groups have been converted into aliphatic hydroxyl groups of the PPO grafted units. The detailed signal assignments and hydroxyl value analysis of the ^{31}P NMR spectra of Kraft lignin and oxypropylated Kraft lignin are summarized in Table 33. The hydroxyl index (I_{OH}), a term often used in PU research, is defined as the weight of KOH (mg) that will neutralize the acetic anhydride capable of reacting by acetylation with 1 g of polyol [20]. Here, I_{OH} of Kraft lignin polyol was determined as the result of the total hydroxyl value (mmol g^{-1}) multiplied by the molecular weight of KOH, which is 387 mg KOH/g.

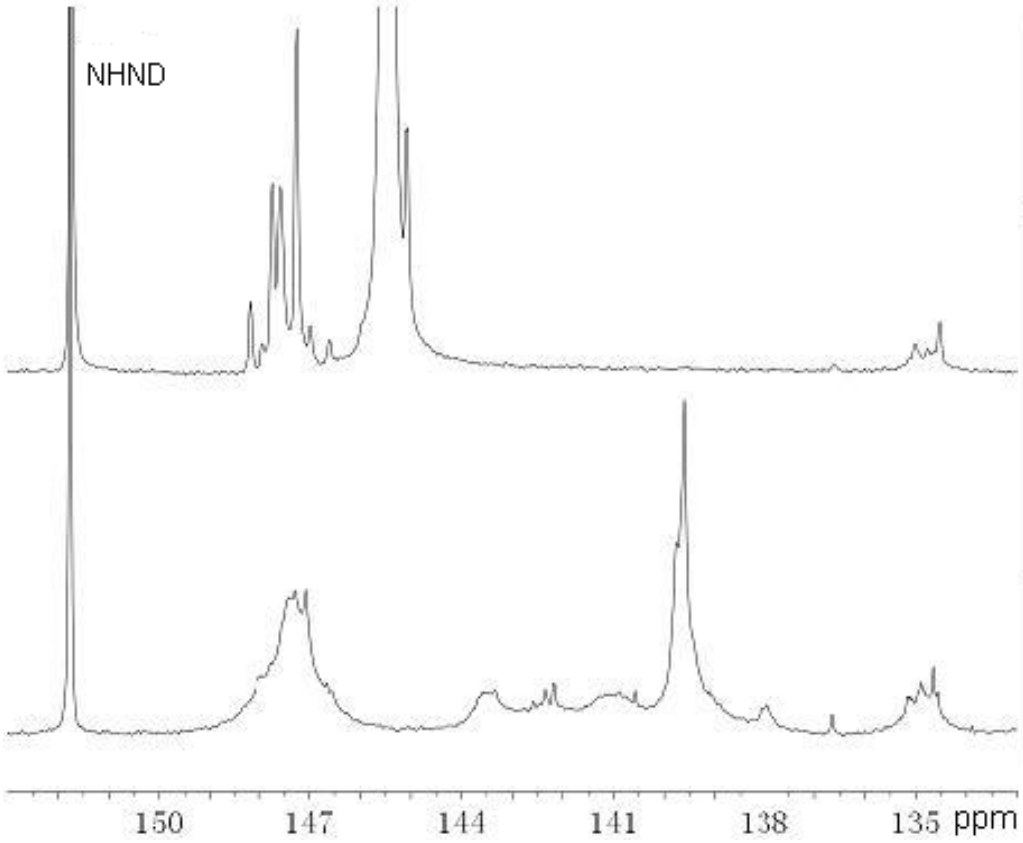

Figure 44. Quantitative ^{31}P NMR spectra of Kraft lignin (bottom) and lignin polyol (top). TMDP: 2-chloro-4,4,5,5-tetramethyl-1,3,2-dioxaphospholane.

Table 33. Signal assignments and hydroxyl value analysis of quantitative ^{31}P NMR spectra of Kraft lignin and oxypropylated Kraft lignin.

Hydroxyl groups	Integration region (ppm)	OH value of Kraft lignin (mmol g^{-1})	OH value of Lignin polyol (mmol g^{-1})
Aliphatic	144.3-150.2	1.95	6.82
Condensed phenolic	140.3-144.3	1.39	-
Guaiacyl phenolic	136.4-140.3	1.85	-
Carboxylic	133.3-136.4	0.43	0.09
Total	-	5.62	6.91

Kraft lignin-based rigid PU foams of varying formulations were prepared under the same experimental conditions. The densities of foams were measured to be ~30 kg m^{-3}. However, the SEM images in Figure 45 show a difference in close-cell diameter between 60%, 100% (750 μm) Kraft lignin-based foams and others (650 μm). Moreover, shrinkage occurred with the two foams that have larger cell sizes when cured at room temperature. The cream time corresponding to the start of bubble rise decreased with increasing lignin polyol contents as shown in Table 34. This result suggests that the lignin polyol has a higher reactivity towards polymeric MDI under the same reaction conditions.

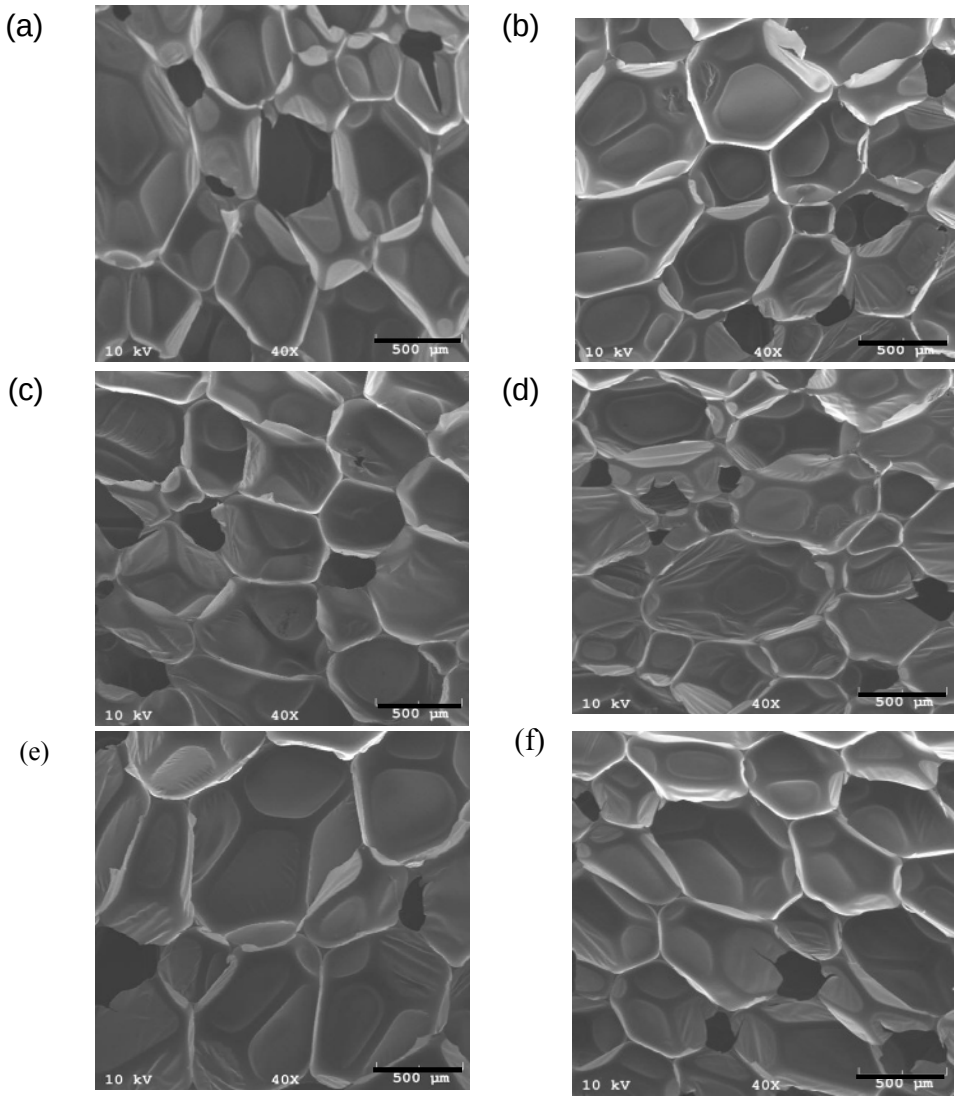

Figure 45. SEM images of rigid PU foams prepared with (a) 0 wt%, (b)10 wt%, (c)30 wt%, (d)60 wt%, (e)100 wt% of Kraft lignin polyol based on the weight of sucrose polyol of the control foam, and (f) only lignin polyol.

Table 34. Different cream times of rigid PU foams prepared with varying lignin polyol contents.

Lignin polyol (wt%)	Cream time (s)
0	40
10	38
30	34
60	26
100	23
Only lignin polyol	17

A key objective of this study was to optimize the mechanical properties of the rigid PU foams as a function of the starting reagents formulation. A series of stress-strain curves was generated by compression testing of the prepared rigid polyurethane foams (Figure 46). According to literature [216], density plays an important role on the mechanical performance of rigid PU foam and their relationship can be depicted by Power law. However, in present study, the density of all foams was close to 30 kg m^{-3}, and therefore the mechanical properties were simply and directly compared in terms of average yield strength and compressive modulus (Table 35). The yield strength of all foams was almost the same except being increased by 44% for the one prepared from only lignin polyol. The compressive modulus were slightly increased at 10% and 30% lignin polyol contents, and then dropped below the values of the control foam at 60% and 100% lignin polyol contents. The drop could be due to the high content of low functionality polyols, i.e., PPO oligomers and glycerol polyol, which are generally not favorable polyols for highly crosslinked rigid PU foam preparation. The optimal mechanical properties were obtained with foam prepared with only lignin polyol without the addition of any other commercial polyols. Its yield strength and compressive modulus were improved by 44% and 135%, respectively, as compared to the control foam. It could be primarily attributed to the rigidity of lignin aromatic structure and the high functionality of lignin hydroxyl groups which introduced more crosslinking to the polyurethane network resulting in a higher crosslinking density compared to the control foam.

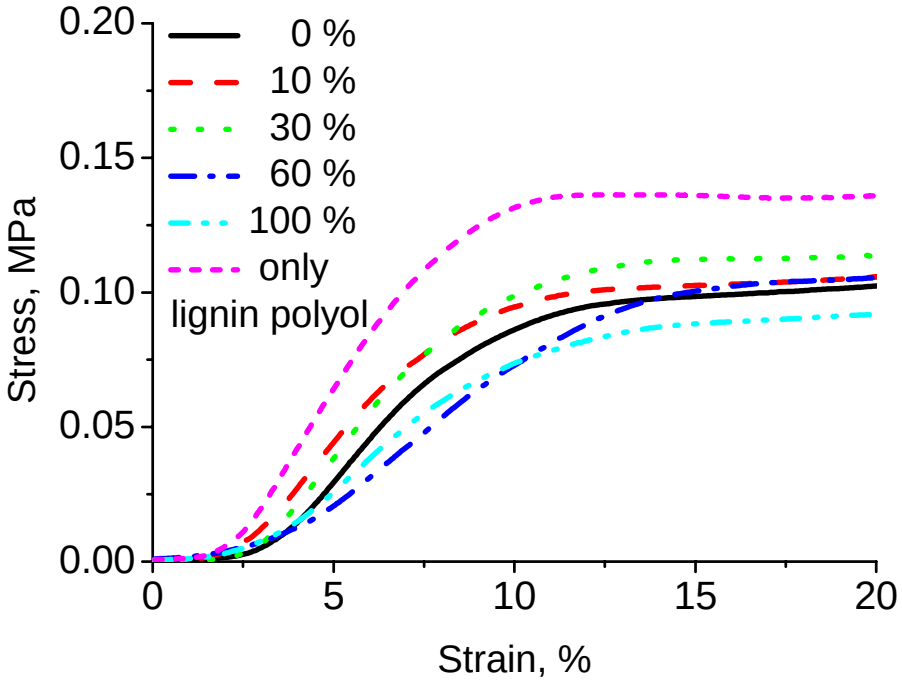

Figure 46. Compressive stress-strain curves of prepared rigid PU foams.

Table 35. Yield strength and compressive modulus of prepared rigid PU foams.

Lignin polyol (wt%)	Strength (MPa)	Modulus (MPa)
0	0.10 ± 0.01	1.45 ± 0.07
10	0.10 ± 0.01	1.56 ± 0.05
30	0.11 ± 0.01	1.58 ± 0.05
60	0.10 ± 0.01	1.13 ± 0.01
100	0.09 ± 0.01	1.11 ± 0.03
Only lignin polyol	0.14 ± 0.01	3.41 ± 0.39

5.4 Conclusion

Kraft pine lignin was derivatized to a liquid polyol through oxypropylation. The resulting polyol was characterized by GPC, FT-IR, H^1, C^{13} and P^{31} NMR and was

compared to commercial polyols in view of the mechanical properties of the corresponding rigid polyurethane foams. Oxypropylation of Kraft pine lignin was proved to be a successful way to modify solid lignin into a liquid polyol, which possessed a suitable hydroxyl index between 300 and 800 for rigid PU foam preparation. Additionally, oxypropylation made it possible to incorporate a higher content of lignin in the PU formulation, and also provided superior and a better control of the properties of polyol and resulting PU, comparing to directly reacting solid lignin with diisocyanate [267], or polyethylene glycol/glycerol and diisocyanate [268], or polyether triol and diisocyanate [222-223] as previously reported by other researchers. A series of lignin-based PU was synthesized by replacing varying weight percentages of the amount of sucrose polyol and glycerol polyol, two commonly used commercial polyols employed in the control foam preparation. All foams showed a low density of ~30 Kg m^{-3} and typical linkages of polyurethane in the FT-IR spectra. The diameter of closed-cells was ~650 μm for most of the foams as revealed by SEM images. This study has shown that it is not only feasible to use lignin polyol solely for rigid PU foam making without the addition of any other polyols or chain extenders, e.g., glycerol [236], but also afford a rigid PU foam with better mechanical properties than its commercial counterpart, primarily attributed to the rigidity of lignin aromatic structure and the high functionality of lignin hydroxyl groups. The results suggest a broad application of lignin polyol in the future polyurethane industry.

CHAPTER 6

ETHANOL ORGANOSOLV LIGNIN-BASED RIGID POLYURETHANE FOAM REINFORCED WITH CELLULOSE NANOWHISKERS[4]

6.1 Introduction

With an ever-increasing societal focus on environmental and economical sustainability, biorenewable energy and materials from non-food bioresources, especially wood, are drawing increasing attentions from consumers, governments, industries, and research institutes. Cellulose and lignin existing in wood cell walls are abundant biopolymers in nature, corresponding to an annual industrial production of 1.5×10^{12} and 5×10^{7} tons, respectively [1, 269]. Due to their renewable and biodegradable nature, extremely wide availability, non-agricultural based economy, and high reactivity attributed to various functional groups, cellulose and lignin have been exploited in many applications [111, 270-281].

Cellulose nanowhiskers are a group of needle-like nanoparticles hydrolyzed from cellulose fibers. It has a wide size range and is normally 100 to 300 nm in length and 3-15 nm in width for wood or cotton-based CNWs [134]. Its tensile strength and modulus are approximately 10 GPa and 150 GPa, respectively [3, 16]. There has been a growing interest in CNWs reinforced nanocomposites in the last decade, including polyurethane. Up to 5 wt%, 30 wt%, and 1 wt% of CNWs reinforced thermoplastic PU

[4] This manuscript was accepted for publication in RSC Advances, 2012. It is entitled as "Ethanol Organosolv Lignin-based Rigid Polyurethane Foam Reinforced With Cellulose Nanowhiskers". The other author is Arthur J. Ragauskas from the Institute of Paper Science and Technology and School of Chemistry and Biochemistry at Georgia Institute of Technology.

films were studied by Marovich et al. [8], Cao et al. [4, 93], and Auad et al. [110, 215]. SEM images of the resulting nanocomposites indicated well-dispersed CNWs in the polymer, and the FT-IR spectra revealed strong hydrogen bonding and chemical reactions between CNWs and isocyanates. Tensile property of the nanocomposites were shown to be significantly improved with increasing CNWs contents, primarily attributed to the rigidity of the additives and the higher crosslinking density compared to the neat film. It was also found that CNWs addition favored a phase separation of soft and hard domains which led to an upward shift in melting temperature of crystalline phase, an increase in Young's modulus, and a decrease in deformation at break [110, 215].

With the growing application of organosolv pretreatment as an environmentally benign biomass pretreatment technology for biofuels, large amounts of ethanol organosolv lignin is anticipated to be produced by treatment of biomass with ethanol. EOL is usually high-purity, low molecular weight and sulfur free lignin which has less condensed products and a narrower molecular weight distributions than lignin obtained from other methods [139, 177-178]. The large amount of hydroxyl groups in lignin structure, as well as, the potential benefits it can provide to polyurethane namely antioxidative and fire retardant properties, make it a promising candidate for polyurethane synthesis. This research was initially focused on direct incorporation of lignin [222]. However, further development of a lignin polyol could not only improve the lignin content in polyurethane formulation but also result in easier processing and better performance of the product. Oxypropylation of lignin, first studied by Glasser and co-workers [228] and further developed by other researchers [235, 240], has been recognized as the most promising method to derive solid lignin into a liquid polyol.

A formulation optimization study of Kraft lignin-based rigid PU foam showed that the optimal mechanical property was obtained by using only Kraft lignin polyol without the assistance of any other polyols [282]. Based on the above result, herein, EOL-based rigid PU foams were synthesized by directly reacting EOL polyol with polymeric MDI which was catalyzed by DMCHA and a Mannich base catalyst. Silicone surfactant was added to reduce the surface tension of closed cells. Pentane was used as a physical blowing agent. Foam reinforced with 0, 1 and 5 wt% of CNWs were prepared by a one-shot method [216]. A water suspension of CNWs was directly mixed with EOL polyol followed by the removal of water under high vacuum. Compared to its DMF suspension [204], this method avoided freeze drying of CNWs which would cause the agglomeration of CNWs and a difficulty in redispersion as well as the large use of DMF.

6.2 Experimental Section

6.2.1 Chemicals

Softwood pine wood chips were used in the ethanol organosolv pretreatment. Cellulose nanowhiskers were prepared from the commercial linerboard softwood Kraft pulp. Polymeric MDI, DMCHA, Mannich base catalyst, and silicone surfactant were commercial products the same as those used in Chapter 4. Other chemicals used in this work were purchased from VWR and used as received.

6.2.2 Ethanol Organosolv Lignin Preparation

Ethanol organosolv lignin was prepared as described in Chapter 3 (3.2.2 Ethanol organosolv lignin preparation).

6.2.3 Oxypropylation of EOL

EOL was rendered into a liquid polyol though oxypropylation as described in Chapter 3 (3.2.3.2 Oxypropylation of ethanol organosolv lignin). During the process, temperature and pressure started to increase progressively from 160°C. After reaching the maximum value, pressure decreased rapidly due to the propylene oxide consumption.

6.2.4 Rigid PU Foam Preparation

EOL-based rigid PU foams were prepared as described in Chapter 3 (3.2.4.3 Preparation from EOL polyol).

6.2.5 Characterization

The molecular weight change of EOL after oxypropylation was analyzed by using GPC. Samples were acetylated before analysis as described in Chapter 3 (3.3.5 GPC analysis of lignin before and after oxypropylation).

FT-IR spectra of EOL and oxypropylated EOL were recorded as described in Chapter 3 (3.3.1.2 FT-IR of lignin and oxypropylated Kraft lignin).

Phosphitylated EOL/oxypropylated EOL samples were characterized by ^{31}P NMR as described in Chapter 3 (3.3.4.3 ^{31}P NMR characterization of Kraft/EOL lignin before and after oxypropylation).

SEM images of the resulting foams were taken by a Hitachi S-800 FE-SEM. The sample preparation and operation conditions were summarized in Chapter 3 (3.3.2.2 SEM of Kraft lignin/EOL-based rigid PU foams). Five images from different parts of the foam were taken for an average cell size analysis.

6.2.6 Mechanical Testing

Compressive properties of the prepared rigid PU foam were studied by

compression testing as described in Chapter 3 (3.3.7.3 Compression testing of Kraft/EOL-based rigid PU foams).

6.2.7 Thermal Analysis

The thermal properties of EOL-based rigid PU foams were studied by DSC and TGA in terms of the glass transition temperature and decomposition temperature. The detailed analysis procedures were summarized in Chapter 3 (3.3.9 Differential scanning calorimetry (DSC) analysis of rigid PU foams and 3.3.10 Thermogravimetric analysis (TGA) of rigid PU foams). Both the T_g and T_d values were determined as the average value of three performances for each foam sample.

6.3 Results and Discussion

EOL was completely rendered into a liquid polyol without any insoluble residues. Pure oxypropylated EOL was separated from poly(propylene oxide) (PPO) by extracting the mixture three times with hot hexane under reflux. PPO accounted for ~55 wt% of the raw product. Oxypropylated EOL has an increased molecular weight （M_w=3.7×10^3 g mol^{-1}）due to the graft of PPO and a narrower polydispersity (D = 2.2) compared to EOL（M_w=2.6×10^3 g mol^{-1}, D = 2.5）as revealed by the GPC results. FT-IR spectra of EOL before and after oxypropylation were normalized to the intensity of the lignin aromatic ring vibrations at 1600 cm^{-1}. Stronger bond intensities at ~2970 cm^{-1} and 1000-1100 cm^{-1} were observed for oxypropylated EOL (Figure 47b) than the original EOL (Figure 47a). Those changes are attributed to CH_3, CH_2, CH and CO stretching vibrations of the PPO grafts. The ^{31}P NMR spectrum (Figure 48a) of phosphitylated

EOL shows phosphorous signals corresponding to aliphatic (144.8-150.8 ppm), condensed phenolic (141.6-144.5 ppm), guaiacyl (136.4-141.6 ppm) and a small amount of carboxylic (134.1-136.2 ppm) hydroxyl groups. In contrast, the phosphitylated EOL polyol (Figure. 46b) exhibited only aliphatic (143.0-148.8 ppm) and carboxylic (133.6-136.9 ppm) hydroxyl signals. All results suggest a successful chain extension reaction of EOL. The hydroxyl index of EOL polyol was calculated to be 380 mg KOH/g based on the integrated analysis of ^{31}P NMR spectrum data, which is a suitable value between 300 and 800 for rigid PU foam preparation [240].

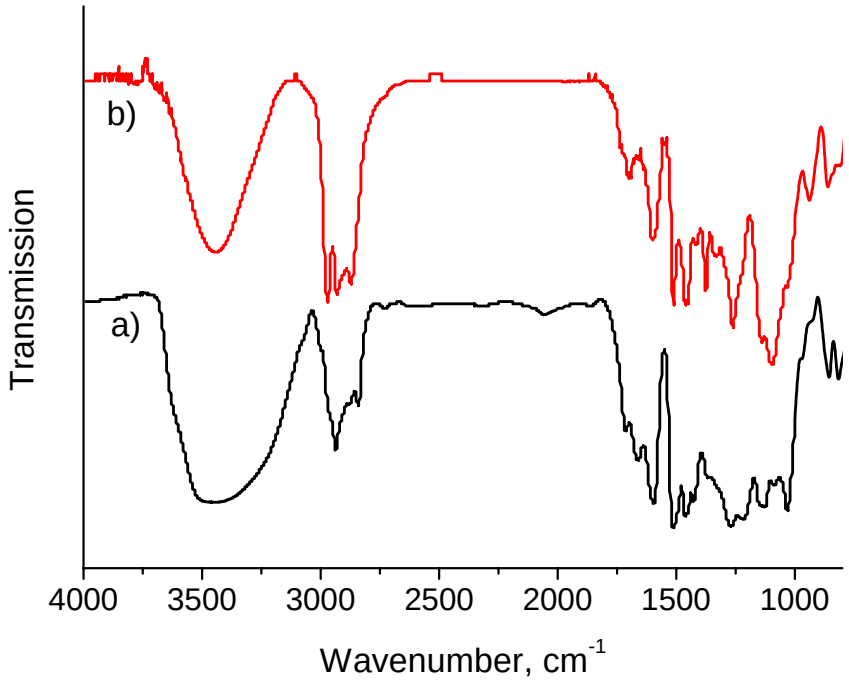

Figure 47. FT-IR spectra of (a) EOL and (b) oxypropylated EOL.

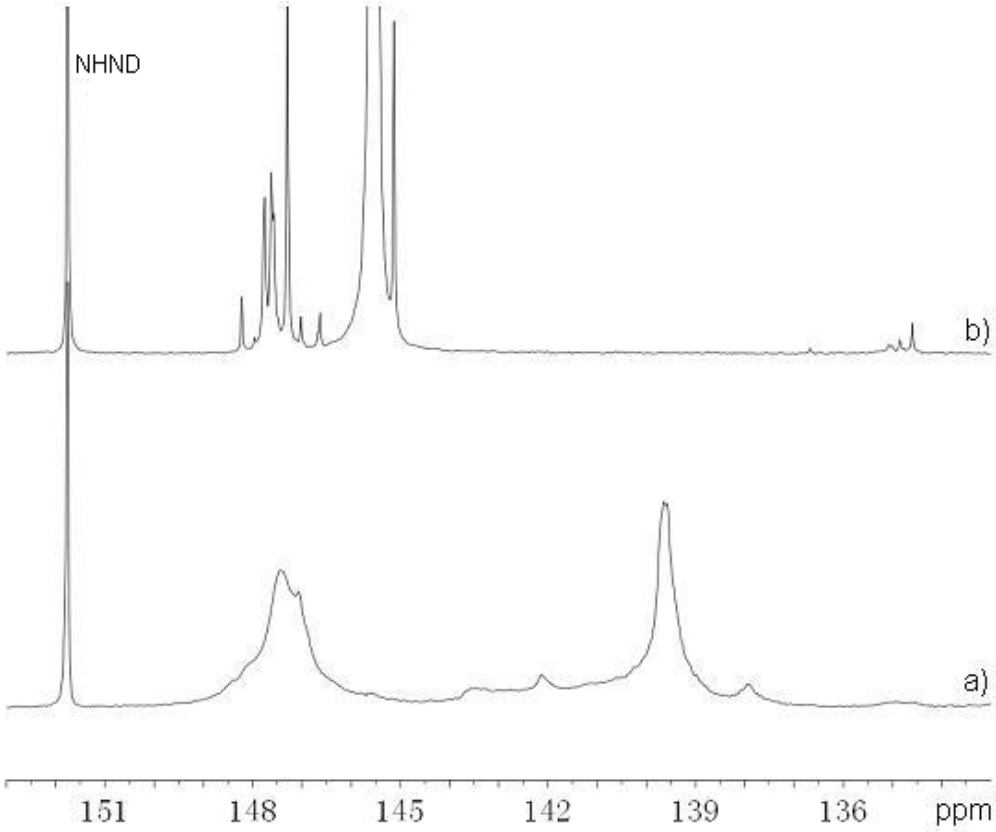

Figure 48. ^{31}P NMR spectra of (a) EOL and (b) oxypropylated EOL.

The FT-IR spectra of prepared rigid PU foams are relatively the same where typical linkages of polyurethane can be readily seen in Figure 49, e.g., N-H stretching and bending vibrations (~3310 cm^{-1} and ~1513 cm^{-1}), aliphatic C-H (~2932 cm^{-1}), OC=O (~1729 cm^{-1}), CO-NH (~1612 cm^{-1}), O-CO (~1227 cm^{-1}) and C-O (~1079 cm^{-1}) stretching vibrations. PU foams showed reduced average cell diameters from 320 ± 20, 269 ± 28, to 191 ± 16 μm with increasing CNWs contents from 0, 1, to 5 wt% as indicated by SEM images (Figure 50), the same observation as in our previous study [204]. It is presumably because CNWs served as nucleation sites to facilitate the cell nucleation process, and the increased number of nucleation sites led to a finer cell structure [253, 283]. The density was calculated as an average value of mass divided by

volume of three samples from each foam (Table 36). The density of rigid PU foam used for thermal insulation in buildings normally ranges between 30 kg m^{-3} and 45 kg m^{-3}. However, it can reach 100 kg m^{-3} for some applications [284]. In present study, the density of the prepared foams increased due to the smaller cell size at higher CNWs contents but still within this range.

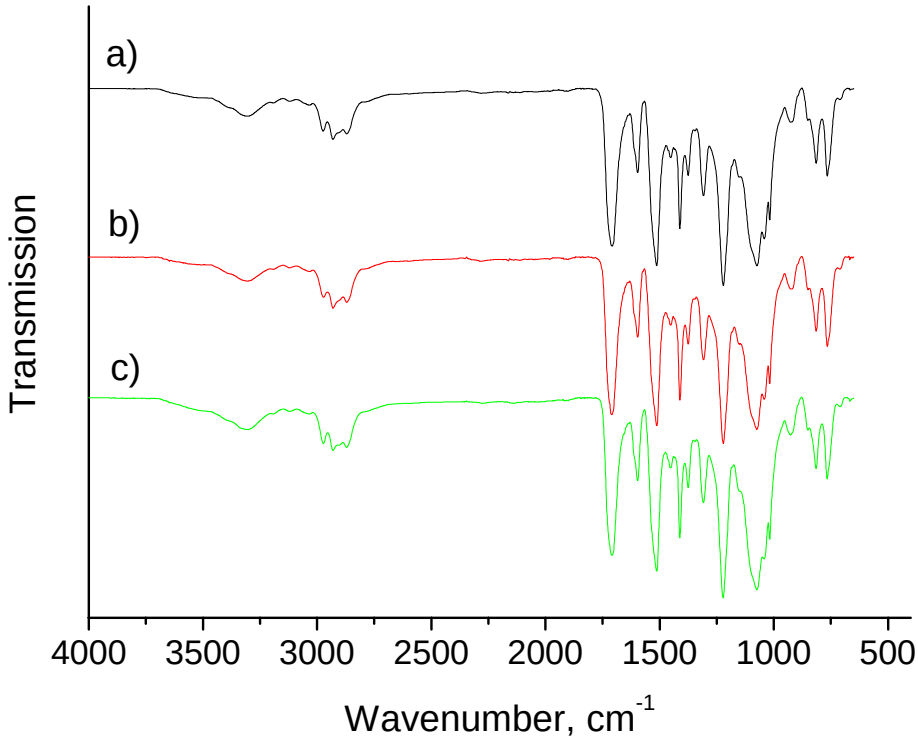

Figure 49. FT-IR spectra of rigid PU foams reinforced with (a) 0 wt%, (b) 1 wt%, and (c) 5 wt% of CNWs.

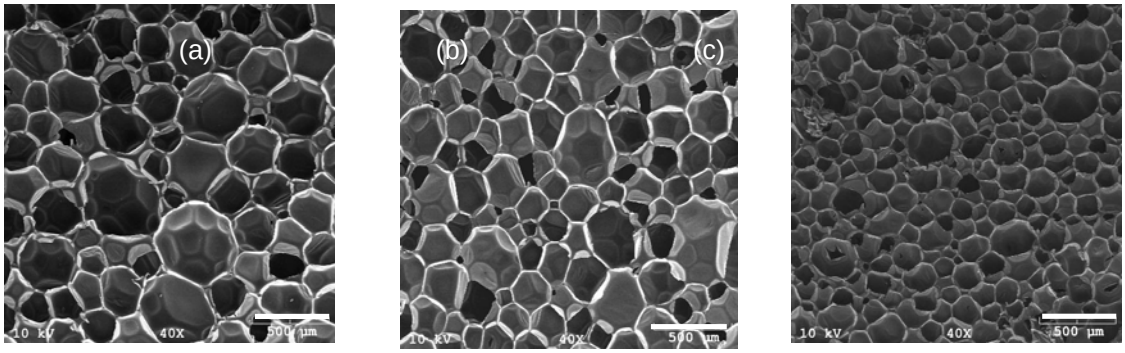

Figure 50. SEM images of rigid PU foams reinforced with (a) 0 wt%, (b) 1 wt%, and (c) 5 wt% of CNWs. Scale bar: 500 μm.

Mechanical property of the resulting rigid PU foams was investigated by compression testing which generated a series of stress-strain curves shown in Figure 51. The yield strength of all foams (Table 36) is higher than 100 KPa which is a sufficient value for many rigid PU foam applications [284]. Since the prepared foams have different density, all the comparisons were made based on the unit mass value of the yield strength and compressive modulus. The control foam (0 wt% CNWs) showed dramastically enhanced mechanical property compared to those synthesized from commercial sucrose polyol and glycerol polyol [204, 282]. Additionally, the yield strength and compressive modulus were increased for the 1 wt% of CNWs reinforced nanocomposite and a more significant improvement for the nanocomposite prepared with addition of 5 wt% of CNWs was observed. It can be partially attributed to the high mechanical property of CNWs, the rigidity of the lignin phenolic structure, and the higher density due to the decrease of cell size. Moreover, CNWs have been proved to be both hydrogen bonded with the polymer matrix and covalently bonded to polyurethane molecular chains through the reaction of hydroxyl groups of CNWs with isocyanate groups of MDI [285]. Together with the high hydroxyl functionality of lignin, it could

possibly result in a higher crosslinking density which is a potential reason for the improvement of compressive properties.

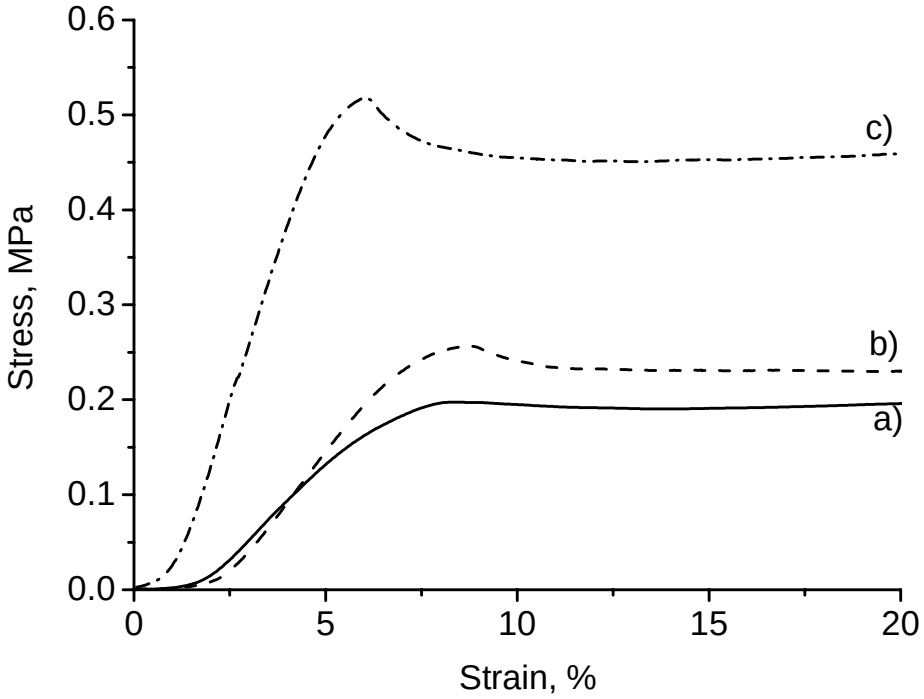

Figure 51. Compressive stress-strain curves of rigid PU foams reinforced with (a) 0 wt%, (b) 1 wt%, and (c) 5 wt% of CNWs.

Thermal property of the prepared rigid PU foams was investigated by DSC and TGA (Figure 52) in terms of glass transition temperature (T_g) and decomposition temperature (T_d). The DSC and TGA results clearly indicated enhanced thermal stability (Table 36). As mentioned above, a reaction took place between CNWs and polymeric MDI which reduced the mobility of the polyurethane chains and caused the increment in T_g and T_d. The same observation and explanation can be found elsewhere regarding cellulose micro/nanocrystals reinforced polyurethane [8].

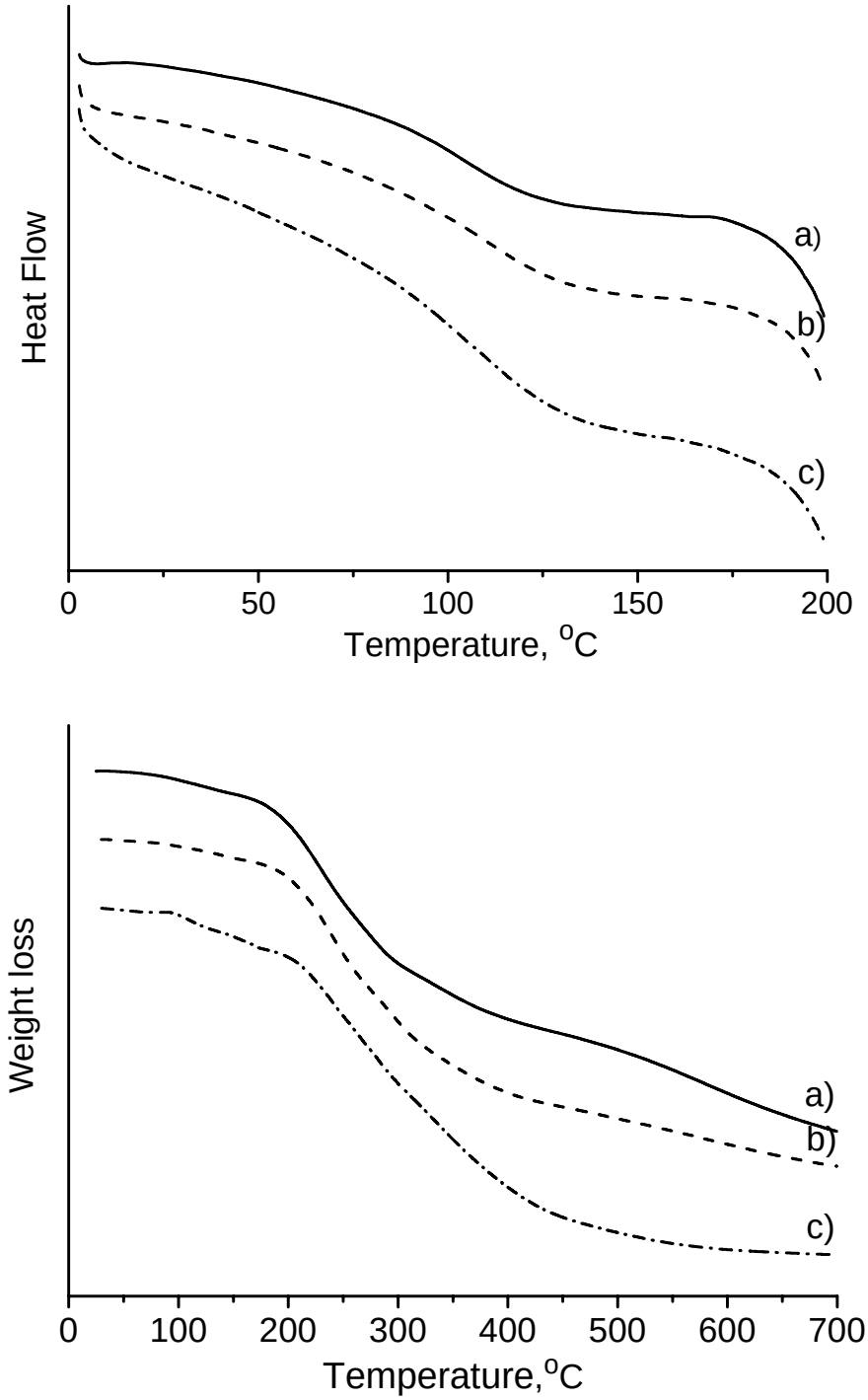

Figure 52. DSC (left) and TGA (right) curves of rigid PU foams reinforced with (a) 0 wt%, (b) 1 wt%, and (c) 5 wt% of CNWs. Both of the DSC and TGA curves were shifted showing a relative value of heat flow or weight loss for easy illustration. Both of the DSC and TGA curves were shifted showing a relative value of heat flow or weight loss for easy illustration.

Table 36. Comparison of compressive and thermal properties of several types of rigid PU foams.

Polyol(s) used	Sucrose and Glycerol polyol	Sucrose and Glycerol polyol	EOL polyol	EOL polyol	EOL polyol
CNW (wt%)	0[33]	0[31]	0	1	5
Density (Kg m^{-3})	53.8 ± 0.5	29.3 ± 0.4	33.6 ± 0.6	37.1 ± 0.6	62.3 ± 0.5
Strength (MPa)	0.15 ± 0.05	0.10 ± 0.01	0.20 ± 0.01	0.26 ± 0.03	0.52 ± 0.01
Strength per unit mass（$\times 10^{-3}$ MPa)	2.79	3.41	5.95	7.01	8.35
Modulus (MPa)	3.3 ± 0.9	1.5 ± 0.1	4.1 ± 0.2	5.4 ± 0.2	12.8 ± 0.1
Modulus per unit mass (MPa)	0.06	0.05	0.12	0.15	0.21
T_g (ºC)	-	-	89 ± 3	104 ± 3	104 ± 2
T_d (ºC)	-	-	247 ± 2	263 ± 3	296 ± 1

6.4 Conclusion

An ethanol organosolv lignin polyol, prepared by reacting lignin with propylene oxide catalyzed by potassium hydroxide, was used to synthesis rigid polyurethane foam which was further reinforced by cellulose nanowhiskers up to 5 wt%. EOL polyol has been proved as a viable and promising polyol to prepared rigid PU foams. The incorporation of CNWs significantly improves both the mechanical and thermal properties of rigid PU nanocomposite foams. It could primarily attributed to the rigid phenolic structure and high functionality of lignin, the high mechanical strength of CNWs, as well as the hydrogen bonding and crosslinking introduced by CNWs. Overall, the combined application of lignin and cellulose in polyurethane synthesis explored a new and economical way to utilize the most abundant natural biopolymers, and at the same time, resulted in greener and more competitive biobased rigid polyurethane foams.

CHAPTER 7

OVERALL CONCLUSIONS

The first thesis study (chapter 4) started with the idea of investigating cellulose nanowhiskers as nanofiller for rigid polyurethane nanocomposite foam preparation due to its attractive features. Cellulose nanowhiskers were hydrolyzed by sulfuric acid from fully bleached softwood Kraft pulp. The dimension of cellulose nanowhiskers was measured to be 150 nm to 250 nm in length and 10 nm to 20 nm in width by AFM. Cellulose nanowhiskers were added in the polyurethane matrix by mixing its DMF suspension with polyol followed by DMF removal under high vacuum. Rigid polyurethane nanocomposite foams reinforced with up to 1.00 wt% of cellulose nanowhiskers were produced. They had low densities suitable for industrial uses and the closed cells of ~350 μm were homogeneously dispersed in the product. Mechanical properties of the nanocomposites, especially compressive properties were significantly improved. In addition to the characteristics of cellulose nanowhisker, i.e., high specific strength, small diameter, and high aspect ratio, other possible reasons for the improvement could be the hydrogen bonding and crosslinking interactions established between cellulose nanowhiskers and the polyurethane matrix and a higher crosslinking density shown by the DMA results. A higher glass transition temperature of the nanocomposites was asctibed to the hydrogen bonding and crosslinking between fillers and matrix resulting in the higher crosslinking density as compared to the control. Moreover, the role of cellulose nanowhisker acting as an insulator and mass transfer barrier during polyurethane decomposition led to a upward shift of the nanocomposites

decomposition temperature.

To further investigate the application of biopolymers in preparation of environmentally friendly polyurethanes, widely available softwood Kraft lignin was oxypropylated to a liquid polyol for rigid polyurethane foam preparation as described in Chapter 5. Kraft lignin was liquefied through a chain extension reaction with propylene oxide under the catalysis of potassium hydroxide. The structure of lignin polyol was characterized by various techniques including FT-IR, GPC and NMR. The phenolic hydroxyl groups were rendered into aliphatic hydroxyl groups after oxypropylation and the oxypropylated lignin had a narrower molecular weight polydispersity compared to the original Kraft lignin. Analyzed from the ^{31}P NMR spectrum of lignin polyol, it had a hydroxyl index of 387 mg KOH/g which was a proper value for rigid PU foam preparation. In the second part of the study in Chapter 5, Kraft lignin polyol was incorporated into polyurethane formulation by replacing sucrose polyol at 10, 30, 60, 100 wt% and then replacing both sucrose polyol and glycerol polyol. All prepared PU foams had a low density of ~30 kg m^{-3} and showed typically polyurethane linkages in the FT-IR spectra. Closed cells of ~650 μm were homogeneously dispersed in the nanocomposites. Compressive properties of the products were characterized in terms of yield strength and compressive modulus according to ASTM standard. Rigid polyurethane foam synthesized by reacting only Kraft lignin polyol with polymeric MDI showed the best mechanical properties. The reinforcement can be attributed to the rigid phenolic structure of lignin and the high functionality of lignin hydroxyl groups resulting in higher crosslinking density of the nanocomposites

In Chapter 6, cellulose nanowhiskers and ethanol organosolv lignin were both

utilized to prepared lignin-based rigid polyurethane nanocomposite foams. The reasons to employ ethanol organosolv lignin are: (1) it has lower molecular weight and less condensed structure compared to Kraft lignin and thus has been reported more reactive towards oxypropylation; (2) the growing market of biorefinery will generate large amount of ethanol organosolv lignin and the utilization of this major byproduct is critical. Since the best formulation in preparation of lignin-based rigid polyurethane foam of the highest mechanical property was found out in Chapter 5, in this study, ethanol organosolv lignin was used as the only polyol for PU synthesis. In order to improve the cellulose nanowhiskers content in polyurethane, the aqueous suspension of cellulose nanowhiskers was directly mixed with polyol instead of the DMF suspension of freeze dried cellulose nanowhiskers. Rigid polyurethane foam reinforced with 1 wt% and 5 wt% of cellulose nanowhiskers were prepared. The closed cell diameter reduced from 320 μm for the control foam to 191 μm for the foam reinforced with 5 wt% of nanowhiskers resulting in an increase density from 33.6 to 62.3 kg m^{-3}. Ethanol organosolv lignin-based rigid polyurethane foam exhibited higher compressive strength and modulus compared to commercial polyols-, namely sucrose polyol and glycerol polyol, based rigid polyurethane foam. It can be primarily ascribed to the rigid phenolic structure of lignin and the high hydroxyl functionality of lignin resulting in the high crosslinking density of lignin-based rigid polyurethane. The nanocomposites, especially the foam reinforced with 5 wt% of cellulose nanowhiskers showed improved mechanical properties and thermal stability as compared to the control foam. It should be the same reason as previously discussed in the first study. Higher char content was found for the lignin-based rigid polyurethane foam in comparison to other commercial counterparts

indicating possible higher flame resistance as the char content was shown to be related with the flame retardant property.

Overall, cellulose nanowhiskers are strong candidate as the nanofiller for rigid polyurethane nanocomposite foam preparation. It can be acid hydrolyzed, enzymatic hydrolyzed or even mechanically disintegrated from wood pulp, cotton, flax, tunicin, algae, etc. Cellulose nanowhiskers undoubtedly possess all characteristics of cellulose, namely wide availability, biodegradability, renewability and high surface reactivity. Moreover, it also bears some unique properties, such as high aspect ratio, and high mechanical strength and modulus. Its incorporation in the polyurethane synthesis resulted in improved mechanical and thermal properties due to both physical and chemical contributions. The content of up to 5 wt% of cellulose nanowhiskers was shown to be feasible by its aqueous suspension which was simple and avoid using organic solvents. The liquefaction of lignin through oxypropylation produced a polyol of adequate hydroxyl index and viscosity for rigid polyurethane foam synthesis. It was highly reactive towards polymeric MDI and resulted in rigid PU foam of comparable or even better mechanical and thermal properties. This was largely attributed to its rigid phenolic structure and its high functionality of hydroxyl groups resulting in higher crosslinking density.

In conclusion, the co-application of cellulose nanowhisker and lignin in the synthesis of rigid polyurethane nanocomposite foams was desirable and promising. It is not only provides an alternative valorization of the most abundant polymers in nature but also adds some environmentally benign characteristics to polyurethanes, e.g., biodegradability.

CHAPTER 8

RECOMMENDATIONS FOR FUTURE WORK

Several other studies might be conducted to further investigate the application of cellulose nanowhiskers and lignin in preparation of polyurethanes. Some particularly attractive options are as follows:

- Compared to cellulose fiber and cellulose microfibril, cellulose nanowhisker exhibited a better reinforcing effect as the nanofiller in polyurethanes. The nanoscale effect played a critical role. However, cellulose nanowhisker prepared from different sources or under varying conditions shows different dimensions. A more specific future study regards to the size effect within the nanoscale is of interest.
- The highest content of cellulose nanowhiskers studied is 5 wt%. Both mechanical and thermal properties of the rigid polyurethane nanocomposite foams were improved with increasing CNWs addition up to 5 wt%. Higher dosages of CNWs are worth studying to find out a critical value from where the reinforcing effect starts to reduce or shows completely negative effect.
- Other characterizations of lignin polyol, e.g., viscosity measurement and thermal properties can be valuable to conduct for quality control. On the other hand, oxypropylation conditions can be adjusted according to the desired properties of lignin polyol for other uses such as its application in flexible polyurethane foams and polyurethane elastomers.

- As a high performance insulating material, rigid polyurethane foam has the corresponding properties need to investigate such as thermal conductivity, aging property, long term thermal resistance, flexural properties, and etc. The effect of employing cellulose nanowhisker and lignin polyol on those properties of rigid PU foams should be studied.

APPENDIX A

CELLULOSE NANOWHISKER FOAMS BY FREEZE CASTING[5]

A.1 Introduction

Fabrication of materials with homogeneous and well defined architectures has received increasing research interest owing to their broad applications such as tissue engineering, delivery matrices, green packaging, nanocomposites, and automotive industry [286-289]. Several methods including spin coating, layer-by-layer, freeze casting, and eutectic growth in two phase system has been utilized to organize micron/nano size particles to obtain ordered structures. Among the different techniques used, freeze casting has been shown as a versatile, easily implemented, and promising technique to build structures such as scaffolds, porous nanocomposites, and microwire networks with well aligned and controlled porosity [290-292].

Freeze casting technique involves freezing a liquid suspension and sublimation of the solvent there after under reduced pressure. During the freezing process, the suspended particles are organized by rejection from the growing ice crystal front to the intervening space, which results in an ordered structure after sublimation. Fabrication of various materials by this technique suggests that the underlying principle of freeze casting is strongly dependent on simple physics of ice crystals and the physical interaction between the growing solidification front and the inert particles of the slurry

[5] This manuscript was accepted for publication in Carbohydrate Polymers, 2012. It is entitled as "Cellulose Nanowhisker Foams by Freezing Casting". The first author is Rajalaxmi Dash from the Institute of Paper Science and Technology and School of Chemistry and Biochemistry at Georgia Institute of Technology. The other authors are Yang Li and Arthur J. Ragauskas from the Institute of Paper Science and Technology and School of Chemistry and Biochemistry at Georgia Institute of Technology.

[293-295]. Depending on the choice of solvent, slurry formulation, and solidification conditions, the final porosity and pore morphologies can be readily tuned. However, the solidification conditions remain as the key factor since all the features of porosity are created during this stage and thereby, controlling the formation and growth of ice crystals would yield materials with specific microstructure. For instance, in case of unidirectional freezing, a porous structure with unidirectional channel is obtained. In fact, this approach has been utilized to prepare variety of ceramic structures such as silica fiber bundles, tubular supports with radially aligned pores, micro-honeyecombs as well as polymeric scaffolds [296-298].

Cellulose nanowhiskers, derived sustainably from biomass represent a relatively new raw material that has gained significant attention due to their intrinsically appealing physical, chemical as well as mechanical properties [2, 83, 134, 299]. Cellulose nanowhiskers designate a class of rod like nanoparticles which are mainly prepared by controlled acid hydrolysis of native cellulose fibers. The size and properties of nanowhiskers depend on the source and hydrolysis conditions of cellulose fibers and typically are 5-10 nm in width and 100-300 nm in length for wood-based nanowhiskers [87, 108]. A number of non-periodic highly porous structures known as aerogels from micro and nano cellulose fibers as well as cellulose derivatives have been reported in literature and they are commonly prepared by solvent exchange of a wet gel followed by supercritical CO_2 drying [299-302]. However, porous structures with regular pattern can be obtained by controlling the freezing temperature of the slurry followed by subsequent freeze drying.

Recently, Deng et al. [303] reported the preparation of layered cellulose foams

through directional freezing technique emphasizing the effect of fiber concentration and freezing temperature on the microstructure and mechanical properties of microfibril foams. They have also measured the compressive strength of cellulose nanowhisker foams but a detailed examination on their microstructure is lacking. Utilizing the facile freeze casting technique, we attempt to fabricate aligned porous cellulose nanowhisker structures and investigate the relationship between the freezing conditions and the microstructures obtained, which has not been reported so far. We expect that ice growth strategy of freeze casting technique will allow the fabrication of well ordered cellulose nanowhisker structures, opening their use as a template for layered composites, filters, and storage material.

A.2 Experimental Section

A.2.1 Materials

A fully bleached commercial softwood Kraft pulp was used as a source for cellulose nanowhiskers preparation. Polyvinyl alcohol (PVA) was purchased from VWR International (M_w: 15000, Degree of hydrolysis: 87-89%).

A.2.2 Preparation of H_2SO_4-hydrolyzed Cellulose Nanowhiskers

The cellulose nanowhiskers were prepared by sulfuric acid hydrolysis of a bleached softwood pulp based on a literature procedure [108]. In brief, 60.00 g (oven dried weight) of the pulp was mixed with H_2SO_4 solution (64%, w/w, 1:10 g mL^{-1}) with continuous stirring at 45˚C for 45 min. The hydrolysis reaction was halted by adding excess (10-fold) of distilled water followed by the removal of acidic solution through

successive centrifugation at 12,000 rpm for 10 min until the supernatant became turbid. The sediment was collected and dialyzed (MWCO: 12-14,000) against tap water until the solution pH did not change anymore. After dialysis, the content was sonicated for 10 min and centrifuged for 5 min at 10,000 rpm. The cloudy supernatant, containing nanowhiskers, was collected and the remaining sediment was again mixed with distilled water, sonicated, and centrifuged to obtain additional nanowhisker; this step was repeated till the supernatant was clear.

A.2.3 Preparation of Porous Samples

Porous cellulose nanowhisker samples were prepared by freezing a suspension of nanowhiskers and polyvinyl alcohol under different freezing conditions and then drying under vacuum. Cellulose nanowhisker suspension (10mL, 2 wt %) was mixed with different amounts of PVA (20% and 50%, w/w) and slowly stirred at room temperature for 4 h in order to avoid the generation of bubbles. Then, the mixture was poured in to small glass vials and freezed by two methods: (i) dipping in liquid nitrogen (ii) placing these vials in two different freezers for 2 h, where the cooling rates were measured to be 4.5 and 13˚C min^{-1}, respectively. Frozen solids were subsequently dried in a freeze dryer for 24 h to sublimate the water under vacuum. Control samples were prepared in absence of PVA.

A.2.4 Characterization

Surface morphology of the porous samples was studied by JEOL-1530 thermally-assisted field emission (TFE) scanning electron microscope (SEM). Before acquiring images, the surfaces of all the samples were coated with gold in a sputter

coater.

A.3 Results and Discussion

Cellulose nanowhisker suspension was mixed with PVA and solidification of the slurry was carried out by two ways: (i) quenching the slurry in liquid nitrogen (ii) freezing the slurry at two different cooling rates, i.e., 13˚C min^{-1} and 4.5˚C min^{-1}. Freeze drying of the solvent created the final nanowhisker porous structure as a replica of ice crystals that generated during freezing. PVA was used as a binder due to its solubility in water and its compatibility with cellulose nanowhiskers [304]. Cellulose whisker concentration (2.0 wt %) was chosen as an attempt to be in semi-dilute concentration range especially to obtain a template for potential multilayered nanocomposite applications.

It was observed that irrespective of the cooling rate, when compared to the samples in PVA, the samples prepared in absence of PVA (Figure 53) collapsed during the sublimation process resulting in a structure with no particular alignment of the pores created. It suggests that PVA acts as a support to the nanowhiskers, which could be due to the hydrogen bonding between PVA and nanowhiksers, facilitating the formation of a stable oriented porous architecture. The influence of PVA content on the microstructure of the nanowhisker materials prepared was also studied. The images of the samples freezed at 13˚C min^{-1} cooling rate are shown here (Figure 53). At 20 wt % PVA content, the samples exhibited a well oriented porous structure with equally spaced lamellar walls (Figure 53b), while at 50 wt % of PVA, a dense structure with some locally aligned pores

were found (Figure 53c) instead of the long range order lamellar walls. The possible physical interactions among nanowhiskers and between nanowhiskers and the growing solidification fronts during the freezing leads to different growth mechanisms, which could be the reason for the loss in alignment at high slurry concentrations. Similar phenomenon was also observed for samples prepared at 4.5°C min^{-1} cooling rate, however, for samples freezed in liquid nitrogen, the effect of PVA concentration on the alignment of pores and its morphology was found to be insignificant.

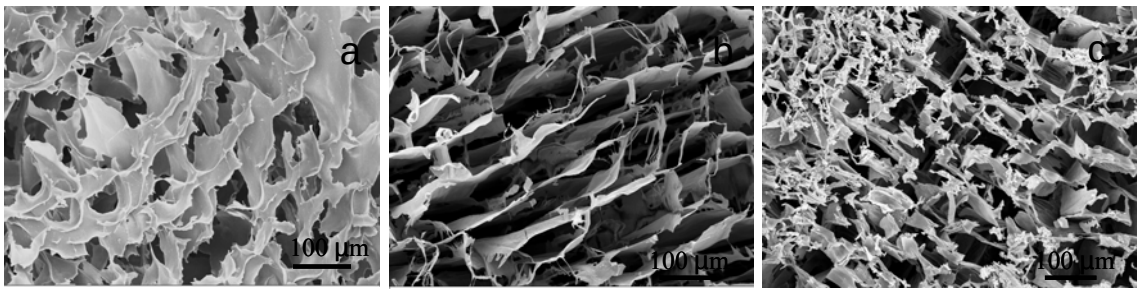

Figure 53. Morphology of cellulose nanowhisker samples freezed at 13°**C** min^{-1} cooling rate (a) 0 wt %, (b) 20 wt % and (c) 50 wt % of PVA.

An overview of the porous cellulose nanowhisker material and its microstructure is shown in Figure 54a. The bottom part of the microstructure can be characterized as a dense cellular structure with some randomly distributed pores whereas the upper part exhibits an oriented and highly porous structure. It implies that after growth initiation step at the bottom, the ice crystals started growing regularly in a vertical direction leaving behind open pore channels after sublimation. Eventually, the growth was terminated at the top of the suspension and formed a surface which has a different microstructure (Figure 54c) as compared to the outer side of the sample, where open, uniform, and oriented pores were observed as shown in 53b. Based on the detailed microstructural

observation of the sample a schematic diagram is shown in Figure 54d simply indicating the growth pattern of ice crystals.

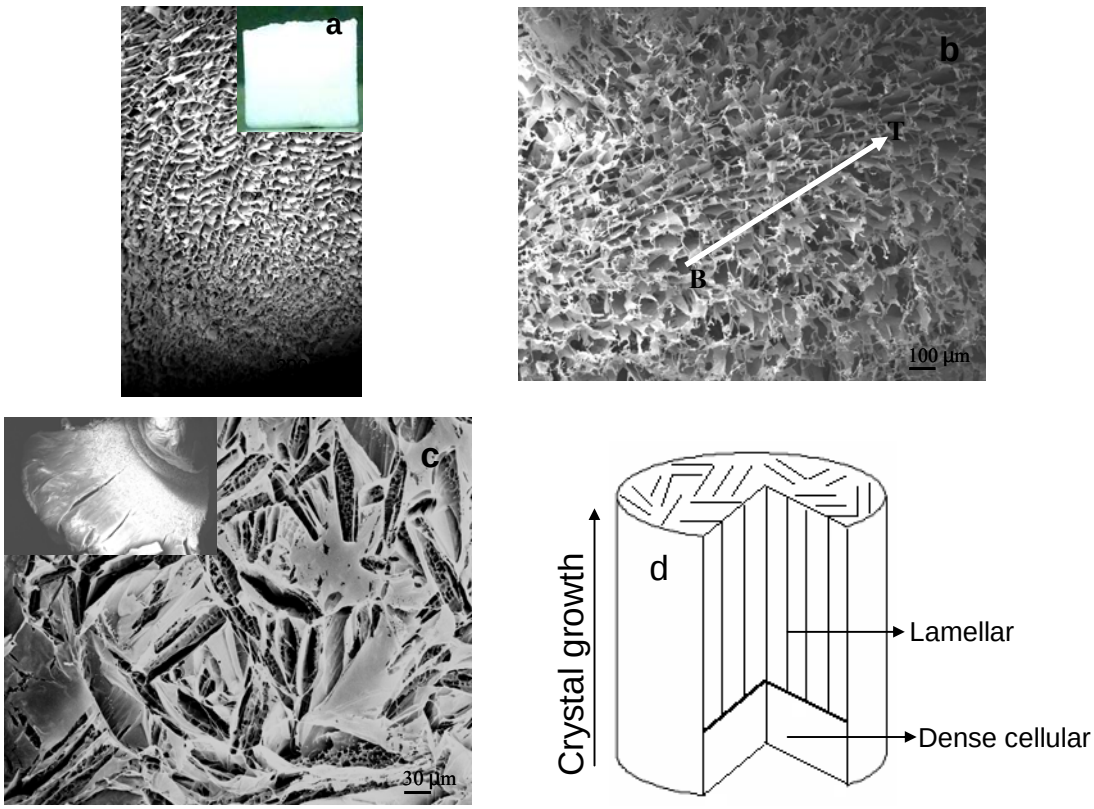

Figure 54. (a) Overview of the sample and its microstructure, (b) side (B: bottom and T:Top of the sample) and (c) top view of the porous nanowhisker structure and (d) schematic diagram showing the growth pattern of ice crystals.

Studies on various materials including ceramic and metallic particles reveal that solidification has a critical role in determining the final pore morphology and microstructure of the porous materials [305-306]. Our results are well consistent with literature results as the pore size of the resulted cellulose nanowhisker structure and the pore orientation were both affected by the cooling rate. It was observed that freezing the slurry in liquid nitrogen created a fine and perfectly aligned lamellar structure in the

vertical direction with a small pore size of 10-20 μm. The lamellae walls are thinner and inter lamellae spaces are smaller at this fast freezing condition (Figure 55a), whereas a decrease in cooling rate gradually increased the pore size (~100 μm) and lamellae thickness as observed in Figure 55b and 55c. Similar behavior was also found in other polymeric and ceramics materials; as faster the freezing rate, finer the resulting structure, on the other hand slow cooling noticeably scaled up the microstructure [306].

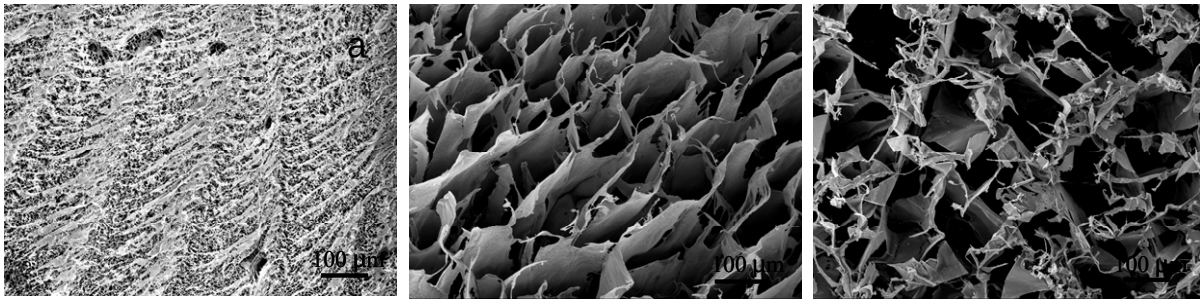

Figure 55. Effect of cooling rate on the pore structure of 20 wt % PVA samples (a) Liquid nitrogen, (b) 13˚C min^{-1} and (c) 4.5˚C min^{-1}.

In each case, the cellulose nanowhiskers and PVA slurries were frozen at a constant cooling rate starting from room temperature. As a consequence, the subsequent drying process resulted in a lamellar porous microstructure with long range order (Figure 56). This is a typical phenomenon observed under steady state freezing conditions as well as in cases where water is being used as a solvent. The mechanism of lamellar structure formation can be well understood through the basic physics of water freezing which has been already explained in literature [291, 306]. Moreover, the lamellar surface exhibits two different types of surface dendrites. The first type of dendrite grows in between the lamellae whereas the second type corresponds to a fine tortuous

morphology protruding from the top of the lamellae. The relative size of these dendrites depends not only on different freezing conditions applied to the suspension but also on the concentration of the solution. For instance, faster cooling rates with liquid nitrogen leads to finer and smaller dendrites while the dendrite size increases in case of slow cooling or with a more concentrated solution. The formation of the dendritic feature was also observed in porous ceramic structures and it was proposed to be influenced by a number of factors such as nature of the solvent, freezing conditions, and the characteristics of starting powder [307-308].

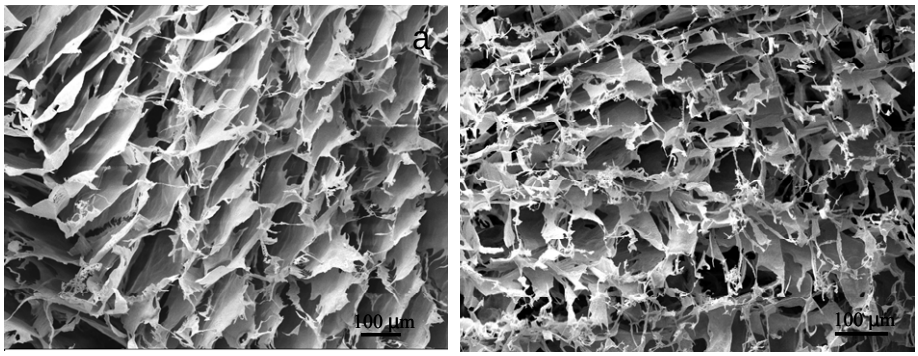

Figure 56. Microstructure showing (a) lamellar walls and (b) surface dendrites.

.

A.4 Conclusions

In conclusion, our results illustrate a simple approach to produce long range ordered porous cellulose nanowhisker structure with PVA as a support material. The resultant microstructure and pore morphology can be controlled by modifying the freezing rate and the slurry concentration. Finally, considering their lamellar and interconnected pore structure combined with the renewable nature of cellulose, ordered

cellulose nanowhisker based materials with designed orientation of pore channels can be prepared through precise control of thermal gradients, which has potential applications especially as a template for layered composites, molecular filtration, delivery matrix, and tissue engineering scaffold.

APPENDIX B

COPYRIGHT PERMISSIONS

B.1 Permission from Nano-Micro Letters

Creative Commons License Deed

Attribution 3.0 Unported (CC BY 3.0)

This is a human-readable summary of the Legal Code (the full license).
Disclaimer

You are free:

- **to Share** — to copy, distribute and transmit the work
- **to Remix** — to adapt the work
- to make commercial use of the work
-

Under the following conditions:

- **Attribution** — You must attribute the work in the manner specified by the author or licensor (but not in any way that suggests that they endorse you or your use of the work).

  What does "Attribute this work" mean?

  The page you came from contained embedded licensing metadata, including how the creator wishes to be attributed for re-use. You can use the HTML here to cite the work. Doing so will also include metadata on your page so that others can find the original work as well.

With the understanding that:

- **Waiver** — Any of the above conditions can be waived if you get permission from the copyright holder.
- **Public Domain** — Where the work or any of its elements is in the public domain under applicable law, that status is in no way affected by the license.
- **Other Rights** — In no way are any of the following rights affected by the license:
    - Your fair dealing or fair use rights, or other applicable copyright exceptions and limitations;
    - The author's moral rights;
    - Rights other persons may have either in the work itself or in how the work is used, such as publicity or privacy rights.
- **Notice** — For any reuse or distribution, you must make clear to others the license terms of this work. The best way to do this is with a link to this web page.

This work is licensed under a Creative Commons Attribution 3.0 Unported License.

B.2 Permission from Journal of Nanoscience and Nanotechnology

RE: copyright permission
From: Chen, Wei [weichen@uta.edu]
Sent: Tuesday, March 27, 2012 2:33 PM
To: Yang Li

Your article and your thesis, no need permissions.

Wei Chen, Ph. D.
Associate Professor
Nano-Bio Physics
Department ment of Physics
The University of Texas at Arlington
502 Yates, Arlington, TX 76019-0059
Phone: 817-272-1064, Fax: 817-272-3637
http://www.uta.edu/physics/main/faculty/wchen/index.html

Editor-in-Chief*, *Reviews in Nanoscience and Nanotechnology
American Editor, Journal of Nanoscience and Nanotechnology
Associate Editor, Journal of Biomedical Nanotechnology

From: Yang Li [mailto:Yang.Li@ipst.gatech.edu]
Sent: Tuesday, March 27, 2012 2:08 PM
To: Chen, Wei
Subject: copyright permission

Dear Dr. Chen,

Could you please let me know how to get the copyright permission to use my article (Rigid Polyurethane Foam/Cellulose Whisker Nanocomposites: Preparation, Characterization,
and Properties) in thesis?

Thank you,

Yang Li
Georgia Institute of Technology
500 10th St. NW
Atlanta, GA, USA 30332

B.3 Permission from InTech

Advances in Diverse Industrial Applications of Nanocomposites

Edited by Boreddy S. R. Reddy

Published by InTech

Janeza Trdine 9, 51000 Rijeka, Croatia

Publishing Process Manager Iva Lipovic

Technical Editor Teodora Smiljanic

Cover Designer Martina Sirotic

Image Copyright Olegusk, 2010. Used under license from Shutterstock.com

First published March, 2011

Printed in India

A free online edition of this book is available at www.intechopen.com

Additional hard copies can be obtained from orders@intechweb.org

Advances in Diverse Industrial Applications of Nanocomposites,

Edited by Boreddy S. R. Reddy

p. cm.

ISBN 978-953-307-202-9

B.4 Permission from Journal of Wood Chemistry and Technology

RightsLink®

Home | Account Info | Help

Title:	Kraft Lignin-Based Rigid Polyurethane Foam
Author:	Yang Li, Arthur J. Ragauskas
Publication:	Journal of Wood Chemistry and Technology
Publisher:	Taylor & Francis
Date:	Jul 1, 2012

Copyright © 2012 Taylor & Francis

Logged in as:

yang li

Account #:
3000515589

LOGOUT

Thesis/Dissertation Reuse Request

Taylor & Francis is pleased to offer reuses of its content for a thesis or dissertation free of charge contingent on resubmission of permission request if work is published.

BACK | CLOSE WINDOW

B.5 Permission from RSC Advances

RE: Permission request to use full article in thesis
From: CONTRACTS-COPYRIGHT (shared) [Contracts-Copyright@rsc.org]
Sent: 28 March 2012 0:27
To: Yang Li

Dear Dr Li

The Royal Society of Chemistry (RSC) hereby grants permission for the use of your paper(s) specified below in the printed and microfilm version of your thesis. You may also make available the PDF version of your paper(s) that the RSC sent to the corresponding author(s) of your paper(s) upon publication of the paper(s) in the following ways: in your thesis via any website that your university may have for the deposition of theses, via your university's Intranet or via your own personal website. We are however unable to grant you permission to include the PDF version of the paper(s) on its own in your institutional repository. The Royal Society of Chemistry is a signatory to the STM Guidelines on Permissions (available on request).

Please note that if the material specified below or any part of it appears with credit or acknowledgement to a third party then you must also secure permission from that third party before reproducing that material.

Please ensure that the thesis states the following:

Reproduced by permission of The Royal Society of Chemistry

and include a link to the paper on the Royal Society of Chemistry's website.

Please ensure that your co-authors are aware that you are including the paper in your thesis.

Regards

Gill Cockhead
Publishing Contracts & Copyright Executive

Gill Cockhead (Mrs), Publishing Contracts & Copyright Executive
Royal Society of Chemistry, Thomas Graham House
Science Park, Milton Road, Cambridge CB4 0WF, UK
Tel +44 (0) 1223 432134, Fax +44 (0) 1223 423623
http://www.rsc.org

From: Yang Li [mailto:Yang.Li@ipst.gatech.edu]
Sent: 28 March 2012 02:41
To: CONTRACTS-COPYRIGHT (shared)
Subject: Permission request to use full article in thesis

Hi,

I am the author of the following article,

Title:	Ethanol organosolv lignin-based rigid polyurethane foam reinforced with cellulose nanowhiskers
Author:	Yang Li,Arthur J. Ragauskas
Publication:	RSC Advances
Publisher:	Royal Society of Chemistry
Date:	Feb 24, 2012

I went through Rightslink to obtain a permission to use this article in my thesis both in an electronic and print format, but the system shows the reuse is not allowed.

Can I be granted the copyright for the electronic format for this article?

Thanks,

Yang Li
Graduate student
School of Chemistry and Biochemistry
Georgia Institute of Technology
500 10th St. NW, Atlanta, GA, USA 30332

B.6 Permission from Carbohydrate Polymers

ELSEVIER LICENSE
TERMS AND CONDITIONS

Mar 27, 2012

This is a License Agreement between yang li ("You") and Elsevier ("Elsevier") provided by Copyright Clearance Center ("CCC"). The license consists of your order details, the terms and conditions provided by Elsevier, and the payment terms and conditions.

All payments must be made in full to CCC. For payment instructions, please see information listed at the bottom of this form.

Supplier	Elsevier Limited The Boulevard,Langford Lane Kidlington,Oxford,OX5 1GB,UK
Registered Company Number	1982084
Customer name	yang li
Customer address	4816 via ventura apt 416 mesquite, TX 75150
License number	2877310954794
License date	Mar 27, 2012
Licensed content publisher	Elsevier
Licensed content publication	Carbohydrate Polymers
Licensed content title	Cellulose nanowhisker foams by freeze casting
Licensed content author	Rajalaxmi Dash,Yang Li,Arthur J. Ragauskas
Licensed content date	2 April 2012
Licensed content volume number	88
Licensed content issue number	2
Number of pages	4
Start Page	789
End Page	792
Type of Use	reuse in a thesis/dissertation
Intended publisher of new work	other
Portion	full article

Format	both print and electronic
Are you the author of this Elsevier article?	Yes
Will you be translating?	No
Order reference number	appendix A
Title of your thesis/dissertation	APPLICATIONS OF CELLULOSE NANOWHISKERS AND LIGNIN IN PREPARATION OF RIGID POLYURETHANE NANOCOMPOSITE FOAMS
Expected completion date	May 2012
Estimated size (number of pages)	200
Elsevier VAT number	GB 494 6272 12
Permissions price	0.00 USD
VAT/Local Sales Tax	0.0 USD / 0.0 GBP
Total	0.00 USD
Terms and Conditions	

INTRODUCTION

1. The publisher for this copyrighted material is Elsevier. By clicking "accept" in connection with completing this licensing transaction, you agree that the following terms and conditions apply to this transaction (along with the Billing and Payment terms and conditions established by Copyright Clearance Center, Inc. ("CCC"), at the time that you opened your Rightslink account and that are available at any time at http://myaccount.copyright.com).

GENERAL TERMS

2. Elsevier hereby grants you permission to reproduce the aforementioned material subject to the terms and conditions indicated.

3. Acknowledgement: If any part of the material to be used (for example, figures) has appeared in our publication with credit or acknowledgement to another source, permission must also be sought from that source. If such permission is not obtained then that material may not be included in your publication/copies. Suitable acknowledgement to the source must be made, either as a footnote or in a reference list at the end of your publication, as follows:

“Reprinted from Publication title, Vol /edition number, Author(s), Title of article / title of chapter, Pages No., Copyright (Year), with permission from Elsevier [OR APPLICABLE SOCIETY COPYRIGHT OWNER].” Also Lancet special credit - “Reprinted from The Lancet, Vol. number, Author(s), Title of article, Pages No., Copyright (Year), with permission from Elsevier.”

4. Reproduction of this material is confined to the purpose and/or media for which permission is hereby given.

5. Altering/Modifying Material: Not Permitted. However figures and illustrations may be altered/adapted minimally to serve your work. Any other abbreviations, additions, deletions and/or any other alterations shall be made only with prior written authorization of Elsevier Ltd. (Please contact Elsevier at permissions@elsevier.com)

6. If the permission fee for the requested use of our material is waived in this instance, please be advised that your future requests for Elsevier materials may attract a fee.

7. Reservation of Rights: Publisher reserves all rights not specifically granted in the combination of (i) the license details provided by you and accepted in the course of this licensing transaction, (ii) these terms and conditions and (iii) CCC's Billing and Payment terms and conditions.

8. License Contingent Upon Payment: While you may exercise the rights licensed immediately upon issuance of the license at the end of the licensing process for the transaction, provided that you have disclosed complete and accurate details of your proposed use, no license is finally effective unless and until full payment is received from you (either by publisher or by CCC) as provided in CCC's Billing and Payment terms and conditions. If full payment is not received on a timely basis, then any license preliminarily granted shall be deemed automatically revoked and shall be void as if never granted. Further, in the event that you breach any of these terms and conditions or any of CCC's Billing and Payment terms and conditions, the license is automatically revoked and shall be void as if never granted. Use of materials as described in a revoked license, as well as any use of the materials beyond the scope of an unrevoked license, may constitute copyright infringement and publisher reserves the right to take any and all action to protect its copyright in the materials.

9. Warranties: Publisher makes no representations or warranties with respect to the licensed material.

10. Indemnity: You hereby indemnify and agree to hold harmless publisher and CCC, and their respective officers, directors, employees and agents, from and against any and all claims arising out of your use of the licensed material other than as specifically authorized pursuant to this license.

11. No Transfer of License: This license is personal to you and may not be sublicensed, assigned, or transferred by you to any other person without publisher's written permission.

12. No Amendment Except in Writing: This license may not be amended except in a writing signed by both parties (or, in the case of publisher, by CCC on publisher's behalf).

13. Objection to Contrary Terms: Publisher hereby objects to any terms contained in any purchase order, acknowledgment, check endorsement or other writing prepared by you,

which terms are inconsistent with these terms and conditions or CCC's Billing and Payment terms and conditions. These terms and conditions, together with CCC's Billing and Payment terms and conditions (which are incorporated herein), comprise the entire agreement between you and publisher (and CCC) concerning this licensing transaction. In the event of any conflict between your obligations established by these terms and conditions and those established by CCC's Billing and Payment terms and conditions, these terms and conditions shall control.

14. Revocation: Elsevier or Copyright Clearance Center may deny the permissions described in this License at their sole discretion, for any reason or no reason, with a full refund payable to you. Notice of such denial will be made using the contact information provided by you. Failure to receive such notice will not alter or invalidate the denial. In no event will Elsevier or Copyright Clearance Center be responsible or liable for any costs, expenses or damage incurred by you as a result of a denial of your permission request, other than a refund of the amount(s) paid by you to Elsevier and/or Copyright Clearance Center for denied permissions.

LIMITED LICENSE

The following terms and conditions apply only to specific license types:

15. **Translation**: This permission is granted for non-exclusive world **English** rights only unless your license was granted for translation rights. If you licensed translation rights you may only translate this content into the languages you requested. A professional translator must perform all translations and reproduce the content word for word preserving the integrity of the article. If this license is to re-use 1 or 2 figures then permission is granted for non-exclusive world rights in all languages.

16. **Website**: The following terms and conditions apply to electronic reserve and author websites:
Electronic reserve: If licensed material is to be posted to website, the web site is to be password-protected and made available only to bona fide students registered on a relevant course if:
This license was made in connection with a course,
This permission is granted for 1 year only. You may obtain a license for future website posting,
All content posted to the web site must maintain the copyright information line on the bottom of each image,
A hyper-text must be included to the Homepage of the journal from which you are licensing at http://www.sciencedirect.com/science/journal/xxxxx or the Elsevier homepage for books at http://www.elsevier.com , and
Central Storage: This license does not include permission for a scanned version of the material to be stored in a central repository such as that provided by Heron/XanEdu.

17. **Author website** for journals with the following additional clauses:

All content posted to the web site must maintain the copyright information line on the bottom of each image, and
he permission granted is limited to the personal version of your paper. You are not allowed to download and post the published electronic version of your article (whether PDF or HTML, proof or final version), nor may you scan the printed edition to create an electronic version,
A hyper-text must be included to the Homepage of the journal from which you are licensing at http://www.sciencedirect.com/science/journal/xxxxx , As part of our normal production process, you will receive an e-mail notice when your article appears on Elsevier's online service ScienceDirect (www.sciencedirect.com). That e-mail will include the article's Digital Object Identifier (DOI). This number provides the electronic link to the published article and should be included in the posting of your personal version. We ask that you wait until you receive this e-mail and have the DOI to do any posting.
Central Storage: This license does not include permission for a scanned version of the material to be stored in a central repository such as that provided by Heron/XanEdu.

18. **Author website** for books with the following additional clauses:
Authors are permitted to place a brief summary of their work online only.
A hyper-text must be included to the Elsevier homepage at http://www.elsevier.com

All content posted to the web site must maintain the copyright information line on the bottom of each image
You are not allowed to download and post the published electronic version of your chapter, nor may you scan the printed edition to create an electronic version.
Central Storage: This license does not include permission for a scanned version of the material to be stored in a central repository such as that provided by Heron/XanEdu.

19. **Website** (regular and for author): A hyper-text must be included to the Homepage of the journal from which you are licensing at
http://www.sciencedirect.com/science/journal/xxxxx. or for books to the Elsevier homepage at http://www.elsevier.com

20. **Thesis/Dissertation**: If your license is for use in a thesis/dissertation your thesis may be submitted to your institution in either print or electronic form. Should your thesis be published commercially, please reapply for permission. These requirements include permission for the Library and Archives of Canada to supply single copies, on demand, of the complete thesis and include permission for UMI to supply single copies, on demand, of the complete thesis. Should your thesis be published commercially, please reapply for permission.

21. **Other Conditions**:

B.7 Permission from John Wiley & Sons Ltd.

RE: Republication/Electronic Request Form
From: Permission Requests - UK [permissionsuk@wiley.com]
Sent: 2012-4-11 5:33
To: Yang Li

Dear Yang Li,

Thank you for your request.

Permission is hereby granted for the use requested subject to the usual acknowledgements (author, title of material, title of book/journal, ourselves as publisher).

Any third party material is expressly excluded from this permission. If any of the material you wish to use appears within our work with credit to another source, authorisation from that source must be obtained.

This permission does not include the right to grant others permission to photocopy or otherwise reproduce this material except for versions made by non-profit organisations for use by the blind, visually impaired and other persons with print disabilities (VIPs).

Best Wishes

Verity Butler
Permissions Assistant
John Wiley & Sons Ltd.

From: Yang Li [mailto:Yang.Li@ipst.gatech.edu]
Sent: 04 April 2012 14:49
To: Permission Requests - UK
Subject: 答复: Republication/Electronic Request Form

Dear Ms. Willcox,

I want to reuse the attached figure (volume growth of the global polyurethane market) in my Ph.D. thesis which will be in both print and electronic form (adobe acrobat). It will not appear in the "software program". Sorry I don't have the book on my hand right now so don't know the exact page number. Please let me know if it does matter. Thank you.

Best regards,

Yang Li

From: Permission Requests - UK [mailto:permissionsuk@wiley.com]
Sent: 2012-4-4 5:45
To: Yang Li
Subject: FW: Republication/Electronic Request Form

Dear Yang Li,

Thank you for your permission request.

Please state the exact material that you wish to reuse, including word count, page numbers or figure numbers as appropriate.

Please also state how our material will appear in the "Software Program" and how this differs from the print and eBook versions.

Kind Regards

Emma Willcox
Permissions Assistant
John Wiley & Sons Ltd.

-----Original Message-----
From: PermissionsUS@wiley.com on www.wiley.com [mailto:webmaster@wiley.com]
Sent: Tuesday, March 27, 2012 5:59 PM
To: Permissions - US
Subject: Republication/Electronic Request Form

A01_First_Name: yang
A02_Last_Name: li
A03_Company_Name: georgia institute of technology
A04_Address: 500 10th St. NW
A05_City: Atlanta
A06_State: GA
A07_Zip: 30332
A08_Country: USA
A09_Contact_Phone_Number: 6789383429
A10_Fax:
A11_Emails: yli@ipst.gatech.edu
A12_Reference:
A13_Book_Title: The Polyurethanes Book
A40_Book_or_Journal: Book

A14_Book_Author: David Randall and Steve Lee
A15_Book_ISBN: 978-0-470-85041-1
A16_Journal_Month:
A17_Journal_Year:
A18_Journal_Volume:
A19_Journal_Issue_Number:
A20_Copy_Pages: figure:Volume growth of the global polyurethane market
A21_Maximum_Copies: 7
A22_Your_Publisher: georgia institute of technology
A23_Your_Title: APPLICATIONS OF CELLULOSE NANOWHISKERS AND LIGNIN IN PREPARATION OF RIGID POLYURETHANE NANOCOMPOSITE FOAMS
A24_Publication_Date:
A25_Format: print,E-Book,Software Program
A41_Ebook_Reader_Type: adobe acrobat
A26_If_WWW_URL:
A27_If_WWW_From_Adopted_Book:
A28_If_WWW_Password_Access:
A45_WWW_Users:
A29_If_WWW_Material_Posted_From:
A30_If_WWW_Material_Posted_To:
A42_If_Intranet_URL:
A32_If_Intranet_From_Adopted_Book:
A33_If_Intranet_Password_Access:
A48_Intranet_Users:
A34_If_Intranet_Material_Posted_From:
A35_If_Intranet_Material_Posted_To:
A50_If_Software_Print_Type: powerpoint
A60_If_Other_Type:
A37_Comments_For_Request:

B.8 Permission from Trends in Plant Science

ELSEVIER LICENSE
TERMS AND CONDITIONS

Mar 27, 2012

This is a License Agreement between yang li ("You") and Elsevier ("Elsevier") provided by Copyright Clearance Center ("CCC"). The license consists of your order details, the terms and conditions provided by Elsevier, and the payment terms and conditions.

All payments must be made in full to CCC. For payment instructions, please see information listed at the bottom of this form.

Supplier	Elsevier Limited The Boulevard,Langford Lane Kidlington,Oxford,OX5 1GB,UK
Registered Company Number	1982084
Customer name	yang li
Customer address	4816 via ventura apt 416 mesquite, TX 75150
License number	2877290127193
License date	Mar 27, 2012
Licensed content publisher	Elsevier
Licensed content publication	Trends in Plant Science
Licensed content title	Lignins and lignocellulosics: a better control of synthesis for new and improved uses
Licensed content author	Alain M Boudet,Shinya Kajita,Jacqueline Grima-Pettenati,Deborah Goffner
Licensed content date	December 2003
Licensed content volume number	8
Licensed content issue number	12
Number of pages	6
Start Page	576
End Page	581

Type of Use	reuse in a thesis/dissertation
Portion	figures/tables/illustrations
Number of figures/tables/illustrations	1
Format	both print and electronic
Are you the author of this Elsevier article?	No
Will you be translating?	No
Order reference number	Figure 2. Schematic representation of the secondary cell wall containing cellulose, hemicelluloses and lignin
Title of your thesis/dissertation	APPLICATIONS OF CELLULOSE NANOWHISKERS AND LIGNIN IN PREPARATION OF RIGID POLYURETHANE NANOCOMPOSITE FOAMS
Expected completion date	May 2012
Estimated size (number of pages)	200
Elsevier VAT number	GB 494 6272 12
Permissions price	0.00 USD
VAT/Local Sales Tax	0.0 USD / 0.0 GBP
Total	0.00 USD
Terms and Conditions	

INTRODUCTION

1. The publisher for this copyrighted material is Elsevier. By clicking "accept" in connection with completing this licensing transaction, you agree that the following terms and conditions apply to this transaction (along with the Billing and Payment terms and conditions established by Copyright Clearance Center, Inc. ("CCC"), at the time that you opened your Rightslink account and that are available at any time at http://myaccount.copyright.com).

GENERAL TERMS

2. Elsevier hereby grants you permission to reproduce the aforementioned material subject to the terms and conditions indicated.

3. Acknowledgement: If any part of the material to be used (for example, figures) has appeared in our publication with credit or acknowledgement to another source, permission must also be sought from that source. If such permission is not obtained then that material may not be included in your publication/copies. Suitable acknowledgement to the source must be made, either as a footnote or in a reference list at the end of your publication, as

follows:

“Reprinted from Publication title, Vol /edition number, Author(s), Title of article / title of chapter, Pages No., Copyright (Year), with permission from Elsevier [OR APPLICABLE SOCIETY COPYRIGHT OWNER].” Also Lancet special credit - “Reprinted from The Lancet, Vol. number, Author(s), Title of article, Pages No., Copyright (Year), with permission from Elsevier.”

4. Reproduction of this material is confined to the purpose and/or media for which permission is hereby given.

5. Altering/Modifying Material: Not Permitted. However figures and illustrations may be altered/adapted minimally to serve your work. Any other abbreviations, additions, deletions and/or any other alterations shall be made only with prior written authorization of Elsevier Ltd. (Please contact Elsevier at permissions@elsevier.com)

6. If the permission fee for the requested use of our material is waived in this instance, please be advised that your future requests for Elsevier materials may attract a fee.

7. Reservation of Rights: Publisher reserves all rights not specifically granted in the combination of (i) the license details provided by you and accepted in the course of this licensing transaction, (ii) these terms and conditions and (iii) CCC's Billing and Payment terms and conditions.

8. License Contingent Upon Payment: While you may exercise the rights licensed immediately upon issuance of the license at the end of the licensing process for the transaction, provided that you have disclosed complete and accurate details of your proposed use, no license is finally effective unless and until full payment is received from you (either by publisher or by CCC) as provided in CCC's Billing and Payment terms and conditions. If full payment is not received on a timely basis, then any license preliminarily granted shall be deemed automatically revoked and shall be void as if never granted. Further, in the event that you breach any of these terms and conditions or any of CCC's Billing and Payment terms and conditions, the license is automatically revoked and shall be void as if never granted. Use of materials as described in a revoked license, as well as any use of the materials beyond the scope of an unrevoked license, may constitute copyright infringement and publisher reserves the right to take any and all action to protect its copyright in the materials.

9. Warranties: Publisher makes no representations or warranties with respect to the licensed material.

10. Indemnity: You hereby indemnify and agree to hold harmless publisher and CCC, and their respective officers, directors, employees and agents, from and against any and all claims arising out of your use of the licensed material other than as specifically authorized pursuant to this license.

11. No Transfer of License: This license is personal to you and may not be sublicensed, assigned, or transferred by you to any other person without publisher's written permission.

12. No Amendment Except in Writing: This license may not be amended except in a writing signed by both parties (or, in the case of publisher, by CCC on publisher's behalf).

13. Objection to Contrary Terms: Publisher hereby objects to any terms contained in any purchase order, acknowledgment, check endorsement or other writing prepared by you, which terms are inconsistent with these terms and conditions or CCC's Billing and Payment terms and conditions. These terms and conditions, together with CCC's Billing and Payment terms and conditions (which are incorporated herein), comprise the entire agreement between you and publisher (and CCC) concerning this licensing transaction. In the event of any conflict between your obligations established by these terms and conditions and those established by CCC's Billing and Payment terms and conditions, these terms and conditions shall control.

14. Revocation: Elsevier or Copyright Clearance Center may deny the permissions described in this License at their sole discretion, for any reason or no reason, with a full refund payable to you. Notice of such denial will be made using the contact information provided by you. Failure to receive such notice will not alter or invalidate the denial. In no event will Elsevier or Copyright Clearance Center be responsible or liable for any costs, expenses or damage incurred by you as a result of a denial of your permission request, other than a refund of the amount(s) paid by you to Elsevier and/or Copyright Clearance Center for denied permissions.

LIMITED LICENSE

The following terms and conditions apply only to specific license types:

15. **Translation**: This permission is granted for non-exclusive world **English** rights only unless your license was granted for translation rights. If you licensed translation rights you may only translate this content into the languages you requested. A professional translator must perform all translations and reproduce the content word for word preserving the integrity of the article. If this license is to re-use 1 or 2 figures then permission is granted for non-exclusive world rights in all languages.

16. **Website**: The following terms and conditions apply to electronic reserve and author websites:
Electronic reserve: If licensed material is to be posted to website, the web site is to be password-protected and made available only to bona fide students registered on a relevant course if:
This license was made in connection with a course,
This permission is granted for 1 year only. You may obtain a license for future website posting,
All content posted to the web site must maintain the copyright information line on the bottom of each image,

A hyper-text must be included to the Homepage of the journal from which you are licensing at http://www.sciencedirect.com/science/journal/xxxxx or the Elsevier homepage for books at http://www.elsevier.com , and
Central Storage: This license does not include permission for a scanned version of the material to be stored in a central repository such as that provided by Heron/XanEdu.

17. **Author website** for journals with the following additional clauses:

All content posted to the web site must maintain the copyright information line on the bottom of each image, and
he permission granted is limited to the personal version of your paper. You are not allowed to download and post the published electronic version of your article (whether PDF or HTML, proof or final version), nor may you scan the printed edition to create an electronic version,
A hyper-text must be included to the Homepage of the journal from which you are licensing at http://www.sciencedirect.com/science/journal/xxxxx , As part of our normal production process, you will receive an e-mail notice when your article appears on Elsevier's online service ScienceDirect (www.sciencedirect.com). That e-mail will include the article's Digital Object Identifier (DOI). This number provides the electronic link to the published article and should be included in the posting of your personal version. We ask that you wait until you receive this e-mail and have the DOI to do any posting.
Central Storage: This license does not include permission for a scanned version of the material to be stored in a central repository such as that provided by Heron/XanEdu.

18. **Author website** for books with the following additional clauses:
Authors are permitted to place a brief summary of their work online only.
A hyper-text must be included to the Elsevier homepage at http://www.elsevier.com

All content posted to the web site must maintain the copyright information line on the bottom of each image
You are not allowed to download and post the published electronic version of your chapter, nor may you scan the printed edition to create an electronic version.
Central Storage: This license does not include permission for a scanned version of the material to be stored in a central repository such as that provided by Heron/XanEdu.

19. **Website** (regular and for author): A hyper-text must be included to the Homepage of the journal from which you are licensing at
http://www.sciencedirect.com/science/journal/xxxxx. or for books to the Elsevier homepage at http://www.elsevier.com

20. **Thesis/Dissertation**: If your license is for use in a thesis/dissertation your thesis may be submitted to your institution in either print or electronic form. Should your thesis be published commercially, please reapply for permission. These requirements include

permission for the Library and Archives of Canada to supply single copies, on demand, of the complete thesis and include permission for UMI to supply single copies, on demand, of the complete thesis. Should your thesis be published commercially, please reapply for permission.

21. **Other Conditions**:

v1.6

If you would like to pay for this license now, please remit this license along with your payment made payable to "COPYRIGHT CLEARANCE CENTER" otherwise you will be invoiced within 48 hours of the license date. Payment should be in the form of a check or money order referencing your account number and this invoice number RLNK500748666.
Once you receive your invoice for this order, you may pay your invoice by credit card. Please follow instructions provided at that time.

Make Payment To:
Copyright Clearance Center
Dept 001
P.O. Box 843006
Boston, MA 02284-3006

For suggestions or comments regarding this order, contact RightsLink Customer Support: customercare@copyright.com or +1-877-622-5543 (toll free in the US) or +1-978-646-2777.

Gratis licenses (referencing $0 in the Total field) are free. Please retain this printable license for your reference. No payment is required.

B.9 Permission from Nature Reviews Genetics

NATURE PUBLISHING GROUP LICENSE
TERMS AND CONDITIONS

Mar 27, 2012

This is a License Agreement between yang li ("You") and Nature Publishing Group ("Nature Publishing Group") provided by Copyright Clearance Center ("CCC"). The license consists of your order details, the terms and conditions provided by Nature Publishing Group, and the payment terms and conditions.

All payments must be made in full to CCC. For payment instructions, please see information listed at the bottom of this form.

License Number	2877291063011
License date	Mar 27, 2012
Licensed content publisher	Nature Publishing Group
Licensed content publication	Nature Reviews Genetics
Licensed content title	Plant genetic engineering for biofuel production: towards affordable cellulosic ethanol
Licensed content author	Mariam B. Sticklen
Licensed content date	Jun 1, 2008
Volume number	9
Issue number	6
Type of Use	reuse in a thesis/dissertation
Requestor type	academic/educational
Format	print and electronic
Portion	figures/tables/illustrations
Number of figures/tables/illustrations	1
High-res required	no
Figures	Figure 3. Schematic representation of plant cell
Author of this NPG article	no
Your reference number	Figure 3. Schematic representation of plant cell
Title of your thesis /	APPLICATIONS OF CELLULOSE NANOWHISKERS AND LIGNIN

dissertation	IN PREPARATION OF RIGID POLYURETHANE NANOCOMPOSITE FOAMS
Expected completion date	May 2012
Estimated size (number of pages)	200
Total	0.00 USD

Terms and Conditions

Terms and Conditions for Permissions

Nature Publishing Group hereby grants you a non-exclusive license to reproduce this material for this purpose, and for no other use, subject to the conditions below:

1. NPG warrants that it has, to the best of its knowledge, the rights to license reuse of this material. However, you should ensure that the material you are requesting is original to Nature Publishing Group and does not carry the copyright of another entity (as credited in the published version). If the credit line on any part of the material you have requested indicates that it was reprinted or adapted by NPG with permission from another source, then you should also seek permission from that source to reuse the material.

2. Permission granted free of charge for material in print is also usually granted for any electronic version of that work, provided that the material is incidental to the work as a whole and that the electronic version is essentially equivalent to, or substitutes for, the print version. Where print permission has been granted for a fee, separate permission must be obtained for any additional, electronic re-use (unless, as in the case of a full paper, this has already been accounted for during your initial request in the calculation of a print run). NB: In all cases, web-based use of full-text articles must be authorized separately through the 'Use on a Web Site' option when requesting permission.

3. Permission granted for a first edition does not apply to second and subsequent editions and for editions in other languages (except for signatories to the STM Permissions Guidelines, or where the first edition permission was granted for free).

4. Nature Publishing Group's permission must be acknowledged next to the figure, table or abstract in print. In electronic form, this acknowledgement must be visible at the same time as the figure/table/abstract, and must be hyperlinked to the journal's homepage.

5. The credit line should read:
   Reprinted by permission from Macmillan Publishers Ltd: [JOURNAL NAME] (reference citation), copyright (year of publication)
   For AOP papers, the credit line should read:
   Reprinted by permission from Macmillan Publishers Ltd: [JOURNAL NAME], advance online publication, day month year (doi: 10.1038/sj.[JOURNAL

ACRONYM].XXXXX)

Note: For republication from the *British Journal of Cancer*, the following credit lines apply.
Reprinted by permission from Macmillan Publishers Ltd on behalf of Cancer Research UK: [JOURNAL NAME] (reference citation), copyright (year of publication) For AOP papers, the credit line should read:
Reprinted by permission from Macmillan Publishers Ltd on behalf of Cancer Research UK: [JOURNAL NAME], advance online publication, day month year (doi: 10.1038/sj.[JOURNAL ACRONYM].XXXXX)

6. Adaptations of single figures do not require NPG approval. However, the adaptation should be credited as follows:

   Adapted by permission from Macmillan Publishers Ltd: [JOURNAL NAME] (reference citation), copyright (year of publication)

   Note: For adaptation from the *British Journal of Cancer*, the following credit line applies.
   Adapted by permission from Macmillan Publishers Ltd on behalf of Cancer Research UK: [JOURNAL NAME] (reference citation), copyright (year of publication)

7. Translations of 401 words up to a whole article require NPG approval. Please visit http://www.macmillanmedicalcommunications.com for more information. Translations of up to a 400 words do not require NPG approval. The translation should be credited as follows:

   Translated by permission from Macmillan Publishers Ltd: [JOURNAL NAME] (reference citation), copyright (year of publication).

   Note: For translation from the *British Journal of Cancer*, the following credit line applies.
   Translated by permission from Macmillan Publishers Ltd on behalf of Cancer Research UK: [JOURNAL NAME] (reference citation), copyright (year of publication)

We are certain that all parties will benefit from this agreement and wish you the best in the use of this material. Thank you.

Special Terms:

v1.1

If you would like to pay for this license now, please remit this license along with your payment

made payable to "COPYRIGHT CLEARANCE CENTER" otherwise you will be invoiced within 48 hours of the license date. Payment should be in the form of a check or money order referencing your account number and this invoice number RLNK500748672.
Once you receive your invoice for this order, you may pay your invoice by credit card. Please follow instructions provided at that time.

Make Payment To:
Copyright Clearance Center
Dept 001
P.O. Box 843006
Boston, MA 02284-3006

For suggestions or comments regarding this order, contact RightsLink Customer Support: customercare@copyright.com or +1-877-622-5543 (toll free in the US) or +1-978-646-2777.

Gratis licenses (referencing $0 in the Total field) are free. Please retain this printable license for your reference. No payment is required.

B.10 Permission from Cellulose

SPRINGER LICENSE
TERMS AND CONDITIONS

Mar 27, 2012

This is a License Agreement between yang li ("You") and Springer ("Springer") provided by Copyright Clearance Center ("CCC"). The license consists of your order details, the terms and conditions provided by Springer, and the payment terms and conditions.

All payments must be made in full to CCC. For payment instructions, please see information listed at the bottom of this form.

License Number	2877291455373
License date	Mar 27, 2012
Licensed content publisher	Springer
Licensed content publication	Cellulose
Licensed content title	Quantification of cellulose forms in complex cellulose materials: a chemometric model
Licensed content author	Kristina Wickholm
Licensed content date	Jun 1, 2001
Volume number	8
Issue number	2
Type of Use	Thesis/Dissertation
Portion	Figures
Author of this Springer article	No
Order reference number	Figure 6. A proposed representation of the fibril structure
Title of your thesis / dissertation	APPLICATIONS OF CELLULOSE NANOWHISKERS AND LIGNIN IN PREPARATION OF RIGID POLYURETHANE NANOCOMPOSITE FOAMS
Expected completion date	May 2012
Estimated size(pages)	200
Total	0.00 USD
Terms and Conditions	

If you would like to pay for this license now, please remit this license along with your payment made payable to "COPYRIGHT CLEARANCE CENTER" otherwise you will be invoiced within 48 hours of the license date. Payment should be in the form of a check or money order referencing your account number and this invoice number RLNK500748676.
Once you receive your invoice for this order, you may pay your invoice by credit card. Please follow instructions provided at that time.

Make Payment To:
Copyright Clearance Center
Dept 001
P.O. Box 843006
Boston, MA 02284-3006

For suggestions or comments regarding this order, contact RightsLink Customer Support: customercare@copyright.com or +1-877-622-5543 (toll free in the US) or +1-978-646-2777.

Gratis licenses (referencing $0 in the Total field) are free. Please retain this printable license for your reference. No payment is required.

B.11 Permission from Chemical Reviews

Home | Account Info | Help

Title: Cellulose Nanocrystals: Chemistry, Self-Assembly, and Applications
Author: Youssef Habibi et al.
Publication: Chemical Reviews
Publisher: American Chemical Society
Date: Jun 1, 2010
Copyright © 2010, American Chemical Society

Logged in as:

yang li

LOGOUT

PERMISSION/LICENSE IS GRANTED FOR YOUR ORDER AT NO CHARGE

This type of permission/license, instead of the standard Terms & Conditions, is sent to you because no fee is being charged for your order. Please note the following:

- Permission is granted for your request in both print and electronic formats.
- If figures and/or tables were requested, they may be adapted or used in part.
- Please print this page for your records and send a copy of it to your publisher/graduate school.
- Appropriate credit for the requested material should be given as follows: "Reprinted (adapted) with permission from (COMPLETE REFERENCE CITATION). Copyright (YEAR) American Chemical Society." Insert appropriate information in place of the capitalized words.
- One-time permission is granted only for the use specified in your request. No additional uses are granted (such as derivative works or other editions). For any other uses, please submit a new request.

BACK | CLOSE WINDOW

B.12 Permission from Bioresources Technology

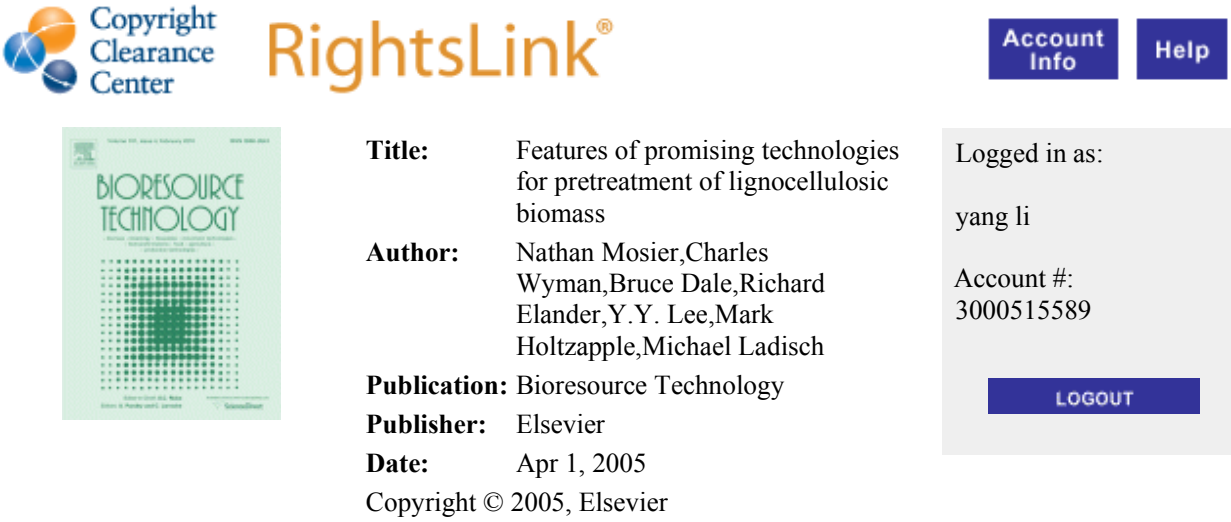

Copyright Clearance Center RightsLink®

Account Info | Help

Title: Features of promising technologies for pretreatment of lignocellulosic biomass

Author: Nathan Mosier,Charles Wyman,Bruce Dale,Richard Elander,Y.Y. Lee,Mark Holtzapple,Michael Ladisch

Publication: Bioresource Technology

Publisher: Elsevier

Date: Apr 1, 2005

Copyright © 2005, Elsevier

Logged in as:

yang li

Account #: 3000515589

LOGOUT

Order Completed

Thank you very much for your order.

This is a License Agreement between yang li ("You") and Elsevier ("Elsevier"). The license consists of your order details, the terms and conditions provided by Elsevier, and the payment terms and conditions.

License number	Reference confirmation email for license number
License date	Mar 27, 2012
Licensed content publisher	Elsevier
Licensed content publication	Bioresource Technology
Licensed content title	Features of promising technologies for pretreatment of lignocellulosic biomass
Licensed content author	Nathan Mosier,Charles Wyman,Bruce Dale,Richard Elander,Y.Y. Lee,Mark Holtzapple,Michael Ladisch
Licensed content date	April 2005
Licensed content volume number	96
Licensed content issue number	6
Number of pages	14
Type of Use	reuse in a thesis/dissertation
Portion	figures/tables/illustrations

Number of figures/tables/illustrations	1
Format	both print and electronic
Are you the author of this Elsevier article?	No
Will you be translating?	No
Order reference number	Figure 21. The effect of pretreatment on lignocellulosic materials
Title of your thesis/dissertation	APPLICATIONS OF CELLULOSE NANOWHISKERS AND LIGNIN IN PREPARATION OF RIGID POLYURETHANE NANOCOMPOSITE FOAMS
Expected completion date	May 2012
Estimated size (number of pages)	200
Elsevier VAT number	GB 494 6272 12
Billing Type	Invoice
Billing address	4816 via ventura apt 416
	mesquite, TX 75150
	United States
Customer reference info	
Permissions price	0.00 USD
VAT/Local Sales Tax	0.00 USD / GBP
Total	0.00 USD

CLOSE WINDOW

REFERENCES

[1] D. Klemm, B. Heublein, H. P. Fink, and A. Bohn, "Cellulose: Fascinating Biopolymer and Sustainable Raw Material," *Angewandte Chemie-International Edition,* 44, pp. 3358-3393, 2005.

[2] M. Samir, F. Alloin, and A. Dufresne, "Review of Recent Research into Cellulosic Whiskers, Their Properties and Their Application in Nanocomposite Field," *Biomacromolecules,* 6, pp. 612-626, 2005.

[3] A. Sturcova, G. R. Davies, and S. J. Eichhorn, "Elastic Modulus and Stress-Transfer Properties of Tunicate Cellulose Whiskers," *Biomacromolecules,* 6, pp. 1055-1061, 2005.

[4] X. D. Cao, H. Dong, and C. M. Li, "New Nanocomposite Materials Reinforced with Flax Cellulose Nanocrystals in Waterborne Polyurethane," *Biomacromolecules,* 8, pp. 899-904, 2007.

[5] M. Samir, F. Alloin, J. Y. Sanchez, N. El Kissi, and A. Dufresne, "Preparation of Cellulose Whiskers Reinforced Nanocomposites from an Organic Medium Suspension," *Macromolecules,* 37, pp. 1386-1393, 2004.

[6] G. Siqueira, J. Bras, and A. Dufresne, "Cellulose Whiskers Versus Microfibrils: Influence of the Nature of the Nanoparticle and Its Surface Functionalization on the Thermal and Mechanical Properties of Nanocomposites," *Biomacromolecules,* 10, pp. 425-432, 2009.

[7] M. O. Seydibeyoglu and K. Oksman, "Novel Nanocomposites Based on Polyurethane and Micro Fibrillated Cellulose," *Composites Science and Technology,* 68, pp. 908-914, 2008.

[8] N. E. Marcovich, M. L. Auad, N. E. Bellesi, S. R. Nutt, and M. I. Aranguren, "Cellulose Micro/Nanocrystals Reinforced Polyurethane," *Journal of Materials Research,* 21, pp. 870-881, 2006.

[9] Y. Pu, J. Zhang, T. Elder, Y. Deng, P. Gatenholm, and A. J. Ragauskas, "Investigation into Nanocellulosics Versus Acacia Reinforced Acrylic Films," *Composites Part B-Engineering,* 38, pp. 360-366, 2007.

[10] F. G. Calvo-Flores and J. A. Dobado, "Lignin as Renewable Raw Material," *Chemsuschem,* 3, pp. 1227-1235, 2010.

[11] R. J. A. Gosselink, E. de Jong, B. Guran, and A. Abacherli, "Co-Ordination Network for Lignin - Standardisation, Production and Applications Adapted to Market Requirements (Eurolignin)," *Industrial Crops and Products,* 20, pp.

121-129, 2004.

[12] R. W. Thring, M. N. Vanderlaan, and S. L. Griffin, "Polyurethanes from Alcell (R) Lignin," *Biomass & Bioenergy,* 13, pp. 125-132, 1997.

[13] D. Stewart, "Lignin as a Base Material for Materials Applications: Chemistry, Application and Economics," *Industrial Crops and Products,* 27, pp. 202-207, 2008.

[14] S. Sarkar and B. Adhikari, "Synthesis and Characterization of Lignin-Htpb Copolyurethane," *European Polymer Journal,* 37, pp. 1391-1401, 2001.

[15] C. A. Cateto, M. F. Barreiro, and A. E. Rodrigues, "Monitoring of Lignin-Based Polyurethane Synthesis by Ftir-Atr," *Industrial Crops and Products,* 27, pp. 168-174, 2008.

[16] S. Kamel, "Nanotechnology and Its Applications in Lignocellulosic Composites, a Mini Review," *Express Polymer Letters,* 1, pp. 546-575, 2007.

[17] I. Banik and M. M. Sain, "Water Blown Soy Polyol-Based Polyurethane Foams of Different Rigidities," *Journal of Reinforced Plastics and Composites,* 27, pp. 357-373, 2008.

[18] G. Oertel, *Polyurethane Handbook: Chemistry, Raw Materials, Processing, Application*. New York: Mac-Millan Publishing Co. Inc., 1985.

[19] I. Global Industry Analysts, "Foamed Plastics (Polyurethane): A Global Strategic Business Report ", San Jose2011.

[20] T. AbiSaleh, M. Anderson, M. Barker, G. Biesmans, J. Bosman, D. Daems, and e. al., "Introduction to Polyurethanes," in *The Polyurethanes Book*, D. Randall and S. Lee, Eds., New York: Wiley, 2003, pp. 1-8.

[21] G. Woods, *The ICI Polyurethane Book*, R. L. Heath, Ed., New York: Wiley, 1990.

[22] P. Kumar, D. M. Barrett, M. J. Delwiche, and P. Stroeve, "Methods for Pretreatment of Lignocellulosic Biomass for Efficient Hydrolysis and Biofuel Production," *Industrial & Engineering Chemistry Research,* 48, pp. 3713-3729, 2009.

[23] D. Fengel and G. Wegener, *Wood Chemistry, Ultrastructure, Reactions*. Berlin: Walter de Gruyter 1984.

[24] A. J. Ragauskas, M. Nagy, D. H. Kim, C. A. Eckert, J. P. Hallett, and C. L. Liotta, "From Wood to Fuels: Integrating Biofuels and Pulp Production," *Industrial Biotechnology* 2, pp. 55-65, 2006.

[25] A. M. Boudet, S. Kajita, J. Grima-Pettenati, and D. Goffner, "Lignins and

Lignocellulosics: A Better Control of Synthesis for New and Improved Uses," *Trends in Plant Science,* 8, pp. 576-581, 2003.

[26] B. C. Saha, "Hemicellulose Bioconversion," *Journal of Industrial Microbiology & Biotechnology,* 30, pp. 279-291, 2003.

[27] Suhas, P. J. M. Carrott, and M. Carrott, "Lignin - from Natural Adsorbent to Activated Carbon: A Review," *Bioresource Technology,* 98, pp. 2301-2312, 2007.

[28] M. B. Sticklen, "Plant Genetic Engineering for Biofuel Production: Towards Affordable Cellulosic Ethanol (Retracted Article. See Vol 11, Pg 308, 2010)," *Nature Reviews Genetics,* 9, pp. 433-443, 2008.

[29] Shafizadeh F and McGinnis GD, Eds., *Morphology and Biogenesis of Cellulose and Plant Cell-Walls. In: Advances In* (Advances in Carbohydrate Chemistry and Biochemistry. New York: Academic Press, 1971, p.^pp. Pages.

[30] Y. Q. Pu, D. C. Zhang, P. M. Singh, and A. J. Ragauskas, "The New Forestry Biofuels Sector," *Biofuels Bioproducts & Biorefining-Biofpr,* 2, pp. 58-73, 2008.

[31] W. Helbert, J. Y. Cavaille, and A. Dufresne, "Thermoplastic Nanocomposites Filled with Wheat Straw Cellulose Whiskers .1. Processing and Mechanical Behavior," *Polymer Composites,* 17, pp. 604-611, 1996.

[32] S. J. Eichhorn, C. A. Baillie, N. Zafeiropoulos, L. Y. Mwaikambo, M. P. Ansell, A. Dufresne, K. M. Entwistle, P. J. Herrera-Franco, G. C. Escamilla, L. Groom, M. Hughes, C. Hill, T. G. Rials, and P. M. Wild, "Review: Current International Research into Cellulosic Fibres and Composites," *Journal of Materials Science,* 36, pp. 2107-2131, 2001.

[33] A. P. Mathew and A. Dufresne, "Morphological Investigation of Nanocomposites from Sorbitol Plasticized Starch and Tunicin Whiskers," *Biomacromolecules,* 3, pp. 609-617, 2002.

[34] A. Morin and A. Dufresne, "Nanocomposites of Chitin Whiskers from Riftia Tubes and Poly(Caprolactone)," *Macromolecules,* 35, pp. 2190-2199, 2002.

[35] M. Ioelovich and A. Leykin, "Accessibility and Supermolecular Structure of Cellulose," *Cellulose Chemistry and Technology,* 43, pp. 379-385, 2009.

[36] M. Ioelovich, "Accessibility and Crystallinity of Cellulose," *Bioresources,* 4, pp. 1168-1177, 2009.

[37] M. Ioelovich and E. Larina, "Parameters of Crystalline Structure and Their Influence on the Reactivity of Cellulose I," *Cellulose Chemistry and Technology,* 33, pp. 3-12, 1999.

[38] M. Y. Ioelovich, "A Study on Formation of Supermolecular Structure of Cotton

Cellulose," *Vysokomolekulyarnye Soedineniya Seriya a & Seriya B,* 35, pp. B268-B271, 1993.

[39] M. Grunert and W. T. Winter, "Nanocomposites of Cellulose Acetate Butyrate Reinforced with Cellulose Nanocrystals," *Journal of Polymers and the Environment,* 10, pp. 27-30, 2002.

[40] N. Duran, A. P. Lemes, M. Duran, J. Freer, and J. Baeza, "A Minireview of Cellulose Nanocrystals and Its Potential Integration as Co-Product in Bioethanol Production," *Journal of the Chilean Chemical Society,* 56, pp. 672-677, 2011.

[41] P. T. Larsson, K. Wickholm, and T. Iversen, "A Cp/Mas C-13 Nmr Investigation of Molecular Ordering in Celluloses," *Carbohydrate Research,* 302, pp. 19-25, 1997.

[42] P. T. Larsson, E. L. Hult, K. Wickholm, E. Pettersson, and T. Iversen, "Cp/Mas C-13-Nmr Spectroscopy Applied to Structure and Interaction Studies on Cellulose I," *Solid State Nuclear Magnetic Resonance,* 15, pp. 31-40, 1999.

[43] K. Wickholm, P. T. Larsson, and T. Iversen, "Assignment of Non-Crystalline Forms in Cellulose I by Cp/Mas C-13 Nmr Spectroscopy," *Carbohydrate Research,* 312, pp. 123-129, 1998.

[44] Y. Q. Pu, C. Ziemer, and A. J. Ragauskas, "Cp/Mas (13)C Nmr Analysis of Cellulase Treated Bleached Softwood Kraft Pulp," *Carbohydrate Research,* 341, pp. 591-597, 2006.

[45] P. Sannigrahi, A. J. Ragauskas, and S. J. Miller, "Effects of Two-Stage Dilute Acid Pretreatment on the Structure and Composition of Lignin and Cellulose in Loblolly Pine," *Bioenergy Research,* 1, pp. 205-214, 2008.

[46] K. Wickholm, E. L. Hult, P. T. Larsson, T. Iversen, and H. Lennholm, "Quantification of Cellulose Forms in Complex Cellulose Materials: A Chemometric Model," *Cellulose,* 8, pp. 139-148, 2001.

[47] Y. Nishiyama, J. Sugiyama, H. Chanzy, and P. Langan, "Crystal Structure and Hydrogen Bonding System in Cellulose 1(Alpha), from Synchrotron X-Ray and Neutron Fiber Diffraction," *Journal of the American Chemical Society,* 125, pp. 14300-14306, 2003.

[48] P. Sannigrahi, A. J. Ragauskas, and G. A. Tuskan, "Poplar as a Feedstock for Biofuels: A Review of Compositional Characteristics," *Biofuels Bioproducts & Biorefining-Biofpr,* 4, pp. 209-226, 2010.

[49] A. C. Osullivan, "Cellulose: The Structure Slowly Unravels," *Cellulose,* 4, pp. 173-207, 1997.

[50] E. Shefter and Truebloo.Kn, "Crystal and Molecular Structure of D(Plus)-Barium

Uridine-5'-Phosphate," *Acta Crystallographica,* 18, pp. 1067-1077, 1965.

[51] Y. Nishiyama, P. Langan, and H. Chanzy, "Crystal Structure and Hydrogen-Bonding System in Cellulose 1 Beta from Synchrotron X-Ray and Neutron Fiber Diffraction," *Journal of the American Chemical Society,* 124, pp. 9074-9082, 2002.

[52] A. Buleon and H. Chanzy, "Single-Crystals of Cellulose-Ii," *Journal of Polymer Science Part B-Polymer Physics,* 16, pp. 833-839, 1978.

[53] F. J. Kolpak and J. Blackwell, "Determination of the Structure of Cellulose Ii," *Macromolecules,* 9, pp. 273-278, 1976.

[54] C. Woodcock and A. Sarko, "Packing Analysis of Carbohydrates and Polysaccharides .11. Molecular and Crystal-Structure of Native Ramie Cellulose," *Macromolecules,* 13, pp. 1183-1187, 1980.

[55] K. Okamura, "Structure of Cellulose," in *Wood and Cellulosic Chemistry*, D. N.-S. Hon and N. Shiraishi, Eds., ed New York: Marcel Dekker,, 1991, pp. 89-111.

[56] M. Tsuboi, "Infrared Spectrum and Crystal Structure of Cellulose," *Journal of Polymer Science,* 25, pp. 159-171, 1957.

[57] J. Mann and H. J. Marrinan, "Crystalline Modifcations of Cellulose. Part Ii. A Study with Plane-Polarised Infrared Radiation," *Journal of Polymer Science,* 32, pp. 357-370, 1958.

[58] C. Y. Liang and R. H. Marchessault, "Infrared Spectra of Crystalline Polysaccharides .1. Hydrogen Bonds in Native Celluloses," *Journal of Polymer Science,* 37, pp. 385-395, 1959.

[59] R. H. Marchessault and C. Y. Liang, "Infrared Spectra of Crystalline Polysaccharides .3. Mercerized Cellulose," *Journal of Polymer Science,* 43, pp. 71-84, 1960.

[60] K. H. Gardner and J. Blackwell, "The Structure of Native Cellulose " *biopolymers,* 13, pp. 1975-2001, 1974.

[61] A. P. Heiner, J. Sugiyama, and O. Teleman, "Crystalline Cellulose I-Alpha and I-Beta Studied by Molecular-Dynamics Simulation," *Carbohydrate Research,* 273, pp. 207-223, 1995.

[62] H. Yamamoto and F. Horii, "Cp Mas C-13 Nmr Analysis of the Crystal Transformation Induced for Valonia Cellulose by Annealing at High-Temperatures," *Macromolecules,* 26, pp. 1313-1317, 1993.

[63] Y. H. P. Zhang and L. R. Lynd, "Toward an Aggregated Understanding of Enzymatic Hydrolysis of Cellulose: Noncomplexed Cellulase Systems,"

Biotechnology and Bioengineering, 88, pp. 797-824, 2004.

[64] A. L. Dupont and G. Mortha, "Comparative Evaluation of Size-Exclusion Chromatography and Viscometry for the Characterisation of Cellulose," *Journal of Chromatography A,* 1026, pp. 129-141, 2004.

[65] E. Sjöholm, "Size Exclusion Chromatography of Cellulose and Cellulose Derivatives," in *Handbook of Size Exclusion Chromatography and Related Techniques*, C. Wu, Ed., ed New York: Marcel Dekker, 2004, pp. 311-354.

[66] D. Klemn, B. Philipp, T. Heinze, U. Heinze, and W. Wagenknecht, "Analytical Methods in Cellulose Chemistry," in *Fundamentals and Analytical Methods*, ed New York: Wiley-VCH, 1998, pp. 167-247.

[67] R. Kumar, G. Mago, V. Balan, and C. E. Wyman, "Physical and Chemical Characterizations of Corn Stover and Poplar Solids Resulting from Leading Pretreatment Technologies," *Bioresource Technology,* 100, pp. 3948-3962, 2009.

[68] X. Pan, D. Xie, K. Y. Kang, S. L. Yoon, and J. N. Saddler, "Effect of Organosolv Ethanol Pretreatment Variables on Physical Characteristics of Hybrid Poplar Substrates," *Applied Biochemistry and Biotechnology,* 137, pp. 367-377, 2007.

[69] J. M. Martinez, J. Reguant, M. A. Montero, D. Montane, J. Salvado, and X. Farriol, "Hydrolytic Pretreatment of Softwood and Almond Shells. Degree of Polymerization and Enzymatic Digestibility of the Cellulose Fraction," *Industrial & Engineering Chemistry Research,* 36, pp. 688-696, 1997.

[70] M. S. Jahan and S. P. Mun, "Studies on the Macromolecular Components of Nonwood Available in Bangladesh," *Industrial Crops and Products,* 30, pp. 344-350, 2009.

[71] M. S. Jahan and S. P. Mun, "Effect of Tree Age on the Cellulose Structure of Nalita Wood (Trema Orientalis)," *Wood Science and Technology,* 39, pp. 367-373, 2005.

[72] K. Klemanleyer, E. Agosin, A. H. Conner, and T. K. Kirk, "Changes in Molecular-Size Distribution of Cellulose During Attack by White Rot and Brown Rot Fungi," *Applied and Environmental Microbiology,* 58, pp. 1266-1270, 1992.

[73] R. Cohen, K. A. Jensen, C. J. Houtman, and K. E. Hammel, "Significant Levels of Extracellular Reactive Oxygen Species Produced by Brown Rot Basidiomycetes on Cellulose," *Febs Letters,* 531, pp. 483-488, 2002.

[74] W. Xu, N. Reddy, and Y. Q. Yang, "Extraction, Characterization and Potential Applications of Cellulose in Corn Kernels and Distillers' Dried Grains with Solubles (Ddgs)," *Carbohydrate Polymers,* 76, pp. 521-527, 2009.

[75] J. L. Snyder and T. E. Timell, "Molecular Properties of Native Balsam Fir

Cellulose," *Sven papperstidn* 58, pp. 851-859, 1955.

[76] T. E. Timell, "Chain Length and Chain-Length Distribution of Native White Spruce Cellulose," *Pulp Paper Mag Can* 56, pp. 104-114, 1955.

[77] T. E. Timell, "Molecular Properties of Seven Native Wood Celluloses," *Tappi Journal,* 40, pp. 25-29, 1957.

[78] T. E. Timell, "Molecular Weight and Polymolecularity of White Birch Celluloses," *Sven papperstidn,* 59, pp. 1-11, 1956.

[79] V. P. Puri, "Effect of Crystallinity and Degree of Polymerization of Cellulose on Enzymatic Saccharification," *Biotechnology and Bioengineering,* 26, pp. 1219-1222, 1984.

[80] K. M. KlemanLeyer, M. SiikaAho, T. T. Teeri, and T. K. Kirk, "The Cellulases Endoglucanase I and Cellobiohydrolase Ii of Trichoderma Reesei Act Synergistically to Solubilize Native Cotton Cellulose but Not to Decrease Its Molecular Size," *Applied and Environmental Microbiology,* 62, pp. 2883-2887, 1996.

[81] M. S. Sweet and J. E. Winandy, "Influence of Degree of Polymerization of Cellulose and Hemicellulose on Strength Loss in Fire-Retardant-Treated Southern Pine," *Holzforschung,* 53, pp. 311-317, 1999.

[82] H. Hakansson, P. Ahlgren, and U. Germgard, "The Degree of Disorder in Hardwood Kraft Pulps Studied by Means of Lodp," *Cellulose,* 12, pp. 327-335, 2005.

[83] S. J. Eichhorn, "Cellulose Nanowhiskers: Promising Materials for Advanced Applications," *Soft Matter,* 7, pp. 303-315, 2011.

[84] J. F. Revol, L. Godbout, X. M. Dong, D. G. Gray, H. Chanzy, and G. Maret, "Chiral Nematic Suspensions of Cellulose Crystallites - Phase-Separation and Magnetic-Field Orientation," *Liquid Crystals,* 16, pp. 127-134, 1994.

[85] J. Araki, M. Wada, S. Kuga, and T. Okana, "Influence of Surface Charge on Viscosity Behavior of Cellulose Microcrystal Suspension," *Journal of Wood Science,* 45, pp. 258-261, 1999.

[86] J. Araki, M. Wada, S. Kuga, and T. Okano, "Flow Properties of Microcrystalline Cellulose Suspension Prepared by Acid Treatment of Native Cellulose," *Colloids and Surfaces a-Physicochemical and Engineering Aspects,* 142, pp. 75-82, 1998.

[87] S. Beck-Candanedo, M. Roman, and D. G. Gray, "Effect of Reaction Conditions on the Properties and Behavior of Wood Cellulose Nanocrystal Suspensions," *Biomacromolecules,* 6, pp. 1048-1054, 2005.

[88] P. B. Filson, B. E. Dawson-Andoh, and D. Schwegler-Berry, "Enzymatic-Mediated Production of Cellulose Nanocrystals from Recycled Pulp," *Green Chemistry,* 11, pp. 1808-1814, 2009.

[89] X. M. Dong, T. Kimura, J. F. Revol, and D. G. Gray, "Effects of Ionic Strength on the Isotropic-Chiral Nematic Phase Transition of Suspensions of Cellulose Crystallites," *Langmuir,* 12, pp. 2076-2082, 1996.

[90] X. M. Dong, J. F. Revol, and D. G. Gray, "Effect of Microcrystallite Preparation Conditions on the Formation of Colloid Crystals of Cellulose," *Cellulose,* 5, pp. 19-32, 1998.

[91] J. Araki, M. Wada, S. Kuga, and T. Okano, "Birefringent Glassy Phase of a Cellulose Microcrystal Suspension," *Langmuir,* 16, pp. 2413-2415, 2000.

[92] M. Hasani, E. D. Cranston, G. Westman, and D. G. Gray, "Cationic Surface Functionalization of Cellulose Nanocrystals," *Soft Matter,* 4, pp. 2238-2244, 2008.

[93] X. D. Cao, Y. Habibi, and L. A. Lucia, "One-Pot Polymerization, Surface Grafting, and Processing of Waterborne Polyurethane-Cellulose Nanocrystal Nanocomposites," *Journal of Materials Chemistry,* 19, pp. 7137-7145, 2009.

[94] A. H. Pei, Q. Zhou, and L. A. Berglund, "Functionalized Cellulose Nanocrystals as Biobased Nucleation Agents in Poly(L-Lactide) (Plla) - Crystallization and Mechanical Property Effects," *Composites Science and Technology,* 70, pp. 815-821, 2010.

[95] L. M. Tang and C. Weder, "Cellulose Whisker/Epoxy Resin Nanocomposites," *Acs Applied Materials & Interfaces,* 2, pp. 1073-1080, 2010.

[96] Y. Wang, H. Tian, and L. Zhang, "Role of Starch Nanocrystals and Cellulose Whiskers in Synergistic Reinforcement of Waterborne Polyurethane," *Carbohydrate Polymers,* 80, pp. 665-671, 2010.

[97] N. L. G. de Rodriguez, W. Thielemans, and A. Dufresne, "Sisal Cellulose Whiskers Reinforced Polyvinyl Acetate Nanocomposites," *Cellulose,* 13, pp. 261-270, 2006.

[98] Y. Habibi, L. Foulon, V. Aguie-Beghin, M. Molinari, and R. Douillard, "Langmuir-Blodgett Films of Cellulose Nanocrystals: Preparation and Characterization," *Journal of Colloid and Interface Science,* 316, pp. 388-397, 2007.

[99] Y. Habibi and A. Dufresne, "Highly Filled Bionanocomposites from Functionalized Polysaccharide Nanocrystals," *Biomacromolecules,* 9, pp. 1974-1980, 2008.

[100] J. O. Zoppe, M. S. Peresin, Y. Habibi, R. A. Venditti, and O. J. Rojas,

"Reinforcing Poly(Epsilon-Caprolactone) Nanofibers with Cellulose Nanocrystals," *Acs Applied Materials & Interfaces,* 1, pp. 1996-2004, 2009.

[101] D. G. Liu, T. H. Zhong, P. R. Chang, K. F. Li, and Q. L. Wu, "Starch Composites Reinforced by Bamboo Cellulosic Crystals," *Bioresource Technology,* 101, pp. 2529-2536, 2010.

[102] J. K. Pandey, W. S. Chu, C. S. Kim, C. S. Lee, and S. H. Ahn, "Bio-Nano Reinforcement of Environmentally Degradable Polymer Matrix by Cellulose Whiskers from Grass," *Composites Part B-Engineering,* 40, pp. 676-680, 2009.

[103] V. Favier, H. Chanzy, and J. Y. Cavaille, "Polymer Nanocomposites Reinforced by Cellulose Whiskers," *Macromolecules,* 28, pp. 6365-6367, 1995.

[104] M. N. Angles and A. Dufresne, "Plasticized Starch/Tunicin Whiskers Nanocomposites. 1. Structural Analysis," *Macromolecules,* 33, pp. 8344-8353, 2000.

[105] N. Ljungberg, J. Y. Cavaille, and L. Heux, "Nanocomposites of Isotactic Polypropylene Reinforced with Rod-Like Cellulose Whiskers," *Polymer,* 47, pp. 6285-6292, 2006.

[106] G. Siqueira, J. Bras, and A. Dufresne, "New Process of Chemical Grafting of Cellulose Nanoparticles with a Long Chain Isocyanate," *Langmuir,* 26, pp. 402-411, 2010.

[107] M. Samir, F. Alloin, J. Y. Sanchez, and A. Dufresne, "Cross-Linked Nanocomposite Polymer Electrolytes Reinforced with Cellulose Whiskers," *Macromolecules,* 37, pp. 4839-4844, 2004.

[108] D. Bondeson, A. Mathew, and K. Oksman, "Optimization of the Isolation of Nanocrystals from Microcrystalline Cellulose by Acid Hydrolysis," *Cellulose,* 13, pp. 171-180, 2006.

[109] W. Bai, J. Holbery, and K. C. Li, "A Technique for Production of Nanocrystalline Cellulose with a Narrow Size Distribution," *Cellulose,* 16, pp. 455-465, 2009.

[110] M. L. Auad, M. A. Mosiewicki, T. Richardson, M. I. Aranguren, and N. E. Marcovich, "Nanocomposites Made from Cellulose Nanocrystals and Tailored Segmented Polyurethanes," *Journal of Applied Polymer Science,* 115, pp. 1215-1225, 2010.

[111] H. Y. Liu, D. G. Liu, F. Yao, and Q. L. Wu, "Fabrication and Properties of Transparent Polymethylmethacrylate/Cellulose Nanocrystals Composites," *Bioresource Technology,* 101, pp. 5685-5692, 2010.

[112] P. Terech, L. Chazeau, and J. Y. Cavaille, "A Small-Angle Scattering Study of Cellulose Whiskers in Aqueous Suspensions," *Macromolecules,* 32, pp.

1872-1875, 1999.

[113] S. J. Hanley, J. Giasson, J. F. Revol, and D. G. Gray, "Atomic Force Microscopy of Cellulose Microfibrils - Comparison with Transmission Electron-Microscopy," *Polymer,* 33, pp. 4639-4642, 1992.

[114] A. Dufresne, M. B. Kellerhals, and B. Witholt, "Transcrystallization in Mcl-Phas/Cellulose Whiskers Composites," *Macromolecules,* 32, pp. 7396-7401, 1999.

[115] D. Bondeson and K. Oksman, "Polylactic Acid/Cellulose Whisker Nanocomposites Modified by Polyvinyl Alcohol," *Composites Part a-Applied Science and Manufacturing,* 38, pp. 2486-2492, 2007.

[116] K. Oksman, A. P. Mathew, D. Bondeson, and I. Kvien, "Manufacturing Process of Cellulose Whiskers/Polylactic Acid Nanocomposites," *Composites Science and Technology,* 66, pp. 2776-2784, 2006.

[117] L. Rahkamo, M. Vehvilainen, L. Viikari, P. Nousiainen, and J. Buchert, *Enzyme Applications in Fiber Processing*. Washington: American Chemical Society, 1997.

[118] G. Joksimovic and Z. Markovic, "Investigation of the Mechanism of Acidic Hydrolysis of Cellulose " *Acta Agriculturae Serbica,* XII, pp. 51-57, 2007.

[119] Organic Esters:Http://Wpage.Unina.It/Avitabil/Testi/Acetilcellulosa.Pdf.

[120] N. Bhatt, P. K. Gupta, and S. Naithani, "Preparation of Cellulose Sulfate from Alpha-Cellulose Isolated from Lantana Camara by the Direct Esterification Method," *Journal of Applied Polymer Science,* 108, pp. 2895-2901, 2008.

[121] M. Roman and W. T. Winter, "Effect of Sulfate Groups from Sulfuric Acid Hydrolysis on the Thermal Degradation Behavior of Bacterial Cellulose," *Biomacromolecules,* 5, pp. 1671-1677, 2004.

[122] Http://Www.Standardbase.Com/Tech/Finalhutechcond.Pdf.

[123] I. Z. Selim, A. A. F. Zikry, and S. H. Gaber, "Physicochemical Properties of Prepared Cellulose Sulfates: Ii. From Linen Pulp Bleached by the H2o2 Method," *Polymer-Plastics Technology and Engineering,* 43, pp. 1387-1402, 2004.

[124] D. Williams and C. B. Carter, *Transmission Electron Microscopy*, Plenum Press, 1996.

[125] R. A. Wilson and H. A. Bullen. Introduction to Scanning Probe Microscopy (SPM)-Basic Theory -Atomic Force Microscopy (AFM).

[126] http://www.nanoandmore.com/afm-tips.php#afm-tips-by-shape.

[127] J. K. Pandey, J. W. Lee, W. S. Chu, C. S. Kim, and S. H. Ahn, "Cellulose Nano Whiskers from Grass of Korea," *Macromolecular Research,* 16, pp. 396-398, 2008.

[128] N. Wang, E. Ding, and R. Cheng, "Thermal Degradation Behaviors of Spherical Cellulose Nanocrystals with Sulfate Groups," *Polymer,* 48, pp. 3486-3493, 2007.

[129] M. M. D. Lima and R. Borsali, "Rodlike Cellulose Microcrystals: Structure, Properties, and Applications," *Macromolecular Rapid Communications,* 25, pp. 771-787, 2004.

[130] R. H. Marchessault, F. F. Morehead, and N. M. Walter, "Liquid Crystal Systems from Fibrillar Polysaccharides," *Nature,* 184, pp. 632-633, 1959.

[131] T. E. Strzelecka, M. W. Davidson, and R. L. Rill, "Multiple Liquid-Crystal Phases of DNA at High-Concentrations," *Nature,* 331, pp. 457-460, 1988.

[132] G. Oster, "2-Phase Formation in Solutions of Tobacco Mosaic Virus and the Problem of Long-Range Forces," *Journal of General Physiology,* 33, pp. 445-473, 1950.

[133] Y. Bouligand and F. Livolant, "The Organization of Cholesteric Spherulites," *Journal De Physique,* 45, pp. 1899-1923, 1984.

[134] Y. Habibi, L. A. Lucia, and O. J. Rojas, "Cellulose Nanocrystals: Chemistry, Self-Assembly, and Applications," *Chemical Reviews,* 110, pp. 3479-3500, 2010.

[135] E. Sjöström, *Wood Chemistry: Fundamentals and Applications*. San Diego: Academic Press, 1981.

[136] K. V. Sarkanen and C. H. Ludwig, *Lignin: Occurrence, Formation, Structure and Reactions*. New York: Wiley Interscience, 1971.

[137] S. K. Ritter, "Lignincellulose: A Complex Biomaterial," *Chemical & Engineering News,* p. 15, 2008.

[138] E. A. B. da Silva, M. Zabkova, J. D. Araujo, C. A. Cateto, M. F. Barreiro, M. N. Belgacem, and A. E. Rodriques, "An Integrated Process to Produce Vanillin and Lignin-Based Polyurethanes from Kraft Lignin," *Chemical Engineering Research & Design,* 87, pp. 1276-1292, 2009.

[139] J. Zakzeski, P. C. A. Bruijnincx, A. L. Jongerius, and B. M. Weckhuysen, "The Catalytic Valorization of Lignin for the Production of Renewable Chemicals," *Chemical Reviews,* 110, pp. 3552-3599, 2010.

[140] Y. N. Sazanov and A. V. Gribanov, "Thermochemistry of Lignin," *Russian Journal of Applied Chemistry,* 83, pp. 175-194, 2010.

[141] D. P. Koullas, E. G. Koukios, E. Avgerinos, A. Abaecherli, R. Gosselink, C. Vasile, R. Lehnen, B. Saake, and J. Suren, "Analytical Methods for Lignin Characterization - Differential Scanning Calorimetry," *Cellulose Chemistry and Technology,* 40, pp. 719-725, 2006.

[142] C. G. Boeriu, D. Bravo, R. J. A. Gosselink, and J. E. G. van Dam, "Characterisation of Structure-Dependent Functional Properties of Lignin with Infrared Spectroscopy," *Industrial Crops and Products,* 20, pp. 205-218, 2004.

[143] F. S. Chakar and A. J. Ragauskas, "Review of Current and Future Softwood Kraft Lignin Process Chemistry," *Industrial Crops and Products,* 20, pp. 131-141, 2004.

[144] T. Hatakeyama, Y. Izuta, S. Hirose, and H. Hatakeyama, "Phase Transitions of Lignin-Based Polycaprolactones and Their Polyurethane Derivatives," *Polymer,* 43, pp. 1177-1182, 2002.

[145] Y. Pu, D. Zhang, P. M. Singh, and A. J. Ragauskas, "The New Forestry Biofuels Sector," *Biofuels Bioproducts & Biorefining-Biofpr,* 2, pp. 58-73, 2008.

[146] J. K. Weng and C. Chapple, "The Origin and Evolution of Lignin Biosynthesis," *New Phytologist,* 187, pp. 273-285, 2010.

[147] W. Boerjan, J. Ralph, and M. Baucher, *Lignin Biosynthesis* vol. Volume 54, 2003.

[148] G. Henriksson, "Lignin," in *Ljungberg Textbook. Pulp and Paper Chemistry and Technology. Book 1. Wood Chemistry and Wood Biotechnology* M. Ek, G. Gellerstedt, and G. Henriksson, Eds., ed Stockholm: Fiber and Polymer technology, KTH, 2007, pp. 125-148.

[149] M. Nagy, "Biofuels from Lignin and Novel Biodiesel Analysis," Ph.D., Georgia Institute of Technology, Atlanta, 2009.

[150] Http://Ars.Usda.Gov/Services/Docs.Htm?Docid=10443.

[151] L. V. Kanitskaya, A. V. Rokhin, D. F. Kushnarev, and G. A. Kalabin, "Chemical Structure of Wheat Dioxane Lignin : 1h and 13c Nmr Study," *Vysokomol soedin,* 40, pp. 800-805, 1998.

[152] A. Guerra, I. Filpponen, L. A. Lucia, and D. S. Argyropoulos, "Comparative Evaluation of Three Lignin Isolation Protocols for Various Wood Species," *Journal of Agricultural and Food Chemistry,* 54, pp. 9696-9705, 2006.

[153] E. A. Capanema, M. Y. Balakshin, and J. F. Kadla, "A Comprehensive Approach for Quantitative Lignin Characterization by Nmr Spectroscopy," *Journal of Agricultural and Food Chemistry,* 52, pp. 1850-1860, 2004.

[154] J. W. Choi, O. Faix, and D. Meier, "Characterization of Residual Lignins from Chemical Pulps of Spruce (Picea Abies L.) and Beech (Fagus Sylvatica L.) by

Analytical Pyrolysis-Gas Chromatography/Mass Spectrometry," *Holzforschung,* 55, pp. 185-192, 2001.

[155] P. C. Pinto, D. V. Evtuguin, and C. P. Neto, "Effect of Structural Features of Wood Biopolymers on Hardwood Pulping and Bleaching Performance," *Industrial & Engineering Chemistry Research,* 44, pp. 9777-9784, 2005.

[156] R. Samuel, Y. Pu, B. Raman, and A. J. Ragauskas, "Structural Characterization and Comparison of Switchgrass Ball-Milled Lignin before and after Dilute Acid Pretreatment," *Applied Biochemistry and Biotechnology,* 162, pp. 62-74, 2010.

[157] M. Galbe and G. Zacchi, "Pretreatment of Lignocellulosic Materials for Efficient Bioethanol Production," in *Biofuels*. vol. 108, L. Olsson, Ed., ed, 2007, pp. 41-65.

[158] N. Mosier, C. Wyman, B. Dale, R. Elander, Y. Y. Lee, M. Holtzapple, and M. Ladisch, "Features of Promising Technologies for Pretreatment of Lignocellulosic Biomass," *Bioresource Technology,* 96, pp. 673-686, 2005.

[159] J. E. Holladay, J. F. White, J. J. Bozell, and D. Johnson, "Results of Screening for Potential Candidates from Biorefinery Lignin," in *Top Value Added Candidates from Biomass*, P. Werpy and G. Petersen, Eds., ed Richland: Pacific Northwest National Laboratory, 2007, pp. 53-55.

[160] S. E. Lebo, J. D. Gargulak, and J. M. Timothy, *Lignin in Kirk-Othmer Encyclopedia of Chemical Technology (4th Ed.)*. New York: John Wiley & Sons, 2001.

[161] I. Brodin, E. Sjoholm, and G. Gellerstedt, "The Behavior of Kraft Lignin During Thermal Treatment," *Journal of Analytical and Applied Pyrolysis,* 87, pp. 70-77, 2010.

[162] D. R. Robert, M. Bardet, G. Gellerstedt, and E. L. Lindfors, "Structural-Changes in Lignin During Kraft Cooking .3. On the Structure of Dissolved Lignins," *Journal of Wood Chemistry and Technology,* 4, pp. 239-263, 1984.

[163] J. H. Lora and W. G. Glasser, "Recent Industrial Applications of Lignin: A Sustainable Alternative to Nonrenewable Materials," *Journal of Polymers and the Environment,* 10, pp. 39-48, 2002.

[164] W. G. Glasser, "Classification of Lignins According to Chemical and Molecular Structure," in *Lignin – Historical, Biological, and Materials Perspectives*. vol. ACS Symp. Ser. No. 742, W. G. Glasser, R. A. Northey, and T. P. Schultz, Eds., ed, 1999, pp. 216-238.

[165] R. A. Fenner and J. O. Lephardt, "Examination of the Thermal-Decomposition of Kraft Pine Lignin by Fourier-Transform Infrared Evolved Gas-Analysis," *Journal of Agricultural and Food Chemistry,* 29, pp. 846-849, 1981.

[166] Food and Agriculture Organization of the United Nations 2008: www.fao.org/forestry.

[167] J. D. Gargulak and S. E. Lebo, "Commercial Use of Lignin-Based Materials," in *Lignin : Historical, Biological, and Materials Perspectives*. vol. 742, W. G. N. R. A. S. T. P. Glasser, Ed., ed, 2000, pp. 304-320.

[168] X. Pan, N. Gilkes, J. Kadla, K. Pye, S. Saka, D. Gregg, K. Ehara, D. Xie, D. Lam, and J. Saddler, "Bioconversion of Hybrid Poplar to Ethanol and Co-Products Using an Organosolv Fractionation Process: Optimization of Process Yields," *Biotechnology and Bioengineering,* 94, pp. 851-861, 2006.

[169] X. Pan, J. F. Kadla, K. Ehara, N. Gilkes, and J. N. Saddler, "Organosolv Ethanol Lignin from Hybrid Poplar as a Radical Scavenger: Relationship between Lignin Structure, Extraction Conditions, and Antioxidant Activity," *Journal of Agricultural and Food Chemistry,* 54, pp. 5806-5813, 2006.

[170] X. J. Pan, D. Xie, R. W. Yu, D. Lam, and J. N. Saddler, "Pretreatment of Lodgepole Pine Killed by Mountain Pine Beetle Using the Ethanol Organosolv Process: Fractionation and Process Optimization," *Industrial & Engineering Chemistry Research,* 46, pp. 2609-2617, 2007.

[171] V. B. Diebold, W. F. Cowan, and J. K. Walsh, "Solvent Pulping Process," US Patent 4.100.016, 1978.

[172] M. N. Vanderlaan and R. W. Thring, "Polyurethanes from Alcell (R) Lignin Fractions Obtained by Sequential Solvent Extraction," *Biomass & Bioenergy,* 14, pp. 525-531, 1998.

[173] E. K. Pye and J. H. Lora, "The Alcell Process: A Proven Alternative to Kraft Pulping," *TAPPI,* 74, pp. 113-118, 1991.

[174] P. Stockburger, "An Overview of near-Commercial and Commercial Solvent-Based Pulping Processes," *Tappi Journal,* 76, pp. 71-74, 1993.

[175] J. H. Lora, E. K. Pye, P. Tech Assoc, and I. N. D. Paper, "The Alcell(R) Process," in *Solvent Pulping Symposium*, 1992, pp. 27-34.

[176] N. Brosse, P. Sannigrahi, and A. Ragauskas, "Pretreatment of Miscanthus X Giganteus Using the Ethanol Organosolv Process for Ethanol Production," *Industrial & Engineering Chemistry Research,* 48, pp. 8328-8334, 2009.

[177] P. Sannigrahi, A. J. Ragauskas, and S. J. Miller, "Lignin Structural Modifications Resulting from Ethanol Organosolv Treatment of Loblolly Pine," *Energy & Fuels,* 24, pp. 683-689, 2010.

[178] R. El Hage, N. Brosse, L. Chrusciel, C. Sanchez, P. Sannigrahi, and A. Ragauskas, "Characterization of Milled Wood Lignin and Ethanol Organosolv Lignin from

Miscanthus," *Polymer Degradation and Stability,* 94, pp. 1632-1638, 2009.

[179] X. Pan, D. Xie, R. W. Yu, and J. N. Saddler, "The Bioconversion of Mountain Pine Beetle-Killed Lodgepole Pine to Fuel Ethanol Using the Organosolv Process," *Biotechnology and Bioengineering,* 101, pp. 39-48, 2008.

[180] H. Sixta, *Handbook of Pulp*. Weinheim: Wiley-VCH Verlag GmbH & Co. KGaA, 2006.

[181] F. J. Lu, L. H. Chu, and R. J. Gau, "Free Radical-Scavenging Properties of Lignin," *Nutrition and Cancer-an International Journal,* 30, pp. 31-38, 1998.

[182] R. J. A. Gosselink, M. H. B. Snijder, A. Kranenbarg, E. R. P. Keijsers, E. de Jong, and L. L. Stigsson, "Characterisation and Application of Novafiber Lignin," *Industrial Crops and Products,* 20, pp. 191-203, 2004.

[183] C. I. Simionescu, M. M. Macoveanu, C. Vasile, F. Ciobanu, M. Esanu, A. Ioanid, P. Vidrascu, and N. GeorgescuBuruntea, "Polyolefins/Lignosulfonates Blends," *Cellulose Chemistry and Technology,* 30, pp. 411-429, 1996.

[184] M. Rusu and N. Tudorachi, "Biodegradable Composite Materials Based on Polyethylene and Natural Polymers. I. Mechanical and Thermal Properties," *Journal of Polymer Engineering,* 19, pp. 355-369, 2000.

[185] N. Tudorachi, M. Rusu, C. N. Cascaval, L. Constantin, and V. Rugina, "Biodegradable Polymeric Materials I. Polyethylene-Natural Polymer Blends," *Cellulose Chemistry and Technology,* 34, pp. 101-111, 2000.

[186] N. Tudorachi, C. N. Cascaval, and M. Rusu, "Biodegradable Polymer Blends Based on Polyethylene and Natural Polymers. Degradation in Soil," *Journal of Polymer Engineering,* 20, pp. 287-304, 2000.

[187] G. J. Cui, H. L. Fan, W. B. Xia, F. J. Ai, and J. Huang, "Simultaneous Enhancement in Strength and Elongation of Waterborne Polyurethane and Role of Star-Like Network with Lignin Core," *Journal of Applied Polymer Science,* 109, pp. 56-63, 2008.

[188] M. Turunen, L. Alvila, T. T. Pakkanen, and J. Rainio, "Modification of Phenol-Formaldehyde Resol Resins by Lignin, Starch, and Urea," *Journal of Applied Polymer Science,* 88, pp. 582-588, 2003.

[189] J. L. Popp, T. K. Kirk, and J. S. Dordick, "Enzymic Modification of Lignin for Use as a Phenolic Resin," *Enzyme Microb. Technol.,* 13, pp. 964-968, 1991.

[190] G. A. Doering, "Lignin Modified Phenol-Formaldehyde Resins," US Patent 5,202,403, 1993.

[191] G. Vazquez, C. Rodriguez-Bona, S. Freire, J. Gonzalez-Alvarez, and G. Antorrena,

"Acetosolv Pine Lignin as Copolymer in Resins for Manufacture of Exterior Grade Plywoods," *Bioresource Technology,* 70, pp. 209-214, 1999.

[192] T. Sellers, J. H. Lora, and M. Okuma, "Organosolv-Lignin-Modified Phenolics as Strandboard Binder .1. Organosolv Lignin and Modified Phenolic Resin," *Mokuzai Gakkaishi,* 40, pp. 1073-1078, 1994.

[193] T. Sellers, J. H. Lora, and M. Okuma, "Organosolv-Lignin-Modified Phenolics as Strandboard Binder .2. Strandboard Manufacture and Properties," *Mokuzai Gakkaishi,* 40, pp. 1079-1084, 1994.

[194] N. S. Cetin and N. Ozmen, "Use of Organosolv Lignin in Phenol-Formaldehyde Resins for Particleboard Production - I. Organosolv Lignin Modified Resins," *International Journal of Adhesion and Adhesives,* 22, pp. 477-480, 2002.

[195] L. M. Cotoruelo, M. D. Marques, J. Rodriguez-Mirasol, T. Cordero, and J. J. Rodriguez, "Adsorption of Aromatic Compounds on Activated Carbons from Lignin: Equilibrium and Thermodynamic Study," *Industrial & Engineering Chemistry Research,* 46, pp. 4982-4990, 2007.

[196] Z. B. Xu, X. L. Tang, A. J. Gu, and Z. P. Fang, "Novel Preparation and Mechanical Properties of Rigid Polyurethane Foam/Organoclay Nanocomposites," *Journal of Applied Polymer Science,* 106, pp. 439-447, 2007.

[197] H. Lim, S. H. Kim, and B. K. Kim, "Effects of Silicon Surfactant in Rigid Polyurethane Foams," *Express Polymer Letters,* 2, pp. 194-200, 2008.

[198] X. Cao, L. J. Lee, T. Widya, and C. Macosko, "Polyurethane/Clay Nanocomposites Foams: Processing, Structure and Properties," *Polymer,* 46, pp. 775-783, 2005.

[199] M. Szychers, *Szycher`S Handbook of Polyurethanes*. Boca Raton: CRC press, 1999.

[200] S.-T. Lee and N. S. Ramesh, *Polymeric Foams: Mechanisms and Materials*: CRC press, 2004.

[201] Y. H. Kim, J. W. Lee, S. J. Choi, M. S. Han, J. M. Kim, S. B. Vim, and W. N. Kim, "Properties of Rigid Polyurethane Foams Blown by Hfc-365mfc and Distilled Water," *Journal of Industrial and Engineering Chemistry,* 13, pp. 1076-1082, 2007.

[202] H. Fleurent and S. Thijs, "The Use of Pentanes as Blowing Agent in Rigid Polyurethane Foam," *Journal of Cellular Plastics,* 31, pp. 580-&, 1995.

[203] Y. X. Wang, H. F. Tian, and L. N. Zhang, "Role of Starch Nanocrystals and Cellulose Whiskers in Synergistic Reinforcement of Waterborne Polyurethane," *Carbohydrate Polymers,* 80, pp. 665-671, 2010.

[204] Y. Li, H. F. Ren, and A. J. Ragauskas, "Rigid Polyurethane Foam/Cellulose Whisker Nanocomposites: Preparation, Characterization, and Properties," *Journal of Nanoscience and Nanotechnology,* 11, pp. 6904-6911, 2011.

[205] V. P. Saraf and W. G. Glasser, "Engineering Plastics from Lignin .3. Structure Property Relationships in Solution Cast Polyurethane Films," *Journal of Applied Polymer Science,* 29, pp. 1831-1841, 1984.

[206] B. S. Raymond and B. K. George, "Polyurethanes: A class of modern versatile materials," *Journal of Chemical Education*, 69(11), pp. 909-911, 1992.

[207] M. Ionescu, *Chemistry and Technology of Polyols for Polyurethanes*: Smithers Rapra Technology 2005.

[208] A. Gandini, M. N. Belgacem, Z.-X. Guo, and S. Montanari, "Lignin as Macromonomers for Polyesther and Polyurethanes," in *Chemical Modification, Properties, and Usage of Lignin*, T. Q. Hu, Ed., ed New York: Kluwer Academic Plenum Publishers, 2002, pp. 57-80.

[209] K. Nakamura, R. Morck, A. Reimann, and K. Kringstad, "Compression Properties of Polyurethane Foam Derived from Kraft Lignin," in *Wood Processing Andutilisation*, J. F. Kennedy, G. O. Phillips, and P. A. Williams, Eds., ed Chichester: Ellis Horwood Limited, 1989, pp. 175-180.

[210] J. Bicerano and J. L. Brewbaker, "Reinforcement of Polyurethane Elastomers with Microfibers Having Varying Aspect Ratios," *Journal of the Chemical Society-Faraday Transactions,* 91, pp. 2507-2513, 1995.

[211] M. Johnson and S. Shivkumar, "Filamentous Green Algae Additions to Isocyanate Based Foams," *Journal of Applied Polymer Science,* 93, pp. 2469-2477, 2004.

[212] M. C. Silva and G. G. Silva, "A New Composite from Cellulose Industrial Waste and Elastomeric Polyurethane," *Journal of Applied Polymer Science,* 98, pp. 336-340, 2005.

[213] Q. J. Wu, M. Henriksson, X. Liu, and L. A. Berglund, "A High Strength Nanocomposite Based on Microcrystalline Cellulose and Polyurethane," *Biomacromolecules,* 8, pp. 3687-3692, 2007.

[214] M. A. Mosiewicki, U. Casado, N. E. Marcovich, and M. I. Aranguren, "Polyurethanes from Tung Oil: Polymer Characterization and Composites," *Polymer Engineering and Science,* 49, pp. 685-692, 2009.

[215] M. L. Auad, V. S. Contos, S. Nutt, M. I. Aranguren, and N. E. Marcovich, "Characterization of Nanocellulose-Reinforced Shape Memory Polyurethanes," *Polymer International,* 57, pp. 651-659, 2008.

[216] M. Thirumal, D. Khastgir, N. K. Singha, B. S. Manjunath, and Y. P. Naik, "Effect

of Foam Density on the Properties of Water Blown Rigid Polyurethane Foam," *Journal of Applied Polymer Science,* 108, pp. 1810-1817, 2008.

[217] Y. G. Yao, M. Yoshioka, and N. Shiraishi, "Rigid Polyurethane Foams from Combined Liquefaction Mixtures of Wood and Starch," *Mokuzai Gakkaishi,* 41, pp. 659-668, 1995.

[218] R. H. F. Li Y., Ragauskas A. J., "Rigid Polyurethane Foam Reinforced with Cellulose Whiskers: Synthesis and Characterization," *Nano-Micro Letters,* 2, p. 6, 2010.

[219] W. G. Glasser, W. De Oliveira, S. S. Kelley, and L. S. Nieh, "Method of Producing Star-Like Polymers from Lignin," US Patent 5,066,790, 1991.

[220] K. R. Kurple, US Patent PCT/US96/20140, WO97/24362, 2000.

[221] H. Yoshida, R. Morck, and K. P. Kringstad, US Patent PCT/SE86/00237, WO 86/07070, 1986.

[222] H. Yoshida, R. Morck, K. P. Kringstad, and H. Hatakeyama, "Kraft Lignin in Polyurethanes .1. Mechanical-Properties of Polyurethanes from a Kraft Lignin Polyether Triol Polymeric Mdi System," *Journal of Applied Polymer Science,* 34, pp. 1187-1198, 1987.

[223] H. Yoshida, R. Morck, K. P. Kringstad, and H. Hatakeyama, "Kraft Lignin in Polyurethanes .2. Effects of the Molecular-Weight of Kraft Lignin on the Properties of Polyurethanes from a Kraft Lignin Polyether Triol Polymeric Mdi System," *Journal of Applied Polymer Science,* 40, pp. 1819-1832, 1990.

[224] C. A. Cateto, M. F. Barreiro, A. E. Rodrigues, M. C. Brochier-Solan, W. Thielemans, and M. N. Belgacem, "Lignins as Macromonomers for Polyurethane Synthesis: A Comparative Study on Hydroxyl Group Determination," *Journal of Applied Polymer Science,* 109, pp. 3008-3017, 2008.

[225] C. Pavier and A. Gandini, "Oxypropylation of Sugar Beet Pulp. 2. Separation of the Grafted Pulp from the Propylene Oxide Homopolymer," *Carbohydrate Polymers,* 42, pp. 13-17, 2000.

[226] H. Nadji, C. Bruzzese, M. N. Belgacem, A. Benaboura, and A. Gandini, "Oxypropylation of Lignins and Preparation of Rigid Polyurethane Foams from the Ensuing Polyols," *Macromolecular Materials and Engineering,* 290, pp. 1009-1016, 2005.

[227] W. G. Glasser, L. C. F. Wu, and J. F. Selin, "Synthesis, Structure and Some Properties of Hydroxylpropyl Lignins," in *Wood and Agricultural Residues-Research on the Use for Feed, Fuels and Chemicals*, E. J. Soltes, Ed., ed New York: Academic Press, 1983, pp. 149-166.

[228] L. C. F. Wu and W. G. Glasser, "Engineering Plastics from Lignin .1. Synthesis of Hydroxypropyl Lignin," *Journal of Applied Polymer Science,* 29, pp. 1111-1123, 1984.

[229] A. M. A. Nada, M. A. Yousef, K. A. Shaffei, and A. M. Salah, *Pigment Resin Technol,* 28, p. 143, 1999.

[230] V. P. Saraf, W. G. Glasser, and G. L. Wilkes, "Engineering Plastics from Lignin .7. Structure Property Relationships of Poly(Butadiene Glycol)-Containing Polyurethane Networks," *Journal of Applied Polymer Science,* 30, pp. 3809-3823, 1985.

[231] V. P. Saraf, W. G. Glasser, G. L. Wilkes, and J. E. McGrath, "Engineering Plastics from Lignin .6. Structure Property Relationships of Peg-Containing Polyurethane Networks," *Journal of Applied Polymer Science,* 30, pp. 2207-2224, 1985.

[232] W. G. Glasser, O. H.-H. Hsu, D. L. Reed, R. C. Forte, and L. C.-F. Wu, *ACS Symp. Ser.,* pp. 172, 311, 1081.

[233] W. de Oliveira and W. G. Glasser, *ACS Symp. Ser.,* pp. 397, 414, 1989.

[234] S. S. Kelley, W. G. Glasser, and T. C. Ward, "Engineering Plastics from Lignin .15. Polyurethane Films from Chain-Extended Hydroxypropyl Lignin," *Journal of Applied Polymer Science,* 36, pp. 759-772, 1988.

[235] W. G. Glasser, J. F. Selin, P. L. Hall, and S. W. Drew, in *the 6th Int. Symp. Wood Pulping Chem.*, 1981, p. 39.

[236] B. Ahvazi, O. Wojciechowicz, T. M. Ton-That, and J. Hawari, "Preparation of Lignopolyols from Wheat Straw Soda Lignin," *Journal of Agricultural and Food Chemistry,* 59, pp. 10505-10516, 2011.

[237] W. G. Glasser and R. H. Leitheiser, "Engineering Plastics from Lignin .11. Hydroxypropyl Lignins as Components of Fire Resistant Foams," *Polymer Bulletin,* 12, pp. 1-5, 1984.

[238] A. K. Kaw. (2005). *Mechanics of Composite Materials, Second Edition*.

[239] W. Soboyejo. (2002). *Mechanical Properties of Engineered Materials*.

[240] C. A. Cateto, M. F. Barreiro, A. E. Rodrigues, and M. N. Belgacem, "Optimization Study of Lignin Oxypropylation in View of the Preparation of Polyurethane Rigid Foams," *Industrial & Engineering Chemistry Research,* 48, pp. 2583-2589, 2009.

[241] Y. Li and A. J. Ragauskas, "Ethanol Organosolv Lignin-Based Rigid Polyurethane Foam Reinforced with Cellulose Nanowhiskers," *RSC Advances,* 2, pp. 3347-3351, 2012.

[242] A. Granata and D. S. Argyropoulos, "2-Chloro-4,4,5,5-Tetramethyl-1,3,2-Dioxaphospholane, a Reagent for the Accurate Determination of the Uncondensed and Condensed Phenolic Moieties in Lignins," *Journal of Agricultural and Food Chemistry,* 43, pp. 1538-1544, 1995.

[243] M. Nagy, K. David, G. J. P. Britovsek, and A. J. Ragauskas, "Catalytic Hydrogenolysis of Ethanol Organosolv Lignin," *Holzforschung,* 63, pp. 513-520, 2009.

[244] M. Modesti, A. Lorenzetti, and S. Besco, "Influence of Nanofillers on Thermal Insulating Properties of Polyurethane Nanocomposites Foams," *Polymer Engineering and Science,* 47, pp. 1351-1358, 2007.

[245] Y. Q. Pu, J. G. Zhang, T. Elder, Y. L. Deng, P. Gatenholm, and A. J. Ragauskas, "Investigation into Nanocellulosics Versus Acacia Reinforced Acrylic Films," *Composites Part B-Engineering,* 38, pp. 360-366, 2007.

[246] A. J. Svagan, M. A. S. A. Samir, and L. A. Berglund, "Biomimetic Foams of High Mechanical Performance Based on Nanostructured Cell Walls Reinforced by Native Cellulose Nanofibrils," *Advanced Materials,* 20, pp. 1263-1269, 2008.

[247] I. Banik and M. M. Sain, "Role of Refined Paper Fiber on Structure of Water Blown Soy Polyol Based Polyurethane Foams," *Journal of Reinforced Plastics and Composites,* 27, pp. 1515-1524, 2008.

[248] T. U. Patro, G. Harikrishnan, A. Misra, and D. V. Khakhar, "Formation and Characterization of Polyurethane-Vermiculite Clay Nanocomposite Foams," *Polymer Engineering and Science,* 48, pp. 1778-1784, 2008.

[249] H. Ning, G. M. Janowski, U. K. Vaidya, and G. Husman, "Thermoplastic Sandwich Structure Design and Manufacturing for the Body Panel of Mass Transit Vehicle," *Composite Structures,* 80, pp. 82-91, 2007.

[250] M. C. Saha, M. E. Kabir, and S. Jeelani, "Enhancement in Thermal and Mechanical Properties of Polyurethane Foam Infused with Nanoparticles," *Materials Science and Engineering a-Structural Materials Properties Microstructure and Processing,* 479, pp. 213-222, 2008.

[251] I. Banik and M. M. Sain, "Structure of Glycerol and Cellulose Fiber Modified Water-Blown Soy Polyol-Based Polyurethane Foams," *Journal of Reinforced Plastics and Composites,* 27, pp. 1745-1758, 2008.

[252] A. J. Birch, "Process for Preparing Polyurethane Foam in the Presence of a Hydrocarbon Blowing Agent " US Patent 5,451,615, 1995.

[253] L. J. Lee, C. C. Zeng, X. Cao, X. M. Han, J. Shen, and G. J. Xu, "Polymer Nanocomposite Foams," *Composites Science and Technology,* 65, pp. 2344-2363, 2005.

[254] M. Alexandre and P. Dubois, "Polymer-Layered Silicate Nanocomposites: Preparation, Properties and Uses of a New Class of Materials," *Materials Science & Engineering R-Reports,* 28, pp. 1-63, 2000.

[255] A. Pattanayak and S. C. Jana, "Properties of Bulk-Polymerized Thermoplastic Polyurethane Nanocomposites," *Polymer,* 46, pp. 3394-3406, 2005.

[256] H. H. Wang, Y. H. Ni, M. S. Jahan, Z. H. Liu, and T. Schafer, "Stability of Cross-Linked Acetic Acid Lignin-Containing Polyurethane," *Journal of Thermal Analysis and Calorimetry,* 103, pp. 293-302, 2011.

[257] D. V. Evtuguin, J. P. Andreolety, and A. Gandini, "Polyurethanes Based on Oxygen-Organosolv Lignin," *European Polymer Journal,* 34, pp. 1163-1169, 1998.

[258] B. Guettes, R. Hempel, A. Biedermann, G. Knorr, and U. Rotermund, "Lignin Containing Poly: Hydroxyl Compound Used to Give Polyurethane," DE Patent 19,648,724, 1998.

[259] S. Hirose, "Production of Polyurethane Containing Lignin," JP Patent 63,182,327, 1998.

[260] K. R. Kurple, "Lignin Based Polyols," EP Patent 0,812,326, 1997.

[261] C. Ciobanu, M. Ungureanu, L. Ignat, D. Ungureanu, and V. I. Popa, "Properties of Lignin-Polyurethane Films Prepared by Casting Method," *Industrial Crops and Products,* 20, pp. 231-241, 2004.

[262] S. Baumberger, A. Abaecherli, M. Fasching, G. Gellerstedt, R. Gosselink, B. Hortling, J. Li, B. Saake, and E. de Jong, "Molar Mass Determination of Lignins by Size-Exclusion Chromatography: Towards Standardisation of the Method," *Holzforschung,* 61, pp. 459-468, 2007.

[263] C. E. L. Pasquali and H. Herrera, "Pyrolysis of Lignin and Ir Analysis of Residues," *Thermochimica Acta,* 293, pp. 39-46, 1997.

[264] Q. Liu, S. R. Wang, Y. Zheng, Z. Y. Luo, and K. F. Cen, "Mechanism Study of Wood Lignin Pyrolysis by Using Tg-Ftir Analysis," *Journal of Analytical and Applied Pyrolysis,* 82, pp. 170-177, 2008.

[265] L. L. Landucci, S. A. Ralph, and K. E. Hammel, "C-13 Nmr Characterization of Guaiacyl, Guaiacyl/Syringyl and Syringyl Dehydrogenation Polymers," *Holzforschung,* 52, pp. 160-170, 1998.

[266] L. Yang, F. Heatley, T. G. Blease, and R. I. G. Thompson, "A Study of the Mechanism of the Oxidative Thermal Degradation of Poly(Ethylene Oxide) and Poly(Propylene Oxide) Using H-1- and C-13-Nmr," *European Polymer Journal,* 32, pp. 535-547, 1996.

[267] H. Cheradame, M. Detoisien, A. Gandini, F. Pla, and G. Roux, "Polyurethane from Kraft Lignin," *British Polymer Journal,* 21, pp. 269-275, 1989.

[268] S. Chahar, M. G. Dastidar, V. Choudhary, and D. K. Sharma, "Synthesis and Characterisation of Polyurethanes Derived from Waste Black Liquor Lignin," *Journal of Adhesion Science and Technology,* 18, pp. 169-179, 2004.

[269] D. Klemm, H. P. Schmauder, and T. Heinze, "Biopolymers." vol. 6, E. Vandamme, S. de Beats, and A. Steinbuchel, Eds., ed Weinheim: Wiley-VCH, 2002, pp. 290-292.

[270] B. L. Holt, S. D. Stoyanov, E. Pelan, and V. N. Paunov, "Novel Anisotropic Materials from Functionalised Colloidal Cellulose and Cellulose Derivatives," *Journal of Materials Chemistry,* 20, pp. 10058-10070, 2010.

[271] H. Sehaqui, M. Allais, Q. Zhou, and L. A. Berglund, "Wood Cellulose Biocomposites with Fibrous Structures at Micro- and Nanoscale," *Composites Science and Technology,* 71, pp. 382-387, 2011.

[272] I. Siro and D. Plackett, "Microfibrillated Cellulose and New Nanocomposite Materials: A Review," *Cellulose,* 17, pp. 459-494, 2010.

[273] J. J. Tan, H. L. Kang, R. G. Liu, D. Q. Wang, X. Jin, Q. M. Li, and Y. Huang, "Dual-Stimuli Sensitive Nanogels Fabricated by Self-Association of Thiolated Hydroxypropyl Cellulose," *Polymer Chemistry,* 2, pp. 672-678, 2011.

[274] J. Gajdziok, B. Martina, C. Zuzana, and R. Miloslava, "Oxycellulose as Mucoadhesive Polymer in Buccal Tablets," *Drug Development and Industrial Pharmacy,* 36, pp. 1115-1130, 2010.

[275] Y. Ikeuchi, F. Z. Khan, N. Onishi, M. Shiotsuki, T. Masuda, Y. Nishio, and F. Sanda, "Amino Acid-Functionalized Ethyl Cellulose: Synthesis, Characterization, and Gas Permeation Properties," *Journal of Polymer Science Part a-Polymer Chemistry,* 48, pp. 3986-3993, 2010.

[276] S. Vlad, D. Filip, D. Macocinschi, I. Spiridon, A. Nistor, L. M. Gradinaru, and V. E. Musteata, "New Polyetherurethanes Based on Cellulose Derivative for Biomedical Applications," *Optoelectronics and Advanced Materials-Rapid Communications,* 4, pp. 407-414, 2010.

[277] J. M. Lavoie, W. Bare, and M. Bilodeau, "Depolymerization of Steam-Treated Lignin for the Production of Green Chemicals," *Bioresource Technology,* 102, pp. 4917-4920, 2011.

[278] Q. Shen, T. Zhang, W. X. Zhang, S. A. Chen, and M. Mezgebe, "Lignin-Based Activated Carbon Fibers and Controllable Pore Size and Properties," *Journal of Applied Polymer Science,* 121, pp. 989-994, 2011.

[279] E. M. Nour-Eddine, Q. L. Yuan, and F. R. Huang, "Use of Hydroxymethylated Lignin in Phenol-Formaldehyde Resins," in *Research Progress in Paper Industry and Biorefinery*, R. C. Sun and S. Y. Fu, Eds., ed, 2010, pp. 53-56.

[280] S. Liu and X. Cheng, "Application of Lignin as Antioxidant in Styrene Butadiene Rubber Composite " in *2nd International Symposium on Aqua Science, Water Resource and Low Carbon Energy* Sanya Hainan, (China), 2009, pp. 344-347.

[281] G. Sivasankarapillai and A. G. McDonald, "Synthesis and Properties of Lignin-Highly Branched Poly (Ester-Amine) Polymeric Systems," *Biomass & Bioenergy,* 35, pp. 919-931, 2011.

[282] Y. Li and A. J. Ragauskas, "Kraft Lignin-Based Rigid Polyurethane Foam," *Journal of Wood Chemistry and Technology,* 32, pp. 210-224, 2012.

[283] M. Alexandre and P. Dubois, "Polymer-Layered Silicate Nanocomposites: Preparation, Properties and Uses of a New Class of Materials," *Materials Science and Engineering: R: Reports,* 28, pp. 1-63, 2000.

[284] "Technical Report on Thermal Insulation Materials Made of Rigid Polyurethane Foam (Pur/Pir)," BING-Federation of European Rigid Polyurethane Foam Associations, Brussels, Belgium 1, 2006.

[285] A. H. Pei, J. M. Malho, J. Ruokolainen, Q. Zhou, and L. A. Berglund, "Strong Nanocomposite Reinforcement Effects in Polyurethane Elastomer with Low Volume Fraction of Cellulose Nanocrystals," *Macromolecules,* 44, pp. 4422-4427, 2011.

[286] S. Hoepfner, L. Ratke, and B. Milow, "Synthesis and Characterisation of Nanofibrillar Cellulose Aerogels," *Cellulose,* 15, pp. 121-129, 2008.

[287] U. J. Kim, J. Park, H. J. Kim, M. Wada, and D. L. Kaplan, "Three-Dimensional Aqueous-Derived Biomaterial Scaffolds from Silk Fibroin," *Biomaterials,* 26, pp. 2775-2785, 2005.

[288] T. Rosenau, F. Liebner, A. Potthast, E. Haimer, and M. Wendland, "Ultralightweight Cellulose Aerogels from Nbnmo-Stabilized Lyocell Dopes," *Research Letters in Materials Science,* 2007, p. Article ID 73724, 2007.

[289] X. H. Chang, D. R. Chen, and X. L. Jiao, "Chitosan-Based Aerogels with High Adsorption Performance," *Journal of Physical Chemistry B,* 112, pp. 7721-7725, 2008.

[290] S. A. Barr and E. Luijten, "Structural Properties of Materials Created through Freeze Casting," *Acta Materialia,* 58, pp. 709-715, 2010.

[291] S. Deville, E. Saiz, R. K. Nalla, and A. P. Tomsia, "Freezing as a Path to Build Complex Composites," *Science,* 311, pp. 515-518, 2006.

[292] S. Deville, E. Saiz, and A. P. Tomsia, "Ice-Templated Porous Alumina Structures," *Acta Materialia,* 55, pp. 1965-1974, 2007.

[293] H. F. Zhang, I. Hussain, M. Brust, M. F. Butler, S. P. Rannard, and A. I. Cooper, "Aligned Two- and Three-Dimensional Structures by Directional Freezing of Polymers and Nanoparticles," *Nature Materials,* 4, pp. 787-793, 2005.

[294] M. Kawata, H. Uchida, K. Itatani, I. Okada, S. Koda, and M. Aizawa, "Development of Porous Ceramics with Well-Controlled Porosities and Pore Sizes from Apatite Fibers and Their Evaluations," *Journal of Materials Science-Materials in Medicine,* 15, pp. 817-823, 2004.

[295] C. Tsioptsias, A. Stefopoulos, I. Kokkinomalis, L. Papadopoulou, and C. Panayiotou, "Development of Micro- and Nano-Porous Composite Materials by Processing Cellulose with Ionic Liquids and Supercritical Co(2)," *Green Chemistry,* 10, pp. 965-971, 2008.

[296] W. Mahler and M. F. Bechtold, "Freeze-Formed Silica Fibers," *Nature,* 285, pp. 27-28, 1980.

[297] J. W. Moon, H. J. Hwang, M. Awano, and K. Maeda, "Preparation of Nio-Ysz Tubular Support with Radially Aligned Pore Channels," *Materials Letters,* 57, pp. 1428-1434, 2003.

[298] S. R. Mukai, H. Nishihara, and H. Tamon, "Formation of Monolithic Silica Gel Microhoneycombs (Smhs) Using Pseudosteady State Growth of Microstructural Ice Crystals," *Chemical Communications,* pp. 874-875, 2004.

[299] R. Gavillon and T. Budtova, "Aerocellulose: New Highly Porous Cellulose Prepared from Cellulose-Naoh Aqueous Solutions," *Biomacromolecules,* 9, pp. 269-277, 2008.

[300] O. Aaltonen and O. Jauhiainen, "The Preparation of Lignocellulosic Aerogels from Ionic Liquid Solutions," *Carbohydrate Polymers,* 75, pp. 125-129, 2009.

[301] L. Heath and W. Thielemans, "Cellulose Nanowhisker Aerogels," *Green Chemistry,* 12, pp. 1448-1453, 2010.

[302] H. Sehaqui, M. Salajkova, Q. Zhou, and L. A. Berglund, "Mechanical Performance Tailoring of Tough Ultra-High Porosity Foams Prepared from Cellulose I Nanofiber Suspensions," *Soft Matter,* 6, pp. 1824-1832, 2010.

[303] J. Lee and Y. L. Deng, "The Morphology and Mechanical Properties of Layer Structured Cellulose Microfibril Foams from Ice-Templating Methods," *Soft Matter,* 7, pp. 6034-6040, 2011.

[304] I. Kvien and K. Oksman, "Orientation of Cellulose Nanowhiskers in Polyvinyl Alcohol," *Applied Physics a-Materials Science & Processing,* 87, pp. 641-643,

2007.

[305] S. Deville, "Freeze-Casting of Porous Ceramics: A Review of Current Achievements and Issues," *Advanced Engineering Materials,* 10, pp. 155-169, 2008.

[306] S. Deville, E. Saiz, and A. P. Tomsia, "Freeze Casting of Hydroxyapatite Scaffolds for Bone Tissue Engineering," *Biomaterials,* 27, pp. 5480-5489, 2006.

[307] T. Fukasawa, Z. Y. Deng, M. Ando, T. Ohji, and S. Kanzaki, "Synthesis of Porous Silicon Nitride with Unidirectionally Aligned Channels Using Freeze-Drying Process," *Journal of the American Ceramic Society,* 85, pp. 2151-2155, 2002.

[308] J. A. Sekhar and R. Trivedi, "Solidification Microstructure Evolution in the Presence of Inert Particles," *Materials Science and Engineering a-Structural Materials Properties Microstructure and Processing,* 147, pp. 9-21, 1991.